Functional analysis of a novel DNA binding protein of Streptomyces coelicolor.

Aldridge, Matthew J

Functional analysis of a novel DNA binding protein of *Streptomyces coelicolor*

By

MATTHEW J. ALDRIDGE

A thesis submitted to the College of Medicine, Swansea University in candidature of the degree of Doctor of Philosophy

Swansea University
Prifysgol Abertawe

Institute of Life Science, College of Medicine
Swansea University

April 2012

ProQuest LLC.
789 East Eisenhower Parkway
P.O. Box 1346
Ann Arbor, MI 48106 – 1346

Success is going from failure to failure without loss of enthusiasm.

Winston Churchill

DECLARATION

This work has not previously been accepted in substance for any degree and is not being concurrently submitted in candidature for any degree.

Signed:

Date: 10/04/2012

STATEMENT 1

This thesis is the result of my own investigations, except where otherwise stated. Where correction services have been used, the extent and nature of the correction is clearly marked in a footnote(s).

Other sources are acknowledged by footnotes giving explicit references. A bibliography is appended.

Signed:

Date: 10/04/2012

STATEMENT 2

I hereby give consent for my thesis, if accepted, to be available for photocopying and for inter-library loan, and for the title and summary to be made available to outside organisations.

Signed:

Date: 10/04/2012

Acknowledgements

Firstly I would like to express my thanks and gratitude to my supervisor Prof Paul Dyson for giving me the opportunity to be a part of his research group for his guidance and support for the past many years.

I would also like to thank Dr Ricardo Del Sol for teaching me some of his huge research knowledge his help with problem solving and encouragement with the occasional kick up the backside.

I wish to thank Meirwyn Evans for his valuable help over the years and all my present and past lab-mates: Kate, Lorena, Lindsay, Matt, Paola, Paul Facey, Simon, Suliman and Suzy for making lab life enjoyable and fun.

Finally I would like to thank all my family and friends for all their help and support; Mam, Dad and especially Amy and Sophie as without their support and encouragement I would have never have accomplished this work.

Abstract

Secondary metabolism occurs after the main growth phase in *Streptomyces*. A 'transition phase' occurs to remodel global patterns of gene expression at the onset of physiological and developmental differentiation. Many different signals influence this transition phase, integrating, for example, information on nutritional status, growth rate, and stress responses. Several pleiotropic transcription factors that regulate the transition phase have been identified, but aspects of epigenetic control of gene expression are not well understood.

This study focused on the characterisation of a novel gene *sco2075* in *S. coelicolor* encoding a protein that combines a histone-like domain with a conserved DksA-like domain, the latter considered a ppGpp cofactor. The protein is important for integrating responses to both oxidative and osmotic stresses. The *sco2075*⁻ mutant strain is sensitive to oxidative stress at least in part due to reduced induction of the alternative sigma factor σ^R. SCO2075, similarly to *E. coli* DksA, may play a possible role in the liberation of core RNA polymerase to bind alternative sigma factors such as σ^R. In addition DSCO2075 has an altered topological profile of a reporter plasmid under osmotic stress, showing little alteration in negative supercoiling when compared to the significant increase in wildtype. DSCO2075 also has a reduction in aerial hyphae and a possible reduction in actinorhodin production when grown with osmolyte.

The histone-like domain of SCO2075 binds DNA non-specifically. SCO2075 expression appears to coincide with diffused FtsZ expression prior to Z-ring formation when SCO2075 appears to become nucleoid associated. Analysis of pre-spore compartment lengths showed SCO2075 is one of several nucleoid associated proteins involved in nucleoid compaction during aerial hyphal erection and sporulation. Absence of *sco2075,* however, does not affect the production of unigenomic spore chains. Finally, over-expression of SCO2075 suppresses defects in secondary metabolism of a *relA* mutant affected in ppGpp synthesis.

SCO2075 could potentially be a new type of regulator, likely acting as a node to integrate stress and physiological cues by modulating DNA topology/compaction and RNA polymerase activity.

Abbreviations

2D	Two dimensional
A	Adenine
ADP	Adenosine Diphosphate
AFM	Atomic Force Microscopy
ATP	Adenosine Triphosphate
bp	Base pair(s)
C	Cytosine
CDA	Calcium dependent antibiotic
CIAP	Calf Intestinal Alkaline Phosphatase
DBD	DNA binding Domain
DMSO	Dimethyl sulfoxide
DNA	Deoxyribose nucleic acid
dNTP	Deoxynucleoside Triphosphate
Dps	DNA-binding proteins from starved cells
DTT	Dithiothreitol
EDTA	Ethylene Diamine Tetraacetic acid
EGFP	Enhanced Green Fluorescent Protein
FIS	Factor for inversion stimulation
g	Gram(s)
G	Guanine
h	Hour(s)
H-NS	histone-like nucleoid structuring
HU	Heat unstable nucleoid protein
IHF	integration host factor

IPTG	Isopropyl-β-*D*-thiogalactoside
Kbp	Kilobase pair(s)
kDa	Kilodalton(s)
L or l	Litre
Lk	Linking number
Mb	Megabase(s)
MIC	Minimum Inhibitory Concentration
min	Minute(s)
MW	Molecular Weight
nt	nucleotides
OD	Optical density
ORF	Open Reading Frame
PAGE	Polyarcylamide gel electrophoresis
PCR	Polymerase Chain Reaction
PFGE	Pulse field gel electrophoresis
pI	Isoelectric point
ppGpp	Guanosine tetra- and pentaphosphate
RNA	Ribonucleic acid
RNAP	RNA polymerase
rpm	Revolutions per minute
rrn	Genes encoding rRNA
rRNA	Ribosomal RNA
s	Second(s)
SDS	Sodium Dodecyl Sulphate
T	Thymine
TAE	Tris Acetate EDTA
TBE	Tris Borate EDTA
TEMED	N,N,N',N'-tetramethyl-ethylenediamine

TES	*N*-tris(hydroxymethyl)-*2*-aminoethanesulphonic acid
TPE	Tris Phosphate EDTA
Tris	Tris(hydroxymethyl)amino-methane
tRNA	Transfer RNA
Tw	Twist
UV	Ultraviolet light
V	Volt(s)
W	Watt(s)
Wr	Writhe
xg	Times gravity
X-gal	5-bromo-4-chloro-3-indolyl-β-*D*-galactoside
µ	Micro

Glossary

Negative supercoiling	When the DNA molecule is twisted in the opposite direction to the DNA helix (left-handed direction), there-by under-winding the molecule.
Plectonemic	The conformation of DNA, where the DNA helix is wound around another part of the same molecule in a higher order helix
Positive supercoiling	Where the DNA is twisted in the same direction (right-handed direction) which tightens the helix.
Toroidal DNA or toroidal winding	So called because the axis of the DNA helix lies on the surface of an imaginary torus
Twist (T_w)	How individual strands of DNA coil around the axis of the DNA helix (i.e. around one another).
Writhe (W_r)	How the DNA helix axis coils around itself in space.

Contents

Chapter - 1

Introduction

1.1 Classification

1.1.1 *Actinomycetales*

Actinomycetes, meaning "ray fungus" in Greek (Waksman and Henrici (1943), are the genera of actinobacteria consisting of Gram-positive bacteria with greater than 55% G+C content in the genome that form branching hyphae and asexual spores. Most are aerobic however a small number can survive under anaerobic conditions such as *Actinomyces israelii.* They are well known as secondary metabolite producers with over 10,000 active metabolites produced by actinomycetes (Berdy 2005), of which *Streptomyces* contributes 80% of the naturally derived antibiotics. The genera include *Corynebacterium, Mycobacterium*, *Nocardia*, *Rhodococcus* and *Streptomyces.*

1.1.2 *Streptomyces*

Streptomyces is the largest genus in actinobacteria and falls in the family *Streptomycetaceae* and owes its name to its apparent likeness to filamentous fungi where Waksman and Henrici (1943) combined "actinomyces" meaning "ray fungus" with "streptothrix" meaning "twisted hair". There were over 535 species in the genus *Streptomyces* in the Bergey's Manual in 2009, (August 2009), however, this number is constantly increasing. For example, *Streptomyces aomiensis* was classed as a novel species of the genus in 2010 (Nagai, Khan et al. 2011).

Originally thought to be an intermediate of bacteria and fungi, it was shown in the Strangeways Laboratory using electron microscopy that *Streptomyces* lack a nuclear

membrane which firmly placed them with prokaryotes (Hopwood 1999) as do other characteristics such as antibiotic sensitivity and cell wall composition. *Streptomyces* are mycelial Gram-positive bacteria which have a high guanine (G) and cytosine (C) content. Their complex developmental life cycle is split into three phases, filamentous vegetative growth which leads to the development of aerial hyphae with the subsequent differentiation of these hyphae to unigenomic spores. This complex morphology and ability to produce a variety of active secondary metabolites has generated a lot of interest over the last 50 years. They are generally not pathogenic; however there are a few example species such as: *Streptomyces scabies* that causes potato scab and *Streptomyces acidiscabies,* which causes potato scab in soils having pH values below 5.2 resulting in surface damage on infected tubers (Lambert 1989). Sweet potato small pox is caused by *Streptomyces ipomoea* results in disfiguring lesions to tubers (Zhang, Clark et al. 2003). The only known human pathogens are *Streptomyces somaliensis* and *Streptomyces sudanensis,* which causes actinomycetoma, a chronic subcutaneous infection that, occurs in many parts of the world with subtropical climates (Fahal and Hassan 1992; Quintana, Wierzbicka et al. 2008).

1.1.3 ***Streptomyces coelicolor* A3(2)**

S. coelicolor is the best genetically characterised of the genus and is the model organism for genetic studies. It originates from Strathclyde University (formerly Royal College of Technology in Glasgow) and was then named strain 204F, obtained by Dr David Hopwood in 1954. Hopwood coined the species name *coelicolor* due to the striking blue pigment it produced (Hopwood 1999). *S. coelicolor* produces four

different antibiotics. The colour of the distinctive diffusible blue pigmented antibiotic previously mentioned, called actinorhodin is pH dependent. It also produces undecylprodigiosin (red pigmented), methylenomycin and calcium dependent antibiotic (CDA).

1.2 Life cycle

The complex life cycle of *S. coelicolor* is one of the main reasons why it is so widely studied, forming multicellular colonies comprising of physiologically distinct cells (Chater 1998). The major stages of the life cycle are shown in figure 1.1 where it initially starts with the germination of a single unigenomic spore where one or two germ tubes emerge, growing by apical tip elongation to form long multi-nucleoid filaments, which have branched several times to form vegetative mycelium (Gray, Gooday et al. 1990). The apical tip extension allows the vegetative mycelium also known as substrate mycelium to grow into the immediate environment such as solid media in laboratory conditions. Septa emerge irregularly, separating compartments often with more than one nucleoid present.

Streptomyces is a saprophyte and the growing substrate hyphae excrete extracellular hydrolytic enzymes to solubilise organic compounds. The densely packed filamentous growth allows full utilization of all available nutrients within the soil, allowing *Streptomyces* to colonise solid substrates more efficiently than non-motile microorganisms. As the colony grows older, the mycelium increases in density and piles up where further changes take place. These changes could be due to nutritional limitations, a result of guanosine tetraphosphate (ppGpp) and/or cell density responses

mediated via extracellular signals and an apparent cascade of signals necessary for aerial growth in *S. coelicolor*. This morphogenesis requires *bld* genes and the secretion of a small hydrophobic biosurfacant SapB in *S. coelicolor* which reduces surface tension at the colony-air interface thereby allowing the hyphae to grow into the air (Claessen, de Jong et al. 2006). During the morphological change there is an increase in expression of extracellular enzymes and secondary metabolites such as antibiotics (Champness 1988). Unlike autolysis where the uncontrolled lytic actions of murein hydrolases degrade the cell walls resulting in cell death, in *Streptomyces* the vegetative mycelium mainly undergoes a highly organised progressive disorganisation of the internal cell components, including extensive genome digestion before plasma membrane integrity is compromised (Miguelez, Hardisson et al. 1999). The cell wall only degrades after these events if at all (Anderson and Wellington 2001). After this programmed hyphal death the cell wall collapses with apparent empty cellular content, but retains cell wall structure, which gives mechanical support to the erecting aerial hyphae. Once this transition phase has started and hyphae start to erect, the fate of the substrate mycelium is sealed as it undergoes this ordered disassembly. This disassembly is similar to programmed cell death where it is lysed and nutrients are taken up by the growing aerial hyphae. During this transition phase from vegetative mycelium to aerial erection of hyphae, antibiotics are produced in the lower part of the colony which can protect the nutrients released from dead/ dying cells to support the aerial growth and sporulation (Chater 2006).

To allow this aerial hyphal growth, nutrients are channelled up from the substrate mycelium, passing through a minimum of one septum at the base of the hyphal branch

(i.e. two cell walls). Aerial hyphae development is regulated by a number of *bld* genes, which encode regulatory proteins, with the exception of *bldA,* which encodes a tRNA. *bld* mutants result in a severely reduced aerial hyphae erection and antibiotic production (Lawlor, Baylis et al. 1987).

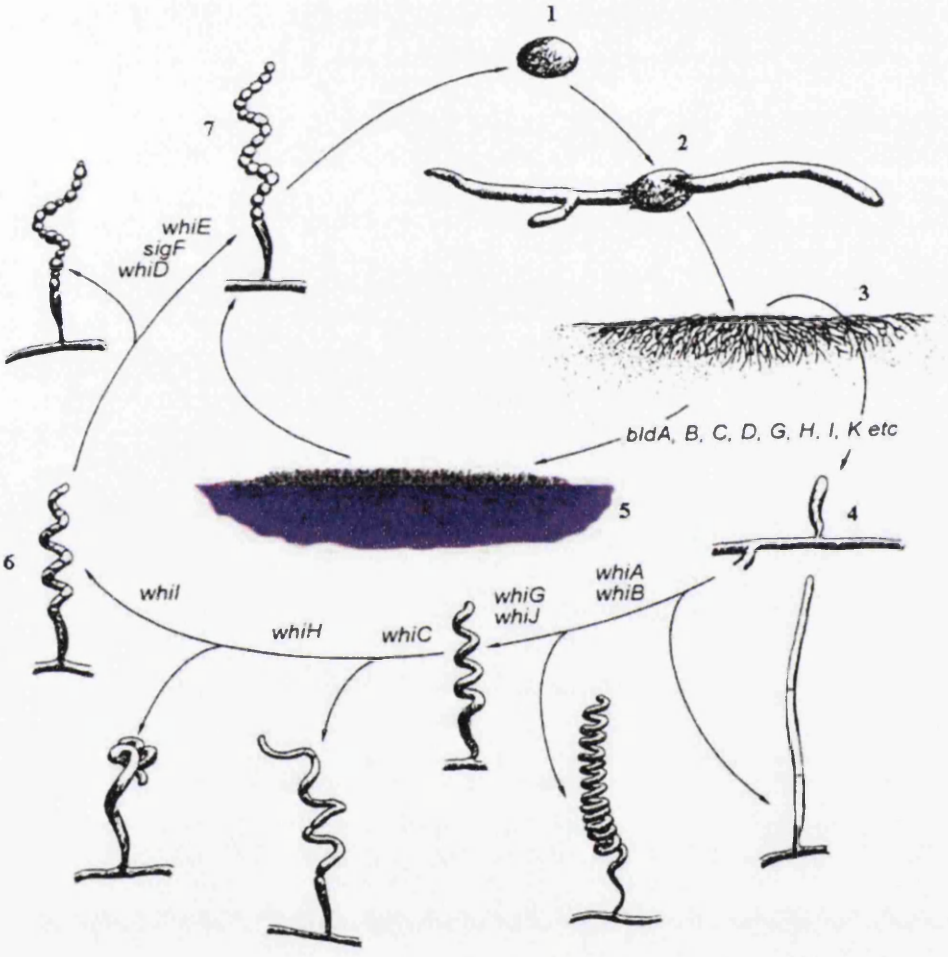

Figure 1.1: Diagram of *Streptomyces* life cycle. Favourable conditions result in a spore (1) germinating (2) extending by apical growth to form a complex vegetative mycelium (3). Under the regulation of the *bld* cascade aerial hyphae emerge from the surface of the colony in conjunction with secondary metabolite production such as the diffusible antibiotic actinorhodin shown as purple (4, 5). Under the regulation of *whi* genes the aerial hyphae undergo multiple septation resulting in the formation of unigenomic prespore compartment chains (6) which finally result in spore chains (7) where the cycle is repeated. Arrows along the cycle preceding the genes show the phenotype of the respective mutants blocked from progressing through the like cycle production (Kieser et al. 2000).

Under the control of six specialised regulatory *whi* genes, hyphal tips undergo multiple synchronous cell divisions to give cylindrical unigenomic prespore compartments. The compartments then round up with spore wall thickening and the accumulation of a grey pigmented polyketide derivative (Kelemen, Brian et al. 1998). The aerial hyphae differ in properties compared to the vegetative mycelia. They are thicker, without branching and have a thin hydrophobic layer which covers the aerial hyphae and spores reducing dehydration while in the air, where as vegetative mycelium is hydrophilic (Del Sol, Armstrong et al. 2007).

1.3 Ecology

Streptomyces are ubiquitous soil bacteria and are responsible for the soil's distinctive 'earthy' aroma through the secretion of chemicals called geosmins (Gerber and Lechevalier 1965; Jiang, He et al. 2007). They are also found in other habits such as fresh water, deep-sea deposits and glaciers (Colquhoun, Heald et al. 1998; Colquhoun, Zulu et al. 2000). Soil is a harsh environment to live in, with sudden alteration of salinity, moisture and temperature only some of the challenges faced by *Streptomyces* which could explain why their genomes have such variability in contingency genes. For example, the σ^B ortholog has been implicated in stress response (Lee, Karoonuthaisiri et al. 2005). However, the *S. coelicolor* genome encodes nine σ^B paralogs which could indicate the complex response strategies imposed by the environment (Cho, Lee et al. 2001; Viollier, Kelemen et al. 2003). Orthologs are genes in different species that evolved from a common ancestral gene by speciation. As *Streptomyces* are non-motile organisms it is no surprise that they have developed a number of strategies to survive

such an unstable environment. These include rapid growth and sporulation, secretion of hydrolytic enzymes to mobilise unusable nutrient sources and secondary metabolism that coincides with morphological development protecting their food source from other microorganisms (Challis and Hopwood 2003).

Streptomyces not only metabolise simple carbohydrates but play a role in the carbon and nitrogen cycle degrading insoluble remains of other organisms such as chitin, starch and lignocellulose which is composed of cellulose, hemicellulose and lignin. *S. coelicolor* has a predicted 819 secreted proteins making up 10.5% of the genome. Of the 819 predicted proteins there are 60 proteases/peptidases, 13 chitinases/ chitosanases, eight cellulases/ endoglucanases, three amylases and two pectate lyases (Bentley, Chater et al. 2002). This clearly shows *S. coelicolor*'s abundant ability to exploit nutrients from its natural habitat. Peripheral carbon sources which include agarase and glycerol utilisation are inducible and subject to catabolite repression (Angell, Lewis et al. 1994). Carbon catabolite repression is common in bacteria and prevents alternative carbon source utilisation where glucose metabolism is made available by glucose ATP-dependent kinase (*glkA*).

1.4 Primary metabolism

As *Streptomyces* are found predominantly in soil environments, the main source of nutrients is from plant biomass, which is rich in carbon compounds and poor in nitrogen and phosphate compounds (Hodgson 2000). *Streptomyces* primary metabolism reflects this nutrient availability. Due to the available and ever changing concentration of a variety of carbon sources in soil, *Streptomyces* have developed a number of catabolic pathways for compounds such as: glycerol, galactose, cellulose and chitin (Hodgson

2000). These catabolic pathways are inducible allowing optimum growth and are subject to carbon catabolic repression (CCR) (Champness 1988; Angell, Lewis et al. 1994; Kwakman and Postma 1994).

Unlike low G-C gram positive bacteria such as *Bacillus subtilis* or gram negative *Escherichia coil* where the phosphoenolpyruvate (PEP)-dependent sugar phosphotransferase system (PTS) plays a major role in CCR, in *S. coelicolor* PTS plays a secondary role (Guzman, Carmona et al. 2005) and responds only to the presence of fructose and *N*-acetylglucosamine (Wang, Xiao et al. 2002; Nothaft, Parche et al. 2003). In contrast, in *S. coelicolor* the ATP dependent glucose kinase (GlkA) plays the major role in CCR in conjunction with its upstream neighbouring gene SCO2127 practical Streptomyces (Kieser 2000; Guzman, Carmona et al. 2005; Guzman, Ramos et al. 2005).

A *glkA* mutant of *S. coelicolor*, initially isolated by Hodgson (1982), was resistant to growth on medium containing the glucose analogue 2-deoxyglucose (2-DOG) which cannot be metabolised and showed decreased levels of GlkA and a lack of glucose repression on other carbon sources. Expression levels of GlkA were restored when these mutants were complemented with *glkA* gene (Ikeda, Seno et al. 1984) although CCR sensitivity was only partially restored. CCR was completely restored with *glkA* and the upstream gene SCO2127 (Angell, Lewis et al. 1994; Guzman, Carmona et al. 2005).

Most *bld* gene mutants fail to erect aerial hyphae on glucose containing medium but can do so on other carbon sources (Merrick 1976; Champness 1988). This could suggest a lack of glucose repression. Recently SCO2127 was shown to be a key factor in CCR of mycelium differentiation by modulating BldKB function in *S. coelicolor*. The

parental strain failed to erect aerial hyphae and undergo septation in the presence of 100mM glucose, whereas a *sco2127* null mutant produced aerial hyphae and septated (Chavez, Forero et al. 2011).

There are two main pathways for nitrogen assimilation mediated by glutamate synthase (GS) and glutamate: 2-oxoglutarate transaminase (GOGAT) (Fisher 1992; Kieser 2000). The GS pathway requires ATP and is energetically unfavourable, functioning at low levels of ammonia and therefore both systems allow *Streptomyces* to grow in the nitrogen limited soil environment (Fisher 1992).

1.5 Secondary metabolism

Secondary metabolites are not essential for growth and maintenance of the producing organism. Secondary metabolism in *S. coelicolor* coincides with the slowing of growth of the vegetative mycelium due to nutrient or physiological limitations such as drought, resulting in the morphological change to aerial hyphae formation (Flardh and Buttner 2009). In liquid culture it is generally confined to stationary phase (Bibb 2005).

Actinomycetes produce over 10,000 bioactive compounds of which *Streptomyces* produce 7,600 and other actinomycetes 2,500 (74% and 25% respectively) (Berdy 2005). These huge numbers are down to the large number of secondary metabolite gene clusters with *S. coelicolor* alone containing 26 (Bentley, Chater et al. 2002). *Streptomyces* produce a large number of novel secondary metabolites and account for 80% of naturally derived antibiotics and as such are exploited and studied by the pharmaceutical industry for their products which also include antitumour, antifungal, antihelminthic, enzyme inhibitors, immunosuppressant activities and also herbicides

(Sanglier, Haag et al. 1993; Sanglier, Wellington et al. 1993; Watve, Tickoo et al. 2001; Paradkar, Trefzer et al. 2003).

Unlike primary metabolism, secondary metabolism is well studied due to its economic importance in the 20th century following the discovery of antibiotics. It has been well documented that the onset of secondary metabolism coincides with morphological changes in *Streptomyces* such as when substrate mycelium is dismantled and lysed, when the colony becomes vulnerable to opportunistic soil microorganisms. The production of antibiotics in particular by the substrate mycelium is thought to be a protective mechanism by inhibiting the growth of antibiotic sensitive micro-organisms (Chater 2006). The onset of morphological differentiation and secondary metabolite production can be triggered by a variety of stimuli such as environmental stresses and both are reliant on some common pathways and some specific pathways which explain their relationship.

.

1.6 Osmoadaptation

Fluctuations in the water content of soil have the potential to inflict physiological damage to bacteria. This can occur by either hypertonic conditions resulting in dehydration by water moving out of the cytoplasm or hypo-osmotic instances which have the potential to lyse the cell. Osmosis provides the bacteria the ability to regulate their cellular water content by adjusting intracellular solute concentrations (Wood, Bremer et al. 2001).

The osmoadaptation response of *Streptomyces* is characterised by the σ^B regulon (Cho, Lee et al. 2001). *sigB* is part of an operon preceded by *rsbA* and *rsbB*, which

encode homologues of the anti-sigma factor RsbW and its antagonist RsbV (Lee, Cho et al. 2004). Under osmotic stress conditions σ^B is dissociated from RsbA by the phosphorylation of RsbV, which allows σ^B to bind to core RNA polymerase (RNAP) resulting in transcription of *sigB*, *osaB* and other σ^B targeted genes (Bishop, Fielding et al. 2004; Fernandez Martinez, Bishop et al. 2009). Excess σ^B activates the kinase domain of OsaC, which phosphorylates a predicted OsaC antagonist thereby releasing OsaC which associates with free σ^B preventing further activation of the σ^B regulon (Fernandez Martinez, Bishop et al. 2009).

1.6.1 Turgor pressure

Turgor pressure is the hydrostatic pressure difference which maintains a balance between the environment and interior of the cell. Osmotic potential is the flow of water from high osmotic potential to areas of low osmotic potential until equilibrium is reached. In order for bacteria to avoid effects of dehydration, protective mechanisms are in place to generate a suitable turgor pressure to stabilise the cell. This osmoadaptation is not only important under stress, but is required for tip extension in developing hyphae, which requires sustained turgor especially to drive the growth of aerial hyphae (Chater 1998).

1.7 Oxidative stress mechanisms

Bacterial cytoplasms are maintained in a reduced state which prevents the inactivation of active site thiols and inappropriate disulfide bridge formation in proteins. (Paget, Kang et al. 1998; Arner and Holmgren 2000). In *E. coli* the major thiol-redox buffer is a cysteine containing tripeptide glutathione with other thiol disulfide

oxidioreductases such as thioredoxin (Figure 1.2) and glutaredoxins in lower concentrations. Oxidised forms of thioredoxin and glutaredoxins are reduced by thioredoxin reductase in the presences of NADPH and glutaredoxin reductase in the presence of NADPH respectively. However glutathione has not been found in *actinomycetes* and therefore alternative mechanisms are used under conditions of thiol stress.

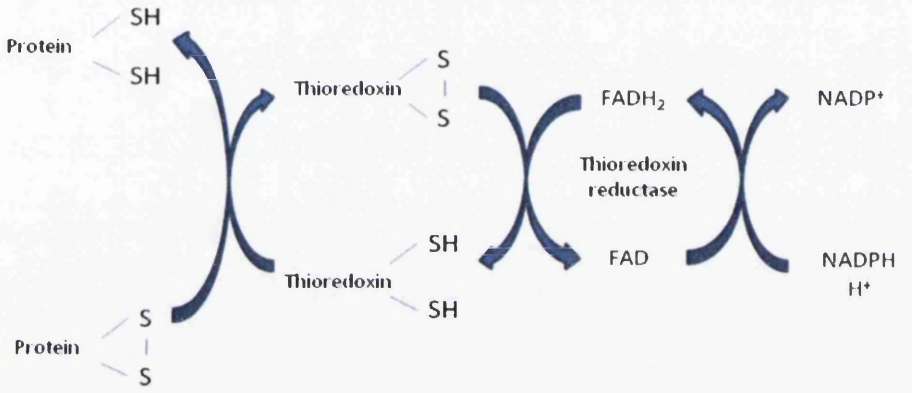

Figure 1.2: schematic overview of thiol reduction mediated by thioredoxin and thioredoxin reductase.

In *Streptomyces*, thiol oxidation is regulated by thioredoxin and σ^R/ RsrA is part of this system that senses and responds to thiol oxidation. Disulphide bond formation in the anti sigma factor RsrA causes conformational changes, releasing σ^R. This mechanism is controlled by a negative feedback loop where thioredoxin reduces RsrA allowing it to sequester σ^R (Kang, Paget et al. 1999). *sigR* mutant strains have reduced levels of disulfide reductase activity and inability to induce activity on exposure to a thiol oxidising agent (Paget, Kang et al. 1998). *trxBA* encodes thioredoxin reductase and thioredoxin and has two promoters separated by 5-6bp. *trxBp1* is transiently induced 50

fold in response to diamide treatment and *in vitro* σ^R directs transcription from this promoter. *trxBp2* is three fold induced under thiol stress and this increase in expression is absent in the *sigR* mutant along with transcription from *trxBp1* which is reduced by >95%.

sigR also has two promoters separated by 173bp. The promoter *sigRp2* is undetectable in the *sigR* mutant strain, however, under thiol stress expression from this promoter is increased 70 fold. It has also been shown *in vitro* that σ^R directs transcription from SigRp2 showing that it positively auto-regulates itself under stress (Figure 1.3).

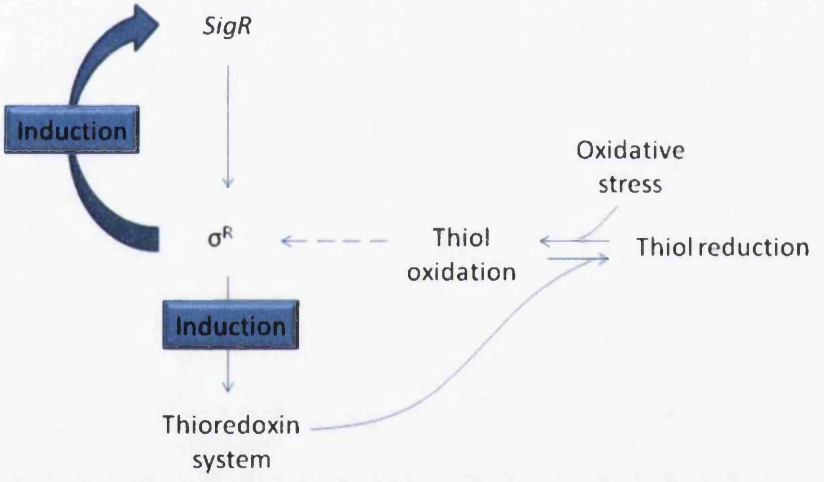

Figure 1.3: Homeostasis of the thioredoxin system of *S. coelicolor*
Exposure to oxidative stress results in thiol oxidation, inducing σ^R activity which increases expression of both thioredoxin and thioredoxin reductase. Positive auto-regulation of *sigR* occurs via *SigRp2* promoter. Figure modified from Paget, Kang et al. (1998).

Unlike *E. coli*, in which OxyR mediates responses to both disulphide and peroxide stress (Aslund, Zheng et al. 1999), *Streptomyces* has two separate response

systems (Paget, Kang et al. 1998). None of the identified targets of σ^R are associated with peroxide stress in *Streptomyces* (Paget, Molle et al. 2001). OxyR has been shown to be a H_2O_2 sensing transcription regulator in *Streptomyces* (Hahn, Oh et al. 2002). Disulfide bond formation between two conserved cysteine residues alters the conformation, allowing OxyR to activate transcription of its own gene *oxyR* and the alkyl hydroperoxide reductase genes *ahpCD,* encoding alkyl hydroperoxide reductase (ahpC), with a five-fold increase in transcription within 10 minutes of H_2O_2 shock. AhpC is maximally produced during early exponential phase and induced by exogenous H_2O_2 under the control of OxyR (Hahn, Oh et al. 2002). Catalase A (*catA)* is a monofunctional catalase which is produced maximally during late exponential phase regulated by a Fur-type repressor, CatR (Hahn, Oh et al. 2000).

1.8 *Streptomyces* Genetics

Streptomyces genetics has been a major topic of research for over half a century with focus on their ability to produce bioactive secondary metabolites and their complex life cycle. Sir David Hopwood was the pioneer in *Streptomyces* genetics starting his career studying a PhD in *Streptomyces* genetics at the University of Cambridge in 1954. During his PhD he made the first chromosome map of a streptomycete by analyzing auxotrophic and antibiotic mutants through natural gene exchange (Hopwood 1958).

The number of genes mapped gradually increased over the years with the improvement of genetic tools and the increase in the number of research groups across the globe. In 1992 a detailed genetic/ physical map was published after using pulse field gel electrophoresis (PFGE) to estimate the chromosome size as 8Mb (Kieser, Kieser et

al. 1992). Within a year, DNA sequences similar to one end of the linear plasmid SLP2 were found in *Streptomyces lividans* chromosome and it was shown by restriction mapping that they represented free ends (Lin, Kieser et al. 1993). PFGE was used to determine that the chromosome is in fact linear which was subsequently confirmed in a number of other *Streptomyces* (Lezhava, Mizukami et al. 1995). It was also shown in *S. lividans* that the chromosome can be circularized by joining the two ends by artificial targeted recombination or by spontaneous deletions spanning both telomeres and still remain viable (Lin, Kieser et al. 1993). The linear chromosome has been subsequently confirmed by genome sequencing of the *S. coelicolor* genome (Bentley, Chater et al. 2002).

The ends of the chromosome comprise of terminal inverted repeats (TIRs) that are covalently bound at the 5′ prime ends to proteins called terminal proteins. Mutations in the gene encoding one of the terminal proteins, *tpgL,* prevented propagation of a linear chromosome but not a circular one, showing that these proteins are essential in linear DNA replication (Bao and Cohen 2001). It has been hypothesised that the linear chromosomes may have been the result of a single crossover between a circular chromosome and a linear plasmid or phage during the evolutionary history of *Streptomyces* (Volff and Altenbuchner 2000; Darvasi and Pisante-Shalom 2002; Yamasaki and Kinashi 2004).

In 2001 the sequencing of *S. coelicolor* was completed at the Sanger centre. The 8,667,507 base pair linear chromosome consists of 7,825 open reading frames (compared to Gram-negative bacterium such as *E. coli* having 4,289) and contains an

unprecedented proportion of regulatory genes likely to be involved in responses to environmental conditions (Bentley, Chater et al. 2002).

Streptomyces spp. have the highest proportion GC content of Gram-positive bacteria, with *S. coelicolor* having 72.12 mole %. The linear chromosome replicates bidirectionally from the origin of replication (*oriC).* The *oriC* is rich in DnaA boxes, containing 19 in 3 clusters compared with 5 in *E. coli* and chromosome replication appears to be controlled mainly by the D78 cluster which DnaA has an eight-fold higher affinity for (Smulczyk-Krawczyszyn, Jakimowicz et al. 2006). Replication proceeds bidirectionaly towards the telomeres where the replication forks reach the ends of the chromosome which leaves a terminal single-stranded gap on the discontinuous strand after removal of the last RNA primer. An unusual process of 'endpatching' by DNA synthesis primed from the terminal protein fills the gap (Hopwood 2006).

Sigma (σ) factors are proteins that act as prokaryotic transcription initiation factors, which must bind to RNAP to direct its binding to a specific promoter region on the DNA. Different sigma factors are activated in response to varying environmental conditions. *Streptomyces* has a huge number of sigma factors, with greater than 65 sigma factors (Bentley, Chater et al. 2002) compared to *E.coli* having as few as 8 sigma factors (Roth, Aigle et al. 2004). 45 of these sigma factors are extra-cytoplasmic function sigma factors, which respond to external stimuli and subsequently activate genes involved with environmental stress, aerial mycelium formation etc (Bentley, Chater et al. 2002).

Four genes in *S. coelicolor, hrdA, hrdB, hrdC* and *hrdD* (*hrd* stands for homolog of *rpoD*) encode RNA polymerase sigma factors extremely similar to the sigma 70 polypeptide of *E. coli* (Tanaka, Shiina et al. 1988). *hrdB* was the only gene, when

disrupted, was lethal, suggesting it to be the principal and essential sigma factor in *S. coelicolor* and was isolated and characterised in 1992 (Buttner, Chater et al. 1990; Brown, Wood et al. 1992; Buttner and Lewis 1992).

1.9 Genome structure

S. coelicolor's linear chromosome has the *oriC* and *dnaA* gene off centre towards the left of the centre of the chromosome by 61kb, which like other microbial genomes has a 55.5% bias towards coding sequences on the leading strand (Bentley, Chater et al. 2002). There is a decrease in the GC bias around *oriC*, thought to be related to DNA replication. The chromosome is split into two regions, the core region extends from 1.5Mb to 6.4Mb and contains essential genes involved in DNA replication, cell division, amino-acid biosynthesis, transcription and translation. The left and right arms contain contingency loci coding for non essential functions such as biosynthesis of secondary metabolites, hydrolytic exoenzymes, conservons and gas vesicle proteins (Bentley, Chater et al. 2002).

In addition to chromosomal DNA, most *Streptomyces* species contain plasmids which are linear or circular and they can be integrative or non-integrative. Most plasmids do not contain antibiotic resistance cassettes or biosynthesis gene clusters required for antibiotic production; however there is one example, SCP1 from *S. coelicolor*, which contains resistance to and biosynthesis genes for the antibiotic methylenomycin (Kirby and Hopwood 1977). Similar to the chromosomal DNA of *Streptomyces* the linear plasmids contain TIRs covalently bond to terminal proteins at the 5' end (Yang, Huang et al. 2002).

Replication of these linear plasmids is similar to the chromosome, starting at a central location and proceeding bidirectionally towards the telomeres. Circular plasmid replication appears dependent on their size; large plasmids replicate bidirectionally via theta replication and are low copy, whereas smaller circular plasmids replicate via a rolling circle mechanism (sigma) and are high copy number, e.g. pIJ101 (Kieser 2000).

S. coelicolor A3(2) contains 3 plasmids: SCP1, SCP2 and SLP1. SCP1 is a 350 kb linear plasmid that contains the genes required for the biosynthesis of methylenomycin. SCP2 is a 30 kb circular, self replicating plasmid that is present at a low copy number. Finally SLP1 is a 17 kb integrative plasmid containing phage like genes *int* (integrase) and *xis* (excisase) required for site-specific integration into the chromosome and was discovered after the genes for pock formation were transferred from *S. coelicolor* to *S. lividans* (Omer and Cohen 1984).

1.10 Nucleoid structuring in *E. coli*

In prokaryotes, DNA is condensed by supercoiling, where half of the supercoils are free while the other half are constrained by nucleoid associated proteins (Bliska and Cozzarelli 1987). The unconstrained DNA is negatively supercoiled and plectonemic in structure as a result of type II topoisomerases such as DNA gyrase. As a result of this conformation, DNA is under constant strain where a nick or double-strand break will release this tension resulting in relaxation. This is a potentially deadly problem for bacteria, in which free negative supercoiling is necessary for viability where hyper negative supercoiling can also inhibit growth (Gellert, O'Dea et al. 1976; Baaklini, Usongo et al. 2008).

The genomic DNA of bacteria is divided in domains which are topologically independent from one another to prevent local changes in topology altering global superhelicity (Worcel and Burgi 1972). At the boundaries of these domains are domain barriers which prevent diffusion of supercoils from one domain to another (Figure 1.4A). Domain barriers must bind to two sites either chromosomally or by an immobilised cellular component. Absence of these domain barriers would result in a single nick or break of the DNA completely unwinding and relaxing the chromosome due to no boundary preventing the spread of relaxation from one domain to another (Hardy and Cozzarelli 2005). Figure 1.4B shows a schematic representation of the chromosome of a domain barrier mutant, where there is a significant reduction in compaction of the chromosome.

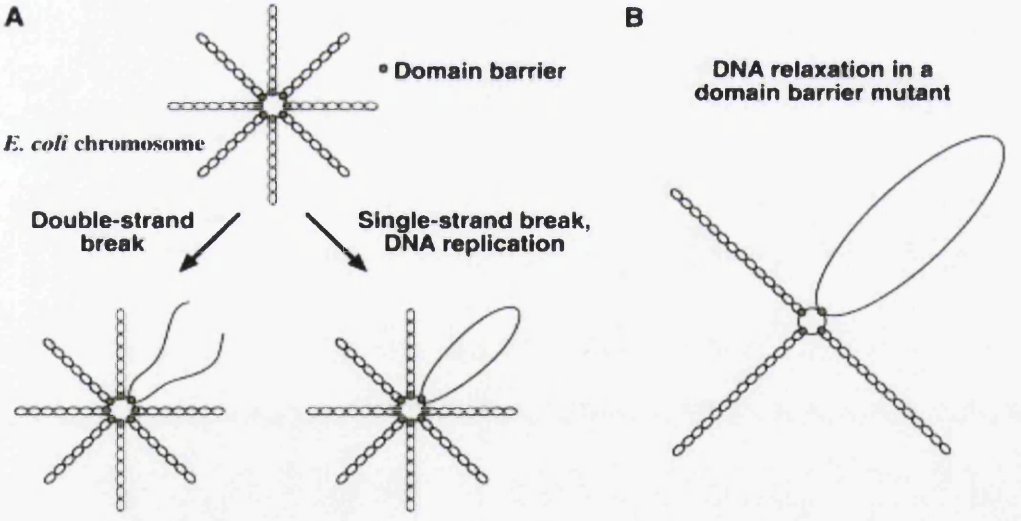

Figure 1.4: *E. coli* topological domains.
(A)The *E. coli* chromosome is divided into topological domains. Supercoiled chromosome represented by black lines indicating double helices of DNA. Only 8 domains are shown for simplicity. Domain barriers are indicated by green circles binding the base of the plectonemic structures. When the DNA is damaged, only the domain containing the damage becomes relaxed allowing the rest of the chromosome to maintain negative supercoiling. (B) A chromosome from a domain barrier mutant containing half as many domains as wild type is depicted. The relaxed domain is thus twice as large as in the wild-type cell shown in A. (Hardy and Cozzarelli 2005).

Global transcription within the genome is influenced by topoisomerases altering the superhelicity of the DNA and the action of nucleoid associated proteins. Bacteria possess proteins similar to eukaryotic histone proteins (Grove 2011). This similarity is based on their size, electrostatic charge and their ability to bind DNA rather than homology at the amino acid sequence level. Consequently they have been termed histone-like proteins. In bacteria, alterations in the superhelicity of DNA and associated chromatin proteins have been shown during the life cycle and in response to environmental stresses (Ali Azam, Iwata et al. 1999; Travers and Muskhelishvili 2005). The stiffness of DNA limits its ability to be bent and twisted over short lengths although such conformational changes are required for the regulation of genes (Becker, Kahn et al. 2007). In the *E. coli* nucleoid there are five highly abundant nucleoid associated proteins involved in overall chromatin structure. Three of these proteins; HU, H-NS and Fis are predominantly associated with growth phase and IHF and Dps with stationary phase cells (Ali Azam, Iwata et al. 1999). HU and IHF have amino acid similarities; however FIS, H-NS and Dps are structurally distinct (Ali Azam, Iwata et al. 1999). These proteins also play a role in regulating gene expression by bending the DNA at certain angles (Dillon and Dorman 2010).

1.11 Nucleoid associated proteins in *E. coli*

1.11.1 Heat unstable nucleoid protein (HU)

HU is a highly abundant DNA architectural protein that is involved in nucleoid compaction and gene transcription (Aki and Adhya 1997; Travers and Muskhelishvili

2005). HU can be either a homodimer or heterodimer of the homologous subunits α and β in *E. coli* (Guo and Adhya 2007). These subunits form long flexible arms that wrap around the DNA forcing a U turn in the DNA without making specific contact with other proteins. There is no specific recognition sequence but HU has been reported to bind more avidly to structural aberrations such as four-way junctions or single stranded regions. HU provides the bending needed to bring distant regions of DNA together in loops to act as a repressor of transcription (Lewis, Geanacopoulos et al. 1999) and can contribute to nucleoid compaction by bending or wrapping DNA (Salerno, Larsson et al. 2009). HU has also been implicated in coordinating the global genomic structure and function by regulating the spatial distribution of RNAP in the nucleoid (Berger, Farcas et al. 2010).

1.11.2 Integration host factor (IHF)

IHF was first discovered as a host factor for bacteriophage λ integration and hence the origin of its name (Kikuchi and Nash 1978). It is a small heterodimeric protein that is related to HU proteins however unlike HU it has specific asymmetric DNA binding sites and bends DNA by 160 degrees and is a member of minor groove-intercalating DNA-bending proteins (Rice, Yang et al. 1996). IHF and HU share a 30% sequence identity with a functional and structural similarity. IHF helps form DNA loops between promoters and distant transcription activators, allowing initiation of transcription (Giladi, Koby et al. 1998). It is also involved in formation of DNA-protein complexes (Segall, Goodman et al. 1994).

1.11.3 Factor for inversion stimulation (FIS)

Fis is the most abundant nucleoid-associated protein during logarithmic growth phase in *E. coli* growing in rich medium (Mallik, Paul et al. 2006) and regulates gene expression as a homodimer (Kostrewa, Granzin et al. 1992) by bending DNA within gene promoter sequences (Yuan, Finkel et al. 1991; Verbeek, Nilsson et al. 1992). Fis forms a concentration gradient between phases of growth, where the concentration of Fis decreases by two orders of magnitude on transition from the exponential phase to the stationary phase (Glazebrook, Doull et al. 1990; Blot, Mavathur et al. 2006). Importantly it plays a role in supercoiling in bacteria, by activating expression of topoisomerase I and down regulating the two genes, *gyrA* and *gyrB,* required for topoisomerase II and gyrase in *E.coli*. Blot, Mavathur et al. (2006) suggested that the *de novo* pathway of nucleotide biosynthesis explicitly involved genes transcribed under high levels of negative supercoiling with most of these having a GC-rich 'discriminator' sequence within the promoter, which confers sensitivity to high negative supercoiling and ppGpp. In a *fis* mutant the concentration of the alarmone ppGpp is increased as well as superhelicity, indicating a homeostatic regulation mechanism (Blot, Mavathur et al. 2006).

1.11.4 Histone-like nucleoid structuring protein (H-NS)

H-NS is predominantly in the form of a homodimer, however, it can form higher oligomeric states with around 10-20,000 molecules per cell in log phase (Ali Azam, Iwata et al. 1999). Unlike the previous histone-like proteins, H-NS does not actively bend DNA; instead it binds preferentially to intrinsically curved DNA (Atlung and

Ingmer 1997). If one of these pre-bent sections of DNA is in close proximity to a promoter region then H-NS acts as a mild repressor to expression by restricting access of RNAP to the DNA. Because of this, H-NS is generally considered a global repressor, keeping gene products down-regulated until required. In *E. coli* it has been shown that H-NS regulated genes are involved in bacterial responses to multiple environmental conditions and/or in cell envelope composition (Hommais, Krin et al. 2001).

1.11.5 Dps (DNA-binding proteins from starved cells)

Dps is predominantly in the form of a dodecamer and binds DNA via positively charged amino acids in the N-terminus that protrude away from the four-helix bundle in the monomer (Ceci, Cellai et al. 2004). Ali Azam, Iwata et al. (1999) determined the relative abundance of twelve nucleoid associated proteins during log growth and stationary phase in *E. coli*. This study showed relatively high abundance of the Dps protein in early and late stationary phases. Unlike the other nucleoid proteins described, Dps can protect DNA via two distinctive alternate mechanisms. Hyper-condensation of DNA by non-specific DNA binding during the stationary phase results in the formation of a crystalline structure, thereby physically protecting the nucleoid (Almiron, Link et al. 1992; Frenkiel-Krispin, Levin-Zaidman et al. 2001; Nair and Finkel 2004). Secondly, under stress conditions the abundance of Dps increases and the Fe(II) chelating activity provided by the ferroxidase centre of the Dps protein protects the DNA from the damage caused by the formation of free radicals formed by Fenton reactions (Facey, Hitchings et al. 2009).

1.11.6 Mutations in nucleoid-associated proteins

Mutations in nucleoid-associated proteins have been shown to alter the topological state of reporter plasmids in a number of species. In *E. coli,* mutations in either *hupA* or *hupB* result in a decrease in negative supercoiling compared to wild type as demonstrated by chloroquine gel electrophoresis (Hsieh, Rouviere-Yaniv et al. 1991; Berger, Farcas et al. 2010). A *hupAB* double mutant strain shows the largest shift in topology compared to wild type. Under osmotic stress the *hupAB* mutant strain was comparable to wild type with the reporter plasmid showing an increase in negative supercoiling in both mutant and parental strain as a result of the osmolyte (Hsieh, Rouviere-Yaniv et al. 1991). Mutations in the HU protein in *Salmonella typhimurium* have also been reported to result in decreased negative supercoiling compared to the parental strain (Hillyard, Edlund et al. 1990). Another nucleoid associated protein, H-NS has also been shown to be involved in modulating the superhelicity of DNA. Mutant strain in the *E. coli* H-NS exhibit the opposite to HU mutant strains and have an increased negative supercoiling profile compared to wild type (Mojica and Higgins 1997). However, this increase is not to the same extent as in a *topA* mutant strain which shows hyper-negative supercoiling (Mojica and Higgins 1997). *topA* encodes topoisomerase I, which is required for relaxation of supercoiled DNA (Tse-Dinh and Wang 1986).

1.12 Nucleoid-associated proteins in *Streptomyces*

In *S. coelicolor* there are currently only three families of nucleoid associated proteins described that are involved in chromatin condensation: HU, SMC (*s*tructural

*m*aintenance of *c*hromosomes that has a functional homologue, MukB in *E. coli*) and Dps (Dedrick, Wildschutte et al. 2009; Facey, Hitchings et al. 2009; Salerno, Larsson et al. 2009).

S. coelicolor encodes two homologs of the nucleoid associated protein HU. A homolog is a gene related to a second gene by descent from a common ancestral DNA sequence. The first of these is HupA, which is a conventional HU protein similar to the alpha and beta HUs of *E.* coli (Yokoyama, Doi et al. 1997; Salerno, Larsson et al. 2009). The second is designated HupS, which has two domains: a typical HU protein N-terminal domain and a highly positively charged C-terminal containing alanines and lysines similar to eukaryotic linker histones (Salerno, Larsson et al. 2009). HupS-like proteins are only found in actinobacteria: some organisms contain HupS alone (Kumar, Sardesai et al. 2010), while others only contain the conventional HU (Salerno, Larsson et al. 2009) and others, including *Streptomyces*, contain both types of HU protein. In *S. coelicolor* the two HU proteins are differentially regulated with HupA expressed during vegetative growth and HupS expressed exclusively during sporulation (Salerno, Larsson et al. 2009). The *hupS* mutant has enlarged nucleoids in spores compared to the parental strain M145 and is defective in heat resistance and spore pigmentation (Salerno, Larsson et al. 2009).

Facey *et al.* (2009) described three Dps proteins in *S. coelicolor*: DpsA, DpsB and DpsC. Unlike other bacteria the Dps proteins in *S. coelicolor* were shown to be involved in nucleoid condensation to permit efficient segregation during sporulation. A *dpsA* mutant strain (*dpsA*$^-$) exhibits a high frequency of pre-spore compartments containing more than one nucleoid with adjacent compartments with reduced DNA

content, suggesting the presence of an incomplete genome (Facey, Hitchings et al. 2009). *dpsB*⁻ or *dpsC*⁻ mutants have smaller nucleoids in prespores and it was proposed that DpsB or DpsC separately, or as a putative DpsBC complex, modulate nucleoid condensation function (Facey, Hitchings et al. 2009).

SMC is highly conserved throughout prokaryotes and is involved in chromosome maintenance and structure (Hirano 1999). It is a 1,186 amino acid protein comprising of two DNA binding domains, one at each N- and C- terminus connected by two coiled-coil regions joined by a hinge (Dedrick, Wildschutte et al. 2009). A Δ*smc* mutant strain of *S. coelicolor* exhibits an increase in anucleate spores (7% compared to wild type 0.8%) (Dedrick, Wildschutte et al. 2009), with defects in DNA partitioning and reduced chromosomal condensation in prespores (no difference in mature spores) (Kois, Swiatek et al. 2009). This was investigated with an SMC-eGFP fusion where SMC foci overlapped uncondensed nucleoids during early sporulation and disappeared when DNA condensed in prespore compartments (Dedrick, Wildschutte et al. 2009). However, it was also shown that DNA was not trapped inside the septa as was observed for the *mukB* mutant in *E. coli* (Niki, Jaffe et al. 1991; Dedrick, Wildschutte et al. 2009).

Understanding nucleoid regulation within actinobacteria is ever expanding with the addition of newly characterised DNA binding proteins. For example, *lsr2* is a small basic protein about ~12KDa in size found in *Mycobacterium* and other actinomycetes such as *Streptomyces*, *Nocardia* and *Rhodococcus* (Chen, Ren et al. 2008), which binds DNA non-specifically; functionally *lsr2* is equivalent to H-NS from gram negative bacteria and has been shown to complement several phenotypes of a H-NS mutant in *E. coli* (Gordon, Imperial et al. 2008; Colangeli, Haq et al. 2009; Werlang, Schneider et al.

2009). Another protein, *Rv3852* from *M. tuberculosis* is another small basic protein ~14KDa which has also been shown to bind non-specifically to DNA, with a slight preference to curved DNA (Werlang, Schneider et al. 2009).

1.13 Supercoiling

DNA exists in a huge variety of different forms (Ghosh and Bansal 2003), however, B-form (right-handed) and Z-form (left-handed) are the predominant forms found in nature (Ghosh and Bansal 2003), B-form DNA, the right-handed double helical structure of DNA (Watson and Crick 1953), is the conformation most commonly found in physiological conditions (Leslie, Arnott et al. 1980; Dickerson, Drew et al. 1982). The Figure 1.5A shows a simplified model of B-form DNA, with a clockwise rotation around the helical axis.

DNA in bacterial cells is always maintained in a negative supercoiled state (Witz and Stasiak 2010). Negative supercoiling is when the DNA molecule is twisted in the opposite direction to the DNA helix (left-handed direction), there-by under-winding the molecule. Positive supercoiling is where the DNA is twisted in the same direction (right-handed direction) which tightens the helix (Bates 1993). It is this superhelicity that contributes to the compaction of the nucleoid and influences global gene expression by altering transcription (Cheung, Badarinarayana et al. 2003). Supercoiling is an abstract mathematical property, and represents the sum of twist and writhe. Twist describes how individual strands of DNA coil around the axis of the DNA helix (i.e. around one another), whereas writhe describes how the helix axis coils in space (Figure 1.5B). Two common conformations that DNA can take are plectonemic and toroidal. Plectonemic is

the conformation of DNA, where the DNA helix is wound around another part of the same molecule in a higher order helix (Figure 1.5B). Toroidal DNA or toroidal winding (Figure 1.5B) is so called because the axis of the DNA helix lies on the surface of an imaginary torus (Bates 1993). A simple example of toroidal winding is a telephone wire, where the coiled wire has substantial writhe but little twist, however if the coil is stretched, the writhe is inter-converted to twist.

DNA supercoiling is an important mechanism used by cells to compact the huge lengths of chromosomal DNA (Stuger, Woldringh et al. 2002). This packaging is aided by histone-like proteins (McGhee and Felsenfeld 1980; Drlica and Rouviere-Yaniv 1987). As chromosomes extend for millions of base pairs, the ends act as if they are anchored allowing localised supercoiling to occur. Negative supercoiling makes DNA more flexible facilitating loop formation, wrapping of DNA around proteins and the formation of left-handed Z-DNA (Drlica 1992).

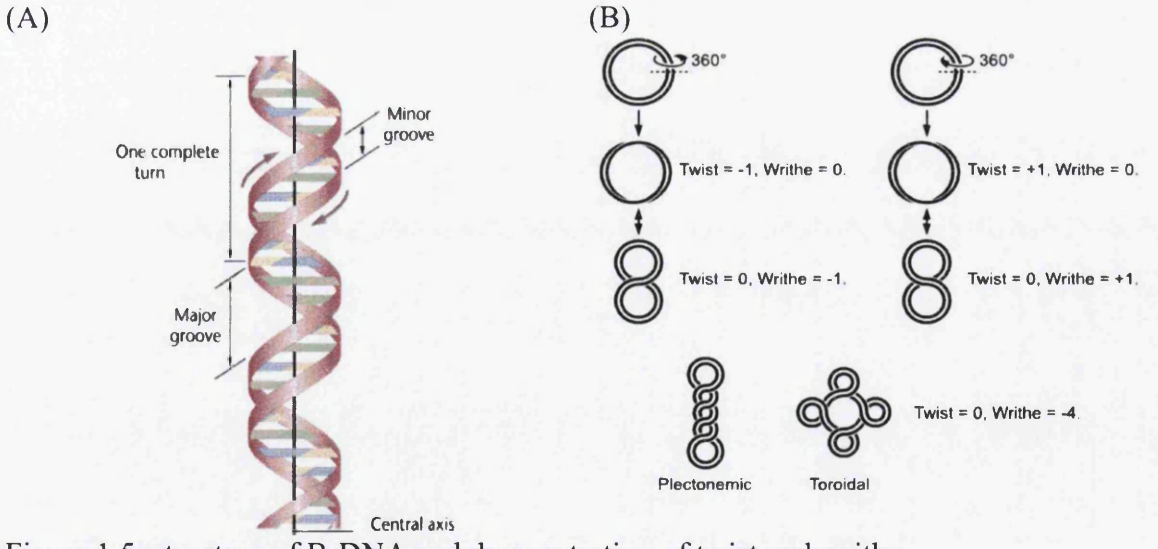

Figure 1.5: structure of B-DNA and demonstration of twist and writhe.
(A) Structure of B-DNA modified from Klug, Cummings et al. (1997). (B) Simplified schematic showing the difference between twist and writhe, and structural conformations which DNA can from.

Supercoiling is the result of changes in linking number of a relaxed DNA molecule. Linking number (*Lk*) is the number of crosses a single strand makes across another strand in a planar projection which must equal the twist (*Tw*) and writhe (*Wr*) of a given molecule of DNA (Figure 1.6A) (Bates 1993). The change in linking number (ΔLk) is the difference between the number of turns (*Lk*) of the plasmid minus the number of turns in the relaxed plasmid Lk^o (Figure 1.6B).

A) $Lk = Tw + Wr$

B) $\Delta Lk = Lk - Lk^o$

Figure 1.6: Equations to calculate linking number *Lk* (A) or change in linking number, ΔLk (B) (Fuller 1971)

1.13.1 DNA topoisomerases

DNA topoisomerases maintain the optimum topological state of DNA in bacteria which is predominantly negatively supercoiled (Lilley 1986). Topoisomerases are not only involved in the compaction of the chromosome but play a key role in the separation of the strands either temporarily for transcription or permanently in the case for replication (Wang 1996). During transcription, DNA preceding the translocating RNAP forms positive supercoiling whilst negative supercoiling is generated behind; these differences in supercoiling are rapidly resolved by DNA gyrase and DNA topoisomerase I (Wu, Shyy et al. 1988; Wang 1998).

DNA gyrase and topoisomerase I were both discovered in *E. coli* (Wang 1971; Yang and Ishiguro 2001). The genes *gyrA* and *gyrB* encode the two subunits of DNA

gyrase and are transcriptionally up-regulated when DNA is relaxed (Menzel and Gellert 1987). In contrast however, *topA,* which encodes topoisomerase I is activated when DNA becomes increasingly negatively supercoiled. (Blot, Mavathur et al. 2006; Dorman 2006). Therefore homeostatic control of negative supercoiling is the result of the combined efforts of gyrase and topoisomerase I in response to relaxed or highly negatively supercoiled DNA, respectively, setting and resetting the linking number, maintaining a balance in keeping with the physiological requirements of the cell (Menzel and Gellert 1983; Pruss, Franco et al. 1986; Dorman and Corcoran 2009).

1.13.2 Classification

DNA cleavage by all topoisomerases is accompanied by the formation of a transient phosphodiester bond between a tyrosine residue in the protein and one of the ends of the broken strand (Roca 1995). DNA topology can be modified during the lifetime of the covalent intermediate, and the enzyme is released as the DNA is re-ligated (Champoux 2001). Those enzymes that cleave only one strand of the DNA are defined as type I and are further classified as either type IA subfamily members if the protein link is to a 5′ phosphate (formerly called type I-5′) or type IB subfamily members if the protein is attached to a 3′ phosphate (formerly called type I-3′) (Wang 1996; Champoux 2001). Topoisomerases that cleave both strands to generate a staggered double-strand break are grouped together in the type II subfamily of topoisomerases (Champoux 2001).

1.13.3 Role of supercoiling in gene regulation and expression

Supercoiling plays a major role not only in DNA replication, but also in response to stress stimuli by activating promoters sensitive to the superhelical state of the genomic DNA (Cheung, Badarinarayana et al. 2003). Microarray analysis of gene expression in *E. coli* demonstrated that expression of 7% of genes is rapidly affected by the loss of chromosomal supercoiling, with 106 genes having increased and 200 decreased expression (Peter, Arsuaga et al. 2004). Consequently, it was proposed that supercoiling acts as a secondary messenger, that rapidly translates environmental changes to the transcriptional machinery to repress or induce genes specifically and independently (Drolet 2006).

Changes in medium osmolarity are known to modify the topological conformation of DNA and thereby modulate the expression of genes in *S. lividans* (Ali, Herron et al. 2002). For example, the promoter *ptipA* in *S. lividans* has an elongated 19bp spacer between the -10 and -35 motifs and in this configuration under normal physiological conditions the -10 and -35 sequences remain out of phase, thereby preventing transcription (Ali, Herron et al. 2002). When a stress such as osmotic shock, which induces negative supercoiling, is applied, the increased negative supercoiling brings the -10 and -35 into phase allowing RNA polymerase recognition and resulting in transcription and translation of the gene (Ali, Herron et al. 2002).

1.14 ppGpp/ DksA

Amino acid starvation in *E. coli* results in global changes in gene expression called the "stringent response" (Haseltine and Block 1973). Under amino acid starvation,

a small highly phosphorylated guanine nucleotide (also known as stringent factor) ppGpp (guanosine 3′–diphosphate 5′–diphosphate) and its precursor (p)ppGpp (guanosine 3′–diphosphate 5′–triphosphate), act as global regulators of gene expression in *E. coli* and *Streptomyces* (Hesketh, Sun et al. 2001; Magnusson, Farewell et al. 2005; Hesketh, Chen et al. 2007). It has been shown that ppGpp causes changes in transcription to genes important for starvation survival and virulence (Pizarro-Cerda and Tedin 2004).

The RelA protein is part of a mechanism involved in the 'stringent response' responsible for the reorganisation of gene transcription under amino acid starvation. (p)ppGpp production in *E. coli* is dependent on two coordinated pathways catalysed by the gene products of *relA* and *spoT*. RelA (GTP pyrophosphokinase), is a (p)ppGpp synthetase via pyrophosphoryl transfer from ATP to GTP (or GDP) and SpoT a ppGpp 3′ pyrophosphohydrolase

The mechanism by which RelA interacts with the ribosome remains to be fully elucidated with a number of mechanisms proposed such as; a 3' extension of mRNA protruding from the ribosome being required for RelA binding, resulting in synthesis of ppGpp, which reduces the affinity of RelA to the ribosome allowing RelA to hop between blocked ribosomal complexes and releasing the uncharged tRNA, which also allows the cell to test the nutritional status (Wendrich, Blaha et al. 2002). The implication of the protein L11 (gene product of *relC*) in the regulation of RelA (Yang and Ishiguro 2001) and the suggestion of RelA forming a higher oligomeric state via its C- terminal domain which is functionally inactive, may be involved in the regulation of ppGpp whereby the oligomeric RelA is functionally activated by reduction of its

oligomeric state to monomers in the stringent response (Gropp, Strausz et al. 2001; Yang and Ishiguro 2001). Nevertheless all mechanisms require the binding of an uncharged tRNA to its cognate codon in the acceptor site of the ribosome.

PpGpp is the sensory mechanism of amino acid starvation or carbon source limitations and causes the down-regulation of expression of stable RNA (rRNA and tRNA), ribosome production and induces expression of enzymes involved in amino acid biosynthesis and transporters (Stephens, Artz et al. 1975; Gallant 1979; Paul, Berkmen et al. 2005). Inhibition of rRNA transcription allows ppGpp indirectly to activate promoters and stimulate expression of proteins involved with amino acid biosynthesis and transport by increasing the number of free RNAP molecules available (Potrykus and Cashel 2008).

The primary source of ppGpp is from the ribosomally associated protein RelA in response to uncharged tRNA occupying the ribosome's acceptor site (A site) (Hogg, Mechold et al. 2004). PpGpp binds to a site adjacent to but not overlapping the active site of RNAP and, although the mechanism of inhibition of transcription initiation is not completely understood, ppGpp decreases the life times of open complexes between RNAP and rRNA promoters liberating enough RNAP to stimulate transcription from amino acid promoters (Barker, Gaal et al. 2001). As the complex formed by RNAP and rRNA promoters is already intrinsically short lived, ppGpp potentiates the effect and prevents transcription from the promoters (Paul, Barker et al. 2004). Although ppGpp's ability to selectively regulate a large number of genes is not fully understood, it has been suggested that base pairing between ppGpp and cytosines in the non-template DNA strand might be an essential component of its transcription control (Artsimovitch, Patlan

et al. 2004). The *dksA* gene was first identified as a high-copy suppressor of *dnaK* mutants (Kang and Craig 1990).

DnaK, originally identified for its DNA replication by bacteriophage l in *E. coli*, is the bacterial HSP70 chaperone (Georgopoulos 1977). DnaK plays an essential role in the initiation of phage lambda DNA replication, where it acts in an ATP-dependent fashion with the DnaJ protein to release lambda O and P proteins from the preprimosomal complex (Hoffmann, Lyman et al. 1992). DnaK is also involved in chromosomal DNA replication, possibly through an analogous interaction with the DnaA protein (Hwang and Kaguni 1991). DnaK also participates actively in the response to hyperosmotic shock (Meury and Kohiyama 1991).

DksA is an RNA polymerase (RNAP) binding protein required for the regulation of a number of promoters, such as controlling expression of the gene *fis* which encodes the nucleoid associated protein Fis. Fis expression extends well into the late logarithmic and stationary growth phases in a *dksA E. coli* mutant (Mallik, Paul et al. 2006). DksA potentiates control of amino acid biosynthesis and rRNA promoters (Paul, Berkmen et al. 2005; Kolmsee, Delic et al. 2011). Cellular levels of DksA in *E. coli* are kept constant at relatively low levels throughout the life cycle and recently Chandrangsu et al. (2011) showed that DksA expression was kept constant by a negative feedback loop in which transcription of the *dksA* promoter is inhibited by DksA in conjunction with its cofactor ppGpp. The transcription factor is crucial for modulating ppGpp's negative control (*in vivo*) on rRNA transcription and directly activates other promoters (Paul, Berkmen et al. 2005). When the 2.0 Å resolution crystalline structure of DksA was resolved by Perederina et al. in 2004 it became immediately evident that the structure resembled

very closely the transcription cleavage factor GreA. With such similarity it was proposed that the coiled coil-domain of the DksA protein protruded into the secondary nucleotide triphosphate (NTP) channel of RNAP rather than directly to the DNA and with two conserved aspartic acid residues ASP71 and ASP74 stabilising the ppGpp-RNAP complex via a Mg^{2+} ion. The stabilisation of ppGpp with DksA reduces the life time of competitor-resistant complexes and thereby decreases the concentration of ppGpp required for inhibition of rRNA expression (Barker, Gaal et al. 2001; Paul, Barker et al. 2004).

Three mechanisms have been proposed for the control of gene transcription by ppGpp and DksA: direct inhibition (Barker, Gaal et al. 2001; Paul, Barker et al. 2004; Paul, Berkmen et al. 2005) , direct activation (Krasny and Gourse 2004; Paul, Berkmen et al. 2005) and indirect activation (Jishage, Kvint et al. 2002; Magnusson, Farewell et al. 2005; Szalewska-Palasz, Wegrzyn et al. 2007). Direct inhibition occurs by interacting directly with the RNAP either by trapping RNAP at the promoter site or by destabilising the complex formed by the RNAP and DNA (magic). Direct activation of genes involves ppGpp and DksA directing the RNAP to promoters (Choy 2000; Potrykus, Wegrzyn et al. 2004) and finally indirect activation of transcription whereby core RNAP is liberated by altering the affinity of σ^{70} to RNAP allowing competition of alternative sigma factors (Jishage, Kvint et al. 2002; Magnusson, Farewell et al. 2005). In the case of σ^{H} and σ^{S} it is proposed that ppGpp and DksA, aid these factors in competing for core RNAP (Jishage, Kvint et al. 2002).

In *S. coelicolor* A3(2), RelA appears to be the only source of ppGpp synthesis (Chakraburtty and Bibb 1997). Under such conditions, RelA protein binds to a ribosome

while an mRNA is bound to the same ribosome and codon specified but uncharged tRNA is bound to the A site (Brun and Shimkets 2000). ppGpp is synthesised in response to occupancy of the ribosomal A-site by the uncharged tRNA (Brun and Shimkets 2000). RelA catalyses the phosphorylation of GTP using ATP hydrolysis. Each round of (p)ppGpp synthesis releases the uncharged tRNA to assess the state of starvation (Potrykus and Cashel 2008). As in *E. coli*, after nutritional down-shift in *S. coelicolor,* there is a decrease in transcription of the *rrnD* gene set, genes encoding ribosomal proteins, genes associated with ribosomal biogenesis/ function and a further 51 genes involved in active growth (Strauch, Takano et al. 1991; Hesketh, Chen et al. 2007).

The *relA* disruption mutant of *S. coelicolor* exhibits continued RNA synthesis upon amino acid depletion (relaxed phenotype) and a loss of actinorhodin and undecylprodigiosin production under nitrogen limitation (Chakraburtty and Bibb 1997). Morphologically, the mutant also has a delay in the onset of aerial hyphal development and sporulation, particularly on the rich medium MYMTE where erection of aerial hyphae is sparse and pigmented antibiotic production is absent (Sun, Hesketh et al. 2001).

Unlike other transcriptional regulators which bind to DNA in or near promoter regions, DksA interacts with rpoC, while ppGpp directly contacts rpoB and rpoC subunits of RNAP (Potrykus and Cashel 2008). This reduces the synthesis of rRNA, tRNA, DNA and protein synthesis (Paul, Berkmen et al. 2005). Specific sequences in the promoters determine which promoters are repressed or induced by ppGpp (Travers 1980). GC-rich discriminator regions between -10 and +1 (start site) result in inhibition

by ppGpp (Travers 1980). Although ppGpp inhibition is not only down to the discriminator sequence but also the length of the linker between -35 and -10, where a slightly shorter 16bp linker also results in inhibition (contrasted to 17bp consensus) (Artsimovitch, Patlan et al. 2004). This is the opposite, however, for ppGpp induced genes, where the discriminator region is AT rich and the linker sequence is longer for example, the *his* promoter is 18bp (Park, Jung et al. 2002; Potrykus and Cashel 2008). There is also evidence that supercoiling influences ppGpp inhibited promoters showing a mechanism of ppGpp hampering the ability of RNAP to melt DNA (Figueroa-Bossi, Guerin et al. 1998).

DksA has also been shown to be involved in maintaining chromosome structure *in vivo* (Hardy and Cozzarelli 2005). *E. coli* DksA was originally isolated as a multicopy suppressor of the temperature-sensitive growth and filamentation of a *dnaK* mutant strain (Kang and Craig 1990) and has been shown to recover the temperature sensitivity of a Δ*mukB* mutant strain (Yamanaka, Mitani et al. 1994). MukB is a functional homologue to *S. coelicolor* SMC, and plays a central role in chromosome condensation and segregation (Petrushenko, Lai et al. 2006). As is the case for bacterial SMC proteins, two non-SMC accessory proteins, MukE and MukF, are required for the full functionality of MukB (Yamazoe, Onogi et al. 1999; Fennell-Fezzie, Gradia et al. 2005). Null mutations in the *mukE* or *mukF* genes, which are encoded within the same operon as MukB, result in a phenotype indistinguishable from that of a *mukB*$^{-}$ mutation (Yamanaka, Ogura et al. 1996). MukB functions as a homodimer, which is essential for chromosome partitioning (Niki, Jaffe et al. 1991; Niki, Imamura et al. 1992). MukB is also involved in negative DNA supercoiling in vivo and compacts chromosomal DNA

(Petrushenko, Lai et al. 2006; Chen, Zinchenko et al. 2008; Cui, Petrushenko et al. 2008).

Genome searches have revealed the presence of three paralogs of DksA in *S. coelicolor*: SCO2075, SCO6164 and SCO6165 with e-values of $8x10^{-11}$, $2x10^{-08}$ and $1x10^{-06}$ respectively (e-value is the expectation value which is the probability of the alignment happening by chance in a database. For example an e-value of $1x10^{-03}$ indicates a 0.001 chance of the alignment existing in the database by chance). SCO2075 also has a weak sequence similarity to the nucleoid associated protein HupS having a 51.4% identity over a 72 amino acid overlap.

1.15 Aims and objectives

The aim of this investigation is to characterise the *dksA* paralog, *sco2075*. In this study *S. coelicolor* M145, a prototrophic derivative of *S. coelicolor* A3(2) strain lacking its two plasmids SCP1 and SCP2, is used as a model organism. *S. coelicolor* is an interesting organism to investigate the role of DksA with the varied environmental conditions with which it has to cope, and with a huge difference in sigma factors involved in this regulation as discussed above as compared to *E. coli*.

The availability of the complete genome sequence of *S. coelicolor* has facilitated the identification of genes encoding paralogs of DksA in this organism. Computational analysis of these proteins will provide insight into their similarity to conventional DksA, characterise the histone-like N-terminal domain and possibly provide a function and phylogenetic relationship with other proteins in bacteria. Mutational analysis and molecular characterisation will shed light on the function and expression of SCO2075

during the complex life cycle of *S. coelicolor*. From the experimental evidence of this study, we hope to get a general understanding of the function of this unique dual domain protein in *S. coelicolor.*

Chapter - 2

Material and Methods

2.1 Bacterial strains

Bacterial strains used during this study are listed in Table 2.1 below.

Table 2.1: Bacterial strains

Bacterial Strain	Genotype	Source
dpsA⁻/ sco2075⁻	M145 *sco2075*::Tn*loxp53* *sco0596*::Tn*5062*	Del Sol R., personal communication
DSC0596, *dpsA⁻*	M145 *dpsA*::Tn*5062*	(Facey, Hitchings et al. 2009)
DSCO1513, *relA⁻*	M145 *relA*::Tn*5062*	This study
DSCO2075, *sco2075⁻*	M145 *sco2075*::Tn*5062*	Del Sol R., personal communication
DSCO5747-1, *osaC⁻*	M145 osaC::Tn*5062*	(Fernandez Martinez, Bishop et al. 2009)
DSCO6164, *sco6164⁻*	M145 *sco6164*::Tn*5062*	Del Sol R., personal communication
DSCO6165, *sco6165⁻*	M145 *sco6165*::Tn*5062*	Del Sol R., personal communication
E. coli BW25113 (pIJ790)	K12 derivative: Δ*araBAD*, Δ*rhaBAD* containing λRED recombination plasmid pIJ790	(Datsenko and Wanner 2000; Gust, Challis et al. 2003)
E. coli BL21(DE3)	: F⁻ *lon⁻ ompT⁻ hsdS*$_B$ (r_B^- m_B^-) *gal dcm met*	Novagen
E. coli ET12567 (pUZ8002)	*dam13*::Tn*9 dcm6 hsdM* *hsdR recF143* 16 *zjj201* ::Tn*10 galK2 galT22* *ara14 lacY1* *xyl5 leuB6 thi1 tonA31* *rpsL136 hisG4*	(Flett, Mersinias et al. 1997)

	tsx78 mtli glnV44, containing the non-transmissible *oriT* mobilizing plasmid, pUZ8002	
Escherichia coli JM109	F' *traD36 proA+B+ lacIq Δ(lacZ)M15/ Δ(lac-proAB) glnV44 e14- gyrA96 recA1 relA1endA1 thi hsdR17*	Promega Corp. (Yanisch-Perron, Vieira et al. 1985)
J2400, Δ*whiG*	M145 *whiG*::*hyg*	(Flardh, Findlay et al. 1999)
M570, *relA*⁻	M600 *relA*⁻::*Hyg*	(Chakraburtty and Bibb 1997)
M600	Prototrophic SCP1⁻ SCP2⁻	(Chakraburtty and Bibb 1997)
S. coelicolor A3(2) M145	Prototrophic SCP1⁻ SCP2⁻ Pgl^+	(Kieser 2000)
sco2075⁻/ *sco6164*⁻	M145 *sco6164*::Tn*5062* *Sco2075*::Tn*loxp53*	This study
Δ*sigH*	M145 *sigH*⁻::*thio*	(Sevcikova, Benada et al. 2001)
Δ*smc*	M145 *smc*⁻::*hyg*	(Dedrick, Wildschutte et al. 2009)
Δ*whiI*	M145 *whiI*⁻::*hyg*	(Ainsa, Parry et al. 1999)

2.2 Plasmids/ Cosmids

Plasmids and cosmids used during this work are listed in Table 2.2 below. The maps and construction details of plasmids originating from this study can be found in the relevant result chapters.

Table 2.2: Plasmids, cosmids and transposon

Plasmid/Cosmid	Characteristics	Source
p2075His1	*Sco2075::[His$_6$]* downstream of native promoter	This work
p2075mch	*Sco2075::mCherry* downstream of native promoter in pSET152	This work
pAL2075	pAlter1 containing fragment from 4A.10.2.D05	Del Sol R., personal communication
pALD12R	pAlter1 containing *sco6163-sco6166*	Del Sol R., personal communication
pALTER1	Tetracycline^R	Promega Corp.
pcDksactd	pET-26b(+) containing truncated C-terminal domain *sco2075* coding sequence fused to His-tag at C-terminal	This work
pcDksAntd	pET-26b(+) containing truncated N-terminal domain *sco2075* coding sequence fused to His-tag at C-	This work

	terminal	
pDksA1	pET-26b(+) containing *sco2075* coding sequence fused to His-tag at C-terminal	This work
pDksA2	pET-16K containing *sco2075* coding sequence fused to His-tag at N-terminal	This work
pDksA3	*Sco2075*::[*His*]$_6$ downstream of *ptipA*, in PIJ8600	This work
pDksA3H	*Sco2075*::[*His*]$_6$ downstream of *ptipA*, in pIJ8600H	This work
pDpsA7	*dpsA::[His$_6$]* downstream of native promoter in pSH152	(Facey, Hitchings et al. 2009)
pET-16k	Expression vector, N-terminal His_{10}. pET-16b with *bla* gene replaced with *kan*	Del Sol R., personal communication
pET-26(b)	Expression vector, C-terminal His_6, *kan*	Novagen
pGEM T-easy	PCR cloning vector, *amp, LacZ*	Promega Corp.
pGEM2075	*sco2075* with native promoter coding sequence missing stop codon in pGEM T-easy	This work
pHL219	pUWL219 derivative, hygromycin^r	(Del Sol, Mullins et al. 2006)

pIJ8600	*tipAp* expression vector, *aac(3)IV, tsr, ori* pUC18, *oriT* RK2, *int* ϕC31, *attP* and *tipA* inducible promoter	(Sun, Kelemen et al. 1999)
pIJ8600H	*tipAp* expression vector, *hyg, tsr, ori* pUC18, *oriT* RK2, *int* ϕC31, *attP* and *tipA* inducible promoter	(Fernandez Martinez, Bishop et al. 2009)
pNA585	Plasmid pEGFP-N2 encoding the C-terminal part of *FtsK* fused to mCherry and with *egfp* deleted	(Ausmees, Wahlstedt et al. 2007)
pnDksactd	pET-16K containing truncated C-terminal domain *sco2075* coding sequence fused to His-tag at N-terminal	This work
pnDksAntd	pET-16K containing a truncated N-terminal domain *sco2075* coding sequence fused to His-tag at N-terminal	This work
pQM5062	pQM5052 containing *egfp;* Tn*5062*	(Bishop, Fielding et al. 2004)
pRB2075	pUWL219 with *sco2075 and native promoter. oriT*	Del Sol R., personal communication
pROT219	Puwl219 with *oriT* cloned *Pst*I-*Pst*I in multiple cloning site	Del Sol R., personal communication

pRT43	Integrative vector for *Streptomyces*, pRT802 with *ftsZ*::*egfp*, *oriT* RK2, *int* ϕBT1, *attP*, *aad9*	Del Sol R., personal communication
pRWHis1	*crgA*::[*His*]*6* downstream of *ptipA* (pIJ8600 background).	(Del Sol, Mullins et al. 2006)
pRWHis2	*crgA*::[*His*]*6* downstream of native promoter	(Del Sol, Mullins et al. 2006)
pSET152	Integrative vector for *Streptomyces; oriT*(RK2) *int attP* (ΦC31) *aac(3)IV*	(Bierman, Logan et al. 1992)
pSH152	*E. coli-S. coelicolor* shuttle vector, hygromycin resistance	(Mistry, Del Sol et al. 2008)
pSH2075	pSH152 containing *sco2075*	This work
pSH6164	pSH152 containing *sco6164*	This work
pSHD12R	pSH152 containing *sco6164-6166*	This work
pUWL219	*E. coli- S. coelicolor* shuttle vector, ampicillin and thiostrepton resistance	(Wehmeier 1995)
SC4A10	Supercos-1 containing chromosomal DNA from *S. coelicolor bla kan*	(Redenbach, Kieser et al. 1996)
SC4A10.1.A08	4A10 containing Tn*5062* in *sco2075 bla kan aac3(IV) oriT*$_{(RK)}$ *eGFP*	(Fernandez-Martinez, Del Sol et al. 2011)
SC9C5	Supercos-1 containing chromosomal DNA from *S. coelicolor bla kan*	(Redenbach, Kieser et al. 1996)
SC9C5.1.C04	9C5 containing Tn*5062* in *RelA bla*	(Fernandez-Martinez, Del Sol

	kan aac3(IV) oriT$_{(RK)}$ *eGFP*	et al. 2011)
Tnloxp53	Tn*5062*; containing hygromycin gene flanked by *loxP* sequences	(Khodakaramian, Lissenden et al. 2006)

2.3 Chemical Reagents

Chemicals used during this study were mostly purchased from SIGMA Chemicals Company, Fisher Scientific Ltd., BHD Chemicals Ltd. and molecular Probes. The chemical solutions and buffers were generally prepared using de-ionised water (dH_2O), provided by a MILLI-RO (reverse osmosis) water purification system. Solutions requiring ultra-pure de-ionised water (ddH_2O) were prepared using ddH_2O provided by a MILLI-Q water purification system. pH of solutions was measured at room temperature. Solutions were routinely autoclaved at 121°C at 103KPa for 15min, when autoclaving was not possible, solutions were filter sterilised using a 0.2μm Millipore filter unit. The components of all the commonly used reagents and buffers are listed in Table 2.3 below.

Table 2.3: Reagents and buffers

Reagents	Ingredients	Quantity per litre dH_20 (unless otherwise stated)
0.1M K2HPO4	K2HPO4	17.42g
0.1M NaH2PO4	NaH2PO4	12.00g
1.5M Tris/ HCl pH8.8	Tris	18.17g
	Adjust pH to 8.8 with HCl	
	dH_2O	Up to 100ml
10% APS (w/v)	Ammonium persulfate	100mg

	dH_2O	Up to 1ml
10% Glycerol solution (v/v)	100% Glycerol	100.00 ml
	dH2O	Up to 1L
10% SDS	SDS	100g
	dH_2O	up to 1L
10% Yeast extract	Yeast extract	10g
	dH_2O	up to 100ml
10x TAE	Tris base	48.4 g
	glacial acetic acid (17.4 M)	11.4 ml
	EDTA	3.7 g
	dH_2O	Up to 1L
10x TBE	Tris	108g
	Boric Acid	55g
	EDTA	9.3g
10x TBS	NaCl	10g
	KCl	0.25g
	Tris base	37.5g
	ddH_2O	Up to 1000ml
1M Tris/ HCl pH6.8	Tris base	12.11g
	Adjust pH to 6.8 with HCl	
	dH_2O	100ml
1M Tris/ HCl, pH8	Tris base	12.11g
	Adjust pH to 8 with HCl	
	dH_2O	100ml
1N NaOH	NaOH	40.00g
	dH2O	up to 1L
2.5M KCl	KCl	18.6
	dH2O	100 ml
2.5M MgCl2	$MgCl_2$	23.80g
	dH_2O	up to 100 ml
20% glycerol (v/v)	Glycerol	20ml
	dH_2O	100ml

20% L-proline (w/v)	L-proline	20.00g
	dH2O	up to 100 ml
20x SSC	NaCl	175.5g
	tri- Sodium citrate	88.2g
5M $CaCl_2.2H_2O$	$CaCl_2.2H_2O$	73.51g
	dH_2O	up to 100 ml
5M NaCl	NaCl	146.1g
	dH_2O	Up to 500ml
Antibody solution for western blots	Blocking Buffer (5%)	15ml
	Antibody glycerol stock	4µl
Binding solution (HisTrap column)	Tris,	6.057g
	NaCl	29.22g
	imidazole	1.36g
	Adjust pH to 7.5 with HCl	
	dH_2O	Up to 1L
Blocking buffer (5%)	TBS / Tween	100 ml
	'Marvel' Semi skimmed milk powder	5g
Bromophenol Blue DNA loading dye	Sucrose	40g
	Bromophenol Blue	60 mg
	1 x TBE	10 ml
	dH_2O	90 ml
Buffer I	Tris	12.1g
	NaCl	8.8g
Buffer II	Blocking reagent	0.25g
	Buffer I	100 ml
	Microwave to dissolve	
Buffer III	1 M Tris-HCl pH9.5	100 ml
	1 M NaCl	100 ml
	0.5 M $MgCl_2$	100 ml
Colour solution	NBT/ BCIP Tablets (Roche)	1 tablet
	ddH_2O	10 ml

Coomassie blue	Coomassie brilliant blue R250	0.25 g
	Methanol	45 ml
	dH_2O	45 ml
	Glacial acetic acid	10 ml
	Filter through Whatman N°.1 filter	
Coomassie de-stain	Methanol	450 ml
	dH_2O	450 ml
	Glacial acetic acid	100 ml
Denaturing Buffer	NaOH	20g
	NaCl	87.75g
Developing solution	Sodium carbonate	1.25 g
	37% Formaldehyde	10 µl
	dH_2O	up to 50ml
Elution buffer 100mM imidazole (HisTrap column)	Tris,	6.057g
	NaCl	29.22g
	imidazole	6.808g
	Adjust pH to 7.5 with HCl	
	dH_2O	Up to 1L
Elution buffer 200mM imidazole (HisTrap column)	Tris,	6.057g
	NaCl	29.22g
	imidazole	13.616g
	Adjust pH to 7.5 with HCl	
	dH_2O	Up to 1L
Elution buffer 300mM imidazole (HisTrap column)	Tris,	6.057g
	NaCl	29.22g
	imidazole	20.424g
	Adjust pH to 7.5 with HCl	
	dH_2O	Up to 1L
Elution buffer 50mM imidazole (HisTrap column)	Tris,	6.057g
	NaCl	29.22g
	imidazole	3.404g

	Adjust pH to 7.5 with HCl	
	dH_2O	Up to 1L
EMSA loading buffer	10mM Tris	1.21g
	80mM NaCl,	4.68g
	1mM DTT,	154mg
	1mM EDTA	372mg
	glycerol	5ml
	Adjust pH to 7.5 with HCl	
Fixing solution	Ethanol	20 ml
	Acetic acid	5 ml
	dH_2O	up to 50ml
Minor elements solution	$ZnSO_4.7H_2O$	1g
	$FeSO_4.7H_2O$	1g
	$MnCl_2.4H_2O$	1g
	$CaCl_2$ (anhydrous)	1g
	dH_2O	up to 1L
Neutralising Buffer	Tris	121g
	NaCl	88g
	pH 7.5	
SMM trace elements	$ZnSO_4.7H_2O$,	1g
	$FeSO_4.7H_2O$,	1g
	$MnCl_2.4H_2O$,	1g
	$CaCl_2.6H_2O$,	1g
	NaCl	1g
	dH_2O	Up to 1L
	Filter sterilise	
Stop reaction	EDTA	0.73 g
	dH_2O	up to 50ml
TBS / Tween	10X TBS	100ml
	Tween 20	1ml
	dH_2O	up to 1L

TE	Tris	1.21g
	EDTA	372 mg
	pH 8.0	
Trace element solution	$ZnCl_2$	40.00 mg
	$FeCl_3.6H_2O$	200.00 mg
	$CuCl_2.2H_2O$	10.00 mg
	$MnCl_2.4H_2O$	10.00 mg
	$Na_2B_4O_7.10H_2O$	10.00 mg
	$(NH4)_6Mo_7O_{24}.4H_2O$	10.00 mg
	dH_2O	up to 1L
Transfer buffer	Tris	5.82g
	Glycine	2.93g
	SDS	0.035g
	Methanol	200ml
	dH_2O	up to 1L

2.4 Commonly used growth media

The bacterial growth media used during this study are described in Table 2.4. Ingredients for Bacterial growth media were purchased from DIFCO, Oxoid Ltd., Gibco BRL., SIGMA Chemical Company and Fisher Scientific Ltd. De-ionized water (dH_2O) required to prepare the media was provided by the MILLI-RO water purification system. pH of the solutions and media was measured at room temperature. Media were routinely autoclaved at 121° C, 15 psi for 15 minutes. Solutions required for media preparation were either autoclaved or filter sterilized as applicable.

Table 2.4 Growth media

Media	Ingredients	Quantity per litre
2x YT	Tryptone	16 g
	Yeast Extract	10 g
	NaCl	5 g
	dH_2O	up to 1L
	adjust pH to 7.0 with NaOH	
Luria Bertani (LB) Broth and Agar	Tryptone	10 g
	Yeast Extract	5 g
	NaCl	5 g
	Glucose	1 g
	dH_2O	up to 1L
	adjust pH to 7.0 with NaOH	
	For plates add 10g agar	
Minimal Medium	L-asparagine	0.5 g
	K_2HPO_4	0.5 g
	$MgSO_4.7H_2O$	0.2 g
	$FeSO_4.7H_2O$	0.01 g
	Agar	10 g
	dH_2O	up to 1L
	adjust to pH7.2 with NaOH	
	Add filter sterilised glucose (1% w/v) after autoclaving	
MYMTE	maltose	4g
	yeast extract	4g
	malt extract	10g
	Difco Bacto agar	20g
	R2YE trace element solution	2ml

	Distilled water to	1000ml
NMMP	$(NH_4)_2SO_4$	2g
	Difco Casaminoacids	5g
	$MgSO_4.7H_2O$	0.6g
	Minor elements solution	1ml
	Agar	20
	dH_2O	up to 800ml
	When plating add:	
	NaH_2PO_4 (0.1M, pH 6.8)	3.25ml each per 25ml plate
	/ K_2HPO_4 buffer (0.1M, pH 6.8)	
Nutrient Agar	Oxoid Nutrient Broth	13 g
	Agar	20 g
	dH_2O	up to 1L
R2YE	Sucrose	103 g
	K_2SO4	0.25 g
	$MgCl_2.{}_6H_2O$	10.12 g
	Glucose	10 g
	Casamino acids	0.1 g
	Agar	22 g
	dH_2O	up to 800 ml
	After autoclaving add (to 200 ml):	
	Trace element solution	0.5 ml
	5.73% TES Buffer pH7.2	25 ml
	0.5% KH_2PO_4	2.5 ml
	5 M $CaCl_2$	1 ml

	20% Proline	3.75 ml
	1N NaOH	1.25 ml
	10% Yeast extract	12.5 ml
R5	Sucrose	103g
	K_2SO_4	0.25g
	$MgCl_2.6H_2O$	10.12g
	Glucose	10g
	Difco Casaminoacids	0.1g
	Trace element Solution	2ml
	TES buffer	5.73g
	Distilled water to	1000ml
	After autoclaving 100ml aliquots with 2.2g agar add	
	KH_2PO_4 (0.5%)	1 ml
	$CaCl_2.2H_2O$ (5M)	0.4 ml
	L-proline (20%)	1.5 ml
	NaOH (1N)	0.75 ml
SFM	Soya Flour	20 g
	Mannitol	20 g
	Agar	20 g
	Tap water	up to 1L
	Autoclave 30 min, 121°C, 15p.s.i.	
Supplemented minimal medium, solid (SMMS)	Difco casaminoacids	2g
	TES buffer	5.73g
	Water	1000ml
	Autoclave.	
	At time of use add:	
	$Na_2H_2PO_4$+K_2HPO_4 50mM each	2ml

	$MgCl_2$ 1M	1ml
	Glucose 50% w/v	3.6ml
	SMM trace elements	0.2ml
Soft nutrient agar	Oxoid Nutrient Broth	13 g
	Agar	5 g
	dH_2O	up to 1L
SOC	Tryptone	20 g
	Yeast Extract	5 g
	1 M NaCl	10 ml
	1 M KCl	2.5 ml
	H_2O	up to 1L
	after autoclaving add:	
	1 M $MgCl_2$	10 ml
	1 M $MgSO_4$	10 ml
	1 M Glucose	10ml

2.5 Antibiotic selection

All antibiotics were made up as stock concentrations (Table 2.5) and unless specified, made up in ddH_2O and filter sterilised. Antibiotics were stored at -20°C except hygromycin solution which was stored at 4°C. Stock concentration and working concentration for respective antibiotic are listed in Table 2.5.

Table 2.5 Concentration of antibiotics, IPTG and X-gal

Antibiotic	Stock concentration (mg ml^{-1})	*E. coli* working concentration (μg ml^{-1})	*Streptomyces* working concentration (μg ml^{-1})
Ampicillin	50	50	-
Apramycin	25	100	25
Chloramphenicol[1]	10	10	-
IPTG	20	25	-
Kanamycin	25	25	25
Naladixic acid[2]	20	20	-
Spectinomycin	50/ 200	50	400
Streptomycin	25	25	50
Tetracycline[3]	10	10	-
Thiostrepton[4]	25	-	25
X-gal[4]	20	25	-

To dissolve use: [1]100% Ethanol, [2]0.25M NaOH, [3]80% Ethanol, [4]DMSO

2.6 Culture conditions

2.6.1 Growth and storage of *E. coli* strains

E. coli cells were grown on LB medium and incubated at 37°C either in a static temperature controlled incubator if being grown on plates or shaken at 220rpm if liquid. Glycerol stocks of *E. coli* strains were prepared from 5ml overnight cultures, spun down and resuspended in 0.5ml of sterile 20% (v/v) glycerol and stored at -20°C or -70°C. Short term storage of culture was possible by storing broths or plates at 4°C.

2.6.2 Growth and storage of *S. coelicolor* strains

S. coelicolor cultures were grown on a variety of solid and liquid media and incubated at 30°C, statically for plates and shaken at 225rpm for liquid cultures. For the preparation of spores, lawns of the relevant strain were grown on SFM agar, containing appropriate selective antibiotic (if applicable) for 4-6 days. Spore suspensions of different *S. coelicolor* strains were stored at -20°C.

2.7 Preparation of spore suspensions of *S. coelicolor* strains

To prepare spore suspensions, *S. coelicolor* cells were grown on SFM agar media as stated above. After the appropriate incubation period, culture plates were flooded with 9ml sterile ddH_2O and gently scraped off the surface with a sterile inoculating loop to release the spores. The resulting suspension was poured into a sterile centrifuge tube, vortexed and filtered through a sterile 10ml syringe containing a non-absorbent cotton wool to remove mycelia fragments. The spores were then pelleted by centrifugation at 5000xg for 5min and resuspended in 1ml of sterile 20% glycerol solution. Stocks were stored in microcentrifuge tubes at -20°C.

2.8 Transformation

2.8.1 Preparation of electrocompetent *E. coli* JM109

1/10 volume of overnight culture was added to 10ml of LB broth and allowed to grow to an OD_{600} of 0.5 to 0.7. Cells were then pelleted for 5min at 2665xg, 4°C. The cells were then put on ice and the supernatant removed. 10ml of ice cold 10% glycerol

was added to the pellet and the cells resuspended gently then centrifuge again. This step was repeated three times. On the final step the supernatant was removed, and the cells resuspended in the remaining glycerol (200-500µl). The cell suspension was aliquoted and stored at -70°C.

2.8.2 Transformation of electrocompetent *E. coli* JM109

10ng of DNA was added to a 40µl aliquot of JM109 cells, mixed gently and incubated for 1minute. The aliquot was then transferred to a pre-chilled electroporation cuvette and electroporated using a MicroPulser ^{tm} (BioRad). 500µl of LB was then added to the cuvette and the cells resuspended fully and transferred to a Bijoux tube and incubated for 90 minutes at 225rpm, 37°C then plated on LB agar with corresponding antibiotics.

2.8.3 Preparation of electrocompetent *E.coli* ET12567

S. coelicolor possesses a potent methyl-specific restriction system which restricts DNA from *dam*$^+$ *dcm*$^+$ *E. coli* (MacNeil 1988). This restriction system is circumvented by DNA passage through a methylase-deficient *E. coli* host, ET12567 (Flett, Mersinias et al. 1997).

ET12567 is a methylation-deficient strain of *E. coli* containing a plasmid containing the machinery used for interspecies conjugal transfer. ET12567 contains a non-transmissible plasmid (pUZ8002), which lacks a *cis*-acting function for its own transfer (Kieser 2000) but allows the mobilisation of a vector containing *oriT* in trans.

Kanamycin and chloramphenicol maintains selection for pUZ8002 and the dam mutation respectively.

A tenth volume of stationary phase cells was used to inoculate LB broth to an OD_{600} of 0.5 to 0.7. Cells were pelleted for 5minutes at 2665xg, 4°C. The cells were then put on ice and the supernatant removed. 10ml of ice cold 10% glycerol was added to the pellet and the cells resuspended gently then centrifuge again. This step was repeated three times. On the final step the supernatant was removed, and the cells resuspended in the remaining glycerol (200-500µl). The cell suspension was aliquoted and stored at -70°C.

2.8.4 Transformation of *E. coli* ET12567

10ng of DNA or 200ng cosmid was added to a 40µl aliquot of electrocompetent ET12567 cells, mixed gently and incubated for 1minute. The aliquot was then transferred to a pre-chilled electroporation cuvette and electroporated using a MicroPulser ™ (BioRad). 500µl of LB was added to the cuvette and the cells resuspended fully and transferred to a Bijoux tube and incubated for 90 minutes at 225rpm, 30°C and were plated on LB agar with kanamycin, chloramphenicol and antibiotic corresponding to the plasmid or cosmid.

2.8.5 Intergeneric conjugation

Intergeneric transfer of plasmids from *E. coli* to *Streptomyces* strains was demonstrated after modifying the mobilisation system established by Simon (1983) Competent ET12567 was prepared as previously mentioned and electroporated with a vector of interest containing an *oriT* to mobilise into *Streptomyces*. A colony was selected and inoculated

into 5ml of LB and incubated in a shaker overnight at 37°C containing kanamycin, chloramphenicol and antibiotic conferring resistance for the selective marker. The following morning a 1 in 25 dilution of the culture into fresh LB containing antibiotics conferring resistance was prepared and grown to exponential phase, ~6hours or OD_{600} of 0.4-0.6. The cells were then centrifuge at 12,100xg and washed three times in 1.5ml of fresh LB taking care resuspending the cells.

While the *E. coli* cells were being washed, 10^8 spores of *Streptomyces* were added to 500µl 2xYT and heat shocked at 50°C for 10minutes after which they were allowed to cool to room temperature. 500µl of *E. coli* was added to the shocked spores and spun briefly to remove most of the supernatant. The mixture was then resuspended, plated on SFM containing 10mM $MgCl_2$ and incubated at 30°C.

After 24hours the plate was overlaid with 1ml MilliQ H_2O containing antibiotics conferring resistance for the selective marker and nalidixic acid to inhibit *E. coli* DNA synthesis. Three to five days later spores were collect and plated on a fresh SFM plate containing nalidixic acid, and other required antibiotics.

2.8.6 Selection of *S.coelicolor* double crossover mutant strains

After 3-5 days of incubation, single colonies of exconjugants on the overlaid SFM plates could be picked and two sets of plates were prepared, one containing the appropriate concentration of the antibiotic whose resistance gene is carried on the plasmid/ cosmid (e.g. kanamycin for supercos1) and the other containing the antibiotic whose resistance gene is carried on the transposon (e.g. apramycin or hygromycin).

Replica plating was then carried out for a large sample of individual colonies (50-100 colonies). Any colonies which grew on apramycin or hygromycin containing media plate but not on kanamycin containing plates were selected as probable double crossover mutant strains, and these were confirmed using Southern hybridisation.

2.9 DNA isolation and manipulation

2.9.1 Plasmid isolation

2.9.1.1 *Streptomyces* plasmid isolation

Supercoiled plasmid DNA was isolated for liquid cultures using an alkaline lysis technique described by Kieser (2000)

50-200ml cultures were inoculated with 5- 10ml of 24hour precultures and grown for predetermined lengths of time. Mycelium was centrifuged at 12,500xg (and all remaining centrifugations unless stated otherwise), and the alkaline lysis psupernatant removed and rinsed in a 10.3% sucrose solution. The mycelium was then resuspended in 4ml of buffered solution (25mM Tris pH8 10mM EDTA and 0.3M sucrose) containing 50mg/ml RNaseA. *Streptomyces* being Gram-positive bacteria have cell walls composed of approximately 90% peptidoglycan that forms multiple layers of the cell wall structure. Lysozyme, a 14.4kDa enzyme extracted from chicken egg-white catalyzes the hydrolysis of 1, 4-beta-linkages between N-acetylmuramic acid and N-acetyl-D-glucosamine residues in peptidoglycan and between N-acetyl-D-glucosamine

residues in chitodextrin. This produces a strained conformation whereby the glycosidic bond is easily broken.

8ml lysis solution was added, containing 1% Sodium Dodecyl Sulfate (SDS), an ionic detergent that destabilizes hydrophobic interactions and 0.2N NaOH that denatures the macromolecules due to its high pH. At this stage the solution cleared as the mycelium lysed, spilling out its content increasing the concentration of macromolecules in solution.

During the neutralisation step, 6ml of 3M potassium acetate pH4.7 and 0.6ml phenol chloroform (reduces nicking, no separate phase formed) was added to neutralise NaOH, allowing renaturation of macromolecules. The samples were then placed on ice for up to 15 minutes to allow the aggregation of protein/lipid/chromosomal DNA- SDS complexes.

After centrifugation for 35minutes the lysate was transferred into a clean tube containing 10.6ml isopropanol and incubated at -80°C for 30minutes to allow DNA precipitation to occur. The sample was centrifuged for 40minutes and supernatant removed. 1ml of 70% ethanol was added to the sample and centrifuge for a further 5minutes.

The pellet was resuspended in 400µl of TE pH8 and transferred to a 1.5ml eppendorf. 800µl of 100% ice cold ethanol and 120µl 3M sodium acetate pH5.5 was added, incubated for 20min at -80°C and centrifuge at 12,500xg for 20minutes. This step reduces RNA and salt contamination.

The pellet was then dried and resuspended in buffer RP from Bioneer Accuprep plasmid mini prep kit and manufacturer's instructions followed and eluted in TE pH8.

2.9.1.2 *E. coli* plasmid isolation

E. coli plasmids were isolated from overnight 3ml cultures using DNA binding matrices. Using Bioneer's AccuPrep Plasmid Extraction Kit, 3ml cultures of *E. coli* containing the desired plasmid were spun down at 12,100xg and resuspended in 250µl resuspension buffer (RP; containing RNaseA). Once fully resuspended, 250µl lysis buffer (LP) was added to the resuspended cells, inverted gently 4 times and incubated at room temperature until the lysate became clear. 350µl neutralisation buffer (NP) was added to the lysate and centrifuged at 12,100xg for 10minutes to pellet the precipitate. The clear lysate was then transferred to a DNA binding tube and centrifuge for 30seconds. 700µl wash buffer was added to the binding tube, centrifuge at 12,100xg for 1 minute and repeated for a further minute to completely remove any remaining ethanol from the matrix. Plasmid DNA was then eluted using MilliQ H_2O.

2.9.2 Genomic DNA isolation from *S. coelicolor*

The FastDNA® SPIN Kit for Soil (BIO 101 systems) from Q-BIOgene was used, using the supplied buffers, to rapidly isolate genomic DNA by lysing the cells using ceramic and silica particles. Lysing matrix tubes containing 978 µl sodium phosphate buffer and 122 µl MT buffer, were filled to 7/8 volume with mycelia from 24 h cultures grown on LB agar plates. The tubes were securely fastened into the FastPrep instrument and processed for 30sec at speed 5.5. After processing the cell debris and lysis matrix were centrifuged to the bottom at 12100xg for 1 min. After centrifugation the supernatant was transferred to a 15ml tube and incubated, gently shaking, for 2 min with

1 ml binding matrix suspension. Once the DNA was bound to the matrix it was left to settle for 3 min then transferred into a spin filter, which captures the matrix and the bound DNA. The bound DNA was washed with 500µl SEWS-M and eluted into a fresh catch tube with 50µl DNase/ Pyrogen free water. Total DNA from *S. coelicolor* was used for southern blots and as a PCR template for amplification of specific genes.

2.9.3.1 Enzymatic reactions

Restriction digestions were performed using restriction endonucleases purchased from New England Biolabs (NEB) or Promega Corp. All reactions were carried out according to manufacturer guidelines. For blunt ending of 3' and 5' DNA overhangs, T4 DNA polymerase from NEB was used. T4 DNA ligase was purchased from Promega or NEB. To remove 5' phosphate group from DNA Alkaline Phosphatase, Calf Intestinal (CIP) or Antarctic Phosphatase from NEB was used.

2.9.3.2 Ligations reactions

Prior to ligation, DNA fragments were purified from enzymatic reactions by the QIAquick PCR purification Kit (Qiagen). 5 volumes of Buffer PB were mixed with 1 volume of the enzymatic reaction and applied to QIAquick column and centrifuge for 1 minute at 12,100xg to bind the DNA. The matrix was then washed with 750µl Buffer PE. After an additional centrifugation step for 1 minute to fully removing any residual ethanol, the DNA was eluted by applying 50µl H_2O.

DNA from TBE agarose gels was purified using illustra GFX PCR DNA and Gel Band Purification Kit (GE Healthcare). 10µl capture buffer was added to every 10mg of

agarose containing the DNA and incubated at 60°C until fully dissolved. The sample was loaded into a GFX MicroSpin column and incubated at room temperature for 1 minute. Centrifuge for 1 minute and flow through removed. 500µl of wash buffer was added to the column and centrifuged for one minute. 50µl milliQ H_2O was added to the column and centrifuge to elute the DNA.

The ratio of vector to insert was estimated by agarose gel, and a ratio of 1:3 used in 1XNEB buffer in total volume of 20µl overnight at 14°C.

2.9.6 REDIRECT

The REDIRECT system from *E. coli* (Datsenko and Wanner 2000) was adapted for use in *Streptomyces* by Gust, Challis et al. (2003). This process greatly enhances the ability to construct targeted mutants in *Streptomyces* by manipulating cosmids within *E. coli*. 4A10.1.A08 was electroporated into BW25113 containing the λ red recombination plasmid pIJ790.

pIJ790 confers chloramphenicol resistance and contains a temperature sensitive replication gene *repA101ts*, an L-arabinose inducible promoter and the λ red recombination genes *bet* (encoding a single strand DNA binding protein), *gam* (inhibits host exonuclease V) and *exo* (an exonuclease gene which promotes recombination) (Gust, Challis et al. 2003).

Cosmid 4A10.1.A08 was electroporated into BW25113/pIJ790 and grown over night on LB at 30°C containing chloramphenicol and apramycin to maintain pIJ790, and Tn*5062* insertion respectively. Next morning colonies of BW25113/pIJ790 containing 4A10.1.A08 were picked and inoculated into 10ml LB containing chloramphenicol,

apramycin, $MgSO_4$ and 10mM final concentration of arabinose to induce λ red recombination genes for 3-4 hours at 200rpm, 30°C. After the cells have reached an OD_{600} of ~ 0.4 the culture was transferred to a 15ml centrifuge tube and spun at 2665xg for 5minutes at 4°C (from now on kept on ice). The supernatant is removed and cells resuspended gently in 10ml 10%glycerol. Wash step was repeated a further 2 times, on final wash the supernatant was removed and resuspended in the remaining glycerol (circa 200-500µl) and aliquot about 50µl.

A *Pvu*II restricted fragment containing Tn*loxP53* was added to an aliquot of electrocompetent *E. coli* BW25113/pIJ790 containing cosmid 4A10.1.A08, electroporated and incubated for 90minutes in LB (arabinose is not required as sufficient concentration of enzyme remains in the cells from previous induction). As the plasmid pIJ790 containing the red recombination genes is not required anymore the culture was inoculated onto an LB plate overnight with hygromycin at 37°C.

After 16h of growth, there were two different size colonies present, where the small background colonies are false positives. At this stage there are still copies of the cosmid containing Tn*5062* and Tn*loxP53* as one copy of a cosmid containing the new cassette was enough to be resistant to the new marker. Larger colonies generally have more copies of the cosmid with the cassette exchanged; therefore large isolated colonies were picked and grown in 5ml LB, hygromycin in a shaker incubator at 37°C. After 6 hours, plasmid was extracted from the cultures and subjected to enzyme digestion to determine if the cassette exchange was successful. Using *Eco*RI, Tn*5062* produces 1 small band of ~800bp where the new Tn*loxP53* insertion produces 800bp and 1100bp.

4A10.1.A08 hyg^R was then electroporated into *E. coli* JM109 and 4A10.1.A08 extracted using AccuPrep Plasmid Extraction Kit (Bioneer, Inc). 200ng is then electroporated into *E. coli* ET12567 and incubated overnight on LB; Km, Cm, Hyg. Colonies were then picked and conjugated into DSCO6164 mutant strain.

2.10 Polymerase chain reaction (PCR)

PCR reactions were cycled on a PTC-200 DNA Engine (M.J. Research Inc.) using Dynazyme EXTTM polymerase (Finnzymes) with a typical PCR cycle shown in Table 2.7. Primers were manually designed and checked using DNAMAN. Primers used in this study are shown in Table 2.6.

Table 2.6: Primers used in PCR reactions.

Primer name	Sequence	Restriction enzyme
2075_FWD	AATCTAGACGCGCCAGAAGTCGAGCA	*Xba*I
2075_REV	AAAGATCTGCGTACCGGCGCTCCTGC	*Bgl*II
DksA_NdeI	AACATATGGTGGCGAAGAAGAAGACG	*Nde*I
2075_trc_BamHI	AAAGGATCCTCGATCTCGGTGCGCA	*Bam*HI
CTD_NdeI	AAACATATGGGCGAGGAACCCTGGACC	*Nde*I

Reactions were carried out in thin-walled 0.5 ml microfuge tubes with a total reaction volume of 50µl.

A typical reaction scheme follows:

Template DNA (approx. 100 µg/ml)	2.0 µl
10X DyNAzyme EXTTM buffer	5.0 µl
Sense primer (10 pmol/µl)	2.0 µl
Antisense primer (10 pmol/µl)	2.0 µl
2.5 mM dNTP mix	4.0 µl
dH_2O	34.0 µl
DyNAzyme EXTTM polymerase	1.0 µl
Total volume	50µl

Table 2.7: Typical PCR cycle program used for the reaction mix was as follows, where a gradient was used for initial PCR reactions with new primers:

	Temperature (°C)	Time (min)	No. cycles
Initial denaturation	95	4.0	1
Denaturation	95	0.5	
Annealing	50-70	0.5	30
Extension	72	1.0	
Final extension	72 4	10.0 Hold	1

2.11 Quantification of DNA

2.11.1 Gel electrophoresis

DNA was separated out according to size by electrophoresis through agarose gels. The percentage of agarose is varied to reflect the size of the DNA of interest. 1% or 0.8% agarose (w/v) gels were used to separate restriction digests of plasmid DNA (0.5kb-15kb), 0.5% gels were used to visualise large pieces of DNA, for example

Streptomyces chromosomal DNA. To separate smaller PCR products 1.5-2% agarose gels were used. Standard 100ml of 1% (w/v) gels containing a final concentration of 0.1μg/ml ethidium bromide were routinely prepared in 1xTBE buffer. The gel was immersed in the BIORAD electrophoresis tank filled with 1xTBE buffer and the samples were loaded into wells after mixing with bromophenol blue DNA loading dye at a ratio of 5:1. Gels were run at 100V using BIORAD power supply, for 45-60min. To estimate the size of DNA samples an appropriate DNA marker was added to the gels (phage lambda DNA digested with *Hind*III).

Once the DNA samples had run the desired distance in the gel, the gel was removed from the tank and exposed to UV light using a BIORAD transilluminator at 254nm and the DNA samples were visualised through BIORAD gel documentation system (GelDoc).

The quality and quantity of DNA was also assayed using a NanoDrop® ND-1000 Spectrophotometer. The quantity of DNA was measured by applying 2μl sample on the pedestal of the instrument after initialising the instrument and setting the blank. The ratio of A_{260}/A_{280} determined the purity of the DNA.

2.11.2 Chloroquine gel electrophoresis

Gels were made up of 0.5%-1% (w/v) agarose in 1xTAE and contained 6μg/ml chloroquine. The 1xTAE buffer also contained 6μg/ml chloroquine. Supercoiled plasmid DNA was electrophoresed in the dark for 25-40hours at 1-1.5V/cm and the buffer re-circulated to reduce buffer exhaustion at 4°C. Gels were rinsed in 1mM $MgCl_2$ for 2 hour

followed by 1 hour in dH_2O then stained for 1 hour in 1μg/ml ethidium bromide followed by a destaining for 30minutes - 1 hour in dH_2O.

2.11.3 Quantification of bands

Images of chloroquine gels were analysed on Quantity One software (BioRad). Density traces of each lane were constructed using the software and the traces lined up horizontally. Using a ruler, a line was drawn vertically from Lk_m (where Lk_m was the most intense distinguishable single topoisomer) of the control strain and change in linking number calculated by counting the difference in topoisomers between Lk_m of the control and the test sample.

2.11.4 Electrophoretic mobility shift assay (EMSA)

The specified amount of the protein (if applicable) was added to a microcentrifuge tube containing 300ng of substrate DNA containing EMSA binding buffer 10mM Tris-HCl pH7.5, 80mM NaCl, 1mM DTT, 1mM EDTA and 5% glycerol (final concentrations) (Werlang, Schneider et al. 2009). The samples were then left at room temperature for 15min, loaded into a 0.8% agarose 1xTAE gel and run at 4°C with buffer recirculation at a constant 48V for 16hours. The gel was then submerged in 1μg/ml ethidium bromide, destained in dH_2O and visualised through a BioRad gel documentation system (GelDoc).

2.12 Southern Hybridization

The successful replacement of wild type gene with transposon disrupted copy of the same gene in *S. coelicolor* mutant chromosomes was confirmed using Southern hybridization analysis. In brief, a restriction digest of chromosomal DNA from the mutant strain and a positive control (often the relevant cosmid) were run on an agarose gel. The DNA samples were then transferred to a nylon membrane and detected immunologically using an appropriately labelled probe, usually Tn*5062*.

2.12.1 Preparation of digoxigenin labelled probes

Suitable DNA fragment(s) were selected and labelled randomly with alkali-labile Digoxigenin-11-2'-deoxy-uridine-5'triphosphate (DIG-11-dUTP) using the DIG DNA Labelling Kit from Roche Applied Sciences. A 3442bp *Pvu*II fragment of Tn5062 DNA excised from pQM5062 was used as a labelled probe. Phage λ DNA digested with *Hin*dIII was labelled and used as a probe to hybridise with the λ *Hin*dIII marker. Random priming method, based on hybridisation of random oligonucleotides to the denatured DNA template, was used to label respective purified DNA fragments, to label the DNA, the DNA fragments were denatured by heating at 95°C for 10 min and cooled quickly on ice, hexanucleotide mix, DIG-11-dUTP/dNTP mixture and Klenow enzyme were added to the denatured DNA. The reaction mixture was mixed thoroughly and incubated at 37°C overnight. The reaction was stopped by the addition of 2µl of 0.2M EDTA pH 8.

A standard reaction scheme:

Denatured DNA	1-15µl (10ng-3µg DNA)
ddH_2O sterile to make final volume to 15µl	x µl
Final volume	15µl
Hexanucleotide mix	2 µl
DIG-11-dUTP/dNTP mixture	2 µl
Klenow polymerase	1 µl
Total reaction volume	20 µl

Prior to hybridisation, 10µl each of labelled probes Tn*5062* and λ *Hin*dIII was denatured by boiling for 10min in a boiling water bath, cooled quickly by keeping it on ice for 1-2min and added to 15-20ml of prehybridisation solution. The solution thus prepared is called 'probe solution' from here after.

2.12.2 Blotting

Chromosomal DNA of interest and the corresponding cosmid DNA control were digested with suitable restriction enzyme and were separated on an 0.8% agarose, 1xTBE gel along with λ *Hin*dIII marker. The gel was visualised under UV transilluminator to check chromosomal DNA was completely digested. The gel was then immersed in neutralisation buffer for 20min with gentle shaking. This step was repeated twice. The gel was then rinsed twice with dH_20, after quick rinse, the gel was immersed in neutralisation buffer for 20min with gentle shaking, repeated twice. During the neutralisation step, a gel sized neutral nylon membrane (Hybond-M. Amersham Pharmacia Biotech) was soaked in H_2O for 20min and then soaked in 10xSSC solution

for 10min. Two pieces of Whatman filter paper cut 1cm larger than membrane, were also soaked in 10x SSC solution for 10min.

A Stratagene Posiblot Pressure blotter was used to transfer DNA from the gel onto the treated nylon membrane prior to hybridisation and immunological detection. The pressure blotter was assembled with Whatman filter paper, soaked in 10x SSC at the bottom, then nylon membrane and on top of this was a plastic mask, containing a hole 0.5cm smaller around the edges of the gel in the centre. Once assembled the gel was positioned on top of the mask sealing the hole and as much 10xSSC buffer was poured on top of the gel without breaking the water tension. The pressure of 1KPa was applied for 1 hour to transfer the DNA efficiently on to the membrane, with 10xSSC topped up on the gel where appropriate. Once transferred the membrane was baked at 80°C for 60min to fix the DNA.

2.12.3 Hybridisation

Once the DNA was fixed to the membrane, it was rinsed in dH_2O and rolled in a piece of nylon mesh soaked in 2xSSC with the DNA facing upwards. The rolled membrane with the mesh was placed into a hybridisation tube (Appligene) and washed with 2xSSC. A 10ml of prehybridisation solution was added in the hybridization tube and incubated at 42°C for 1 hour. After the prehybridisation step the solution was decanted and a 20ml denatured labelled probe solution was added to the tube and incubated at 42°C overnight in a rotating oven. The following day, the probe was collected and stored at -20°C for future use. The membrane was washed twice in wash

solution 1 at 42°C for 5min each and then it was washed twice in wash solution 2 at 68°C for 15min each.

2.12.4 Immunological detection

After a washing with wash solution 2, the membrane was rinsed in Buffer I for 1 min at room temperature and incubated with freshly prepared buffer II (prehybridisation solution) for 30min. After this, the membrane was briefly washed for 1 min with buffer I. The membrane was then incubated with Anti-digoxigenin antibody solution (15ml buffer I with 3µl Anti-digoxigenin AP) for 20min in a rotating oven at room temperature. To remove unbound antibody, the membrane was washed twice in Buffer I for 15min. After the wash steps in the hybridisation tube, the membrane was removed and transferred to a plastic bag where 10ml of colour solution was added and the bag was sealed. To facilitate the colour reaction the membrane was placed flat in the dark, at 37°C. After the bands had sufficiently intensified (20min – 2h) the reaction was stopped by washing the membrane in dH_2O.

2.13 RNA manipulations

2.13.1 RNA isolation

Before working with RNA it is essential to remove potential sources of ribonuclease (RNase) contamination, therefore, all glassware was baked at 240°C overnight. Disposable plasticware was autoclaved twice before use and laboratory equipment and surfaces were dust free. RNA was isolated using Qiagen RNeasy® Midi Kits. *Streptomyces* spores were inoculated onto agar plates covered with sterile

cellophane discs and at appropriate time points; cells were harvested into 800µl Bacterial RNA Protect (Qiagen) and incubated for 5 min. Mycelia were pelleted at 12100xg for 5 min and resuspended into 1 ml TE buffer containing 3 mg ml^{-1} lysozyme. 4 ml of Buffer RLT was added and the bacterial lysate was centrifuged for 5 min at 2665xg to pellet cell debris. The supernatant was transferred to a fresh 15 ml tube and 2.8 ml Ethanol was added gently. The sample, including any precipitate, was applied to an RNeasy midi column and centrifuged for 5 min at 2665xg. Flow through was discarded and an optional on – column DNase step was incorporated. The silica matrix with RNA bound, was washed once with 2 ml Buffer RW1 then 160 µl Buffer RDD (containing 20 µl DNase I stock solution) was incubated on the column at room temperature for 15 min (RNase free DNase Kit, Qiagen). A second wash step, with 2 ml Buffer RW1 was then centrifuged through the column. Finally 2.5 ml Buffer RPE was applied to the column, centrifuged for 5 min at 2665xg, and the RNeasy column transferred to a fresh 15 ml collection tube. 250 µl RNase free water was applied to the column and incubated for 1 min at room temperature. The RNA was eluted by centrifugation then aliquoted and stored at -70°C.

2.14 RT-Quantitative PCR

After RNA isolation, 1µg of RNA was reverse transcribed using random decamer primers (RETROscript™, Ambion, UK). cDNA was amplified using gene specific primer pairs to obtain a PCR product between 75-150bp for each of the genes under study (Beacon Design 2.0, Premier Biosoft, USA). *S. coelicolor hrdB* was used as

a control, and genomic DNA and RNA were used as negative and positive controls respectively.

Amplification reactions were prepared in a volume of 20 µl by adding 10 µl of SYBR-Green Supermix 2X containing the Thermo-Start ® DNA Polymerase (ABgene), 2.5µl of each primer (4 µM) (Table 2.8) and 5µl of serial dilutions of cDNA. RT-PCR amplifications were done in triplicate in 96-well optical reaction plates and run in the BioRad IQ iCycler. Plates were heated first to 95 °C for 15 min to activate the Thermo-Start ® DNA Polymerase enzyme and run for 50 cycles of 15 s at 95 °C, 30s at the optimal annealing temperature for each primer pair and 30s at 72°C, followed by 1 cycle of annealing at 55°C for 30s and 1 cycle of denaturation at 95°C for 30s. To obtain the melting curves for each sample a final step of 40 cycles was performed for 10s at 53°C, increasing the set point temperature by 1°C per cycle up to a maximum temperature of 94°C. No amplicons were obtained using RNA directly in the PCR reaction.

Relative quantification of gene expression data was determined from threshold cycle (Tc) values for each sample. Serial dilutions of cDNA were used to plot a calibration curve, and gene expression levels quantified by plotting Tc values on the curve. Expression levels were normalized with values obtained for the internal reference gene *hrdB*. Once normalized, fold expression was calculated as a ratio of transcript levels between treated and control samples for each gene.

Table 2.8 RT-PCR primers

SigR_RTF1	GCGTCCTTCCACCAGTTCC
SigR_RTR1	CTTCTTGCGGTACGAGTTGATG
hrdBFor	CCTCCGCCTGGTGGTCTC
hrdBRev	CTTGTAGCCCTTGGTGTAGTC

2.15 Native Protein isolation

Spores were inoculated onto the specified agar medium plates covered with sterile cellophane discs and either left or transferred to an alternate plate for stress shock after 16h. At appropriate time points, cells were harvested into 500 µl Sonication buffer containing 1M Tris pH 8.0, 5M NaCl and 0.5M EDTA pH 8.0. Samples were sonicated on ice 3-4 times for 20 seconds at 25% amplitude. The cell debris was pelleted by centrifugation for 10 min at 12100xg at 4°C and the supernatant was transferred to a fresh microfuge tube and stored at -70°C.

2.15.1 Recombinant protein expression

A single colony from a fresh transformation of *E. coli* BL21(DE3) cells containing the relevant plasmid were grown overnight (37°C, 220rpm) in 2xYT/ 1% glucose and kanamycin for plasmid selection. The overnight culture was used to inoculate 500ml – 2L 2xYT/ 1% glucose with kanamycin and incubated at 37°C until OD reached 0.7 at 600nm. 1mM IPTG was added once the OD reached 0.7 and the culture transferred to a 30°C shaker incubator to minimise inclusion bodies for 1 hour. The culture was then centrifuged and supernatant removed and either stored at -80°C or protein was immediately purified.

2.16 Sonication

Samples were suspended in Sonication Buffer [50 mM Tris-HCl, pH 8, 200 mM NaCl, 15 mM EDTA, Complete protease inhibitor cocktail (Roche Diagnostics)] or wash buffer for recombinant protein purifications. Cells or spores were disrupted by sonication (20s burst on ice) until a clear lysate was obtained. Cell-free extracts were obtained by centrifugation at 12100xg for 3 min and the supernatant recovered.

2.17 Purification of His-tagged protein

2.17.1 Assay using Ni-NTA Magnetic agarose beads (Qiagen)

Initial purification were small scale preparations of 10ml cultures of BL21, BL21/pDksA1 and BL21/pDksA2 grown in LB at 37°C from single colonies until OD of 1 when 1mM IPTG was added and incubation temperature reduced to 30°C for 1 hour. The cells were pellets and sonicated (2.16) in wash buffer from Promega MagneHis kit. 50µl of Ni-NTA Magnetic Agarose Beads, which were previously vortexed for 2s, were added and incubated on a shaker at 4°C for an hour; the tube was placed on a suitable magnetic separator for 1 min and the supernatant was carefully removed. 500 µl of Interaction Buffer were added to each tube, mixed and placed for 1 min on the magnetic separator, afterwards the buffer was removed. 500 µl Interaction Buffer was added and incubated on end-over-end shaker for one hour at room temperature. The samples were washed by adding 500 µl of Interaction Buffer, mixed, placed for 1 min on the magnetic separator, and the buffer removed. Finally, 50 µl of Elution Buffer were added, mixed, incubate for 1 min and placed for 1 min on a magnetic separator; the eluate was collected.

2.17.2 Assay using HisTrap HP 1ml column

The columns were first rinsed with 5 column volumes of binding solution to equilibrate the pH and imizdazole concentration after storage. BL21 (DE3) cells containing the appropriate vector from over-expression cultures were resuspended in binding buffer (50mM Tris, 500mM NaCl and 20mM imidazole at pH7.5) and sonicated. The protein extract was spun down to remove cell debris and the supernatant and passed through a 0.2μm syringe filter and kept on ice. The filtered supernatant was then run through the column at 1ml/ min. Once the supernatant was fully passed through the column, 20ml of wash buffer containing 30mM imidazole was run through to remove unbound proteins.

A stepwise gradient was then used to elute the protein in a range of 50, 100, 200 and 300mM imidazole, with 5 column volumes for each concentration with 0.75-1ml fractions collected. Samples of each fraction were then run on a coomassie to verify protein purity/ abundance and quantified. The protein samples were then dialysed overnight in the appropriate buffer to remove remaining imidazole.

2.18 Protein quantification

The BioRad protein assay allows the rapid measurement of protein concentration in the absence of strong alkaline reagents or detergents. BSA was used as a standard; dilutions of BSA along with protein samples were assayed in volumes of 0.8 ml and mixed with 0.2 ml Dye Reagent concentrate. After 5 min (but no longer than 60 min) the optical density was measured at 595nm. A standard curve was plotted of BSA and the concentration of the unknowns was read off the standard curve.

2.19 SDS polyacrylamide gel electrophoresis

Polyacrylamide gels can vary in size and strength according to the resolving power required. Gels were made according to the formulae above (Table 2.3). Protein samples were mixed with loading buffer and boiled for 7 min to maximise dissociation. The gels were run at a constant voltage of 100V in running buffer for 1-2 hours depending on the size of the protein.

2.20 Native gels/ 2D

The first dimension run was a native PAGE gel using BioRad tris 4-15% gradient gels. The gel was removed from packaging, a strip removed and placed into a BioRad Tetra Cell containing 1X SDS PAGE running buffer with the SDS removed and Coomassie G-250 added to the cathode pool. Protein samples were loaded with Invitrogen 4x native loading buffer or 10% glycerol and the gel was run with a voltage of 90V at 4°C.

For 2D, once the dye front reached the end of the gel the lane of interest was cut out and put into the top space above a SDS-PAGE gel (where the stacking gel would be) and the void filled with 0.8% agarose. Marker can be inserted using Whatman paper with 10µl size marker to the running edge of the native gel. Once the agarose had set the gel was run in the same way as an SDS-PAGE gel.

2.21 Protein staining

Polyacrylamide gels were incubated with Coomassie stain (Table 2.3) at room temperature for about one hour in a shaker. After recovery of the stain for future re-use, the gel was destained in destain solution in several 20min steps, adding fresh destain

solution on each step. The steps were repeated until protein bands were visible against background staining. Resolution was improved by leaving the gels in water overnight.

2.22 Western Blotting

The Western blot protocol was developed by Towbin, Staehelin et al. (1979). At the specified time point samples were scraped from cellophane discs, placed in sonication buffer and kept on ice. Where applicable, spore were collected by lightly scraping the surface of the plate with a sterile loop in ddH_2O at time points 72h and 96h and resuspending in water after which they were centrifuged, ddH_2O removed and resuspended in sonication buffer containing 1%SDS. Samples were sonicated, quantified and 20μg of total protein from each time point added. During PAGE the blotting PVDF membrane was activated by immersing the membrane in pure methanol for 5 min, followed by a brief dH_2O wash. The membrane was then e in transfer buffer. After the gel had finished, it was also equilibrated in transfer buffer along with two pieces of thick blotting paper cut to the size of the gel with approximately 0.25cm overhang. The transfer cassette was made up by first laying a piece of blotting paper on the anode; this was pressed onto the surface using a glass rod to expel any possible air bubbles, and bubbles were removed in every subsequent step in a similar manner. The membrane was added next, followed by the gel, and finally the second piece of filter paper was placed on top of the gel. The cassette was run at 20V for 20min. After transfer, the membrane was washed in TBS / Tween briefly before being blocked in 10% milk powder in TBS / Tween for one hour at room temperature. Following the blocking step, the membrane was thoroughly washed in TBS / Tween, at least 4 times for 5 min.

The membrane was then incubated with primary antibody (Penta-His peroxidase conjugate (QIAGEN)) for one hour at room temperature or overnight at 4°C. After the antibody, the membrane was again washed and visualised by using photographic film and colour solution. The system used was the ECL system from Amersham Biosciences. Fold change was calculated by comparing band intensities according to their grayscale images (http://www.lukemiller.org/journal/2007/08/quantifying-western-blots-without.html).

2.23 Calcium dependent antibiotic production

Streptomyces strains were inoculated on LB agar and incubated at 30°C. Nine mm cores were taken from the agar plates from a 48h and 72h sample from the patched area and place in a sterile Petri dish with sufficient distance between them. Using an overnight liquid LB culture of *Bacillus subtilis*, 24.4ml of Soft Nutrient Agar (SNA; cooled below 60°C) with a final concentration of 12mM Ca $(NO_3)_2$ was inoculated. The SNA containing *B. subtilis* was added to the Petri dish and incubate at 37°C. The following morning, the zones of inhibition were measured with a ruler.

2.24 Microscopy Sample preparation

2.24.1 Coverslip impressions

S. coelicolor strains were grown on the surface of relevant medium for the appropriate time. After incubation, a clean coverslip was flamed, cooled and pressed against the surface of the growing culture. Where appropriate cells/ spores were fixed to

the coverslip by placing the coverslip in a clean Petri plate with the aerial mycelium fragments/ spores attached to the upper surface and gently washed with methanol. The methanol was removed and allowed to completely dry and stained for fluorescence microscopic analysis as described in staining.

2.24.2 Inserted coverslips

S. coelicolor strains were inoculated with 2-5µl spore suspension at the acute angle formed by the inserted coverslip in agar plates of the desired medium. After an appropriate incubation time the coverslip was removed and where appropriate cells/ spores were fixed to the coverslip by placing the coverslip in a clean Petri plate with the aerial mycelium fragments/ spores attached to the upper surface and gently washed with methanol. The methanol was removed and allowed to completely dry and stained for fluorescence microscopic analysis as described in staining.

2.25 Staining

2.25.1 Fluo-WGA/PI staining

The lectin staining protocol described by (Schwedock, McCormick et al. 1997) was used to stain the cell wall and DNA of *S. coelicolor*. For cell wall staining, fluorescein-conjugated wheat germ agglutinin (Fluo-WGA) from Molecular Probes was used at the concentration of 2µg/ml and for DNA staining propidium iodide (PI) was used at 10µg/ml concentration. After fixing the cells as described above, the fixed cells were rehydrated by treating the cells with PBS for 5 min. The PBS was gently removed and the cells were treated in 2% BSA in PBS (w/v) for 5 min. The BSA solution was

removed and the cells were incubated with Fluo-WGA/PI solution for 30 min to 3h in the dark at room temperature. After appropriate incubation period, the cells were washed 4-8 times with PBS containing 10μg/ml PI. Cells were then washed twice with Slow Fade equilibration buffer (SlowFade light antifade kit; Molecular Probe). The second wash was incubated at room temperature for 2-5 min. The buffer was aspirated off and Slow Fade antifade/glycerol or 40% glycerol in PBS solution was added. The coverslip was mounted on a clean slide and excess solution was removed by aspiration. The borders of coverslip were sealed with nail varnish to avoid desiccation and the slide was observed under the microscope.

2.25.2 Syto9/ WGA-Texas Red

To visualise live-cell nucleoids, the protocol was followed as in (Facey, Hitchings et al. 2009), inverted or impression coverslips were place on top of a slide with a drop of Syto9/ glycerol solution. Syto9 (Invitrogen) was diluted 5mM in 20% glycerol. For live cell wall staining WGA-Texas Red (Invitrogen) was used. Coverslips were immersed in 2% BSA/ Texas red/ PBS solution and incubated in the dark for 1 hour. Excess stain was gently removed with PBS washes and similarly mounted on a slide with a drop of Syto9/glycerol.

2.25.3 Visualization of samples under microscope

The samples prepared for microscopy were observed under a Nikon Eclipse E600 epifluroresecent microscope. The microscope is equipped with a FITC filter (Excitation 465-495,DM 505, BA515-555) for visualisation of Fluo-WGA attached to

the cell wall and a G02A filter (Excitation 510-560, DM 575, BA 590) for PI stained chromosomal DNA. Images were captured using a Coolsnap digital camera attached to the microscope. The images obtained were later processed using Adobe Photoshop.

2.26 Zone of inhibition assay

Nutrient agar (NA) plates were prepared as normal and allowed to solidify. Soft nutrient agar (SNA) was allowed to cool sufficiently to inoculate with spores and three ml of SNA/ spores ($1x10^7$/ml) overlaid over the NA agar. Sterile discs were then soaked with varying concentrations of diamide and placed onto the surface of the SNA plates and incubated at 30°C overnight. Plates were done in triplicates and the diameters were measured with a ruler.

2.27 Bioinformatic techniques

2.27.1 Databases

Gene annotation and protein sequences were obtained from publicly available databases: the *S. coelicolor* genome database scoDB (strepdb.streptomyces.org.uk); *S. avermitilis* genome database (avermitilis.ls.kitasato-u.ac.jp/); *S. griseus* genome database (streptomyces.nih.go.jp/griseus); NCBI microbial genome project www.ncbi.nlm.gov/genomes/lproks.cgi); broad institute, *actinomycetales* group database http://www.broadinstitute.org/annotation/genome/streptomyces_group/MultiHome.html, Microbial Genome Database for Comparative Analysis (http://mbgd.genome.ad.jp/); GenoList genome browser (http://genolist.pasteur.fr/).

2.27.2 Blast analysis

Sequence similarity searches were performed by BLASTP (Altschul, Gish et al. 1990) against complete microbial genome sequences deposited in NCBI Microbial Genome Project and genome databases mentioned above.

2.27.3 Multiple alignment and phylogenetic analysis

Multiple alignment of amino acid sequences were constructed using CLUSTALW2 (Larkin, Blackshields et al. 2007) from EMBL-EBI server (http://www.ebi.ac.uk/Tools/msa/clustalw2), standalone version CLUSTALX (Larkin, Blackshields et al. 2007) (http://www.clustal.org/) and MEGA 5.0 version (Tamura, Dudley et al. 2007; Tamura, Peterson et al. 2011) using the sequences shown in Table 2.9. Phylogenetic analyses were conducted using MEGA 5.0. Unrooted trees were computed by the Neighbour-Joining method (Saitou and Nei 1987). The bootstrap value for the consensus tree was set to 5000 replicates.

Table 2.9: Gene bank numbers for the protein sequences used in phylogenetic analysis.

Strains	Accession numbers
Streptomyces griseoflavus tu4000 04650	ZP_07313477.1
Streptomyces ghanaensis 05281	ZP_06579577.1
Streptomyces viridochromogenes 02016	ZP_07303129.1
Streptomyces sp E14 00840	ZP_06707400.1
Streptomyces lividans 05468	ZP_06531578.1
Streptomyces coelicolor SCO2075	NP_626334.1
Streptomyces scabies scab68111	YP_003492347.1
Streptomyces sp. C 01905	ZP_07286284.1
Streptomyces violaceusniger Tu 4113	ZP_07610772.1
Streptomyces bingchenggensis BCW	CP_002047.1
S. pristinaespirals 07067	ZP_06912297.1
Streptomyces sp. SPB74 03716	ZP_06826375.1
Janibacter sp. HTCC2649	EAP_98640.1

Kineococcus radiotolerans	YP_001362918.1
Micromonospora sp. M42 05668	MCBG_05668.1 (Broad Institute)
Salinispora tropica CNB-440	ABP_55637.1
Micromonospora carbonacea ATCC 39149 01203	ZP_04604946.1
Micromonospora sp. M42 01080	MCBG_01080.1 (Broad Institute)
Micromonospora carbonacea ATCC 39149 05446	ZP_04609189.1
Salinispora tropica CNB-440 STROP2148	ABP_54599.1
S. bingchenggensis BCW SBI 03641	ADI_06762.1
S. violaceusniger Tu 4113 ZP 07603026	ZP_07603026.1
E. coli K-12 MG1655 - DksA	AAC_73256.1
Kineococcus radiotolerans KRAD 1413	YP_001361165.1
S. violaceusniger Tu 4113 ZP 07606339	ZP_07291004.1
Streptomyces sp. C 06625	ZP_07304419.1
S. viridochromogenes 03306	ZP 07606339.1
S. lividans 01465	ZP_06527575.1
S.coelicolor SCO6165	NP_733690.1
S. griseoflavus tu4000 05674	ZP_07314501.1
Streptomyces sp. E14 02445	ZP_06709004.1
S. viridochromogenes 06982	ZP_07308095.1
S. scabies SCAB6091	YP_003486375.1
S. pristinaespirals 05552	ZP_06913443.1
S. ghanaensis 00824	ZP_06575109.1
Micromonospora sp. M42 01322	MCBG_01322.1 (Broad Institute)
S. ghanaensis 00375	ZP_06574660.1
S. pristinaespirals 05551	ZP_06913444.1
S. griseoflavus tu4000 05673	ZP_07314500.1
S. ghanaensis 00825	ZP_06575110.1
S. viridochromogenes 06983	ZP_07308096.1
S. scabies SCAB6081	YP_003486374.1
Streptomyces sp. E14 02444	ZP_06709003.1
S. lividans 01466	ZP_06527576.1
S. coelicolor SCO6164	NP_630269.1
S. coelicolor SCO5556	NP_629690.1
S. griseus SGR1926	YP_001823438.1
S. clavuligerus SCLAV4504	EFG_09575.1
S. scabies	CBG_69762.1
Mycobacterium tuberculosis HupB	NP_217502.1
M. tuberculosis H37Rv - H-NS	NP_218369.1
M. tuberculosis GM 1503 - H-NS	ZP_03534436.1
Mycobacterium marinum M - H-NS	YP_001853662.1
Mycobacterium ulcerans - H-NS	YP_908370.1
Mycobacterium avium subsp. *paratuberculosis* K-10	NP_959116.1

-H-NS	
Variovorax paradoxus S110 - histone H1/H5 family protein	YP_002942871.1
Chlamydia trachomatis - histone-like protein Hc2	ADD14367.1
sideroxydans lithotrophicus ES-I - histone h1 family protein nucleoprotein Hc2	YP_003525241.1
Methylibium petroleiphilum PM1- histone H1-like	ABM_96165.1
phytophthora infestans - histone h1 putative	XP_002907205.1
S. violaceusniger Tu 4113 - *gyrB*	AEM80044.1
S. bingchenggensis BCW-1 -*gyrB*	ADI08508.1
Streptomyces sp. C- gyrB	ZP_07287909.1
S. coelicolor - gyrB	CAB92994.1
S. scabiei 87.22 - *gyrB*	YP_003490181.1
*S. lividans - gyr*B	ZP_06528017.1
S. pristinaespiralis - *gyrB*	ZP_06909005.1
Streptomyces sp. E14 - gyrB	ZP_06708903.1
Streptomyces sp. SPB74 - gyrB	ZP_06824684.1
S. viridochromogenes DSM - *gyrB*	ZP_07306970.1
S. griseoflavus Tu4000 - *gyrB*	ZP_07312003.1
S. ghanaensis - gyrB	ZP_06577902.1
Streptomyces sp. C - gyrB	ZP_07287909.1

2.27.4 Protein secondary structure prediction

To predict protein secondary structures, amino acid sequences of the relevant proteins were submitted to both Jpred (Cole, Barber et al. 2008) and psipred (Bryson, McGuffin et al. 2005).

Chapter - 3

Bioinformatics

3.1 Introduction

With the significant number of complete bacterial genomes now available it is possible to use amino acid sequence comparisons to predict the possible structure, function and evolution of genes. Similarity to conserved sequences helps predict functions of uncharacterised genes and find well described orthologs. In this chapter the DksA paralogs within *S. coelicolor* are investigated looking at domain similarities with other proteins, the analysis of gene loci within other *Streptomyces* and relatedness to homologs in other *Streptomyces* species, which have fully annotated genomes.

3.2 Genes encoding DksA like proteins

A BlastP search of *S. coelicolor* revealed there are three paralogs of the *E. coli* DksA protein: SCO2075, SCO6164 and SCO6164 with e-values of $8x10^{-11}$, $2x10^{-08}$ and $1x10^{-06}$ respectively. A paralog is the result of gene duplication within the genome where the duplicated gene evolves a new function. The most conserved of the three, however, has an elongated N-terminal domain extending an additional 93 amino acids (Figure 3.1), which, interestingly, contains a histone H1-like DNA binding domain (Figure 3.7). The other two DksA paralogs, SCO6164 and SCO6165, are situated next to each other, and both have a slightly shorter N-terminal domain than *E. coli* DksA. The *E. coli* DksA protein has a C4 zinc finger domain near the C-terminus and two highly conserved aspartic acid residues at position 71 and 74 which stabilise the Mg^{2+} ions (Perederina, Svetlov et al. 2004). The crystalline structure of DksA revealed a conserved secondary structure similar to the transcription factor GreA which interacts with the secondary channel of RNA polymerase (Perederina, Svetlov et al. 2004).

Using the sequence alignment software ClustalW2, the putative protein products encoded by *sco2075*, *sco6164* and *sco6165* were aligned to look at amino acid conservation (Figure 3.1). The conserved aspartic acid residues within the *E. coli* DksA are also conserved in SCO2075. However, in SCO6164 both the acidic polar aspartic acid residues have been replaced with the neutral non polar amino acid leucine and in SCO6165, one aspartic acid residue is conserved and the other has been replaced by isoleucine. This possibly suggests SCO6164 and SCO6165 are unable to stabilise Mg^{2+}. In all three paralogs the four conserved cysteine residues which form the C4 zinc finger domain are all conserved.

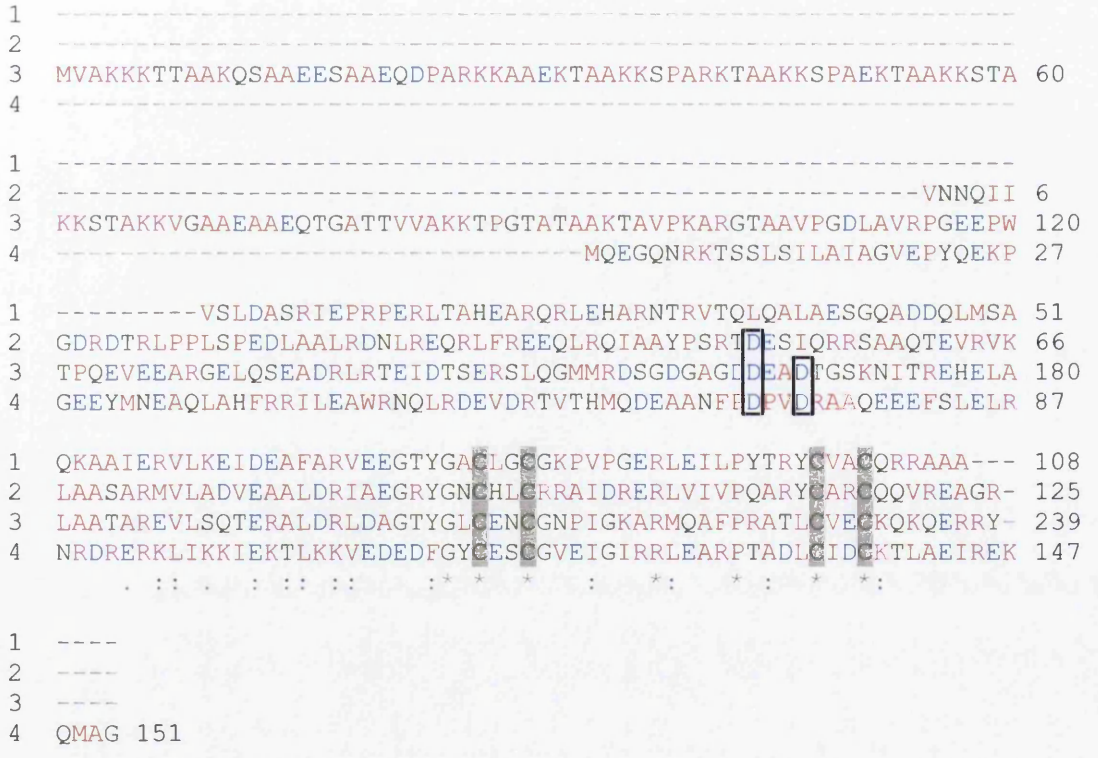

Figure 3.1: Clustalw2 multiple alignment output of SCO6164 (1), SCO6165 (2), SCO2075 (3) and *E. coli* DksA (4). Highlighted in grey are the 4 conserved cysteine residues that form the C4 zinc finger motif and boxed are the conserved aspartic acid residues which have been shown to be required for Mg^{2+} stabilisation of ppGpp. Colours indicate: red- Small (small+ hydrophobic (including aromatic -Y)); blue- acidic; magenta- basic; green- Hydroxyl + sulfhydryl + amine + hydrogen.

In order to analyse the primary amino acid sequences further and to compare the paralogs with the *E. coli* DksA protein, the online secondary structure prediction server, Jpred was employed. The putative primary amino acid sequences of the paralogs SCO2075, SCO6164, SCO6165 and *E. coli* DksA were run in Jpred and the output displayed in Figure 3.2. The *E. coli* DksA crystal structure revealed a globular region consisting of the N- and C- terminal regions (amino acids (AA) 7–33 and 110–134) and a central coiled coil region consisting of two long N- and C-terminal α helices (AA 35–68 and 75–109) connected by a linker at the tip of the coiled coil that comprises two residues (69 and 70) in an extended conformation and an α-helical turn (α turn, residues 71 and 75) (Perederina, Svetlov et al. 2004).

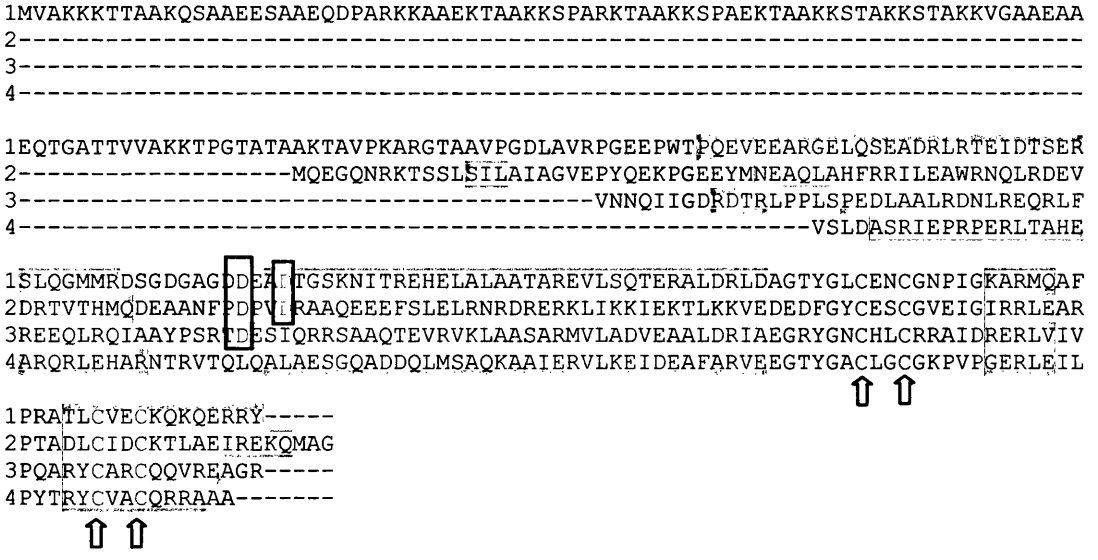

Figure 3.2: JPRED output of predicted secondary structures of SCO2075 (1), *E. coli* DksA (2), SCO6165 (3) and SCO6164 (4). Helix is shown in light grey, C4 zinc finger cysteine residues are shown by the arrows and highly conserved aspartic acid residues boxed which are present in SCO2075.

Interestingly the N-terminal long α helix extends further towards the N-terminus by three residues (starting at AA 32) in the predicted secondary structure of *E. coli* when

compared to the crystal structure data, which must be an error within the secondary structure prediction program. Apart from this variation in helix length between the prediction and the crystalline structure (Perederina, Svetlov et al. 2004), the fundamental secondary structure of two large α helices and two small C-terminal helices appears to be conserved. However, there does appear to be significant variation in length of the N-terminal coiled domain with SCO2075 having the longest by 93 amino acids compared to the *E. coli* DksA and the paralogs SCO6164 and SCO6165 being 36 and 21 amino acids shorter respectively.

3.3 Genome organisation of *sco2075* loci in *Streptomyces*

Conserved gene clusters are a prominent feature of bacterial genomes, and are kept in close proximity due to natural selection pressures on the genes (Demerec 1959). *sco2075* is within the central region of the *S. coelicolor* linear chromosome which spans from 1.5Mb to 6.4Mb, where essential genes for growth and propagation are located and where the most conservation is observed throughout *Streptomyces* genomes (Bentley, Chater et al. 2002; Ventura, Canchaya et al. 2007). *sco2075* is in close proximity to the *ftsZ* gene (six genes upstream in *S. coelicolor*) which is an essential protein for sporulation (McCormick, Su et al. 1994). As a result of the proximity of *sco2075* to *ftsZ*, the genomic location of *sco2075* and its homologs were looked at in other *Streptomyces* species (Figure 3.3). It is evident that the homologs of *sco2075* have all been maintained in a similar relative position to *ftsZ* with a maximum variation of three genes between a given *sco2075* homolog and the respective *ftsZ* gene (Figure 3.3). However, all the additional genes are hypothetical proteins, raising the possibility that the additional

genes may be errors in open reading frame predictions in the respective annotated genomes. This nevertheless shows that there is conservation of the locus throughout *Streptomyces* species and indicating a probable important function in *Streptomyces* species.

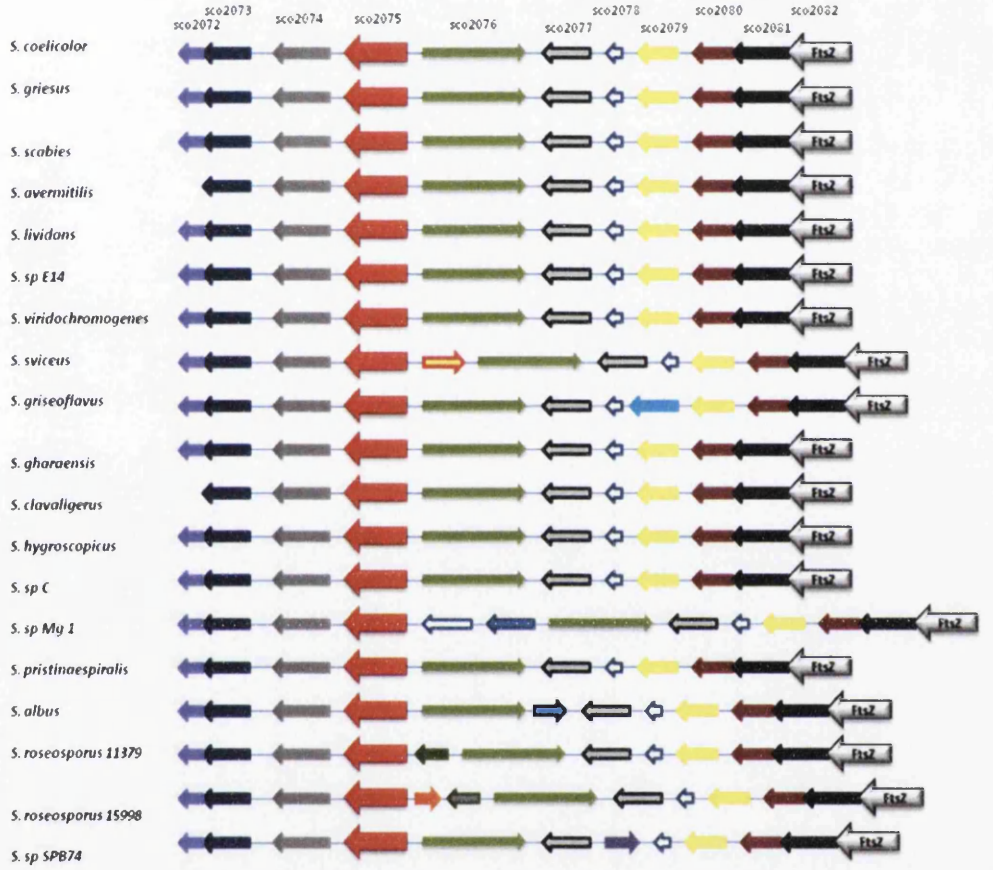

Figure 3.3: Comparison of *sco2075* loci from different species of *Streptomyces*. *sco2075* and its homologs are shown in red, *ftsZ* in light grey. *sco2072*- Acetyltransferase (GNAT) family protein, *sco2073*- putative ribosomal large subunit pseudouridine synthase, *sco2074*- putative signal peptidase, *sco2075*- putative DNA-binding protein, *sco2076*- putative isoleucyl-tRNA synthetase, *sco2077- divIVA*, *sco2078*- putative membrane protein, *sco2079*- conserved hypothetical protein, *sco2080*- conserved hypothetical protein, *sco2081*- conserved hypothetical protein, *sco2082- ftsZ*. All additional proteins in the other *Streptomyces* species shown are hypothetical proteins. Figure not to scale.

The paralogs *sco6164* and *sco6165,* however, are not as well conserved in *Streptomyces* with 8 species containing *sco6164* and *sco6165* orthologs (at time of

writing), which show a lower degree of conservation compared to 34 species containing *sco2075* orthologs (at time of writing). A recent paper has shown that *sco6165* is co-transcribed with *sco6166*, an *mreB*-like gene, which is highly expressed only during vegetative growth (Heichlinger, Ammelburg et al. 2011). However no information is currently available for *sco6164* expression.

3.4 Phylogenetic analysis

A BlastP search of actinobacteria genome sequences using the full length protein sequence of SCO2075 was performed revealing a number of genomes containing more than one DksA-like protein. To look at the relationship between the three paralogs within *Streptomyces,* only genomes which contained more than one DksA were used to construct phylogenetic trees. A bootstrapped neighbour joining tree with 5000 replicates was constructed after aligning the sequences using the default settings of gap opening penalty 10 and gap extension penalty 1 for both pair wise and multiple alignment (Figure 3.4).

As can be seen from the tree in Figure 3.4, there are at least three clades that emerge containing groups of proteins related to SCO2075, SCO6164 or SCO6165. A clade is a group of organisms/ genes/ proteins which descend from a single common ancestor. Due to the close proximity of *sco6164* and *sco6165* in the genome and from the phylogenetic tree where their homologs produce a sister clade, it can be concluded that at some point a gene duplication event has occurred as they appear to share a common ancestral gene, with the potential of the ancestral gene being a descendant of the more highly conserved *sco2075* gene or the result of lateral acquisition. A sister clade is when one member of a

pair of clades originating when a single lineage splits into two, sharing an exclusive common ancestry and are mutually most closely related to one another in terms of common ancestry.

As a result of gene duplication or lateral transfer, they are potentially free from selection pressures, which could possibly explain why the highly conserved aspartic acid residues are absent within SCO6164 and SCO6165, although interestingly the four conserved cysteine residues, which form the zinc finger domain, are retained.

As SCO2075 is the only paralog in *S. coelicolor* to have an extended N-terminal domain and to see whether the N-terminal and C-terminal domains co-evolved or evolved separately, phylogenetic trees were constructed using the amino acid sequences from twelve *Streptomyces* species and one *Janibacter* species used in the previous analysis (Figure 3.4). Two trees were constructed using the first 108 AA which contains the extended N-terminal domains (histone like) for one tree (Figure 3.5A) and the remainder of the protein (131 AA) containing the C-terminal domains (DksA like) for the second tree (Figure 3.5B). As previously, sequences were aligned using ClustalW2 and bootstrapped neighbour joining (NJ) phylogenetic trees constructed using the default settings of gap opening penalty 10 and gap extension penalty of 1 for both pair wise and multiple alignment were used for the analysis with 5000 replicates using Mega 5.0 software.

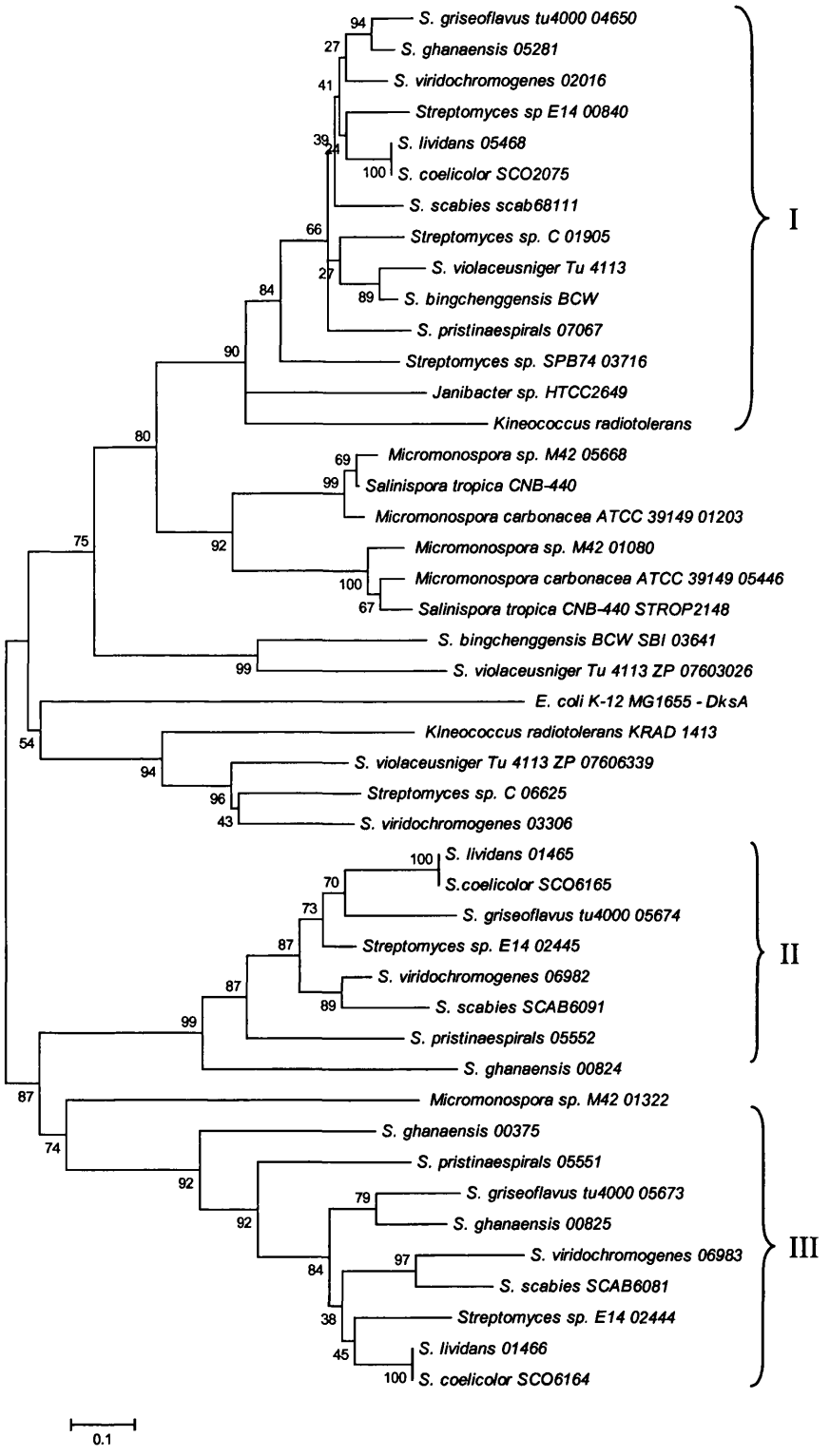

Figure 3.4: Bootstrap neighbour joining (NJ) phylogenetic tree with 5000 replicates of amino acid sequences from genomes which contain multiple DksA like proteins from actinobacteria and *E. coli*. Three clades are bracketed containing SCO2075 like proteins (I), SCO6165 like proteins (II) and SCO6164 like proteins (III).

If the two terminal domains co-evolved, the positions of each species would remain relatively in the same position and branched with the same species. Alternatively if the two domains evolved separately then the two trees would be significantly different with no correlation between one another.

(A)

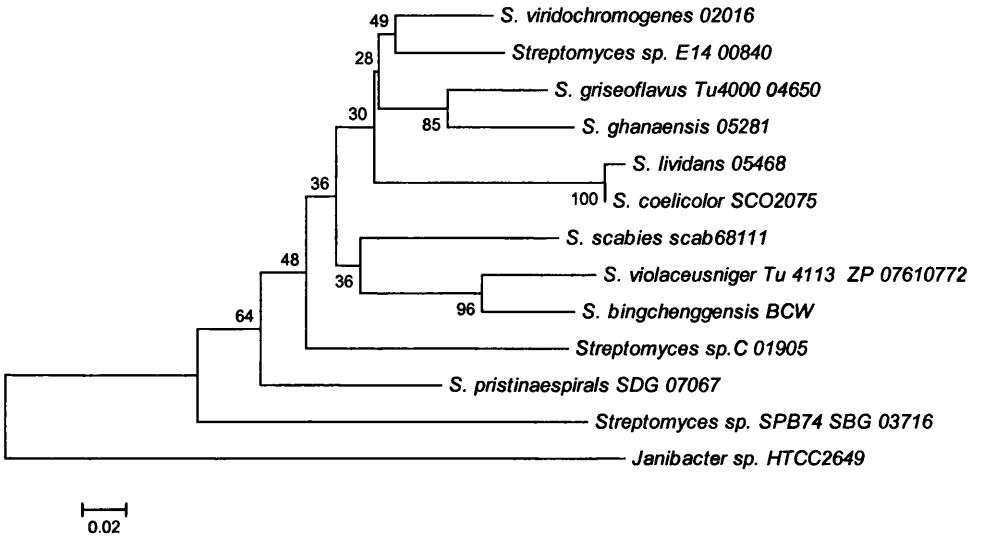

(B)

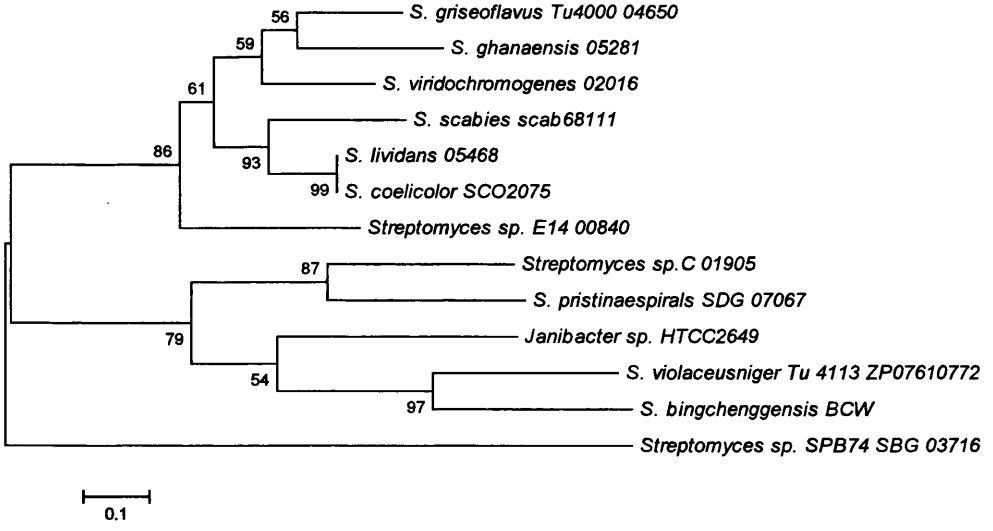

Figure 3.5: Bootstrapped NJ phylogenetic tree analysis of amino acid sequences from N-terminal histone-like domain (A) of SCO2075 and homologs including paralogs from *Janibacter* and C-terminal DksA-like domain (B) with all the same protein sequences with 5000 replicates.

The two NJ phylogenetic trees in Figure 3.5 based on the N-terminal domain (A) and C-terminal domain (B), appear to have some correlation between some species with the N- and C-terminal portion of the proteins clustering with the same species in both trees. *S. coelicolor* and *S. lividans, S. violaceusniger* and *S. bingchenggensis, S. ghanaensis* and *S. griseoflavus* cluster together in both trees. There is no correlation between the remaining species when comparing the two NJ phylogenetic trees.

The resulting similarities between the two phylogenetic trees could be a result of how close the relationship is between the strains prior to speciation and potentially the N-terminal domain evolved/ and or evolving separately from the more defined C-terminal DksA like domain of the protein.

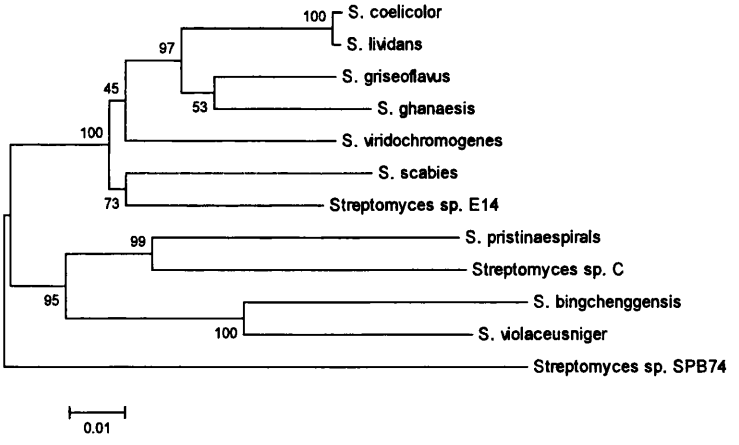

Figure 3.6: Bootstrapped NJ phylogenetic tree analysis of *gyrB* homologs from *Streptomyces* strains used in the phylogenetic analysis in Figure 3.5).

In order to investigate this further, a NJ phylogenetic tree was constructed for the *Streptomyces* species using the gene *gyrB* (Figure 3.6). As previously, sequence alignments were constructed in ClustalW2 and a bootstrapped NJ phylogenetic tree was constructed using the default settings of gap opening penalty 10 and gap extension penalty of 1 for both pair wise and multiple alignment were used for the analysis with

5000 replicates using Mega 5.0 software. From the NJ phylogenetic tree in Figure 3.6, which is based on the *gyrB* gene, it appears that the correlation between *S. coelicolor* and *S. lividans, S. violaceusniger* and *S. bingchenggensis, S. ghanaensis* and *S. griseoflavus* does appear to be the result of the proximity of their relationship prior to speciation.

3.5 A novel DNA binding domain (DBD)?

The N-terminal domain of SCO2075 has a eukaryotic histone H1-like domain with a sequence similar to H-NS-like protein from *mycobacterium*, HU-like protein from *Mycobacterium* and *Streptomyces* and H1 HC2 like proteins from *Chlamydia* (Figure 3.7A). The alignments in Figure 3.7A are separated, as SCO2075 has not been defined into a specific family of DNA binding proteins and a combined alignment greatly reduced the number of conserved amino acids when comparing to three different families of DNA binding protein. Blast searches result in E-values of $1x10^{-14}$ with H1 Hc2 like protein from *C. trachomatis,* $2x10^{-09}$ with Rv3852 (H-NS-like protein from *M. tuberculosis*) and $5x10^{-14}$ with SCO5556 (HU-like protein of *S. coelicolor* with an extended C-terminal domain).

The N-terminal domain of SCO2075 is a highly basic sequence of amino acids with a pI of 10.5 and this alone suggests the likely probability of being able to bind to DNA. There are sequence similarities to the pentapeptide motif consisting of three small or aliphatic side chained amino acids followed by two basic residues (using single letter amino acid code the first three amino acids can be A, P, G, S, T, V and the final two either R or K) of the histone H1 Hc2 like DNA binding protein from *Chlamydi*a (Perara,

Ganem et al. 1992). Like the *Chlamydia* histone-like protein, the conservation of the number of repeats is varied, with some homologs only containing one pentapeptide. The location of this single pentapeptide appears to be highly conserved within the homologs of SCO2075 starting at position 81 shown in Figure 3.7B, while others contain several more pentapeptide repeats than SCO2075. What does differ, however, between the *Chlamydia* proteins and SCO2075 is that there appears to be tetrapeptide repeats within the homologs of SCO2075 (Figure 3.7B) which are found in other histone-like proteins in *Streptomyces* and *M. tuberculosis*.

```
A1)
gi|ADD14367.1     MLGVQKKCSTRKTAARKTVV-----RKPAAKKTAAKKAPVRKVAAKK---
SCO2075           MVAKKKTTAAKQSAAEESAAEQDPARKKAAEKTAAKKSPARKTAAKKSPA
                  *:. :*. :::::**.::..     ** **:******:*.**.****

gi|ADD14367.1     --TVAKKATAKKAPVRKV----AAKKTVAKKATAKKAPVRKAVAKKTV--
SCOSCO2075        EKTAAKKSTAKKSTAKKVGAAEAAEQTGATTVVAKKTPGTATAAKTAVPK
                    *.***:****:..:**    **::* *....***:*   :.**.:*

gi|ADD14367.1     ARKTVAKK-TVAAR---KPVAKRVASTKKSSIAVKAGVC
SCOSCO2075        ARGTAAVPGDLAVRPGEEPWTPQEVEEARGELQSEADR-
                  ** *.*    :*.*   :* : : ..  :..:  :*.
A2)
SCO5556        SGSKKLPKNDIAVKKAPKGSLSGPPPTISKAAGKKAAAKKATGAAKKTTGAAKKTSAAAK
SCO2075        ----------------------------------MVAKKKTTAAKQS--AAEES--AAE
                                                  .*** * ***::  **:::  **:
SCO5556        KTTAKKTTGAAKTTAKKTTAKKSAAKTTTAAAKKTAAKKAPAKKATAKKAPAKKSTARKT
SCO2075        QDPARKKA-AEKTAAKKSPARKTAAKKS--PAEKTAAKKSTAKKSTAKKVGAAEA-AEQT

               : .*:*.: * **:***:.*:*:***.:  .*:******:.***:****. * :: *.:*

SCO5556         TAKKATARKK 130
SCO2075         GATTVVAKK- 86
                 *....*:*
A3)
rv3852         -----MPDPQDRPDSEPSDASTPPAKKLPAKK-AAKKAPARKTPAKKAPAKKTPAKGAKS
SCO2075        MVAKKKTTAAKQSAAEESAAEQDPARKKAAEKTAAKKSPARKTAAKKSPAEKTAAK--KS
                     . . .:. :* * *.  **:* .*:* ****:*****.***:**:**.**  **

rv3852          APPKPAEAPVSLQQRIETNGQLAAAAKDAAA
SCO2075         TAKKSTAKKVGAAEAAEQTGATTVVAKK---
                :. *.:   *.  :  * .*  :..**.
```

B)

```
MVAKKKTTAAKQSAAEESAAEQDPARKKAAEKTAAKKSPARKTAAKKSPAEKTAAKKSTAKKSTAKKVGAA
EAAEQTGATTVVAKKTPGTATAA
```

Figure 3.7: A) Clustalw2 alignment of the N-terminal histone-like domain of SCO2075 with full length *Chlamydia trachomatis* H1 Hc2 protein (A1), extended C- terminal domain of SCO5556 (A2) and the DNA binding domain of Rv3852 (A3). B) N- terminal domain sequences of SCO2075 showing pentapeptide repeats in light and dark grey and tetrapeptide similar to other histone-like proteins from prokaryotes shown in yellow. Underline shows the most highly conserved pentapeptide.

The H-NS-like protein such as Rv3852 in *M. tuberculosis* has no sequence homology to a conventional H-NS such as that of *E. coli*, however, it also appears to have a histone-like sequence in the N- terminal domain of the protein like SCO2075. However, from experimental data the protein has similar characteristics to *E. coli* H-NS (Werlang, Schneider et al. 2009). Interestingly the histone-like domain of Rv3852 is like that of SCO2075 and is highly variable between other *Mycobacterium* species (Sharadamma, Harshavardhana et al. 2010).

To determine whether the DNA binding domain of SCO2075 is related to an existing predefined protein or is novel, several SCO2075 orthologs were aligned with an equivalent number of HU-like, H-NS-like and H1 Hc2-like proteins and a NJ bootstrapped phylogenetic tree constructed with 5000 replicates using the default settings of gap opening penalty of 10 and gap extension penalty of 1 for both pair wise and multiple alignments. The NJ phylogenetic trees were left unrooted in order to make it easier to define SCO2075 within an existing group and is shown in Figure 3.8. Using the full length sequences of SCO2075 and its orthologs, the orthologs form their own clade as an outgroup, with no relationship to the other DNA-binding proteins previously mentioned (Figure 3.8A). However, when the C-terminal domain is deleted from the SCO2075 sequence and its orthologs and the same analysis carried out as with the full length sequences, there appears to be some sequence relationship with the

actinobacterial HU proteins with extended C-terminal domains as they form a sister clade (Figure 3.8B). This indicates the possibility of the HU-like proteins sharing some common ancestral gene, with the histone H1-like proteins from *Chlamydia* diverging before the HU-like proteins and SCO2075 orthologs split.

From this analysis there appears to be some sort of relationship between SCO2075 orthologs, the actinobacterial HUs with extended C-terminal domains and the *Chlamydia* H1 Hc2 proteins. The similarity with the HU proteins is obviously related to the sequence similarity with the extended C-terminal portion of these proteins and the *Chlamydia* H1 HC2. However, it does not clearly define the function of this N-terminal DNA domain in SCO2075, with some similarities to the Hlp protein from *M. Smegmatis.* There is a possibility of this region being involved in repair/ recombination or the regulation of gene activity during stress conditions (Mukherjee, Bhattacharyya et al. 2008).

Due to the sequence similarity with the *E. coli* DksA protein, it is possible that the extended N-terminal DNA binding domain portion of SCO2075 is due to lateral gene acquisition and subsequent fusion possibly with H1 Hc2-like protein of *Chlamydia* or even actinobacterial HU-like protein with an extended C-terminal DNA binding domain which also contains a similar motif of pentapeptide repeats.

(A)

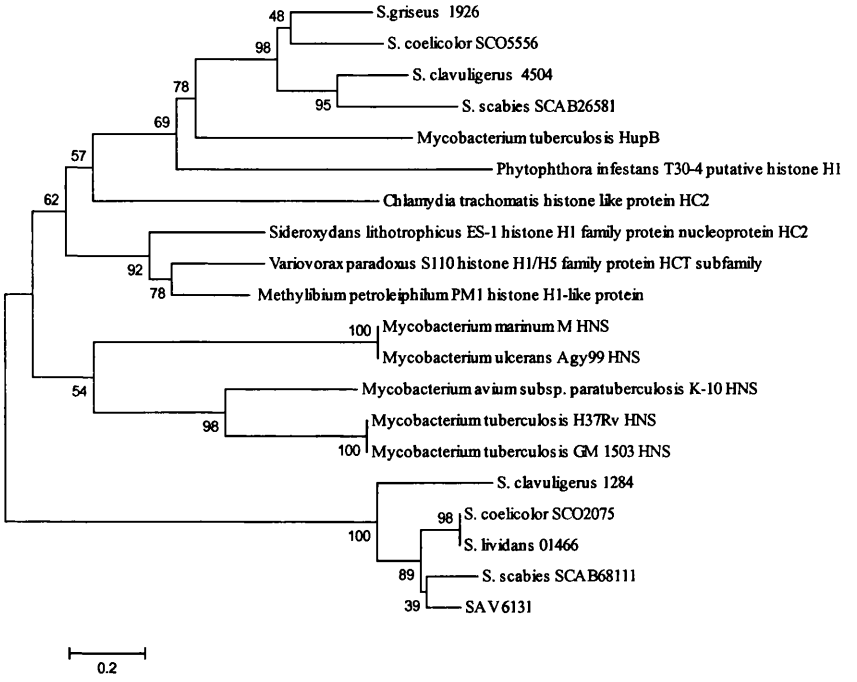

(B)

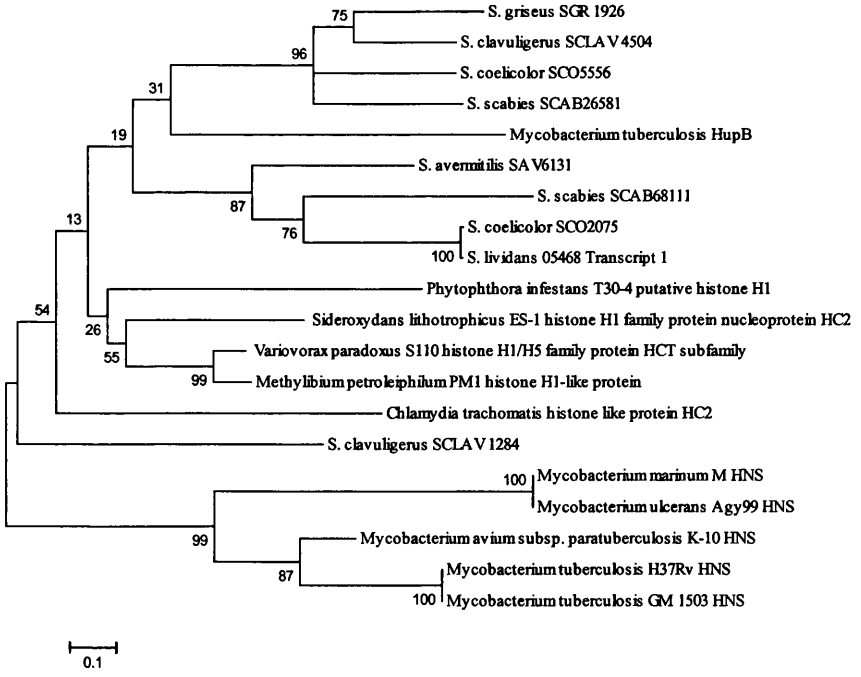

Figure 3.8: Phylogenetic analysis of the N-terminal domain of SCO2075 with predefined nucleoid associated proteins. A) Phylogenetic analysis using full length SCO2075 and orthologs. B) Phylogenetic analysis of N-terminal domain portion (first 108AA) with the same nucleoid associated proteins as A. Bootstrap numbers are displayed at the root of each branch.

3.6 Summary

SCO2075 is the most conserved DksA paralog with an extended N-terminal domain, with SCO6164 and SCO6165 missing two essential aspartic acid residues. However secondary structure predictions based on the putative protein products show similar structures to that of *E. coli* DksA, with variations in the helix lengths of up to eight amino acids in the N-terminal large helix which could alter how far the protein protrudes into the RNA polymerase's secondary channel, potentially affecting the ability to stabilise ppGpp.

sco2075 loci appear to be conserved in the *Streptomyces* species analysed in relation to the essential cell-division gene *ftsZ*. SCO6164 and SCO6165 form a sister clade and are likely a result of gene duplication forming an outgroup in relation to the traditional DksA-like proteins such as that of *E. coli*. However, SCO2075 appears to be a direct descendent of the ancestral DksA, residing in the clade with traditional DksAs.

Evolution of the N- and C-terminal domains appears to be separate, with the closest related species clustering in both phylogenetic trees. The N-terminal domain is highly basic and is related to the extended C-terminal portion of actinobacterial HUs such as HupS of *S. coelicolor* and H1 Hc2 of *Chlamydia*. Possible DNA binding motifs include pentapeptide repeats and a tetra peptide motif within the most basic region of the domain.

Chapter - 4

Phenotyping

4.1 Introduction

Construction of an ordered cosmid library mutagenised with Tn*5062* has accelerated production and subsequently the availability of mutant strains in *S. coelicolor* (Bishop, Fielding et al. 2004). By producing multiple insertions in a single gene there is the potential of not only disrupting the gene in question but also the possibility of looking at the effect of domain disruption in multi domain proteins. Contained in Tn*5062* is a promoterless *egfp*, when inserted into the correct orientation allows transcriptional coupling of the *egfp* to the promoter of interest allowing a quantitative analysis of gene expression.

4.2 Phenotypic analysis of an *sco2075*⁻ mutant strain

DSCO2075 mutant was previously produced using the transposon mutated cosmid 4A10.1.A08, which has transposon Tn*5062* inserted into *sco2075*. For phenotypic analysis of the DSCO2075, *S. coelicolor* M145 and DSCO2075 strains were plated on a number of commonly used agar media. The DSCO2075 mutant was then visually assessed for any variation from parental strain M145 such as antibiotic production and spore pigmentations plated on LB, 2xYT, SMMS, SFM, minimal media with glucose or mannitol, R5 and NMMP with and without 250mM KCl. All plates were incubated at 30°C for 3 days. DSCO2075 grew similarly to wild type in spore pigmentation and antibiotic production, except when plated on NMMP with 250mM KCl with a slight delay in sporulation and a possible increase in actinorhodin production. To confirm that the phenotype of DSCO2075 is not the result of polar effects on downstream genes, DSCO2075 was complemented by plasmid pSH2075,

which contains a single copy of *sco2075* and promoter region that integrates at the ϕC31 *att* site in the *S. coelicolor* chromosome (figure 4.2). This also confirmed that the promoter for *sco2075* is within the 650bp upstream region.

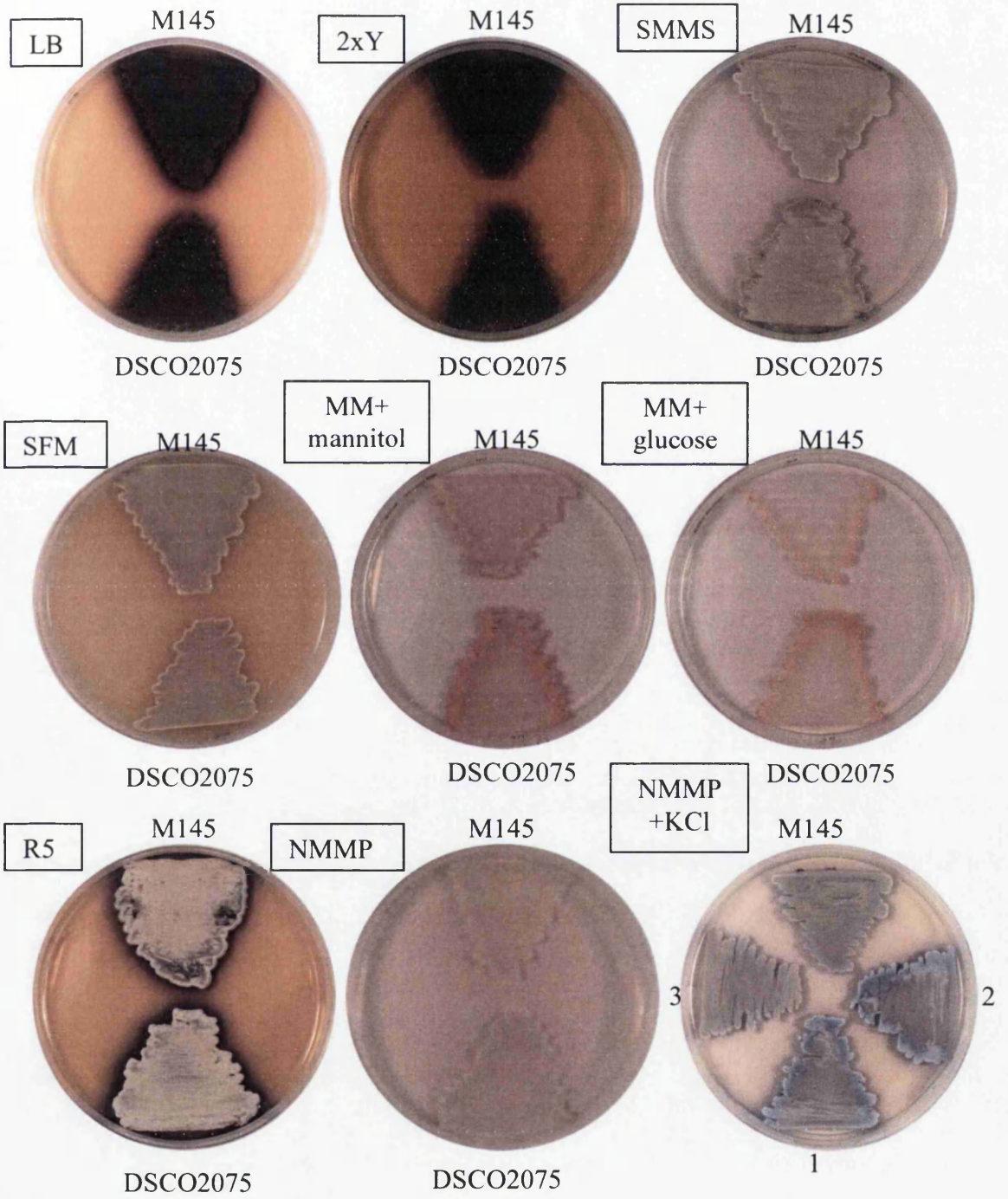

Figure 4.1: Phenotypic analysis of DSCO2075 mutant and parental strain *S. coelicolor* M145 on different media. Strains were grown for 3 days at 30° C on LB, 2xYT, SMMS, SFM, MM + mannitol, MM + glucose, R5, NMMP, NMMP + 250mM KCl. The name of each medium is indicated in rectangle. 1- DSCO2075, 2- DSCO2075/pSH152, 3- DSCO2075/pSH2075.

To construct a plasmid with *sco2075* and its native promoter, plasmid pAL2075 was digested with *Sal*I and *Avr*II, to produce a 1.9Kbp fragment containing *sco2075* and a partial fragment of *sco2076.* The fragment was blunt-ended, purified and cloned into plasmid pSH152 which was restriction digested with *Eco*RV. Blue white selection was used to obtain plasmid pSH2075 (Figure 4.2). Restriction digest and sequencing was used to confirm plasmid pSH2075.

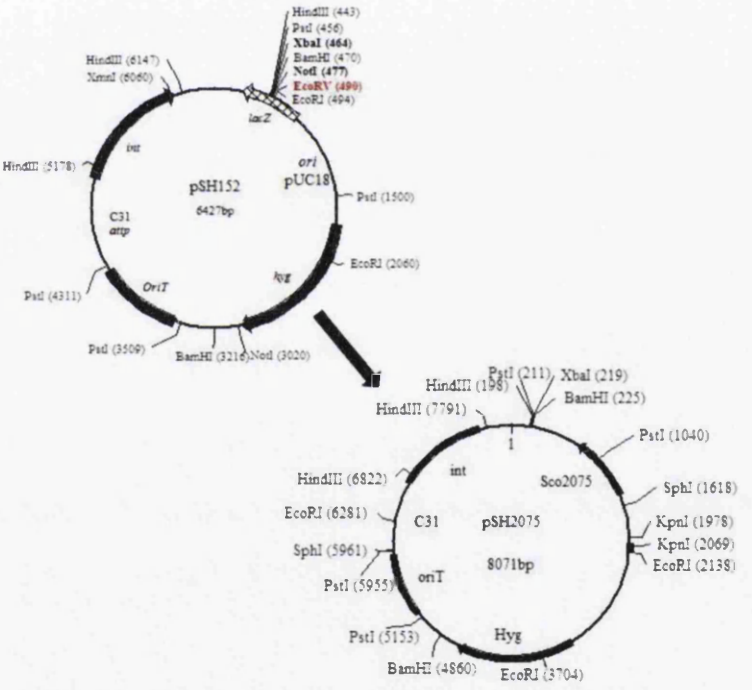

Figure 4.2: construction of plasmids pSH2075.
Plasmid pAL2075 was digested with *Sal*I and *Avr*II and blunt-ended to obtain a 1.9Kbp fragment containing *sco2075* and 650bp upstream region while pSH152 was digested with *Eco*RV. Blue white selection was used to obtain plasmid pSH2075.

4.3 Oxidative stress

Bacterial cytoplasms are maintained in a reduced state which prevents the inactivation of active site thiols and inappropriate disulfide bridge formation in proteins. (Paget, Kang et al. 1998; Arner and Holmgren 2000). In *Streptomyces*, thiol oxidation is regulated by thioredoxin and σ^R/ RsrA is part of this system that senses and responds to thiol oxidation (Kang, Paget et al. 1999). A *sigR* mutant strain in S. coelicolor has a reduced level of disulfide reductase activity and an inability to induce activity on exposure to a thiol oxidising agent (Paget, Kang et al. 1998).

Diazene dicarboxylic acid bis (N, N-dimethylamide) or now commonly called diamide is a thiol specific oxidising agent that causes toxic formation of cytoplasmic disulfides in low molecular weight thiols and proteins (Kosower and Kosower 1995). Thiol stress was analysed by overlaying nutrient agar plates with soft nutrient agar containing fresh spores of either parental strain M145 or the mutant strain DSCO2075 (Paget, Kang et al. 1998).

(A)

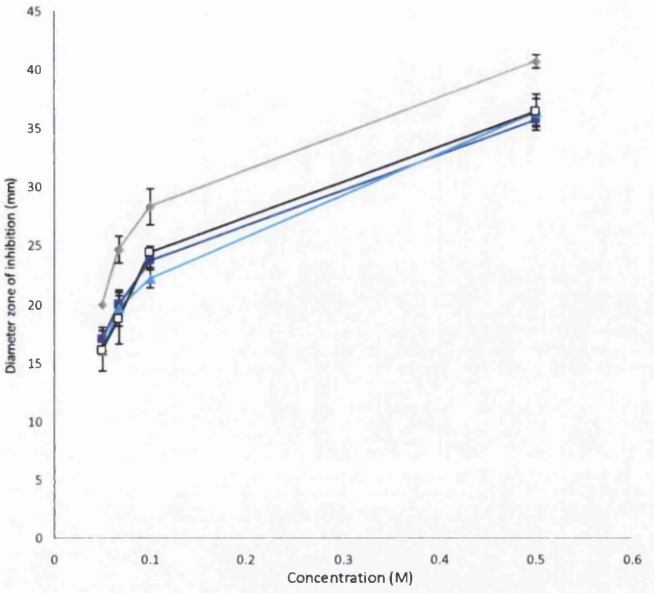

(B)

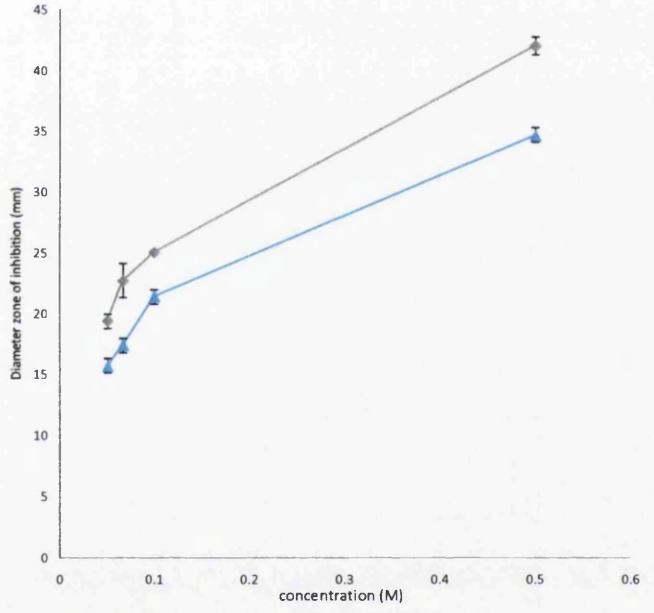

Figure 4.3: Zone of inhibition analysis of thiol stress.
Lawns of the specified strain were generated by overlaying nutrient agar plates with soft nutrient agar containing fresh spores. Immediately after plating, paper discs soaked in a variety of concentrations of diamide were added, and plates were photographed after 24 h incubation at 30°C. Zone diameters were measured in mm. (A) Comparison of DSCO2075, DSCO2075 complemented with plasmid pSH2075 (single copy *sco2075*) and pRB2075 (high copy number plasmid containing single copy *sco2075*) compared to parental strain M145. Grey diamonds – DSCO2075, light blue triangles M145, blue squares DSCO2075/ pSH2075, open squares DSCO2075/ pRB2075. (B) As above with the exception of 250mM KCl added to the media. Grey diamonds – DSCO2075 and light blue triangles - M145.

Three replicates of each concentration of diamide were used for the analysis of the zones of inhibition, where the diameters of the zones were measured in mm. There is clearly an increase in the zone of inhibition of the DSCO2075 mutant strain compared to the parental strain shown in the graph in Figure 4.4A which is reverted to wild type when complemented with a single integrated copy of the *sco2075* gene and native promoter, pSH2075, or *sco2075* gene and native promoter in a multicopy plasmid pRB2075 based on pUWL219.

As there appears to be a phenotype on medium with osmolyte as shown in Figure 4.1, diamide stress was looked at under osmotic stress. The experiment was repeated with 250mM KCl added to both nutrient agar and soft nutrient agar. However, no discernable difference was observed when comparing the data with osmolyte (Figure 4.3B) and without osmolyte (Figure 4.3A).

As σ^R has been implicated as a main player in the sensing and responding to thiol stress in *Streptomyces* (Paget, Kang et al. 1998), qRT-PCR was used to analyse the transcription of *sigR* in the parental strain M145 and the mutant strain DSCO2075 to see if the phenotype under thiol stress is linked to a change in *sigR* transcription or whether SCO2075 plays a more indirect role.

NMMP plates with cellophane discs were innoculated with either M145 or DSCO2075 and incubated over night at 30°C. The cellophane discs were then transferred to either NMMP or NMMP with a dimade concentration of 0.5mM (final concentration) diamide (Paget, Kang et al. 1998) and incubated at 30^0C for either 15 or 30 minutes.

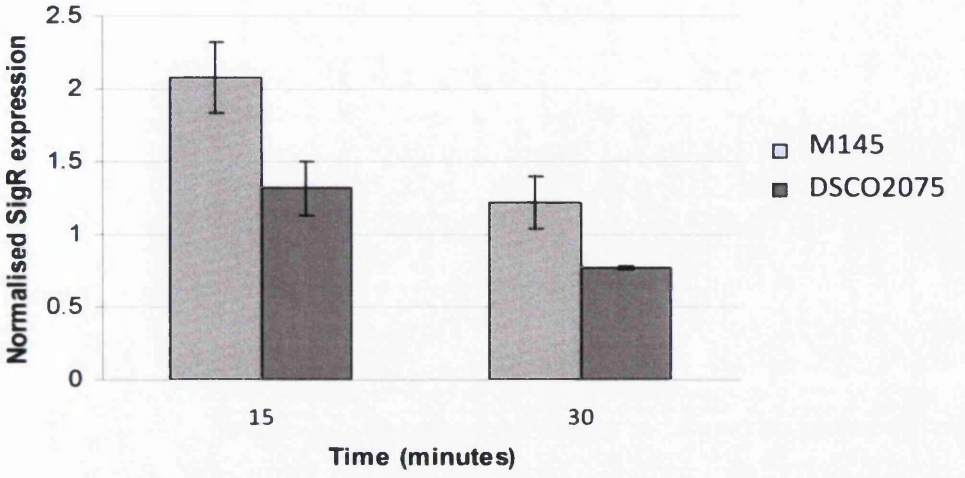

Figure 4.4: QRT-PCR analysis of *sigR* transcripts at 15 and 30 minutes after induction of thiol stress in M145 and DSCO2075. The Data was normalised using *hrdB* as a control. Strains were grown over night on NMMP and transferred to NMMP + 0.5mM diamide.

S. coelicolor hrdB was used to normalise *sigR* transcription (primers in Table 2.8), with three biological and three technical replicates including RNA negative controls and a dilution series of genomic DNA used to calculate a standard curve and the data collected from this analysis is displayed in Figure 4.4. As can be seen from Figure 4.4, *sigR* expression is reduced in the DSCO2075 mutant strain when compared to the parental strain M145 at both 15min and 30min time points resulting in a 0.62 and 0.6 fold change respectively. The data was analysed for statistical significance using One Way Anova in SPSS. Both 15min and 30min time points gave a $P<0.05$ showing statistical significance.

Peroxide oxidative stress was carried out on SFM agar containing 0-1mM H_2O_2. As can be seen from Figure 4.5, which shows the phenotypic analysis of addition of H_2O_2 to the SFM, there is a dose-dependent growth retardation with the mutant strain

DSCO2075 which is fully recovered with complementation via integrative plasmid pSH2075, and not the empty vector pSH152.

Figure 4.5: M145, DSCO2075 and DSCO2075 either containing empty vector pSH152, or complementation plasmid pSH2075 were plated on SFM plates containing either 0, 250μM, 500μM, 750μM or 1mM of H_2O_2 and incubated at 30°C for 5 days.

4.4 Phenotyping dksA paralog mutants

The mutant strains of *sco6164* (DSCO6164) and *sco6165* (DSCO6165) were previously produced using the transposon mutated cosmids 1A9.1.D10 and 1A9.1.G10 respectively. DSCO6164 and DSCO6165 lack actinorhodin production on LB and 2xYT with a lesser effect with respect to DSCO6165 (Figure 4.6).

Phenotypic analysis was also conducted on minimal media (using: mannitol, glucose and glycerol as carbon sources), R2YE, R5, SFM and supplemented minimal medium, solid (SMMS) and calcium dependent antibiotic (CDA) production was assessed. However, no discernable phenotype was observed compared to wild-type M145 (results not shown).

The phenotype on LB agar was also reproduced on LB without sodium chloride for DSCO6164, however DSCO6165 appears to have an initial early production of actinorhodin compared to wild type but does not have full phenotypic recovery (Figure 4.6).

To explore this further, sodium chloride was replaced with magnesium chloride and potassium chloride. Although potassium chloride produced no change in phenotype on LB with NaCl compared to wild type (result not shown), magnesium chloride caused phenotype recovery. On LB agar plates with sodium chloride replaced with magnesium chloride, DSCO6164 and DSCO6165 has restored actinorhodin production similar to parental strain M145. As DSCO6164 had a more profound phenotype, the remaining analysis was conducted exclusively on DSCO6164.

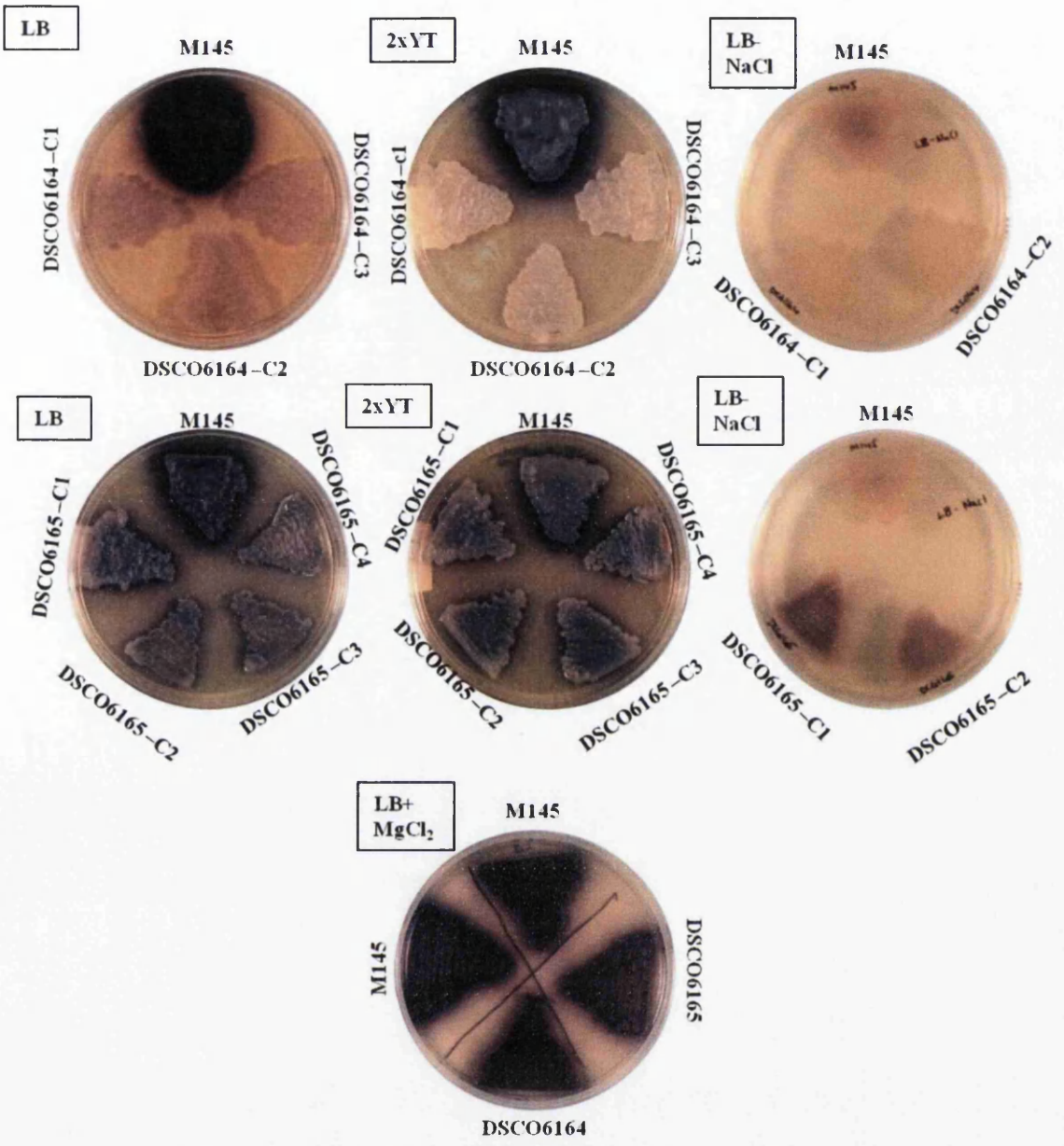

Figure 4.6: Phenotypic analysis of DSCO6164 and DSCO6165 mutant strains with parental strain *S. coelicolor* M145. Strains were grown for 72 days at 30° C on LB, 2xYT and LB with 86mM $MgCl_2$. Images of LB without NaCl taken at 48h and are photos of the bottom of the plates. The name of each medium is indicated in rectangle. C denotes different clones of the same strain.

4.5 Complementation of DSCO6164

To initially complement the mutant phenotype, the mutant strain was complemented with the complete possible operon and upstream region using the plasmid

pALD12R which contains a 3800bp fragment containing the gene cluster: *sco6164*, sco*6165* and *sco6166* and upstream region.

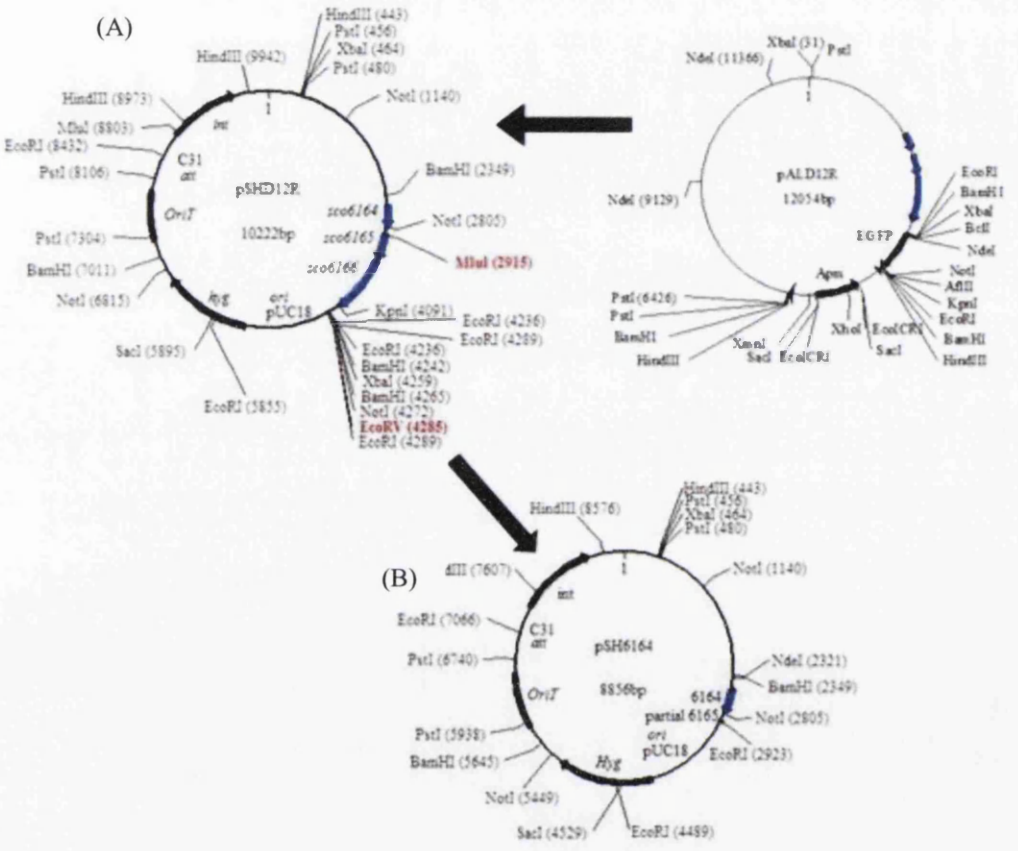

Figure 4.7: (A) plasmid map of pSHD12R, complementation vector containing *sco6164-sco6166* cloned into pSH152 backbone. (B) Plasmid map of pSH6164, the *sco6164* complementation vector with *sco6165* and *sco6166* removed.

Restriction digest of pALD12R with *Xba*I released a fragment containing the genes *sco6164*, *sco6165*,*sco6166* and the upstream region which was inserted into the *Xba*I site of pSH152 to produce pSHD12R (Figure 4.7) using blue/ white selection and checked by restriction digest. This plasmid was introduced into DSCO164 mutant strains by intergeneric conjugal transfer, where exconjugants were selected for hygromycin

resistance. Characterisation of the complementation was carried out on LB agar along with the wild type, DSCO6164 mutant strain and mutant strain with empty vector, pSH152, incubated at 30°C. Introduction of pSHD12R resulted in recovery of actinorhodin production (Figure 4.8), whereas the empty vector, pSH152 resulted in no change.

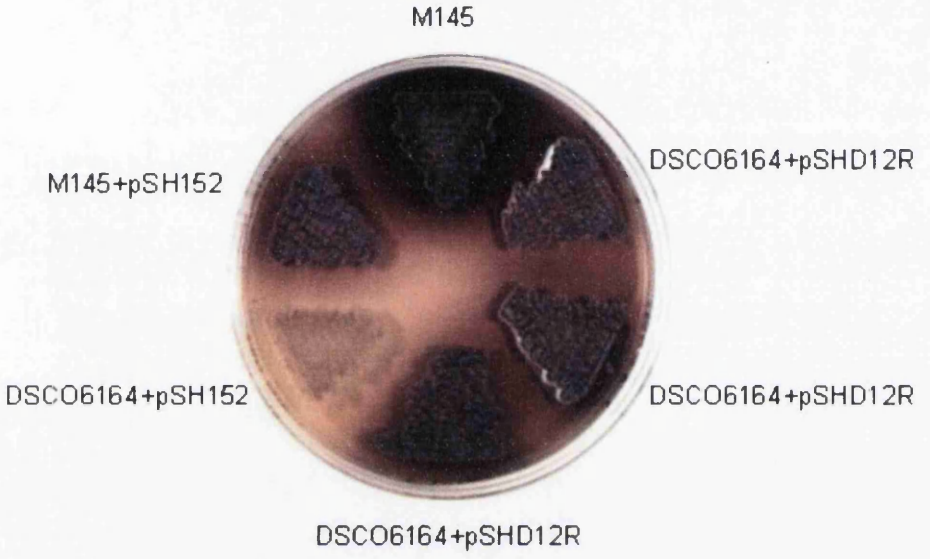

Figure 4.8: Complementation of DSCO6164.
DSCO6164 was complemented with plasmid pSHD12R, grown on LB agar without glucose and incubated for 7 days at 30°C.

As the disruption of the *sco6164* gene resulted in a significant phenotypic difference compared to the parental strain, the complementation test which was successful with the complete possible operon was repeated with the single gene to prove that the phenotype is a direct result of the disruption of the *sco6164* gene and not due to polar effects downstream. In order to complement the mutant DSCO6164 strain, pSHD12R was digested with *Eco*RV and *Mlu*I, where *Mlu*I was blunt ended prior to re-ligation of the plasmid to produce pSH6164 (Figure 4.7B). The plasmid pSH6164 was

confirmed by restriction digest. The newly created plasmid was introduced as previously by intergeneric conjugal transfer into the DSCO6164 mutant strain and phenotypic analysis carried out. As previously, complementation analysis was carried out on LB agar where the DSCO6164 mutant strain containing the complementation vector pSH6164 resulted in a phenotypic recovery compared to parental strain M145 (Figure 4.9), while no change was observed in the empty vector strain.

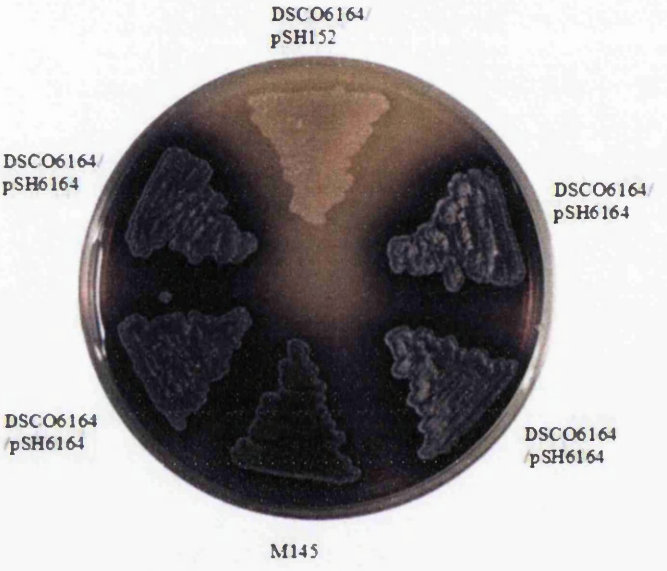

Figure 4.9: Complementation of DSCO6164 with plasmid pSH6164 on LB containing no glucose after 7 days incubation at 30°C.

4.6 Double mutant strain: *sco6164 / sco2075*

DSCO2075 has no discernable phenotypic alteration compared to parental strain M145 (except on NMMP with 250mM KCl), but is the most highly conserved DksA paralog of the three in *S. coelicolor* with two highly conserved Asp residues which potentially stabilises the ppGpp-RNAP complex (Perederina, Svetlov et al. 2004). To look at if there is cross talk between SCO2075 and SCO6164 a double mutant was

made. The easiest way to create a double mutant is changing the resistance cassette from *Apr*^{R} to *Hyg*^{R} The REDIRECT system was used to exchange the transposon in 4A10.1.A08 from Tn*5062* to Tn*loxP53*. As Tn*loxP53* is based on Tn*5062*, the 19nt and 20nt on the left and right of the disruption cassette are identical allowing homologous recombination resulting in insertion of a hygromycin resistant transposon.

(A)

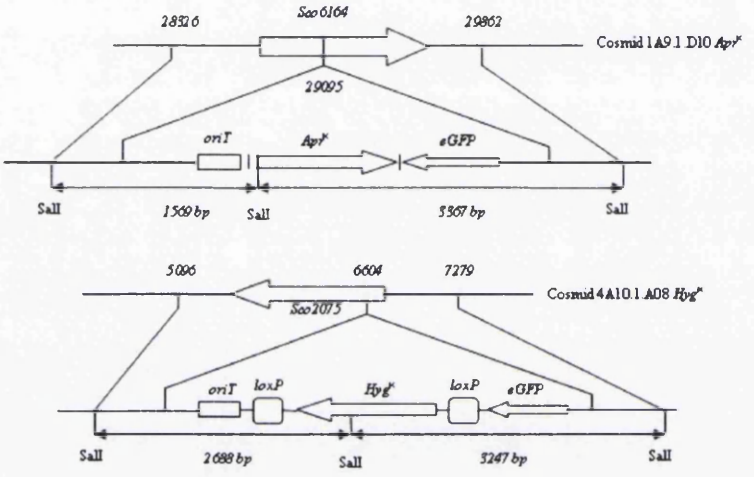

(B)

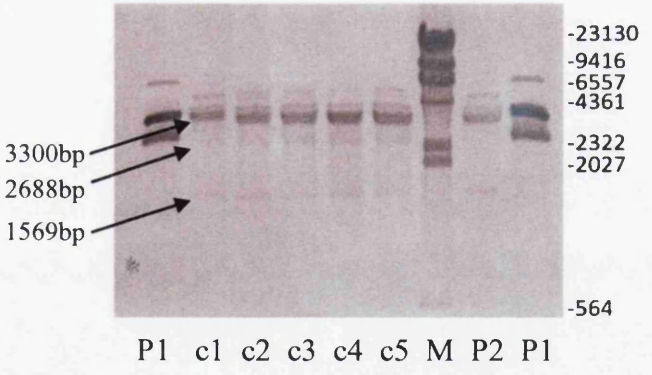

Figure 4.10: Southern blot analysis of *sco2075*$^-$ and *sco6164*$^-$ double mutant strain.
(A) *sco6164* and *sco2075* maps are shown with transposon insertions and *Sal*I restriction sites to calculate expected bands in the southern blot. The position of each *Sal*I and insertion site is indicated in the relevant cosmids. (B) Southern blot of 5 double mutant clones; M – *Hin*dIII digested λ DNA marker (band sizes shown on right in bp); c1-5 clones digested with *Sal*I; P1 is cosmid 4A10.1.A08 *Hyg*^{R} digested with *Sal*I and P2 is chromosomal DNA from DSCO6164 mutant strain. The size of expected bands for each mutant is indicated by arrows. Digoxigenin labelled Tn*5062* was used as a hybridization probe.

The mutated cosmid containing insertion 4A10.1.A08 *Hyg*^{R} was purified from *E. coli* JM109 strain to enrich the cosmid and then transformed into *E. coli* ET12567 (pUZ8002) which was used for conjugation of the cosmid into DSCO6164. Exconjugant colonies of DSCO6164 containing the *hyg*^{R} *sco2075* disruption were obtained by replicate plating on SFM with hygromycin and SFM with kanamycin to obtain double cross-overs. Double cross-overs (hygromycin resistant, kanamycin sensitive) were then plated on apramycin and hygromycin to confirm both transposon insertions are present.

Southern blot analysis was carried out on five selected clones, using digoxigenin labelled Tn*5062* as a probe which cross hybridises with Tn*loxp53* (Figure 4.10). To obtain distinct bands of the transposon insertions, *Sal*I restriction enzyme was selected using DNAMAN software. Cosmid and chromosomal DNA were purified from the relevant sources and digested with *Sal*I. Three bands at positions 3247 to 3367 base pairs (bp), 1568bp and 2688bp would indicate correct double mutant. Clones 2-5 have identical band patterns to the two positive controls confirming the nature of the double cross-over in the *sco2075* gene and that the *sco6164* mutation is present. Clone 1 is missing the 2688bp band from the *Sal*I digest of insertion 4A10.1.A08 *Hyg*^{R} indicating that a double cross over has not occurred. Bands above 3367bp in the Southern blot are the result of incomplete restriction digests with the enzyme *Sal*I.

The *sco6164*$^-$/ *sco2075*- double mutant strain was compared with parental strain M145, on the same media's as previously used (Figure 4.1) and are shown in Figure 4.11. The only phenotypic difference when compared to DSCO2075 is the lack of actinorhodin production on LB and 2xYT which corresponds to the DSCO6164 phenotype.

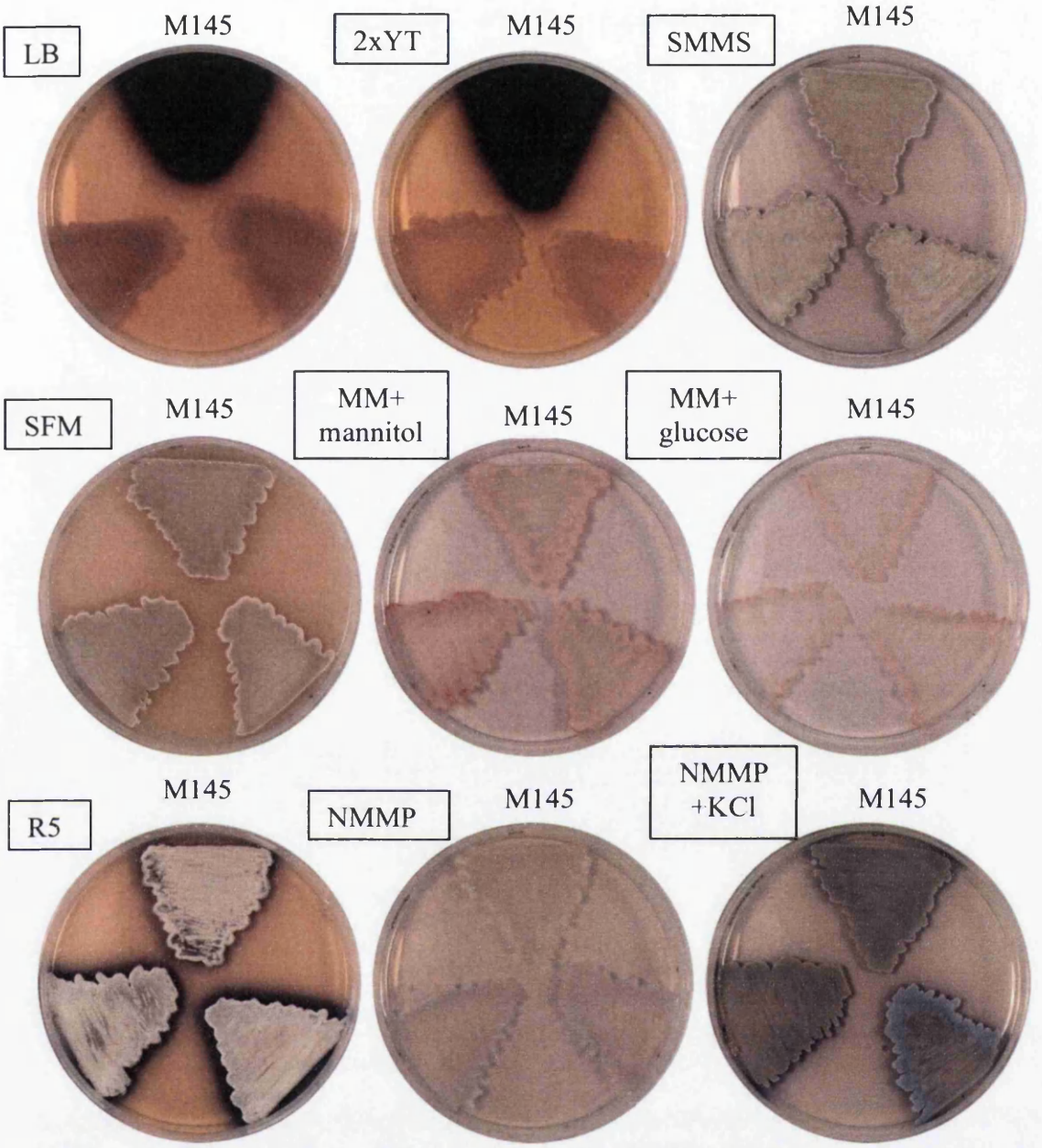

Figure 4.11: Phenotypic analysis of sco*6164*$^{-}$/*sco2075*$^{-}$ double mutant (bottom two) and parental strain *S. coelicolor* M145 (top) on different media. Strains were grown for 3 days at 30° C on LB, 2xYT, SMMS, SFM, MM + mannitol, MM + glucose, R5, NMMP, NMMP + 250mM KCl. The name of each medium is indicated in rectangle. Further analysis of *sco6164*$^{-}$/ *sco2075*$^{-}$ double mutant on NMMP +250mM KCl revealed 4 of the 5 clones had the same phenotype to that of DSCO2075.

4.7 SCO2075 rescues *relA* phenotype

With an absence of a strong phenotype for the DSCO2075 mutant strain, another way to link the function of SCO2075 with that of DksA in *E. coli* was tested. In *E. coli* the relaxed phenotype of a *relA* mutant can be suppressed by over-expression of DksA (Magnusson, Gummesson et al. 2007). To examine this in *S. coelicolor*, firstly the phenotype of a *relA* mutant generated in an M145 background was compared with that of the published M570 mutant (M600 background) (Chakraburtty and Bibb 1997). The effect of over-expression of SCO2075 in these *relA* mutants from both backgrounds was then tested.

RelA is the primary source of ppGpp in *E. coli* and is the only source in *S. coelicolor* and unlike *E. coli* RelA, the gene product of *relA* in *Streptomyces* is capable of synthesising and degrading (p)ppGpp, with a 365 amino acid domain at the N-terminus required for synthesis and a 305 amino acid domain which overlaps from amino acid 93 required for degradation (Martinez-Costa, Fernandez-Moreno et al. 1998). Fragments of 1.46kb and 2.07kb of the N-terminal segment of *relA*, fused to *ptipA* have been shown to restore antibiotic production in *Streptomyces* where shorter sequences fail, confirming the ppGpp synthetase region of the protein in the N-terminus (Sun, Hesketh et al. 2001).

A *relA* mutant strain has been previously characterised in a *S. coelicolor* M600 background (Chakraburtty and Bibb 1997). Deletion of the *relA* gene resulted in loss of ppGpp synthesis upon entry into stationary phase (consistent with a relaxed phenotype) and in nitrogen-limited media following amino acid starvation in exponential growth

(Chakraburtty and Bibb 1997). Under nitrogen-limiting conditions such as SMMS medium, actinorhodin and undecylprodigiosin antibiotic production was absent in M570 (*relA* mutant) (Chakraburtty and Bibb 1997).

A *relA* mutant (DSCO1513) in the *S. coelicolor* M145 strain was constructed using cosmid 9c5.1.c04, which has a transposon inserted at chromosomal position 1618604bp. The mutated cosmid containing 9C5.1.C04 insertion was purified from *E. coli* JM109 strain to enrich the cosmid and then transformed into *E. coli* ET12567 (pUZ8002) which was used for conjugation of the cosmid into *S. coelicolor* M145. Exconjugant colonies of *S. coelicolor* containing the *relA* disruption were obtained by replicate plating on SFM with apramycin and SFM with kanamycin to obtain double cross-overs (apramycin resistant, kanamycin sensitive). Three clones were used for Southern hybridisation to confirm disruption of the *relA* gene, *sco1513* (Figure 4.12).

The Southern blot analysis was carried out on three clones using digoxigenin labelled Tn5062 and *Hind*III-digested lambda DNA to confirm replacement of the wild type *relA* gene with the transposon-inserted gene from the mutated cosmid. Using DNAMAN software the restriction enzyme *Sal*I was chosen for the Southern blot analysis. Chromosomal DNA from the double cross-over clones was purified with mutated cosmid as a positive control and digested with *Sal*I (Figure 4.12). Digestion with *Sal*I results in two defined bands of 2900bp and 800bp. Bands above 2900bp are the result of incomplete restriction digestion by *Sal*I in both cosmid and c1 and the curved bands likely a result of excess chromosomal DNA.

A)

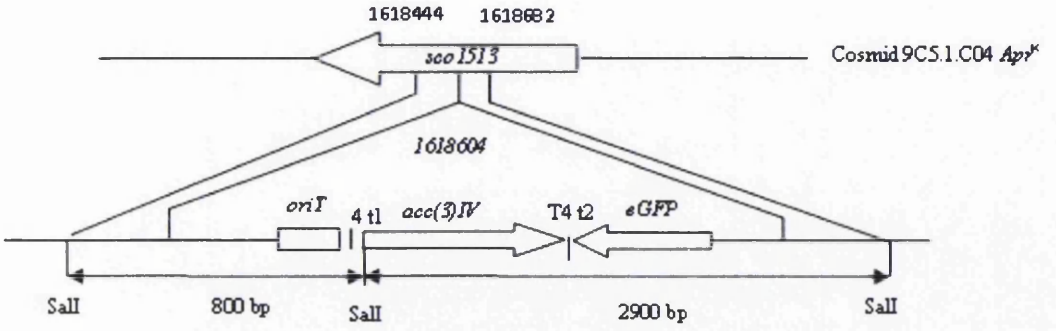

B)

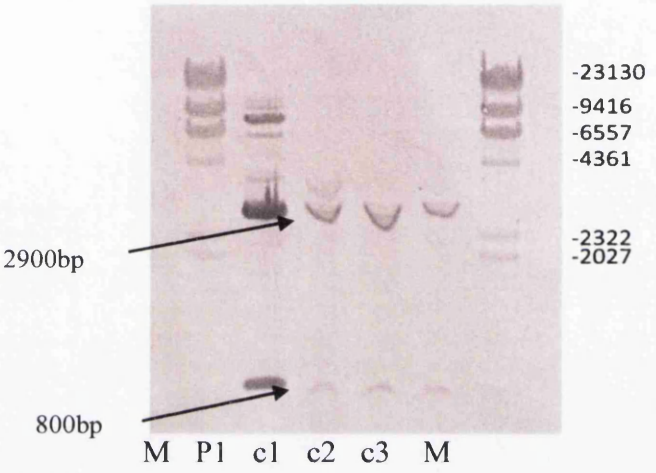

Figure 4.12: Southern blot analysis of DSCO1513.
(A) *sco1513 (relA)* map is shown with transposon insertions and *Sal*I restriction sites to calculate expected bands in the southern blot. The position of each *Sal*I and insertion site is indicated. (B)Southern blot of the three clones; M – *Hin*dIII digested λ DNA marker (band sizes shown on the right in bp); c1-3 clones digested with *Sal*I; P1 9C5.1.C04 cosmid digested with *Sal*I.

Analysis of DSCO1513 was very similar to the published *relA* mutant in the *S. coelicolor* M600 background. Under nitrogen limited medium SMMS actinorhodin production and undecylprodigiosin is absent and in rich medium such as MYMTE very sparse aerial hyphae are erected and again antibiotic production was absent (result not shown).

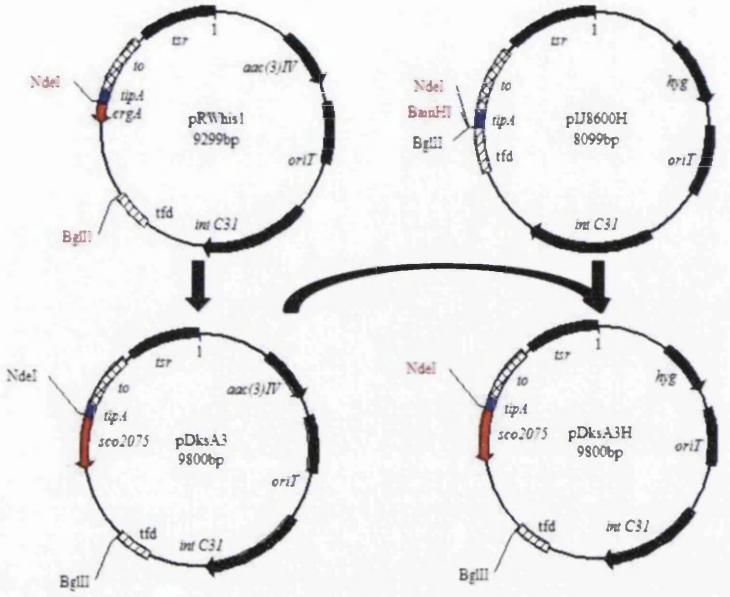

Figure 4.13: construction of pDksA3 and pDksA3H.
Sco2075 was PCR amplified with PCR primers DksA_NdeI and 2075_REV and digested *Nde*I and *Bgl*II. The digested PCR fragment was cloned in to plasmid pRWhis1 (restriction digested with *Nde*I/ *Bam*HI and gel purified) resulting in plasmid pDksA3. To change the plasmid resistance, plasmid pDksA3 was restriction digested with *Nde*I and *Bgl*II. The fragment containing *sco2075* was gel purified and clones into pIJ8600H (restriction digested *Nde*I and *Bam*HI) resulting in plasmid pDksA3H. Plasmids were checked by restriction digest and sequencing.

To over-express SCO2075 in *S. coelicolor*, *sco2075* was amplified by PCR with primers DksA_NdeI and 2075_REV that include an *Nde*I and *Bgl*II site respectively. DksA_NdeI places an *Nde*I site at the start codon and 2075_REV removes the TGA termination codon. The PCR amplified *sco2075* was cleaned, digested with *Nde*I and *Bgl*II, gel purified and cloned in to plasmid pRWhis1 which was restriction digested with *Nde*I and *Bam*HI resulting in plasmid pDksA3 (apramycin resistant) (Figure 4.13). To construct the plasmid with hygromycin resistance, the plasmid pDksA3 was digested with *Nde*I and *Bgl*II, releasing a fragment containing sco2075 transcriptionally fused to the His-tag sequence. The gel purified fragment was then ligated to plasmid pIJ8600H

restriction digested with *Nde*I and *Bgl*II, in frame with the thiostrepton inducible promoter *ptipA,* producing plasmid pDksA3H (Figure 4.13).

The plasmid pDksA3H was conjugated into the M145 background *relA* (DSCO1513) mutant strain and pDksA3 into M570 (M600 background) mutant strain. To look at whether there is phenotypic suppression in the respective *relA*$^-$ mutant strains, spores from fresh SFM plates were used to inoculate SMMS containing varying concentrations of thiostrepton from 0-20μg/ml (Figure 4.14). Expression of *sco2075* via the *tipA* promoter results in undecylprodigiosin production in the M145 background *relA* mutant and in M570 actinorhodin production is restored. Undecylprodigiosin was confirmed using ammonium hydroxide solution. As actinorhodin can be red below a pH of 7, the Petri dish was inverted and 5ml of ammonium hydroxide (pH 11.6) placed into the lid and closed (Rudd and Hopwood 1979) confirming undecylprodigiosin. If the antibiotic was actinorhodin, with the high pH of the ammonium hydroxide, the colour would revert to blue, however if no change occurred then the antibiotic is undecylprodigiosin.

A)

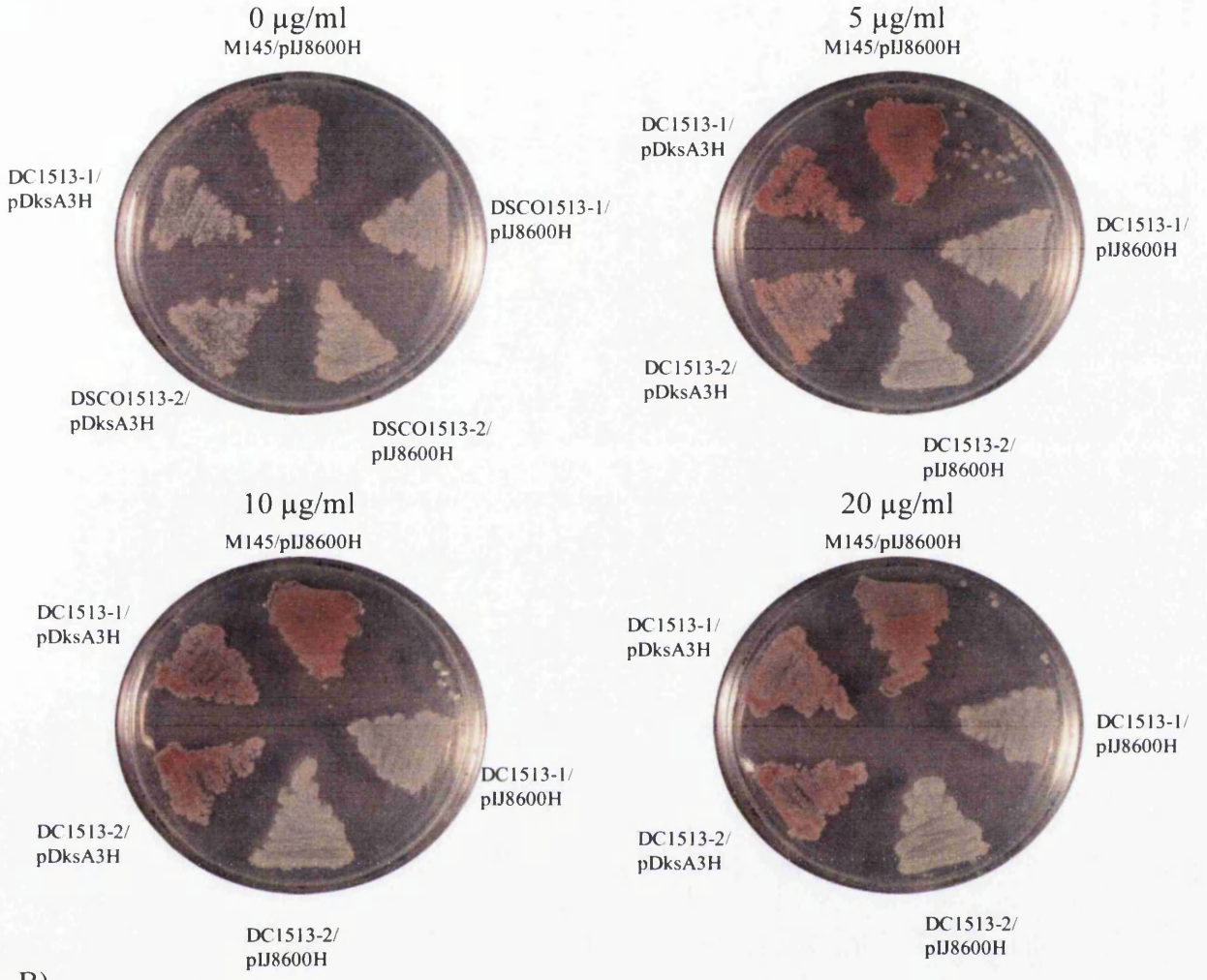

B)

Thiostrepton:

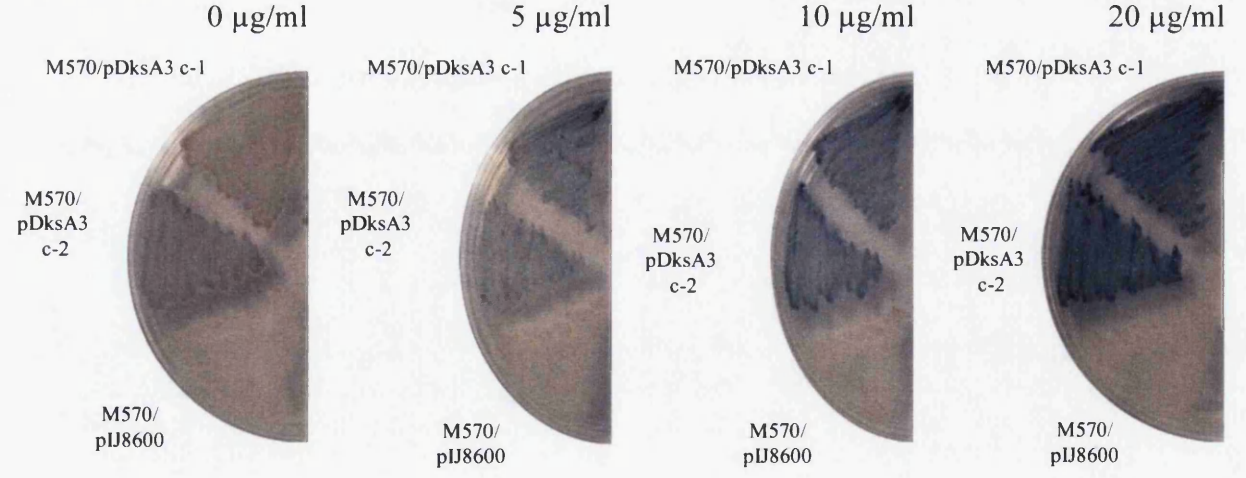

Figure 4.14: Over expression of SCO2075 via plasmid pDksA3H in relA mutant strains in M145 background (A) and over expression of SCO2075 via plasmid pDksA3 in two clones of mutant M570 (M600 background) (B) results in a recovery of antibiotic production which appears dosage dependent. In the DSCO1513 mutant strain, undecylprodigiosin is recovered and in M570, actinorhodin is recovered. Concentration of thiostrepton is show above each plate. All plates are SMMS with the specified concentration of thiostrepton and grown for 5 days at 30°C.

4.8 Summary

sco2075 is not an essential gene in *S. coelicolor* with very little phenotypic alteration compared to the parental M145 except under osmotic stress on NMMP media. DSCO2075 shows higher sensitivity to diamide stress as a result of reduced transcription of *sigR* and is more sensitive to oxidative stress by H_2O_2 when compared to parental strain M145. DSCO6164 and DSCO6165 lack actinorhodin production on LB and 2xYT. The double mutant strain *sco6164⁻/ sco2075⁻* does not show any new phenotypic variations compared to DSCO6164 and DSCO6165. Over-expression of *sco2075* results in recovery of antibiotic production in *relA* mutants of M145 and M600 strains.

Chapter - 5

Analysis of *in vivo* DNA supercoiling

5.1 Introduction

In this chapter the topological states of a reporter plasmid extracted from mutant strains of *S. coelicolor* were analysed by chloroquine gel electrophoresis to determine any changes in global DNA supercoiling. Changes in the osmolarity of media was also investigated with regards to the DSCO2075 mutant strain as evidence exists that certain nucleoid associated proteins in other bacteria (Hsieh, Rouviere-Yaniv et al. 1991; Mojica and Higgins 1997) have the ability to alter DNA topology and influence gene expression by either induction or repression in response to the osmotic conditions.

It has previously been shown that the topological state of a self replicating plasmid within a number of species including *Streptomyces* shows the general superhelical state of genomic DNA (as theoretically plasmid DNA cannot be differentiated from the free cytoplasm bound chromosomal DNA) and an increase in negative supercoiling as a result of osmotic stress (Hsieh, Rouviere-Yaniv et al. 1991; Mojica and Higgins 1997; Ali, Herron et al. 2002).

Mutations in nucleoid-associated proteins have also been shown to alter the topological state of reporter plasmids in a number of species such as *E. coli* and *salmonella tryphimurium* (Hillyard, Edlund et al. 1990; Hsieh, Rouviere-Yaniv et al. 1991; Mojica and Higgins 1997; Berger, Farcas et al. 2010). In addition, DksA has been shown to be involved in maintaining chromosome structure *in vivo. E. coli* DksA was originally isolated as a multicopy suppressor of the temperature-sensitive growth and filamentation of a *dnaK* mutant strain (Kang and Craig 1990) and has been shown to

recover the temperature sensitivity of a Δ*mukB* mutant strain (Yamanaka, Mitani et al. 1994).

A *dksA* mutant strain of *E. coli* has also been shown to affect chromosomal supercoiling *in vivo* (Hardy and Cozzarelli 2005).

Mutant strains of *S. coelicolor* were screened for alterations in supercoiling compared to parental strain M145 under osmotic shock by analysis of plasmid topology using plasmid pROT219, based on pUWL219, a pIJ101 derivative plasmid (high copy number, self replicating). A shift to osmotic stress results in an increase in negative supercoiling in *E .coli* and *Streptomyces* (Hsieh, Rouviere-Yaniv et al. 1991; Ali, Herron et al. 2002). Chlorqouine gel electrophoresis has been shown to be a suitable means of analysing the topological state of a reporter plasmid which represents global alterations to DNA topology within an organism (Alice and Sanchez-Rivas 1997; Piuri, Sanchez-Rivas et al. 2003).

5.2 Chloroquine gel electrophoresis

Chloroquine, like ethidium bromide has a planar polycyclic, aromatic structure (Figure 5.1), which can insert itself between two stacked base pairs of DNA (Sinden 1994). This causes a local unwinding resulting in a decrease in twist and increase in writhe of the DNA. Chloroquine binds weaker to DNA than ethidium bromide which allows the analysis of the distribution of single DNA topoisomers in agarose gels (Shure, Pulleyblank et al. 1977; Bates 1993).

In the presence of low concentrations of chloroquine, more negatively supercoiled DNA migrate down an agarose gel faster than relaxed forms and separates

topoisomers differing by one linking number (Depew and Wang 1975; Keller and Wendel 1975). However with high concentrations, the DNA becomes saturated with chloroquine molecules and initially relaxed and positively supercoiled DNA migrate faster down the gel than negatively supercoiled (Shure, Pulleyblank et al. 1977). For all chloroquine gels a concentration of 6µg/ml of chloroquine was added to the electrophoresis tank running buffer and to the cooled agarose gel prior to pouring which results in faster migration of more negatively supercoiled DNA.

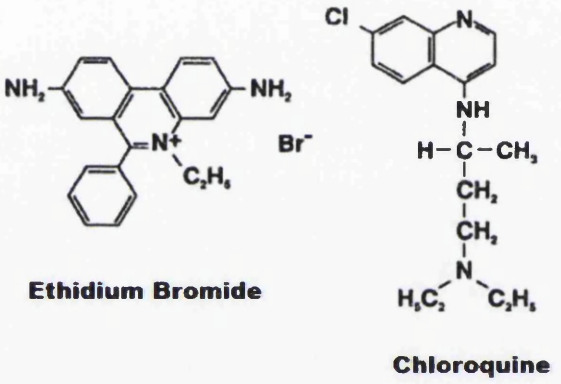

Figure 5.1: Intercalating molecules
Chemical structure of Ethidium Bromide and Chloroquine (Sinden 1994).

5.3 Determination of methods for extracting plasmid DNA

Topicological analysis of the reporter plasmid supercoiling was used to determine the global effects of varying external osmotic stresses. The *E. coli-Streptomyces* shuttle vector pROT219 based on pUWl219 with an *oriT* inserted (Wehmeier 1995) was used for the plasmid analysis. Initially to isolate supercoiled plasmid from 200ml liquid cultures the alkaline lysis method using acid phenol chloroform described in Practical Streptomyces Genetics was used (Kieser 2000). The plasmid was then purified further using Wizard columns according to the manufacturer's

instructions (Promega). However the reproducibility of this method proved difficult and time consuming, so to optimise plasmid isolation from smaller cultures the alkaline lysis (Kieser 2000), described in Chapter 2 was used where acid potassium acetate pH4.7 replaces acid phenol chloroform. Scaling down the cultures volumes to 10ml was looked at, however, it proved difficult to produce adequate amounts of plasmid DNA due to loss during purification and therefore 50ml - 200ml culture volumes were used.

5.4 Determination of running buffer

To obtain maximum resolution of plasmid DNA initially 0.6% agarose gels were used. 1xTBE, 1xTAE and 1xTPE (data not shown) were used as the running buffers and to make the agarose gels with the same concentration of chloroquine (6µg/ml) and run for 26-40 hours at 4°C at 1.5V/cm.

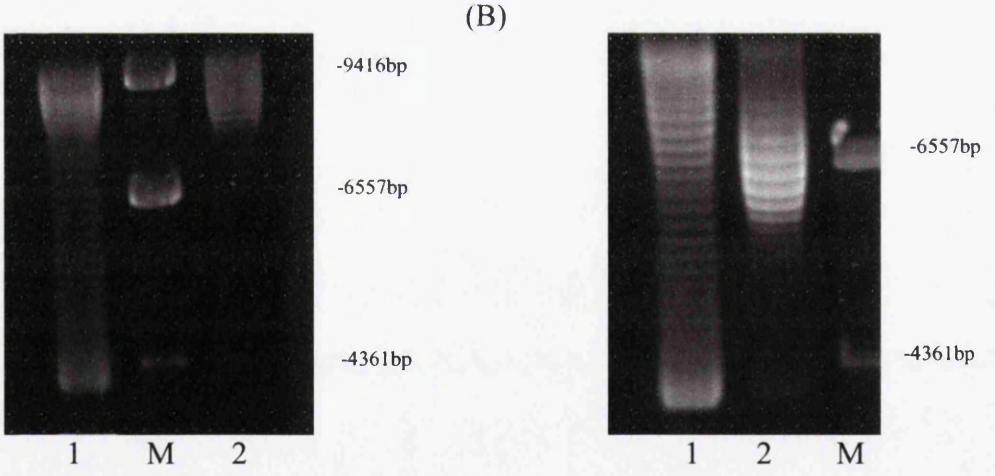

Figure 5.2: Effect of varying gel electrophoresis buffer on topoisomer visualisation. (A)Chloroquine gel containing 6µg/ml chloroquine, 0.5% agarose run for 26 hours at 4°C 1.5v/cm in 1xTBE. Lane 1 plasmid DNA isolated from culture grown in TSB 10g/L yeast extract 5mM $MgCl_2$, lane M lambda DNA *Hin*dIII and plasmid isolated from culture grown in LB, lane 2. (B) Chloroquine gel containing 6µg/ml chloroquine 0.5% agarose run at same conditions as A, however buffer is 1x TAE. Lane 1 - plasmid DNA isolated from culture grown in TSB 10g/L yeast extract 5mM $MgCl_2$; lane 2 - plasmid isolated from culture grown in LB. M- *Hin*dIII digested λ DNA marker (band sizes shown in bp).

Figure 5.2 shows a comparison of identical samples run using two different electrophoresis buffers, 1xTBE and 1xTAE. It is immediately evident, when comparing the two images, that the best resolution of individual topoisomers of supercoiled plasmid DNA extracted from *S. coelicolor* was obtained by using the buffer 1xTAE compared to 1xTBE. As TAE suffers buffer exhaustion with extended electrophoresis runs, the buffer was re-circulated 30min after loading the samples into the agarose gel until completion of the gel run.

5.5 Determination of growth media

TSB supplemented with 5mM $MgCl_2$ and 10g/L yeast extract (Ali, Herron et al. 2002) and LB broth were tested. In Figure 5.2 it is clearly evident that there is quite a contrast between the plasmid supercoiling from cultures grown in TSB and LB, where there is a larger distribution of plasmid topoisomers with a higher proportion more negatively supercoiling from TSB media compared to LB where the topoisomer distribution is more compacted. It is interesting to note even at this stage of analysis that variation in media results in substantial alterations in topological distribution of reporter plasmids and as a result potentially in variations in gene expression. Both medias result in relatively similar changes in linking number when compared to with and without osmolyte (even though topological profiles differ), and as no single media is used for phenotypic analysis of *Streptomyces*, both medias were used for analysis of topoisomer distributions in this chapter.

5.6 Topoisomer distribution in M145 and DSCO2075

To examine the effect of osmolarity, the plasmid pROT219 was used as a reporter and topoisomer distribution analysed in the parental strain M145. As

Streptomyces are unable to metabolise sucrose as a carbon source, filter sterilised sucrose (as opposed to autoclaved, to avoid break down of sucrose to fructose and glucose) was added to 2x TSB or 2x LB-NaCl to the desired concentration and autoclaved dH_2O added to make 1X TSB or 1xLB-NaCl with the desired concentration of osmolyte. Pre-cultures were allowed to grow for 24 hours without osmolyte with 20 μg/ml thiostrepton prior to being used to inoculate larger cultures for 72-96 hours containing the desired concentration of osmolyte and thiostrepton.

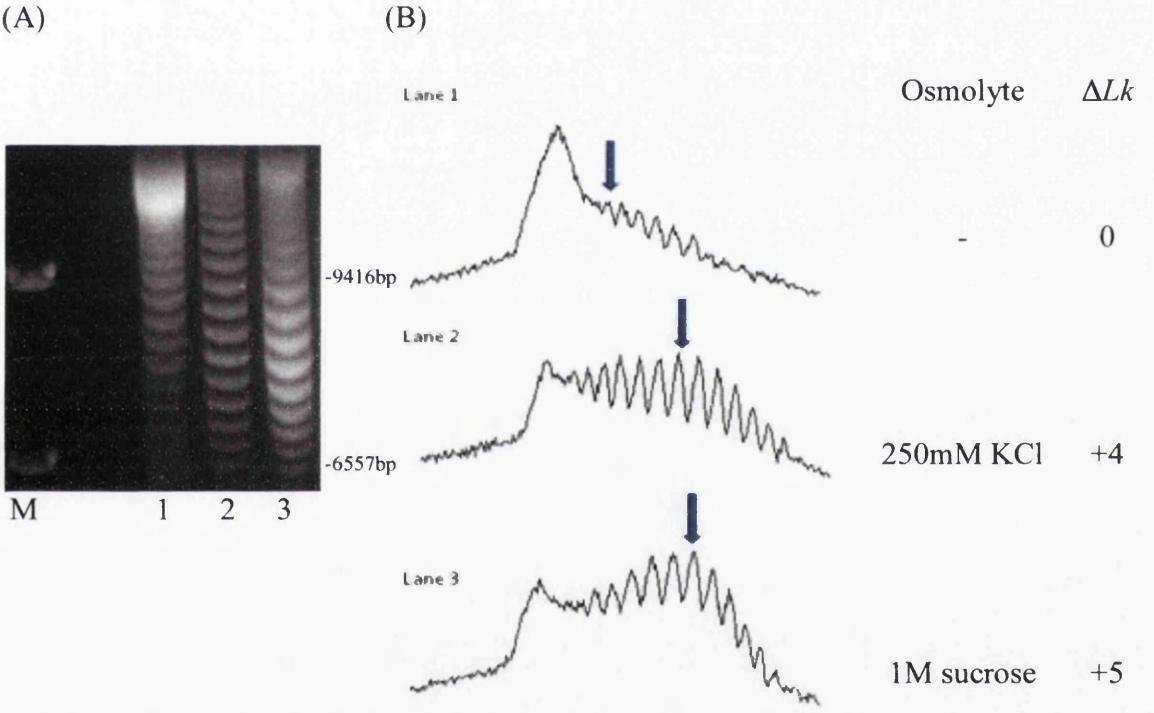

Figure 5.3: The effect of osmolarity on *in vivo* reporter plasmid topology in *S. coelicolor* M145. (A) Chloroquine gel electrophoresis of plasmid pROT219 isolated from M145 cultures grown in TSB with no added osmolyte lane 1; 250mM KCl added in lane 2 and 1M sucrose lane 3. M- *Hin*dIII digested λ DNA marker, sizes in bp on the right hand side. (B) Quantitation of intensity of bands corresponding to individual topoisomers from each lane. Lk_m, the most abundant topoisomer is indicated by the blue arrow and the change in linking number, ΔLk are shown for each lane with KCl or sucrose using no added osmolyte sample as the reference point.

The topoisomer analysis using chloroquine gel electrophoresis was carried out after growing cultures in medium containing either 0.72M non-ionic sucrose, which alters topoisomer distribution of *S. lividans* (Ali, Herron et al. 2002), 1M sucrose, or 250mM of the ionic osmolyte potassium chloride (KCl).

Similarly to other bacteria including *S. lividans,* the density traces from the chloroquine gel in Figure 5.3 were analysed as described in Chapter 2, and shows *S. coelicolor* strain M145 responds as expected to the external osmolyte with a clear shift in topoisomer distribution towards a more negatively supercoiled state. This is shown by the change in mean linking number of +5 with addition of 1M sucrose and +4 with 250mM KCl added (Figure 5.3B), with respect to a reporter plasmid isolated from media without osmolyte. After initial characterisation of plasmids isolated from M145, plasmid DNA was isolated from cultures of DSCO2075 and M145 grown in LB without NaCl (LB-NaCl) media with either 0.72, 1M sucrose and 250mM KCl and analysed using the previous protocol to determine any alteration in mean linking number and/ or distribution of topoisomers.

The chloroquine gels containing samples grown with additional osmolyte of either 0.72M sucrose or 250mM KCl show a distinct difference in range of topoisomers when comparing the mutant DSCO2075 and parental strain M145, where M145 has a larger shift and range of topoisomers which are more negatively supercoiling compared to plasmid isolated from DSCO2075 (Figure 5.4). With the increase in sucrose from 0.72M to 1M there is still this observable alteration in superhelicity between the mutant and the parental strain. Strain M145, shows a ΔLk +6 when comparing topoisomers with and without osmolyte (Figure 5.5A) and from Figure 5.4 and 5.5 the difference in

linking number between DSCO2075 and M145 under osmotic stress was respectively ~ΔLk -4, -7 and -6 for 0.72M sucrose, 1M sucrose and 250mM KCl. Comparing the mutant strain with and without osmolyte there appears to be little change in topoisomer distribution with only a modest increase in negative topoisomers in the mutant strain, which however, does not alter mean linking number.

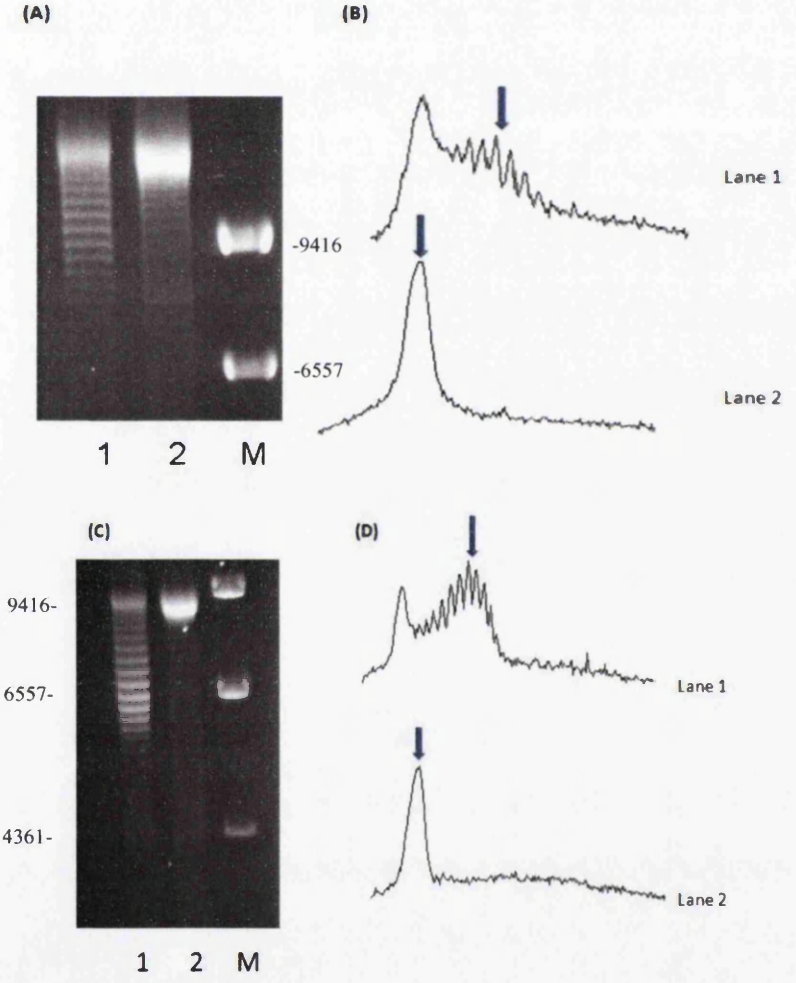

Figure 5.4: Effect of varying osmolytes on *in vivo* supercoiling of a report plasmid from DSCO2075 compared with parental strain M145. (A) Resolved topoisomer distribution of pROT219 isolation from cultures grown with LB-NaCl including 0.72M sucrose. Lane 1- M145, lane 2- DSCO2075 and M- *Hin*dIII digested λ DNA marker. Sizes in bp. (B) Quantitation of intensity of bands from image A. (C) The same as (A) above but with the additional osmolyte changed from sucrose to 250mM KCl. (D) Quantitation of intensity of bands from image C. Blue arrows indicated the Lk_m.

To determine whether the difference in plasmid topoisomer distribution is a result of the *sco2075* mutation, the DSCO2075 mutant was complemented with plasmid pSH2075 introduced by intergeneric conjugal transfer. This is an integrative plasmid, based on pSH152 containing the gene *sco2075* and its upstream region that integrates at the ϕC31 *att* site in the *S. coelicolor* chromosome. Exconjugants were selected by virtue of their hygromycin resistance, which allows the selection for pSH2075 while maintaining the reporter plasmid pROT219 (thiostrepton resistant) and the apramycin resistant Tn*5062 sco2075* insertion. Strains were grown as previous with addition of 1M sucrose as osmolyte and plasmid DNA isolated and analysed using a 0.6% chloroquine agarose gel. From the density traces for the complemented strain compared to M145 there is a comparable recovery with no difference in mean linking number, and distribution of the topoisomers appears similar (Figure 5.5).

DSCO2075 shows somewhat reduced negative supercoiling with ~ΔLk -1 in LB-NaCl compared to parental strain M145 containing the same reporter plasmid. It is also interesting to note that DSCO2075 has an altered topology profile as a result of growth in the presence of additional osmolyte (Fig 5.5A). Although this does not affect the mean linking number of the reporter plasmid it nevertheless shows that there is some response to the increased osmolyte with an increase of negatively supercoiled topoisomers within the same range as the parental strain. These more negatively supercoiled topoisomers do not have the same abundance as the parental strain and this is evident for both non-ionic and ionic osmolytes.

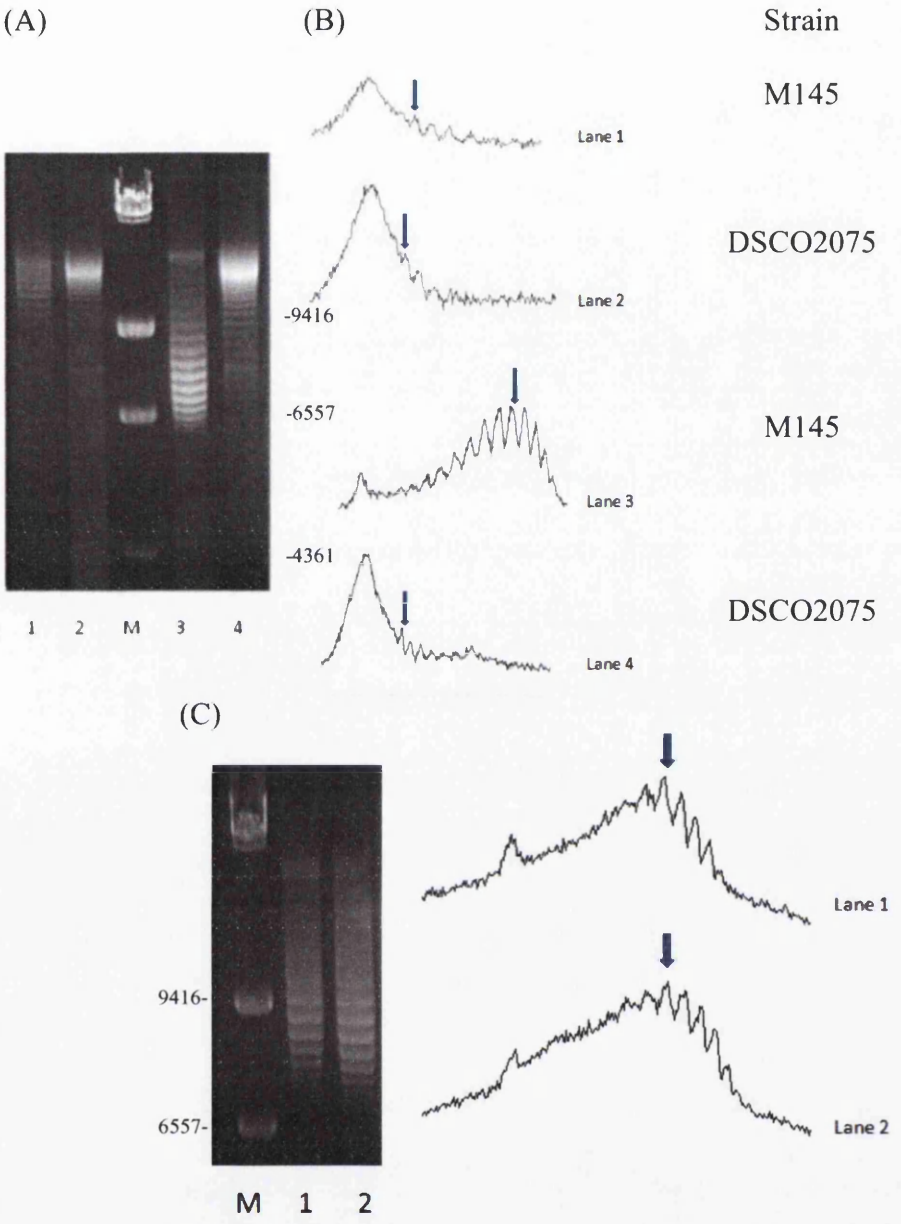

Figure 5.5: The effect of osmolarity on *in vivo* reporter plasmid topology in *S. coelicolor* M145 and DSCO2075. (A) Chloroquine gel electrophoresis of plasmid pROT219 isolated from M145 (lanes 1, 3) or DSCO2075 (lanes 2, 4) grown in LB-NaCl with no added osmolyte lane 1 and lane 2 or with 1M sucrose lanes 3 and 4. (B) Quantitation of intensity of bands corresponding to individual topoisomers from each lane. Lk_m, the most abundant topoisomer is indicated by the blue arrow and the change in linking number, ΔLk are shown for each lane using plasmid isolated from M145 with no osmolyte as a reference point. (C) Complementation of DSCO2075 mutant with pSH2075. Strains were grown as previously with the addition of 1M sucrose and plasmid DNA isolated and analysed on a chloroquine gel. M- *Hin*dIII digested λ DNA marker (band sizes shown in bp), Lane 1, M145 and lane 2 DSCO2075/ pSH2075. Quantitation of intensity of bands corresponding to individual topoisomers from each lane is shown to the right of the gel.

This alteration in plasmid DNA topology DSCO2075 mutant is also evident in an extended run, low voltage 0.6% mini agarose gel without intercalating agents (Fig 5.6). Interestingly, the difference in plasmid topoisomer distribution resulting from cultures grown in the presence of additional osmolyte appears to take time. This is clear when comparing the chloroquine gel from Figure 5.7C with, for example Figure 5.5A; lane 3.

Unlike *E. coli,* which has a rapid change in supercoiling when introduced to osmotic shock with a gradual reduction to a new basal supercoiling level above that of prior to induction (Hsieh, Rouviere-Yaniv et al. 1991), DNA supercoiling in *Streptomyces* appears to change more slowly. Figure 5.7C, lanes 1 and 3 shows little change in topoisomer distribution 120min after addition of osmolyte in M145, compared to a clear shift in cultures grown continuously in the presence of additional osmolyte (Figure 5.5A). This may indicate that changes in DNA topology in *S. coelicolor* after osmotic shock are initially domain specific and not necessarily detected with a plasmid reporter system.

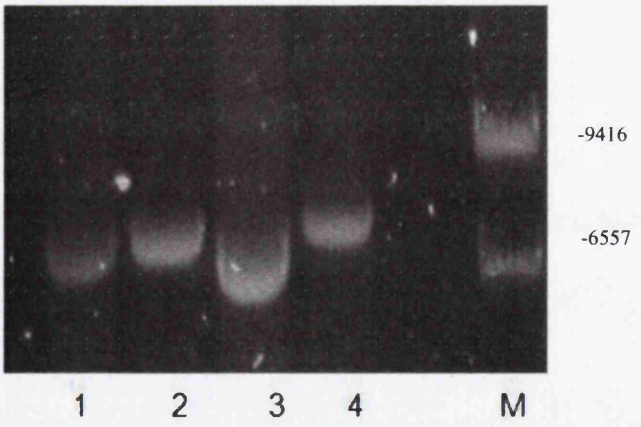

Figure 5.6: Extended mini-gel electrophoresis with 0.6% agarose without intercalating agent. Strains were grown in LB-NaCl (lanes 1, 2) and with 250mM KCl (lanes 3, 4). Lanes 1 and 3 M145; lanes 2 and 4 DSCO2075. M- *Hin*dIII digested λ DNA marker (band sizes shown in bp).

5.7 Reporter topology in other *S. coelicolor* mutants

Plasmid topology was also analysed in other mutants of *S. coelicolor* which could potentially alter the degree of supercoiling. Mutant strains of *osaC,* which functions as a σ^B anti-sigma factor (Fernandez Martinez, Bishop et al. 2009), and *dpsA,* which is strongly induced under osmotic stress and has been shown to be involved in nucleoid condensation during sporulation (Facey, Hitchings et al. 2009), were subjected to osmotic stress. Although initial *in vitro* DNA binding assays have failed to show DpsA to bind DNA (personal communication, Matt Hitchings), Dps proteins from other species have been shown to bind DNA dependent on the N-terminal tail length containing positively charged amino acids with some exceptions for example Dps from *Agrobacterium tumefaciens* (Ceci, Ilari et al. 2003; Ceci, Ilari et al. 2005). Both OsaC and DpsA mutant strains were analysed using 1M sucrose in TSB as shown in Figure 5.7A. From the analysis of the plasmid distributions there appears to be no change in mean linking number, with Lk_m remaining the same in both mutant strains compared to the control parental strain M145.

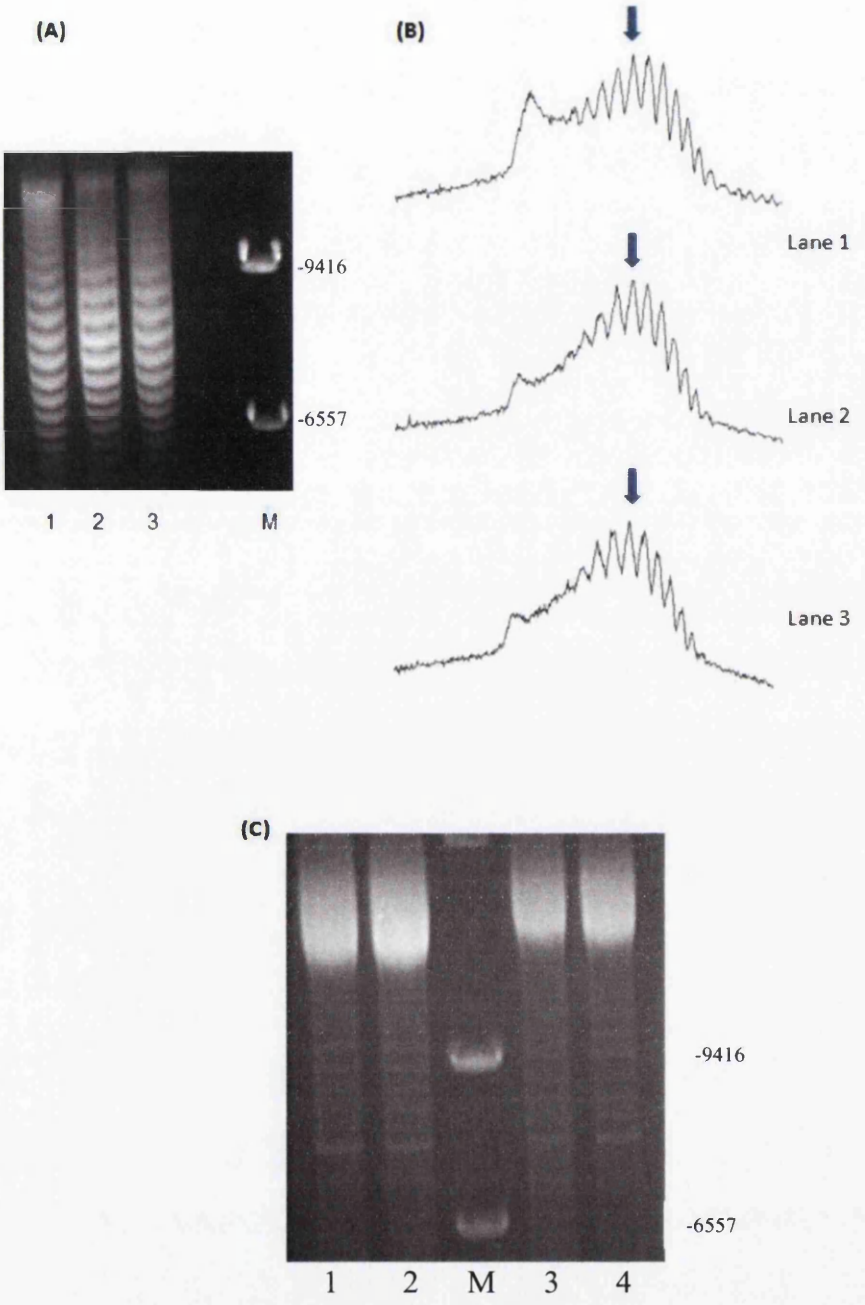

Figure 5.7: (A) Reporter plasmid DNA topological analysis of an *osaC*⁻ mutant strain (lane 1), *dpsA*⁻ mutant strain (lane 2) compared to parental strain M145 (control) (lane 3). All strains containing plasmid pROT219 were grown in TSB with 1M sucrose. (B) Density traces analysis of gel A with mean linking number shown by a blue arrow. (C) analysis of M145 (lanes 1, 3) and *dpsA*⁻ (lanes 2, 4) mutant strain with and without 250mM KCl. 24 hour precultures were used to inoculate 50ml culture of LB-NaCl. After 48hours growth, 250mM KCl was added (lanes 3, 4) and incubated for 120 minutes. M-*Hin*dIII digested λ DNA marker (band sizes shown in bp).

As DpsA protein levels rapidly increase with osmotic up shift to 250mM KCl with significant protein concentrations after two hours (Facey, Hitchings et al. 2009), a short term induction was conducted on the *dpsA*$^-$ mutant strain together with M145. 10ml precultures of the strains were grown in LB-NaCl for 24 hours at 30^{0}C at 225 rpm and used to inoculate 50ml cultures which were grown for a further 48hours when 250mM KCl was added and incubated for a further two hours and plasmid DNA isolated. From Figure 5.7C, there is no difference when comparing either M145 or the *dpsA*$^-$ mutant strain with plasmid isolated from media with and without 250mM KCl.

5.8 Summary

DNA topology of a reporter plasmid was affected by growth media and osmotic stress in *S. coelicolor*. Analysis of plasmid isolated from strain DSCO2075 compared to the parental strain M145 indicated a significant reduction in negative supercoiling in the mutant strain grown in the presence of osmolyte. The degree of negative supercoiling was restored to M145 levels after complementation of DSCO2075. Other mutant strains analysed showed no differences in DNA topology in response to osmotic stress compared to M145 with no changes in mean linking number observed.

Chapter - 6

Proteomics

6.1 Introduction

As *sco2075* is not previously characterised it is important to understand the role of the novel domain architecture and how at a translational level the gene is expressed and to help understand the function of the protein.

In this chapter I examined the expression of *sco2075* during the life cycle of *S. coelicolor* and tried to verify the native oligomeric state of the protein. Also due to the similarities in the NTD portion of the protein to histone-like proteins in bacteria, I investigated the ability of the protein to bind to DNA and looked to see whether this DNA binding ability was domain specific. Following this, the expression of the nucleoid associated protein DpsA (which has a similar expression profile in *S. coelicolor*) was looked at in DSCO2075 and M145 to see if there were any alterations in expression.

6.2 Time course expression of *sco2075*

In order to construct a plasmid with a C-terminal 6xHis residue fusion under the control of the native promoter, pRWHis2 was restriction digested with *Xba*I and *Bam*HI to remove the *crgA* gene and upstream region and gel purified. The *sco2075* gene and upstream region containing *sco2075*'s promoter was amplified by PCR using primers 2075_FWD and 2075_REV with *Xba*I, *Bgl*II respectively (Table 2.6). The PCR product was then cleaned using QIAquick PCR Purification Kit (Qiagen), digested with *Xba*I and *Bgl*II, clean up repeated and then cloned into the purified pRWHis2 *XbaI/ Bam*HI to produce p2075his (Figure 6.1). The resulting plasmid was checked by restriction digest and sequencing.

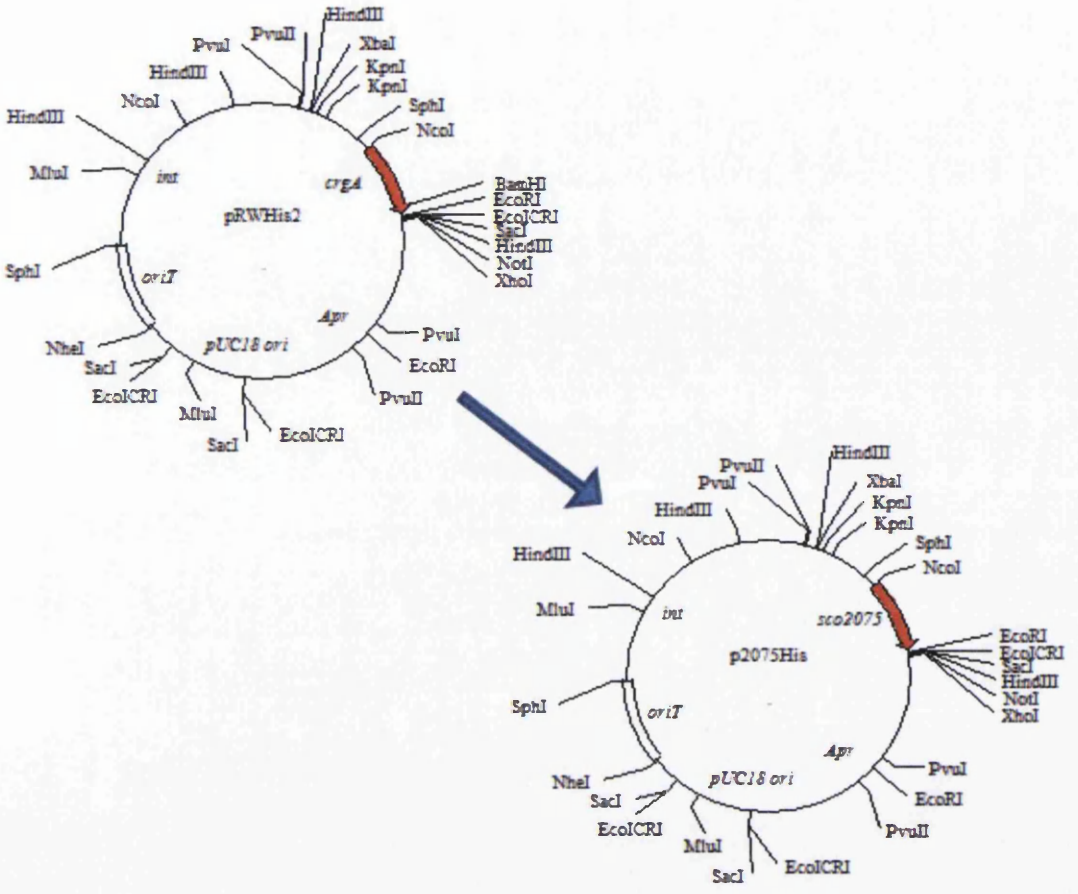

Figure 6.1: Plasmid map and construction of p2075His from pRWHis2. The PCR product containing *sco2075* and upstream region was cloned into pRWHis2 vector at *Xba*I/ *Bam*HI to construct p2075His. Maps are not drawn to the scale.

In order to look at the abundance of SCO2075 within spores and mycelium, samples were grown on agar plates with cellophane discs as described in Chapter 2 and total protein used for Western blot analysis using Penta-His peroxidase conjugate (QIAGEN) to detect His-tagged proteins. The predicted protein size of SCO2075 is 25.5KDa and with a C-terminal 6xHis-tag ~28KDa. However, the predominant band appears at 35KDa which is discussed further in 6.6. From the Western blots shown in Figure 6.2A, protein levels of SCO2075 appear almost undetectable in vegetative

mycelium (lanes 1) with increased concentrations coincident with aerial hyphal formation (Figure 6.2B, lanes 3&4) with highest levels of protein found in spore samples (Figure 6.2A, lanes 3&4).

A.

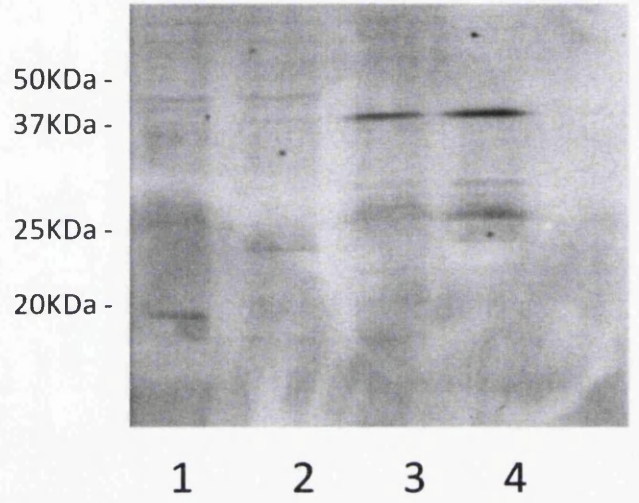

B.

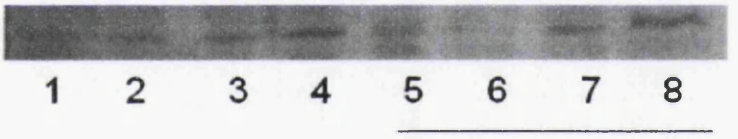

Figure 6.2: A. Western blot of total protein samples run on a 12% SDS PAGE gel at time points: 24, 48, 72, 96 (lanes 1-4) from SFM with cellophane discs. Samples in lanes 3 and 4 are from spores only. Prestained precision plus kaleidoscope marker (Biorad) was used for Mw estimation B. Western blot of samples taken from NMMP with cellophane discs at time points 24h (lanes 1,5) , 48h (lanes 2,6), 72h (lanes 3,7), 96h (lanes 4,8) with and without KCl run on a 12% SDS PAGE gel. Solid line underneath membrane indicates samples grown with KCl. Penta-His peroxidase conjugate (QIAGEN) was used to detect His-tagged proteins.

SCO2075 was also looked at under osmotic stress from innoculation of medium with spores. Agar plates with and without 250mM KCl were prepared with cellophane discs and samples taken at the specified time points from 24h to 96h. Samples were sonicated and quantified. 20µg of total protein from each sample was run on a 12% SDS PAGE. The gel was then used for a western blot analysis. The Western blot in

Figure 6.2B shows SCO2075 protein from time points 24h, 48, 72h and 96h without osmolyte added (lanes 1-4) and with osmolyte added (lanes 5-8). From the western bot there is a slight increase in protein under osmotic shock in protein from 72h to 96h KCl samples compared to uninduced (~1.6 fold).

6.3 Oligomeric state of protein

The crystalline structure of ten *E. coli* DksA protein monomers showed four type II dimers and one type I dimer, where type I are connected by a non-proper two-fold symmetry with ~110° rotation, while type II have more physiological structural characteristics with a proper two-fold symmetry and possesses quite an extensive symmetric interface involving their long Coiled-coil domain (Perederina, Svetlov et al. 2004). As such, the crystalline structure did not fully clarify DksA's native oligomeric state, although it suggested its major functional state was more than likely a monomer as the interactions between the two monomers are easily disrupted in solution. However Perederina, Svetlov et al. (2004) did not rule out the possibility of dimers existing and it was suggested that monomers are most likely with the possibility of a dimer forming that could be involved in other regulatory aspects of DksA.

Clarification of SCO2075 oligomeric state was done using blue native PAGE Tris-Glycine gels as either linear or gradient 4-16% (BioRad). Blue-native PAGE was used with coomassie G-250 as the charge shift molecule in the cathode buffer. Alternate loading buffers and protein concentrations were used including Invitrogen's NativePAGE™ sample loading buffer and 10% glycerol. When comparing lanes 5 and 9 in Figure 6.3A, it is evident that SCO2075 runs as a band, with a slight smear above,

using 10% glycerol (lane 9). However, lane 5, where SCO2075 is loaded in Invitrogen's native loading buffer, SCO2075 migrates as a large smear.

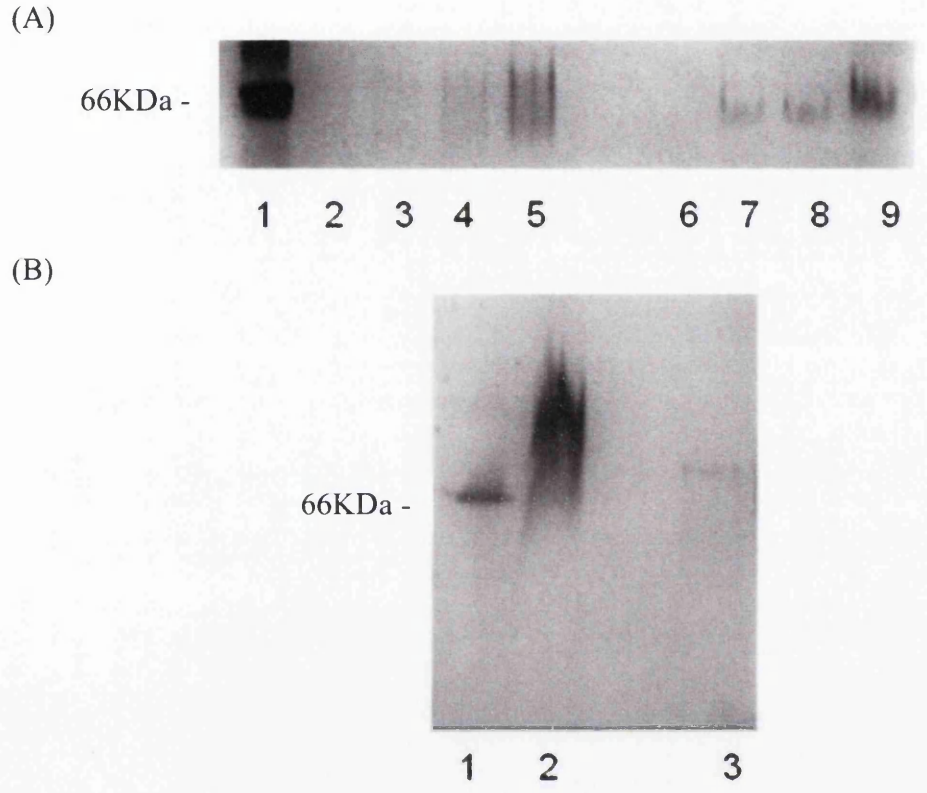

Figure 6.3: Native PAGE analysis of recombinant C-terminally His-tagged SCO2075. A. Blue native PAGE, Straight 7.5% Tris-glycine gel comparing native loading buffer versus 10% glycerol. Lane 1 Invitrogen native MW marker, 0.6, 1, 2, 3μg SCO2075 in native loading buffer, lanes 7-10: 0.6, 1, 2, 3 4μg with glycerol. B. Blue native PAGE 4-16% Tris-glycine gel. Lane 1 contains 2μg BSA, lane 2 2μg SCO2075 in 10% glycerol and lane 3 contains 300ng SCO2075. Gels A and B are both Coomassie stained gels.

To compare the molecular weight of recombinant SCO2075, fresh BSA was prepared each time and 1μg loaded. BSA is predominantly a monomer and has a molecular weight of 66KDa. As BSA is roughly double the protein molecular weight of SCO2075, it can give a good indication of whether its oligomeric state is monomeric or dimeric.

When SCO2075 was run on a 4-16% gradient gel, protein concentrations had to be reduced to 300ng in order to produce a clean band, as 2μg of protein produced a large smear (Figure 6.3B). In both gels, SCO2075 is comparable to BSA in migration, suggesting that SCO2075 is a dimer (Figure 6.3).

6.4 DNA binding activity

It has been shown in *P. aeruginosa* that DksA, at concentrations of 10μM has the ability to bind DNA via the C-terminal domain (Perron, Comte et al. 2005). An intriguing aspect of SCO2075 is the fact that it has an N-terminal domain sequence with similarities (~35-52%) to other bacterial histone-like proteins such as H-NS-like protein from *M. tuberculosis*, HU proteins from *Mycobacterium*, *S. coelicolor* and eukaryotic H1-HC2 like proteins from *Chlamydia* (Chapter 3).

As protein expression levels under its native promoter are relatively low (Figure 6.2A, lanes 1-2), *sco2075* was initially cloned into pIJ8600 under the control of the *tipA* promoter producing pDksA3 (Figure 4.13), for expression in *Streptomyces*. However, protein purifications had significant amounts of protein degradation and/ or a high abundance of other proteins with the ability to bind to the nickel in His-tag purification systems due to the low concentration of diamide required to elute SCO2075 (Figure 6.7C). In order to improve the quality of the preparations, *sco2075* was amplified from chromosomal DNA and cloned into pET expression vectors for recombinant expression of the protein.

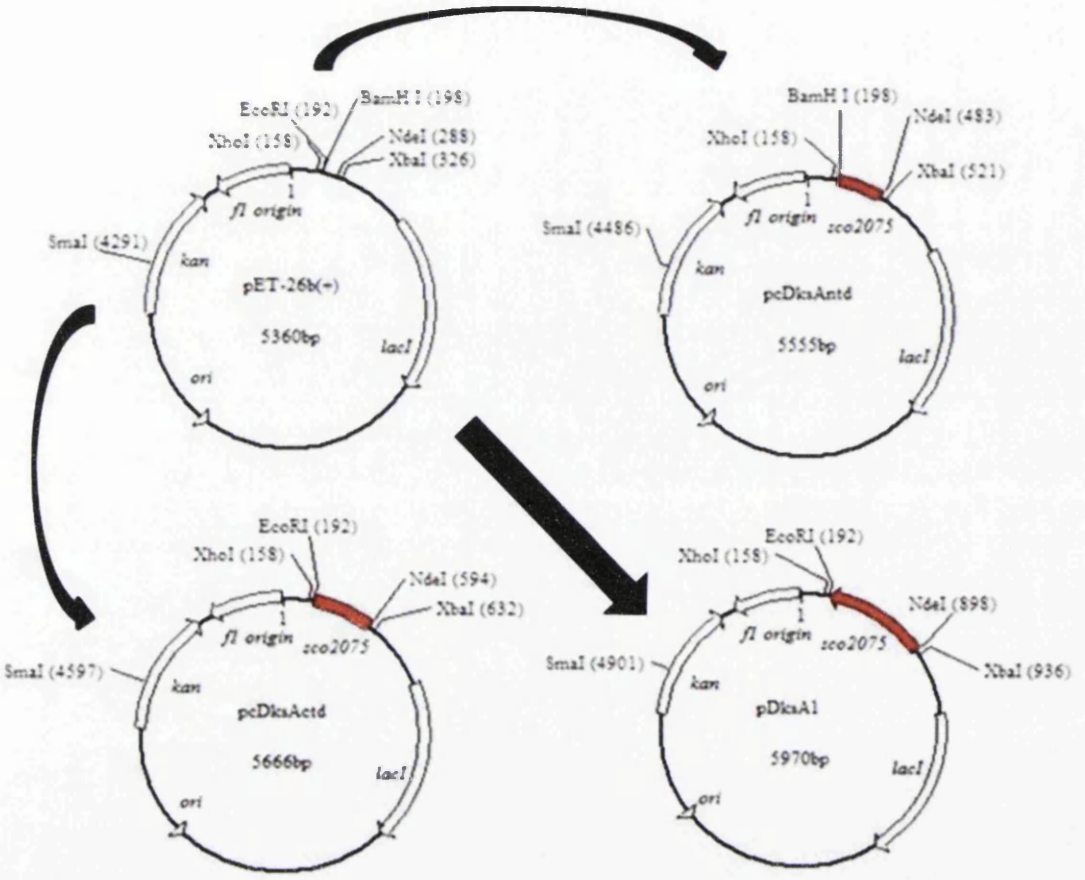

Figure 6.4: Plasmid map used to construct: pDksA1, pcDksActd and pcDksAntd from pET-26b(+). To place the gene under the control of T7 promoter, the PCR products containing the specific gene/ truncation gene were cloned into pET-26b(+) vector at *Nde*I/ *Bam*HI to construct the corresponding plasmids. All plasmids contain a C-terminal 6xHis tag. pDksA1 contains full length *sco2075*, pcDksActd contains the truncated C-terminal domain and pcDksAntd contains the truncated N-terminal domain. Maps are not drawn to the scale.

To analyse the DNA-binding ability of SCO2075, the gene was amplified by PCR with primers DksA_NdeI and 2075_REV that include an *Nde*I and *Bgl*II site respectively (Table 2.6). DksA_NdeI places an *Nde*I site at the start codon to allow control via the T7 promoter and 2075_REV removes the TGA termination codon. The PCR amplified *sco2075* was cleaned, digested with *Nde*I and *Bgl*II, gel purified and cloned in to pET-26b(+) digested with *Nde*I/ *Bam*HI. The resulting plasmid pDksA1

(Figure 6.4) was confirmed by restriction digest analysis and sequencing and electroporated into BL21 competent *E. coli* for expression of recombinant protein under the control of the T7 promoter.

To construct an N-terminal His tagged SCO2075, the gene was amplified by PCR with primers DksA_NdeI and 2075_Rev (Table 2.6) that include *Nde*I and *Bgl*II restriction sites respectively. The PCR amplified *sco2075* gene was purifed, digested with *Nde*I and *Bgl*II, gel purified and cloned in to pET-16k digested with *NdeI/Bam*HI. pET-16k has the backbone from pET-16b with the resistance marker replaced with kanamycin. The plasmid pDksA2 (Figure 6.5) was confirmed by restriction digest analysis and sequencing. The plasmid pDksA2 was then electroporated into BL21 (DE3) for expression of recombinant protein under the control of the T7 promoter.

To construct a truncated SCO2075 protein consisting of the N-terminal domain, the gene was amplified using PCR primers DksA_NdeI and 2075_trc_BamHI (Table 2.6), PCR clean up performed and digested with *Nde*I and *Bam*HI and cloned in pET-26b(+) restriction digested with *NdeI/ Bam*HI (Figure 6.4) to produce a C-terminal His-tagged protein (pcDksAntd), and into pET-16k (Figure 6.5) to produce an N-terminal His-tagged protein (pnDksAntd). Similarly, the C-terminal domain truncated SCO2075 was constructed using primers 2075_REV and CTD_NdeI (Table 2.6) to produce an in-frame deletion corresponding to the N-terminal domain of the protein. The PCR product was cleaned, restriction digested with *NdeI/ Bgl*II and gel purified and cloned into pET-26b(+) restriction digested *NdeI/ Bam*HI producing plasmid pcDksActd (Figure 6.4) and in to pET-16k restriction digested with *NdeI/ Bam*HI to produce plasmid pnDksActd

(Figure 6.5). All plasmid constructs were confirmed by restriction digest and sequencing.

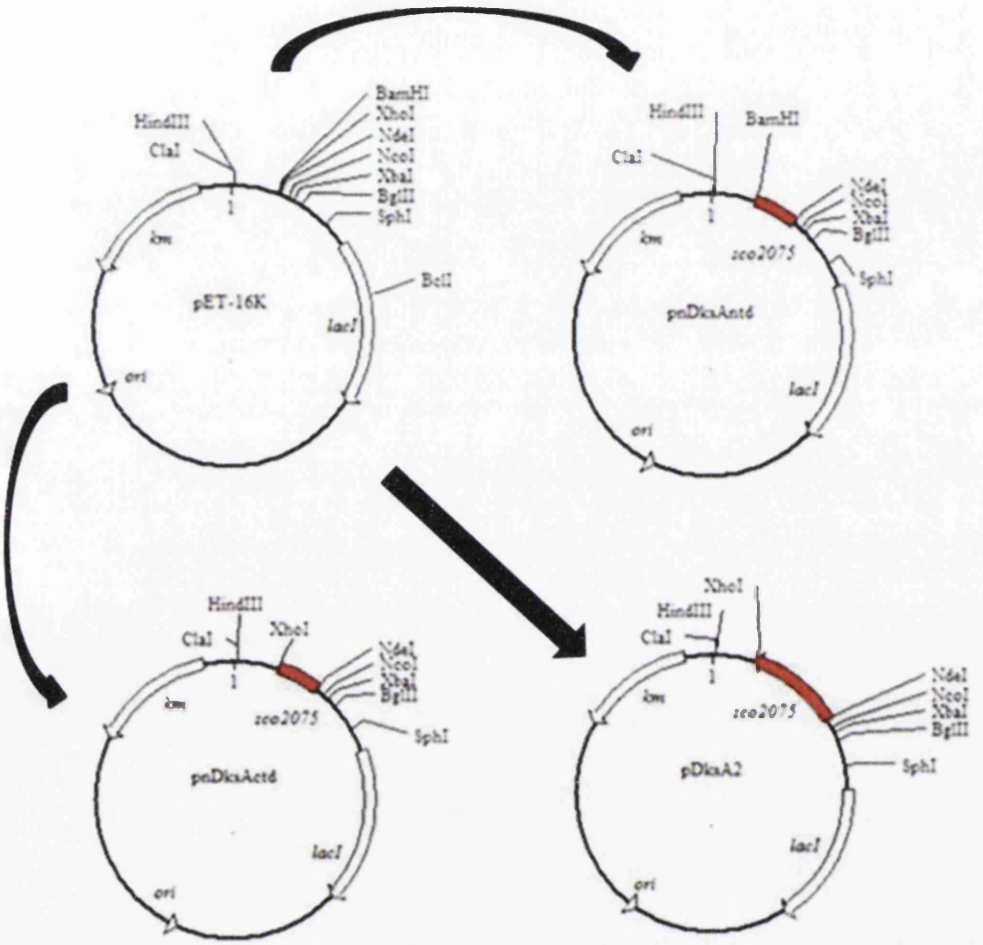

Figure 6.5: Plasmid maps used to construct: pDksA2, pnDksActd and pnDksAntd from pET-16K. To add a 10xHis N-tag to the protein and place the gene under the control of T7 promoter, the PCR products containing the specific gene/ truncation gene were cloned into pET-16k vector at *NdeI/ Bam*HI to construct the corresponding plasmids. pDksA2 contains full length *sco2075*, pnDksActd contains a truncated *sco2075* encoding the C-terminal domain and pnDksAntd contains a truncated *sco2075* encoding the N-terminal domain. Maps are not drawn to the scale.

6.4.1 Recombinant protein purification

In order to test the constructs, pDksA1 and pDksA2 (Figure 6.4/ 6.5) were electroporated into *E. coli* BL21 (DE3), protein expression induced and purified as

described in Chapter 2. Figure 6.6 shows the purified recombinant SCO2075 protein with a C- and N- terminal His-tag (lanes 4 and 8 respectively) compared with an empty vector (lane 2). Purification with the N-terminally His-tagged SCO2075 resulted in a higher yield of purified protein as a result of the higher affinity to the nickel beads due to the 10xHis-tag, where a 6xHis-tag is on the C-terminal protein.

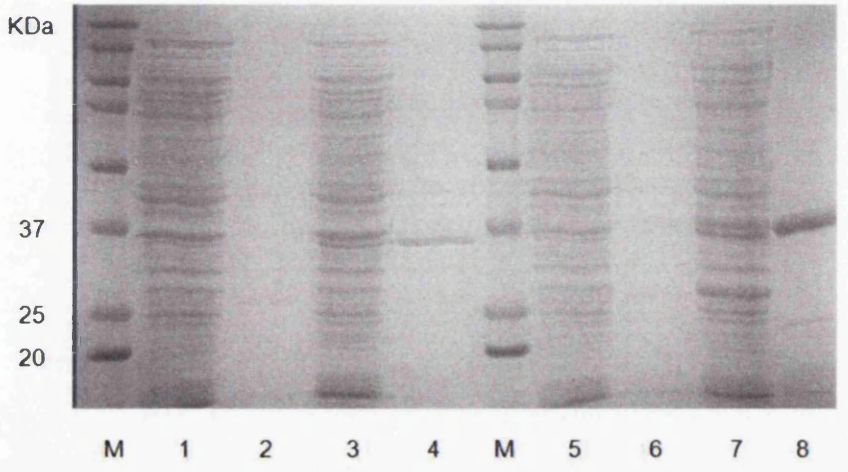

Figure 6.6: Coomassie blue stained 12% SDS-PAGE gel verifying the expression and purification of recombinant protein from plasmids pDksA1 and pDksa2. Lanes 1 and 5 shows protein not bound to the nickel particles from uninduced and induced empty vector strain. Lane 2, elution from empty vector strain without induction and with induction (lane 6). Lanes 3 and 4: induced, unbound protein and eluted purified protein of from plasmid pDksA1 (C-terminal His-tagged protein) respectively. Lanes 7 and 8: induced, unbound protein and eluted purified protein from pDksA2 (N- terminal His-tagged) lane 8. M is BioRad precision plus kaleidoscope marker.

To improve the quality of the C-terminally His-tagged SCO2075, the elution buffer was diluted with wash buffer to create a concentration range from 10mM to 500mM imidazole, which showed that optimum purity was obtained with elutions at 100 to 200mM imidazole (Figure 6.7A lanes 3 and 4). However, due to the low imidazole concentration required to elute the proteins, this optimum purity resulted in a significant loss of protein being eluted at lower concentrations of imidazole. For the remaining

recombinant protein work, GE Healthcare's 1ml HisTrap HP columns were used which has an approximate yield of 40mg His-tagged protein binding affinity (Figure 6.7B).

(A)

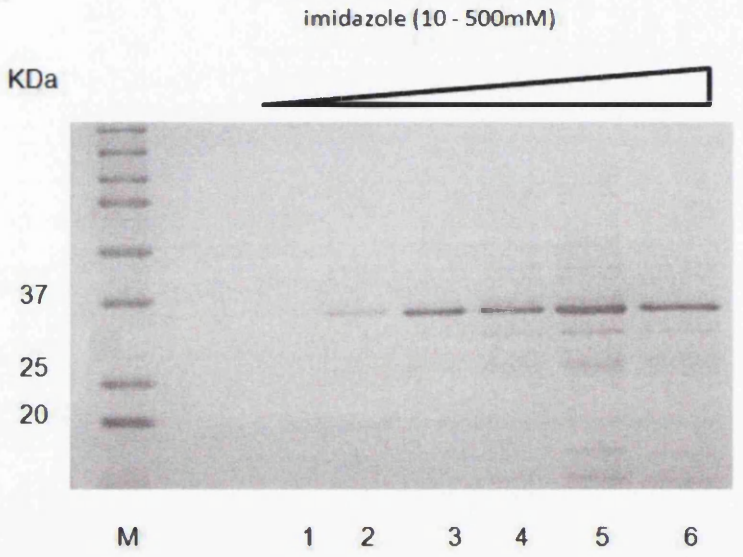

(B)

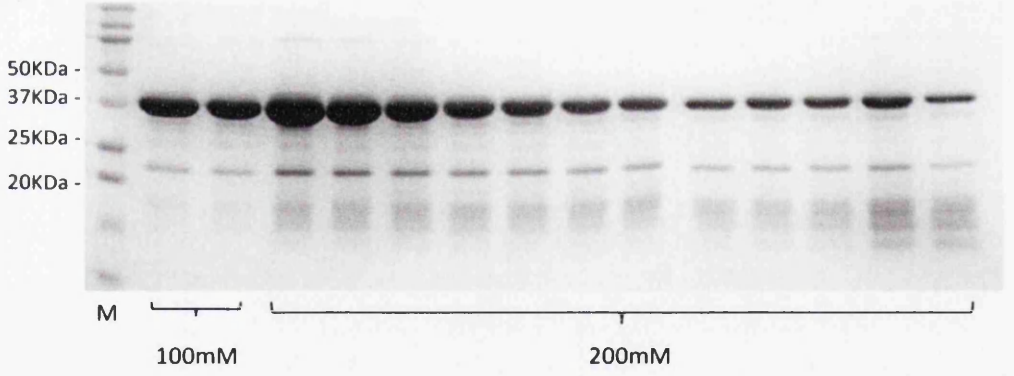

(C)

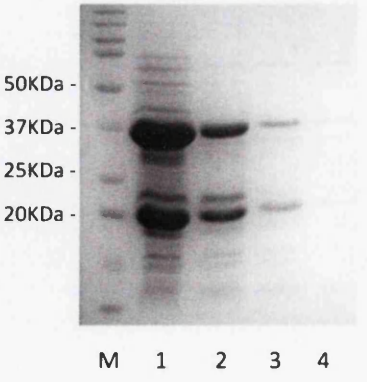

Figure 6.7: Recombinant SCO2075 purification.
(A) 12% SDS-PAGE gel stained with Coomassie blue showing purification of recombinant SCO2075 from pDksA1 (C-terminal His-tag) with an increasing concentration of imidazole in the elution buffer. Lane M is a protein MW ladder proceeded by an elution range of 10mM to 500mM imidazole (lanes 1-6). The open triangle on the top of the gel image denotes increasing concentrations of imidazole. (B) 12% SDS-PAGE gel stained with Coomassie blue showing purification of N-terminal His-tagged SCO2075 purification using HisTrap column. Brackets underneath indicate the last two 100mM imidazole elutions which give the highest purity, and the larger bracket indication 200mM washes. Each lane is a sample of successive 1ml aliquots eluted from the column. (C) 12% SDS-PAGE gel stained with Coomassie blue showing purification of samples from successive 1ml aliquots of the 100mM imidazole elution from *S. coelicolor* preparation using plasmid pDksA3 (lanes 1-4). M denotes the protein marker (Precision plus kaleidoscope protein marker (BioRad)).

6.4.2 Analysis of DNA binding

In order to analyse the ability of the protein to bind to DNA, an electrophoretic mobility shift assay (EMSA) was used (Garner and Revzin 1981). Using the previously mentioned method of purifying recombinant protein, the protein was dialysed overnight in 50mM Tris 50mM NaCl (pH 7.5) to remove remaining imidazole. SCO2075 was incubated with supercoiled pGEM plasmid in loading buffer (Werlang, Schneider et al. 2009) for 15mins prior to loading on to an agarose gels. The plasmids pGEM and pUC18 were both used due to their relatively small plasmid sizes and similarity in size (~3000bp and ~2800bp respectively) and no differences were observed in EMSA (data not shown).

Figure 6.8 shows there is a distinct dose-dependent retardation of the supercoiled pGEM vector with increments of 0, 0.1, 0.25, 0.5, 0.75 and 1μM of recombinant His-tagged SCO2075, whereas BSA had no effect on the migration of the plasmid compared to the supercoiled plasmid run alone. This experiment was also repeated on linearised DNA with similar results and both C- and N- tagged protein which showed no difference

in DNA affinity (data not shown). This indicates that the His-tagged SCO2075 protein binds pGEM in a non specific manner. As a result the N-tagged proteins were used for the rest of the DNA binding assays due to its increased affinity to the HisTrap column.

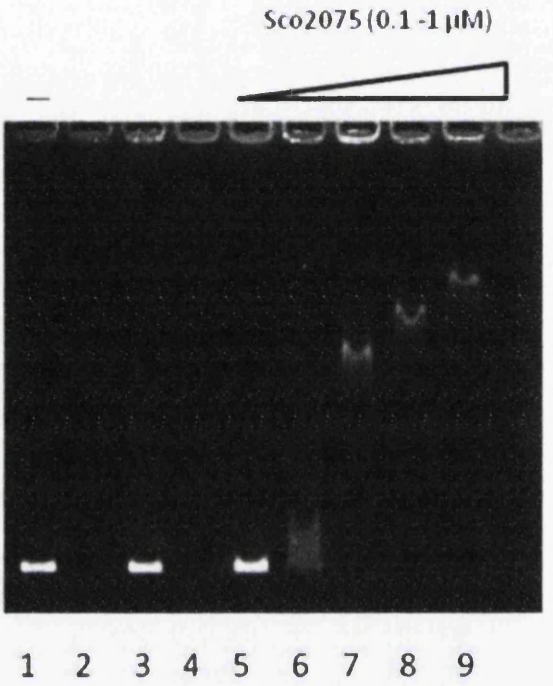

Figure 6.8: Electrophoretic mobility shift assay of increasing amount of SCO2075 (C-terminal His-tagged) with 300ng of supercoiled pGEM plasmid in a 0.8% agarose 1xTAE gel run for 16hours at 48V. Lane 1 contains 300ng pGEM DNA substrate in the absence of protein, lane 2; 1μg BSA, lane 3; 1μg BSA and 300ng DNA, lane 4; 1μg SCO2075. Lanes 5-9 contain pGEM substrate DNA with SCO2075 in a range of 0.1, 0.25, 0.5, 0.75 or 1μM of protein. The open triangle on the top of the gel image denotes increasing concentrations of SCO2075.

To evaluate the DNA binding properties of SCO2075 further and to determine whether it is domain specific or relies on both domains, the protein was separated in to an N-terminal domain (DBD) fragment and C-terminal domain (DksA) fragment with amino acid sequences shown in Figure 6.9C. The resulting plasmids pcDksAntd (DBD) and pcDksActd (DksA) are both C-terminal His-tagged (Figure 6.4), whereas

pnDksAntd (DBD) and pnDksActd (DksA), are both N-terminal His-tagged (Figure 6.5).

A.

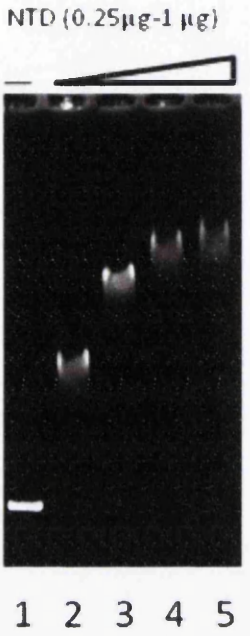

B.

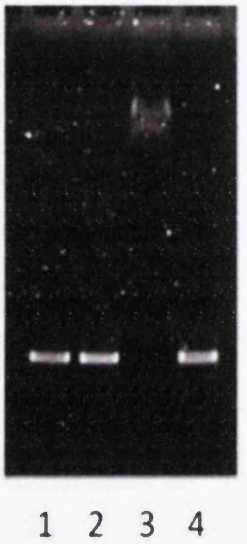

C.

Truncated NTD sequence	MVAKKKTTAA KQSAAEESAA EQDPARKKAA EKTAAKKSPA RKTAAKKSPA EKTAAKKSTA KKSTAKKVGA AEAAEQTGAT TVVAKKTPGT ATAAKTAVPK ARGTAAVPGD LAVRPGEEPW TPQEVEEARG ELQSEADR
Truncated CTD sequence	GEEPWTPQEV EEARGELQSE ADRLRTEIDT SERSLQGMMR DSGDGAGDDE ADTGSKNITR EHELALAATA REVLSQTERA LDRLDAGTYG LCENCGNPIG KARMQAFPRA TLCVECKQKQ ERRY

Figure 6.9: A. EMSA of recombinant SCO2075 DBD fragment. Reactions were performed with 300ng pUC18 substrate DNA in the absence of protein (lane 1) or presence of 0.25, 0.5 0.75 or 1µM of protein (lanes 2-5 respectively). The open triangle on the top of the gel image denotes increasing concentrations of the DBD fragment of SCO2075. B. EMSA of recombinant SCO2075 DksA fragment. All lanes contain supercoiled plasmid pUC18 substrate DNA with 1µM of DksA domain truncated protein in lane1, 300ng pUC18 DNA substrate absent of protein, in lane 2. pUC18 substrate DNA with 1µM full length protein in lane 3 and 1.8µM DksA domain protein with DNA in lane 4 C. Amino acid sequences of the truncated protein used in the EMSAs.

The recombinant DBD and DksA domain protein fragments of SCO2075 were purified as previously and dialysed. The gel retardation assay was also repeated as previously with the exception of supercoiled pUC18 as the DNA probe, with these recombinant protein fragments. EMSA analysis of these fragments showed a dose-dependent retardation of the supercoiled pUC18 with the DBD domain fragment (Figure 6.9A), however, there was no alteration in DNA migrations of lanes containing the DksA domain portion of the protein compared with the negative control (Figure 6.9B). This therefore shows that the DBD domain portion of SCO2075 is sufficient for DNA binding (Figure 6.9).

6.5 DNA binding characteristics

To characterise the DNA binding activity of SCO2075, recombinant N-terminal His-tagged SCO2075 was incubated in a concentration range with pUC18 supercoiled DNA and linearised pUC18 (digested with *Hind*III), using the same protocol as previous. From the EMSA gel in Figure 6.10, there appears to be no preference for linearised DNA over supercoiled with the slight migration difference between supercoiled and linearised samples at the same protein concentration the result of topological differences between linearised and supercoiled DNA affecting migration through the gel.

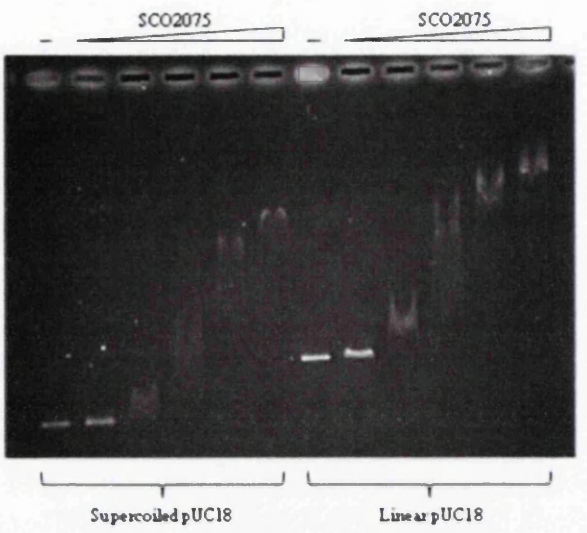

Figure 6.10: EMSA analysis comparing supercoiled pUC18 with linearised pUC18. With protein concentration range from 100ng to 300ng of N-terminal His-tagged SCO2075.

6.6 Post translational modification?

The predicted molecular weight of native SCO2075 is 25.5KDa, while the addition of the His-tag can add up to an additional ~2.5KDa giving a theoretically molecular weight of ~28KDa which results in a discrepancy of 7KDa between the predicted molecular weight of the protein and the most prevalent form visible during SDS-PAGE analysis (Figure 6.11). Western analysis shows that the both bands are indeed SCO2075 as shown in Figure 6.11, which shows a Western blot of C- (lane 1) and N-terminally His-tagged SCO2075 protein (lane 2). The discrepancy when comparing the lower bands (~23KDa) is the result of the size difference between the N-terminal and C-terminal His-tag where the N-terminal tag is larger due to a 10xHis-tag compared to 6xHis in the C-terminal tag). This discrepancy in size could be the result of post translational modification such as acetylation, where twenty three lysine residues are predicted to be acetylated in the N-terminal half of the protein alone using the

software PAIL (PAIL: Prediction of Acetylation on Internal Lysines. Yu Xue, Ao Li, and Xuebiao Yao.). This could potentially be a mechanism for the regulation of the high affinity DNA binding of SCO2075 and/ or the regulation of the DksA domain.

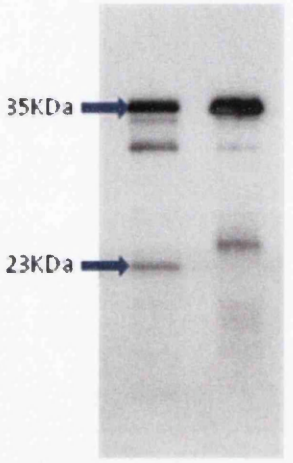

Figure 6.11: Western blot analysis of C- and N- terminally tagged SCO2075.
E.coli purification from C-terminally His-tagged SCO2075 (lane 1) and N-terminally His-tagged 2075 (lane 2). The lower bands run at smaller MW than the predicted full length Sco2075 (Mw Sco2075 ~25kda without His-tag), however, both C- and N-terminal His-tags show similar size lower band which would suggest it is not being cleaved. Penta-His peroxidase conjugate (QIAGEN) was used to detect His-tagged proteins.

6.7 Does SCO2075 bind RNAP?

Using recombinant SCO2075 protein, it was looked at whether SCO2075 binds RNA polymerase *in vitro*. To assess this, native His-tagged RNAP was purified from *S. coelicolor* using strain J1981 (Babcock, Buttner et al. 1997) and purified using HisTrap HP columns.

Both proteins were combined and incubated at room temperature for 15 minutes and then 2D gel electrophoresis using blue native PAGE as the first dimension and the SDS PAGE as 2nd dimension. If an interaction exists, a complex of RNAP and

SCO2075 would be present in the native gel. The 2nd dimension would result in dissociation of this complex and two bands corresponding to SCO2075 (37KDa) and the β' subunit of RNA polymerase (144KDa) in the same lane, while no interaction would show no SCO2075 vertically below the β' subunit of RNA polymerase. From the Western blot analysed in Figure 6.12 there was no detectable interaction, however, this could be a result of transient binding between DksA and RNAP and the amount of SCO2075 bound to the RNAP insufficient to be detected by western blot.

An alternate method to show this interaction would be purifying native RNA polymerase and immobilizing His-tagged SCO2075 on a HisTrap column. The purified RNA polymerase is run through the column and after a large wash volume is passed through the column, SCO2075 is eluted with imidazole. As the native RNA polymerase would be unable to interact with the HisTrap column, any RNA polymerase in the elution would indicate interaction.

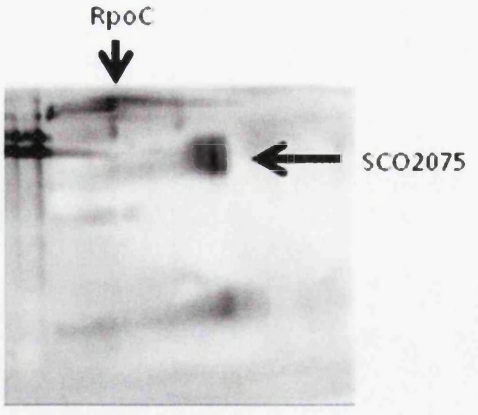

Figure 6.12: Western blot of 2D gel for analysis of interactions between His-tagged SCO2075 and RNAP (His-tagged RpoC). The first dimension was a native blue native PAGE, followed by the second dimension which was a SDS-PAGE. Penta-His peroxidase conjugate (QIAGEN) was used to detect His-tagged proteins.

6.8 DpsA expression in DSCO2075

DpsA has a similar expression profile to that of *sco2075* throughout the life cycle of *S. coelicolor*, with high level of protein within spores compared to mycelium (Facey, Hitchings et al. 2009). However unlike SCO2075 under osmotic stress/ shock DpsA protein levels dramatically increase within 2 hours and are maintained for at least 24h after shock (Facey, Hitchings et al. 2009).

With the similar expression profiles, DpsA was looked at to see if there was an altered protein level as a possibility of compensating any loss of SCO2075. M145 and DSCO2075 both containing plasmid pDpsA7, a vector containing *dpsA* under the control of its native promoter and fused to 6xHistidine residues at the C-terminal, were inoculated onto cellophane discs on NMMP and incubated at 30°C overnight for 16hours. The cellophane was then transferred to NMMP +/- 250mM KCl and incubated an additional 2hours at 30°C.

The western blot in Figure 6.13 shows under osmotic shock there is no apparent difference in DpsA expression between the parental strain M145 and the mutant strain DSCO2075. However, there was a three-fold higher basal DpsA protein level in the DSCO2075 mutant strain compared to parental strain.

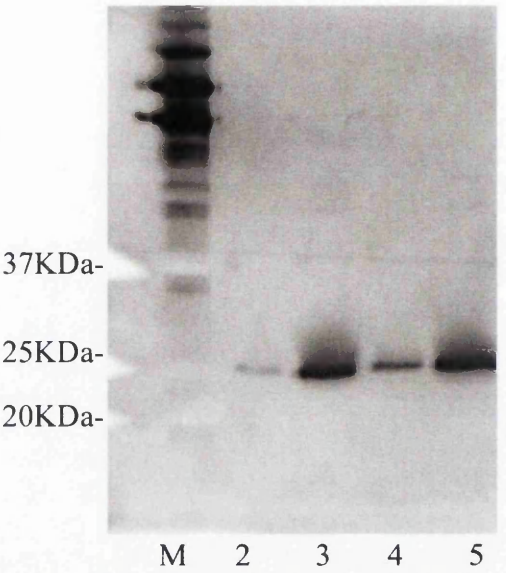

Figure 6.13: Western blot of DpsA expression in M145 and DSCO2075 strains.
DSCO2075 mutant strain and parental strain M145 containing plasmid pDpsA7 were inoculated onto NMMP with cellophane discs and incubated for 16 hours at 30°C. After 16hours they were transferred to NMMP with or without 250mM KCl and incubated for a further 2 hours at 30°C. Lane 1 labelled M contains BioRad kaleidoscope precision plus protein standard, lane 2 and 4 contain sample from M145/ pDpsA7 and DSCO2075/ pDpsA7 grown on NMMP respectively. Lanes 3 and 5 contain M145/pDpsA7 and DSCO2075/pDpsA7 samples from NMMP+250mM KCl respectively. Penta-His peroxidase conjugate (QIAGEN) was used to detect His-tagged proteins.

6.9 Summary

sco2075 increases in expression during the transition phase and growth of aerial hyphae to sporulation, with highest protein levels in spores and has a slight increase in expression under osmotic stress conditions. The predominant oligomeric state of SCO2075 appears to be a dimer.

Recombinant SCO2075 binds DNA in vitro non-specifically to linearised and supercoiled DNA and this ability is due to the histone like domain on the N- terminal portion of the protein. In a DSCO2075 mutant strain, basal DpsA expression is higher compared to parental strain M145, however there is no alteration in protein abundance under osmotic shock.

Chapter -7

Microscopy

7.1 Introduction

This chapter documents microscopic analysis of the cells of the mutant strain DSCO2075 and also to determine localisation of SCO2075 within the cell. With little macroscopic phenotype visible in the DSCO2075 mutant strain, it was important to determine if there were any microscopic morphological differences with the mutant strain compared to parental strain M145 due to its DNA binding ability. Fluorescence microscopy was used to visualise a SCO2075::mCherry fusion protein and to look at nucleoid condensation and septation in aerial hyphae. To define the timing of expression of *sco2075*, the SCO2075/ mCherry fusion protein was used to compare with the timing of expression with respect to Z-ring formation.

7.2 Microscopic analysis

The DSCO2075 mutant strain produces sporogenic hypae with unigenomic spores and is macroscopically morpologically similar to the parental strain M145 from vegetative mycelium through to sporulation (Chapter 4). With the evidence that SCO2075 can bind DNA *in vitro* and Western blot analysis suggesting higher expression levels in spores (Chapter 6), live staining of prespore chains was used to look at nucleoid morphology during vegetative and sporogenic stages of the life cycle. SFM plates were inoculated with strains M145 and DSCO2075 and incubated at 30°C for 48-65 hours when impressions were taken from the surface of the growing colonies with a cover slip and placed onto a slide with a DNA dye and images of prespore chains taken for analysis. Using Syto9 to stain the chromosomal DNA, the nucleoids appear to have an increase in the width along the axis of the hypha and transversally wider resulting in a

'boxier' shape than the parental strain M145 in prespore compartments (Figure 7.2B). This suggests more relaxed nucleoids in the DSCO2075 mutant strain compared to the parental strain.

7.3 Nucleoid measurements

As the DSCO2075 mutant strain proved to have similar macroscopic morphologies to the parental strain M145 as shown in Chapter 4 and as visually there appeared to be differences in nucleoid sizes shown in Figure 7.2B, the dimensions of the pre-spore nuceloids and compartments were quantified for both mutant and parental strains. As previously shown, SCO2075 has DNA binding activity and considering its expression appears during nucleoid condensation during sporulation, it was important to determine whether the absence of SCO2075 affected chromosomal compaction or altered compartment sizes during this phase of development. Sporulating septa were stained using Texas Red WGA, which binds to oligomers of peptidoglycan forming the cell wall, and chromosomal DNA was stained using Syto9 (Figure 7.1).

Spore suspensions were used to inoculated SFM plates and grown for 60-65 hours. Coverslips were used to take impressions from each strain and the nucleoids stained with Syto9 and microscopy immediately conducted and images saved for later analysis. The lengths of at least 400 randomly chosen nucleoids were measured where only nucleoids that formed part of a pre-spore chain were measured and used to calculate the percentage of nucleoids per a 0.1μm length interval using the Scion Image Program.

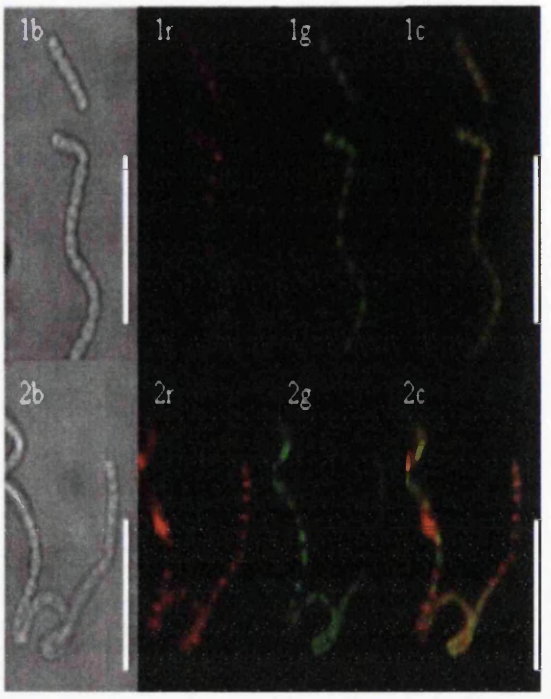

M145

DSCO2075

Fig. 7.1: Fluorescence microscopy of aerial hyphae of parental strain *S. coelicolor* M145 (panel 1) and DSCO2075 mutant strain (panel 2) using Texas Red WGA (cell wall) and Syto9 (chromosomal DNA) staining to visualize sporulating septa and chromosome distribution. Samples were prepared by taking impressions from each strain grown of SFM agar for 60-65 hours showing early-late stage sporulation. Each panel contains a bright field (b), Texas Red WGA (r), Syto9 (g) and the combined images of Texas Red WGA and Syto9 (c) Bar indicates 10μm.

To see if there was any variation in compartment size, the length of the compartments was measured using the Texas Red WGA stained septa from the same sample used for nucleoid measurements. Figure 7.1 shows dual cell wall (WGA Texas Red) and nucleoid (Syto9) live staining of parental strain M145 and DSCO2075 as an example of fluorescence microscopy images of parental strain M145 and DSCO2075 used for these measurements.

As there was an increase in protein expression of DpsA in the DSCO2075 mutant strain (Chapter 6) and DpsA has been shown to affect pre-spore nucleoid lengths (Facey, Hitchings et al. 2009), an *dpsA⁻/ sco2075⁻* double mutant was analysed with DSCO2075

and *dpsA*$^-$ mutant strains. The *dpsA*$^-$/ *sco2075*$^-$ double mutant strain was previously constructed using the insertion mutated cosmid 4A10.1.A08 hyg^R inserted into the *dpsA*$^-$ mutant strain and double cross-over confirmed by Southern Hybridisation.

Figure 7.2A shows the five sets of data collected. The nucleoid length measurements collected for each strain was subjected to statistical analysis to confirm statistical significance. Initially the data were tested with Kolmogorov Smirnov test for normality, which showed that the distributions of strain M145, DSCO2075, *dpsA*$^-$ and *dpsA*$^-$/ *sco2075*$^-$ were not normal with p values of $P<0.05$. The P values shows that the datasets were not normally distributed resulting in a non-parametric test being used to test for statistical significance. The Mann-Whitney U test was used to compare parental strain M145 and DSCO2075 measurements giving $P<0.01$ showing that the difference in nucleoid lengths of the DSCO2075 mutant strain is statistically significant.

Using the same method, the *dpsA*$^-$/ *sco2075*$^-$ mutant was compared to DSCO2075 and *dpsA*$^-$ mutant strains giving a $P<0.05$ also showing that the value for the double mutant is statistical significant. There is a slight variation in compartment lengths between DSCO2075 and M145 shown in figure 7.3, student T-test analysis however shows that it is not significant with $p>0.05$.

From the nucleoid analysis it can be seen that the DSCO2075 mutant strain has a larger positive skewness and elongated right tail compared to the parental strain M145 showing that there is an increase in the number of longer nucleoids as was suspected from the styo9 stained images previously viewed. Nucleoid measurements were also taken from M145 and DSCO2075 grown on NMMP, a minimal medium, using the same

protocol and this positive skewness and elongated right tail is also present as shown in Figure 7.3A.

(A)

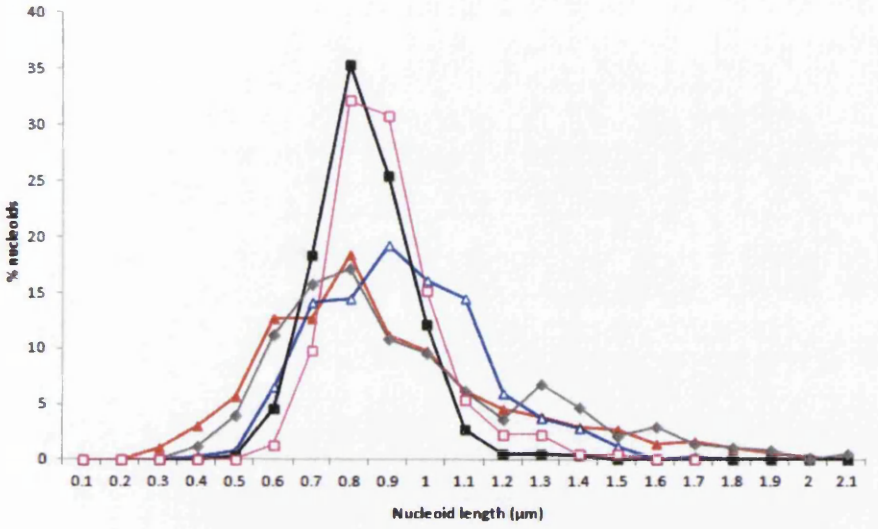

B)

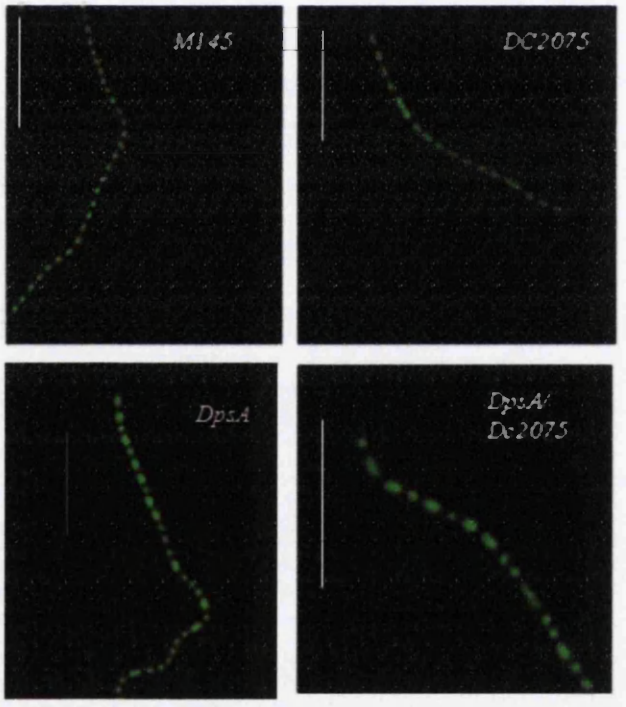

Figure 7.2: Analysis of prespore nucleoids.
(A) Distribution of nucleoid sizes from prespore chains grown on SFM of, M145 black squares, DSCO2075 open blue triangles, *dpsA*⁻ red triangles, double mutant *dpsA*⁻/ *sco2075*⁻ grey diamonds and DSCO2075/ pSH2075 pink open squares. (B) live stained cells - Syto9 stained nucleoids of prespore chains from parental strain M145, DSCO2075, *dpsA*⁻ and *dpsA*⁻/ *sco2075*⁻. Bar indicates 10µm.

While the nucleoid distribution pattern of *dpsA⁻/ sco2075⁻* double mutant strain shows more similarity to the *dpsA⁻* mutant strain profile a small subpopulation of longer nucleoid lengths appears in the double mutant shown in the distribution graph in Figure 7.2. This suggests that the *dpsA⁻* mutant strain is the dominant mutant phenotype of nucleoid lengths, which is somewhat expected as DpsA is more abundant in spores than SCO2075 and the mutation results in a more profound effect. The absence of SCO2075 does not affect the proper segregation of the nucleoids during sporulation.

To confirm that the alteration in nucleoid condensation in DSCO2075 was a result of the mutation, plasmid pSH2075 which integrates at the ϕC31 *att* site, containing a single copy of *sco2075* was conjugated into DSCO2075 and exconjugants selected for hygromycin resistance. Plasmid pSH2075 inserted into DSCO2075 results in recovery of nucleoid compaction comparable to that of parental strain M145 (Figure 7.2A). Median nucleoid lengths for each strain were; 0.78μm, 0.89μm, 0.85μm, 0.9μm and 0.8μm for M145, DSCO2075, *dpsA⁻*, *dpsA⁻/ sco2075⁻* double mutant and DSCO2075/ pSH2075 respectively.

(A)

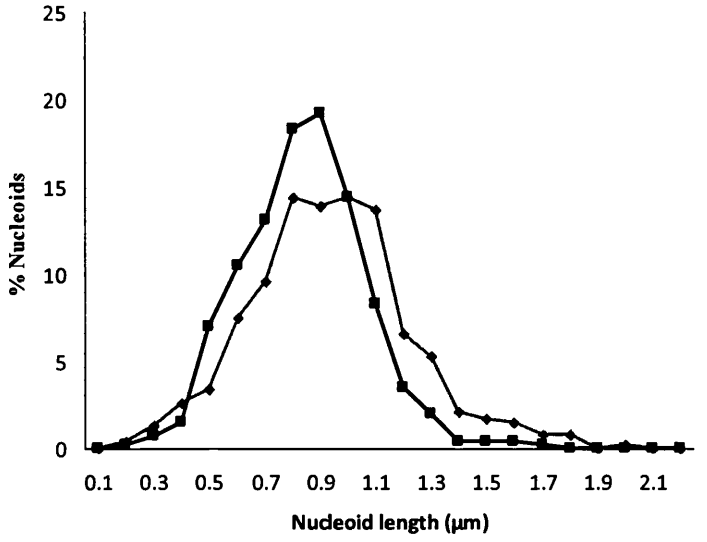

(B)

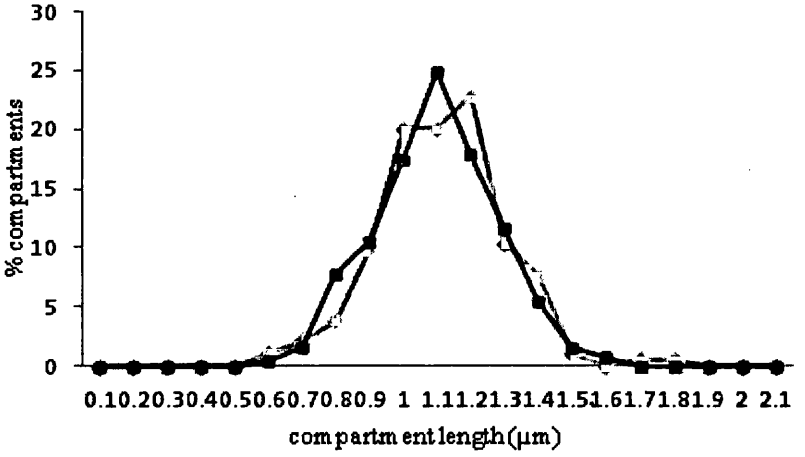

Figure 7.3: (A) Distribution of nucleoid sizes from M145 and DSCO2075 mutant grown on NMMP. Graphs were generated by plotting the percentage of nucleoids per 0.1μm intervals from 0.1- 2.1μm. Black squares – M145, grey diamonds – DSCO2075 (B) Distribution of pre-spore compartment lengths. Black squares- M145, grey diamonds DSCO2075.

7.4 Protein localisation- mCherry fusion

Fluorescent microscopy was used to look at *sco2075* expression and localisation within the complex life cycle of *S. coelicolor* under different environmental conditions. A *sco2075*::mCherry fusion was constructed and conjugated into the parental strain M145. The M145/p2075mCh strain was plated on either NMMP or SFM agar medium with and without KCl and samples examined at varying time points to cover the whole complex life cycle in order to obtain images of each stage of development.

In order to construct the plasmid with a C-terminal mCherry translational fusion under the control of the native promoter, pSET152 was restriction digested with *Xba*I and *Eco*RI and gel purified. The mCherry tag fragment was cut out from pNA585 using *Bam*HI and *Eco*RI and gel purified. The *sco2075* gene and upstream region was amplified by PCR using primers 2075_FWD and 2075_REV (Table 2.6) with *Xba*I, *Bgl*II sites included in these primers respectively. 2075_REV removes the TGA stop codon from *sco2075* allowing a transcriptional fusion. The PCR product was then cleaned using QIAquick PCR Purification Kit (Qiagen) and cloned into pGEM T-easy vector to make pGEM2075. The plasmid pGEM2075 was digested with *Xba*I and *Bgl*II, gel purified and the three gel purified fragments were ligated together at 14°C overnight to produce p2075mCh (Figure 7.4). The plasmid p2075mch was checked by restriction digest and sequencing.

In isolated spores from a spore suspension of M145 containing the plasmid p2075mCh, fluorescence from the mCherry fusion protein is present consistent with the shape of the nucleoid (figure 7.7). Following germination where either one or two germ tubules emerge from the unigenomic spore, SCO2075 appears to defuse from the spore

along the growing mycelium where detectable florescence levels diminish and SCO2075 appears to be absent or at best at very low levels within the vegetative mycelium until aerial hyphae form (Figure 7.5, 7.6).

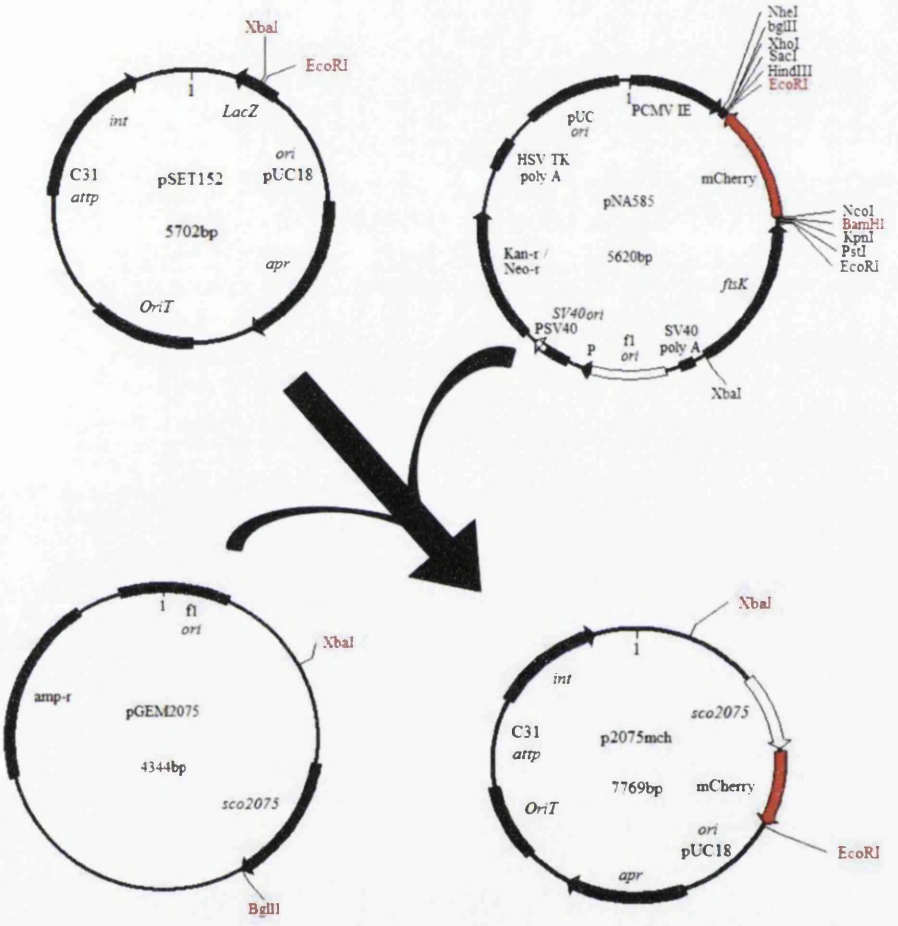

Figure 7.4: Maps of plasmids used to construct p2075mCh containing the sco2075 gene with a C-terminal translationally fused mCherry with the native *sco2075* promoter upstream. Restriction enzymes sites used for the cloning of *sco2075*/ mCherry fusion are shown in red. The maps are not drawn to scale.

Only during the late vegetative mycelium/ aerial hyphal transition phase does fluorescence levels of the SCO2075::mCherry fusion become detectable again. At first, this expression was very low and diffused. Image 2 in Figure 7.6 shows tissue-specific

expression of the SCO2075::mCherry fusion in aerial hyphae. The fluorescence intensity increases as the aerial hypha matures into spore chains (Figure 7.6).

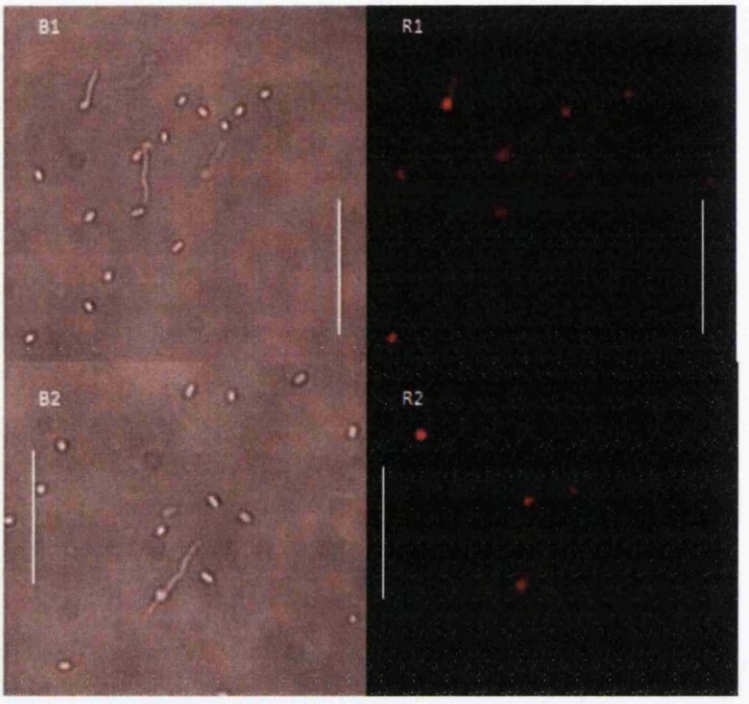

Figure 7.5: fluorescence microscopy images of SCO2075::mCherry fusion protein in spores and germinating spores with single and double germ tubes emerging from SFM. Each panel shows bright field (B) and mCherry fusion emission (R). Scale bar 5μm.

From Figure 7.6 which shows different stages of growth, SCO2075::mCherry appears to have a very low abundance in vegetative hyphae, and only has a diffused protein localisation in early aerial hyphae which remains through sporulation. During late sporulation when the unigenomic spores are mature SCO2075::mCherry fusion protein remains within the spores consistent with the shape of the nucleoid shown in image r4 in Figure 7.6 and image r3 in Figure 7.7.

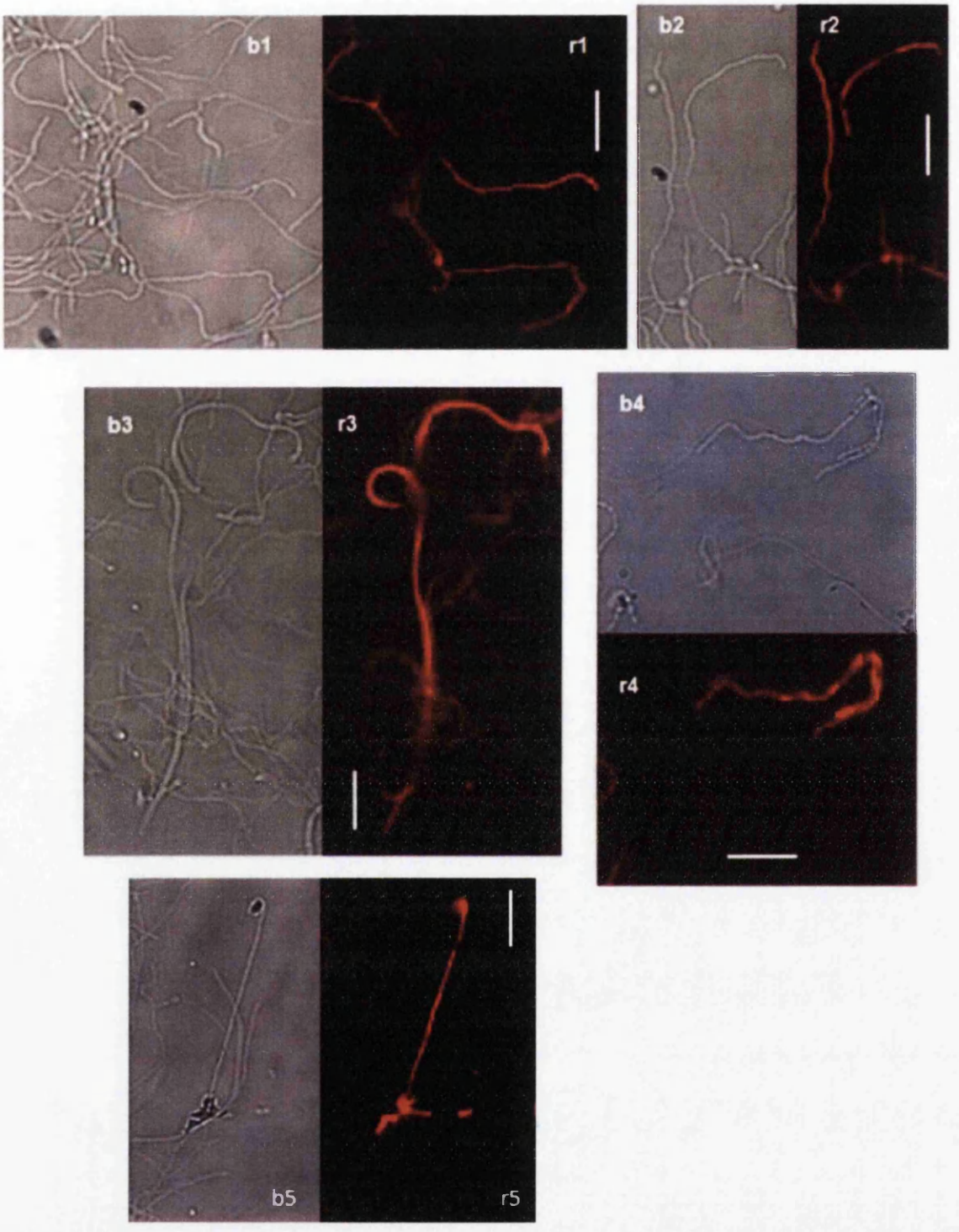

Figure 7.6: Fluorescent microscopy images of SCO2075::mCherry fusion protein in vegetative mycelium, aerial hyphae and spore chains. Each panel shows bright field (b) and mCherry fusion emission (r). Images 1, 2 and three show a mixture of vegetative mycelium with some aerial hyphae and image 4 shows spore chains. Image 5 is a sample grown on SFM with 250mM KCl. Bar indicates 10µm.

This expression and localisation profile was reproduced under osmotic stress conditions with no discernible difference in fluorescence levels of SCO2075::mCherry protein, which remains in the prespores through maturation and subsequently when the spores separate from the chain and the life cycle repeats (image 5, Figure 7.6). Fluorescence appears similar at the same time points in the life cycle when comparing growth on SFM and NMMP (data not shown).

7.5 Co-visualisation of Z-ring formation and *sco2075* expression

Considering that the timing of expression of SCO2075 appears to coincide with development of aerial hyphae, the increased protein abundance was looked at relative to the FtsZ expression and Z ring formation. This was to define whether SCO2075 is up regulated before or after developmental up regulation of FtsZ expression and Z-ring formation.

Unlike in *E. coli* where nucleoid occlusion affects Z-ring formation, in the early stages of sporulation and septation in *Streptomyces* the Z-ring forms over un-segregated chromosomes and nucleoid segregation is not observed until septal constriction (Del Sol, Mullins et al. 2006). The plasmid pRT43, which contains an *ftsZ::egfp* fusion under the control of its native promoter and integrates at the ϕBT1 was inserted in to the strain M145/ p2075mCh (p2075mCh integrates in the ϕC31 site) via intergeneric conjugal transfer. Both proteins were then visualised using fluorescence microscopy using a 465-459nm and 510-560nm filters respectively.

Increased SCO2075 expression appears to precede developmental up regulation of FtsZ. Figure 7.7 shows three different stages of development of the aerial hyphae,

where there is an initial diffuse localisation of SCO2075 with levels above those of FtsZ, followed by Z-ring formation with nucleoid and finally hyphae with visible prespores, which was described by Grantcharova *et al.,* 2005 as stages 2, 5 and 6 respectively. This indicates that SCO2075 is involved in the condensation of the chromosomes during very early stages of aerial development, preceding Z-ring formation.

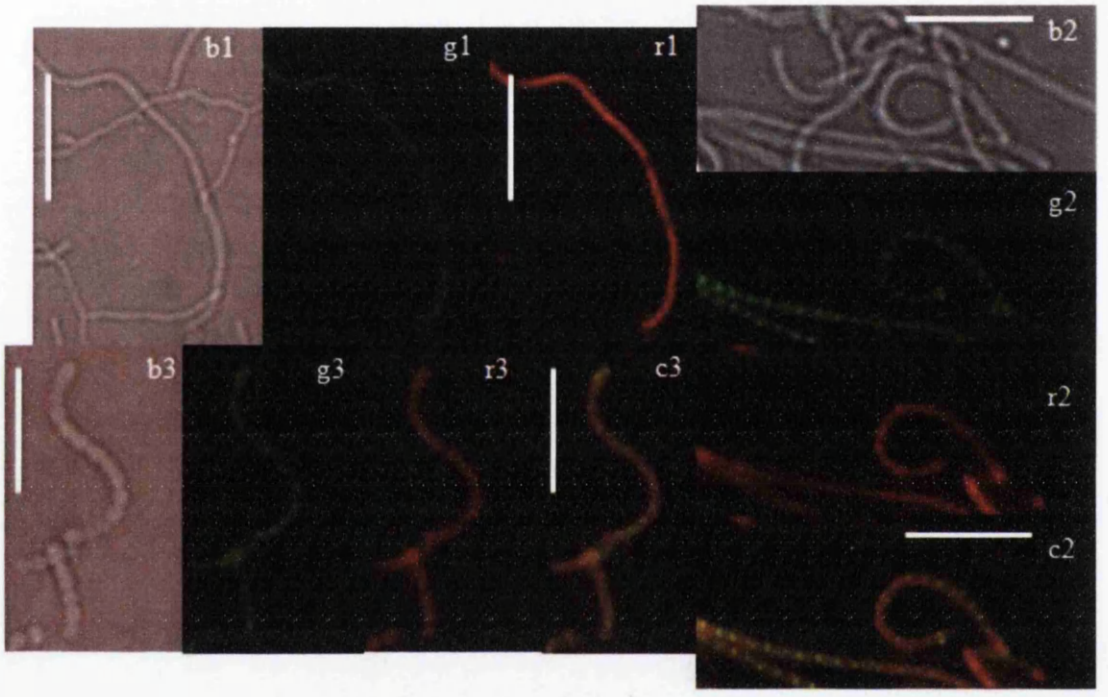

Figure 7.7: Fluorescence microscopy of aerial hyphae with sco2075::mCh and ftsZ::eGFP. (M145/p2075mCh/pRT43). Aerial hyphae (panel 1), early sporulation (panel 2) and late sporulation (panel 3). Samples were taken from inverted cover slips grown in SFM agar for 40 - 48 hours. Each panel contains a bright field (b), Sco2075::mCh fusion (r), ftsZ::eGFP fusion (g) and the combined emission images (c). Bar indicates 10μm.

7.6 SCO2075 localisation in mutants

With the SCO2075::mCherry fusion already constructed, it was placed in a number of mutant strains to see if there was any change in expression and localisation as

a result of the mutation. The plasmid p2075mCh was placed in sigma factor mutant strains Δ*whiG* and Δ*sigH,* Δ*whiI,* a two component regulator, and a nucleoid-associated protein Δ*smc* (Ainsa, Parry et al. 1999; Flardh, Findlay et al. 1999; Sevcikova, Benada et al. 2001; Dedrick, Wildschutte et al. 2009). *ΔwhiG* and Δ*whiI* mutant strains are defective in septa formation during sporulation leading to non sporogenic hyphae (Ainsa, Parry et al. 1999; Flardh, Findlay et al. 1999). The Δ*smc* mutant strain results in anucleate spore compartments and enlarged nuceloids due to a lack of condensation of the nucleoid (Dedrick, Wildschutte et al. 2009) and the alternative sigma factor, SigH which is involved in stress response and morphology produces undifferentiated hyphae with rare spore chains (Sevcikova, Benada et al. 2001).

Mycelium fragments or spore suspensions, where appropriate were used to inoculate the acute angle of inserted cover slips in SFM medium plates incubated at 30°C and samples viewed between 3 and 7 days depending on which strain was being analysed. SCO2075 expression did not appear to be affected in the mutants analysed with florescence visible in aerial hyphae and spores where applicable (Figure 7.8) suggesting that *sco2075* is not regulated differently in these mutants. However this does not rule out completely whether they are involved in minor alterations in expression as these may not be visible and experimental conditions used may require alteration. However from the initial analysis it does not appear that *sco2075* transcription is altered by these mutations.

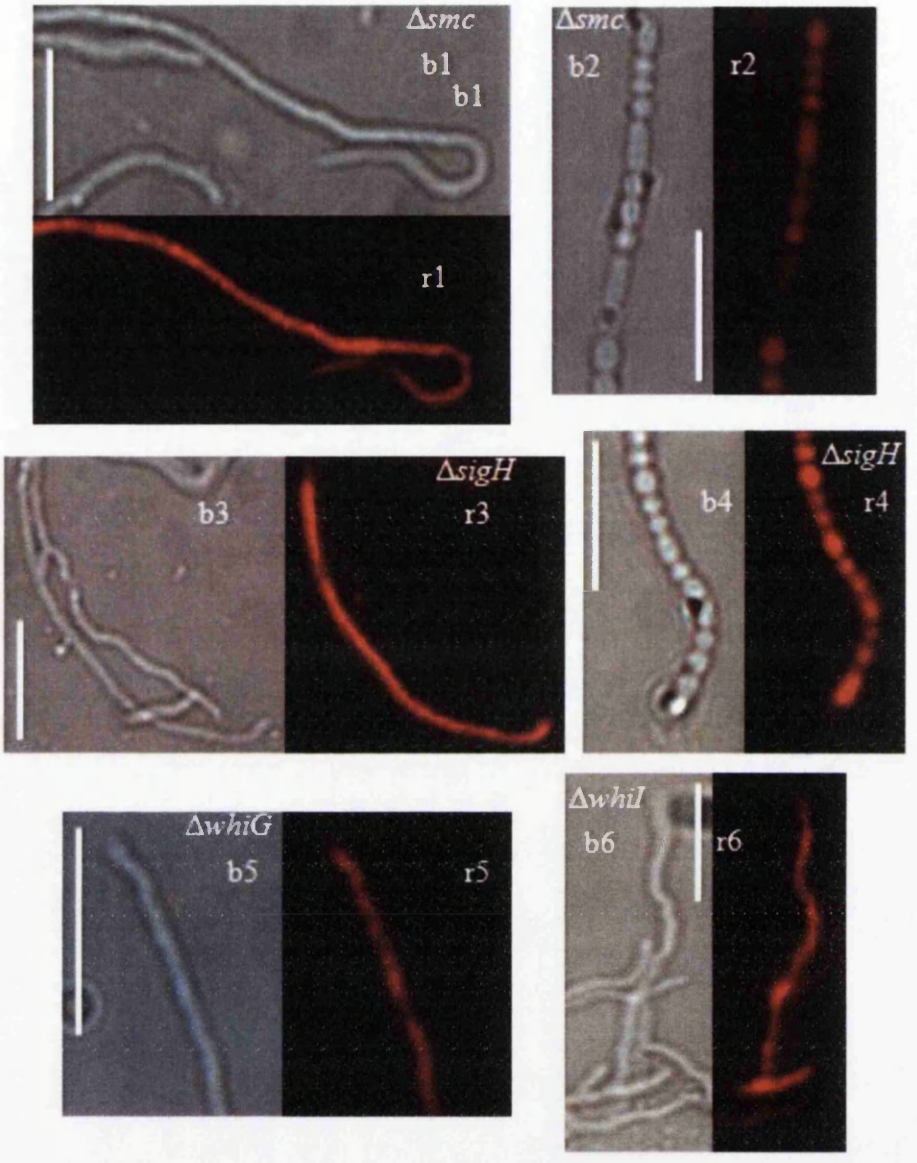

Figure 7.8: Fluorescence microscopy images of the *sco2075*::mCherry under the control of its native promoter in a number of mutant backgrounds. Panels 1 and 2 show Δ*smc* aerial hyphae and sporulation respectively. Panels 3 and 4 show Δ*sigH* aerial hyphae and sporulation respectively while panel 5 and 6 show Δ*whiG* and Δ*whiI* respectively during aerial hyphae. Each panel contains a bright field (b) and *sco2075*::mCh fusion fluorescence (r). Bar indicates 10μm

Mycelium fragments or spore suspensions, where appropriate were used to inoculate the acute angle of inserted cover slips in SFM medium plates incubated at 30°C and samples viewed between 3 and 7 days depending on which strain was being

analysed. SCO2075 expression did not appear to be affected in the mutants analysed with florescence visible in aerial hyphae and spores where applicable (Figure 7.8) suggesting that *sco2075* is not regulated differently in these mutants. However, this does not rule out completely whether they are involved in minor alterations in expression as these may not be visible and experimental conditions used may require alteration. However from the initial analysis it does not appear that *sco2075* transcription is altered by these mutations.

7.7 Summary

Pre-spore chain nucleoids in the DSCO2075 mutant strain are 'boxier' than those of the parental strain, but the mutant strain formed unigenomic spores. When a *dpsA*$^-$/ *sco2075*$^-$ double mutant strain was analysed, the *dpsA*$^-$ phenotype was dominant with a subpopulation of slightly wider nucleoids along the hyphal axis. The *dpsA*$^-$ mutant strain phenotype was dominant in the double mutant, which is expected, due to the milder nucleoid compaction defect displayed in the DSCO2075 mutant strain when compared to the *dpsA*$^-$ mutant strain.

An mCherry fluorescence tagged SCO2075 under the control of the native promoter to analysis expression and localisation in *S. coelicolor* has shown that SCO2075 was present at a number of key stages within the complex life cycle, namely germination, aerial hyphal erection and sporulation. SCO2075's expression appears to precede the formation of Z-rings in aerial hyphae, continuing through to sporulation, suggesting a possible role in the condensation of the nucleoid prior to septation, which is

also evident from the analysis of nucleoid lengths. However, it is not apparently an essential gene for the proper segregation of nucleoids into unigenomic spores.

Analysis of a SCO2075::mCherry fusion in Δ*whiG,* Δ*whiI,* Δ*sigH* and Δ*smc* mutants showed no observable alterations in fluorescence compared to the parental strain in the conditions tested.

Chapter - 8

Discussion

8.1 Introduction

The results chapters (Chapters 3-7) in this thesis describe the preliminary characterisation of the *dksA*-like genes *sco2075*, *sco6164* and *sco6165* during the life cycle of *S. coelicolor*. The overall picture of the function of *sco2075* will be discussed collectively within this chapter, linking current knowledge of DksA and nucleoid-associated proteins from *Streptomyces* and other species to obtain a general understanding. Then finally, possible future experimental approaches to expand the characterisation of SCO2075's DNA-binding domain and DksA like domain will be discussed.

8.2 Features of Sco2075 and gene loci

Bioinformatic analysis of actinomycete genomes have shown a large number of *Streptomyces* genomes with more than one DksA paralog with a maximum of three, which presents the question of why *Streptomyces* needs multiple paralogs when the majority of prokaryotic species only have one? Moreover, there is no evidence to date to suggest even the existence of a single DksA in the genus *Mycobacterium*, however a completely unrelated essential transcription factor CarD can functionally replace DksA for stringent control of rRNA transcription in *E. coli*, even though CarD associates with a different site on the RNAP via its N-terminal domain (Stallings, Stephanou et al. 2009). Primary and secondary structure similarities to the *E. coli* DksA have been established with conservation of critical amino acids for the activity of DksA being present in the paralog SCO2075 (Figure 3.1). However, SCO6164 and SCO6165 lack either both aspartic acid residues or just one, respectively (Figure 3.2). *P aeruginosa* has

a second *dksA* (DksA2) that lacks conserved cysteine residues of the zinc finger domain, however, this does not alter the function of the protein (Blaby-Haas, Furman et al. 2011), and the authors suggest that DksA2 acts as a Zn^{2+}-independent backup of DksA that functions in low Zn^{2+} environments.

Conserved gene clusters are a prominent feature of bacterial genomes, where the genes are kept in close proximity with one another due to natural selection pressures (Demerec 1959). The *sco2075* locus analysis shows its location is within the central core region of the *S. coelicolor* chromosome suggesting a possible requirement for the gene, as the core region has the highest conservation throughout *Streptomyces* genomes (Bentley, Chater et al. 2002; Ventura, Canchaya et al. 2007). Analysis within *Streptomyces* species shows relative close proximity to an essential gene for sporulation, *ftsZ* and a number of other genes including those encoding isoleucyl tRNA synthase, lipoprotein signal peptidase and GNAT acetyl transferase as shown in Figure 3.3. This possibly suggests that although *sco2075* is a non-essential gene, shown in this work, there is a selective pressure maintaining its locus in a number of *Streptomyces* species.

SCO2075 is a dual domained protein, with a histone-like N-terminal domain and a DksA like C-terminal domain. Amino acid conservation appears stronger in the C-terminal domain of the protein than the N-terminal domain which appears variable and with the NJ phylogenetic trees shown in Figure 3.5, suggests the possibility of the latter evolving separately from the C-terminal portion of the protein and the likelihood of the DNA binding domain having been acquired by lateral gene transfer or possibly gene duplication, for example, from the extended C-terminal domain of the *hupS* gene of *S. coelicolor*.

Alignment of the DNA-binding domain separately with Rv3852 (H-NS) from *M. tuberculosis*, HupS from *Streptomyces* and H1 Hc2-like protein from *C. trachomatis* illustrates significant amino acid conservation (Figure 3.7). As a result, phylogenetic analysis of the SCO2075 primary amino acid sequence was undertaken to determine whether the DNA-binding domain was novel or related to a previously characterised histone-like protein. The NJ phylogenetic tree data implies that there is some relationship between the N-terminal domain of SCO2075 and the extended C-terminal HU proteins such as HupS and to a lesser extent H1 Hc2-like proteins of *Chlamydia* (Figure 3.8B). Although the HU protein within *S. coelicolor*, HupS (*sco5556*), has been shown to be involved with the nucleoid (Salerno, Larsson et al. 2009), it has not been explored yet how the extended C-terminal histone domain is involved. Although it has been shown that the C-terminal domain of the orthologous Hlp protein of *M. smegmatis,* has a high affinity to DNA and is involved in end joining in the presence of T4 DNA ligase (Mukherjee, Bhattacharyya et al. 2008).

Primary amino acid analysis of the DNA-binding domain from the N-terminal domain of SCO2075 suggests the possibility of a pentapeptide motif similar to that of the *Chlamydia* H1 Hc2-like protein (Perara, Ganem et al. 1992). Also contained within the N-terminal domain of SCO2075 are tetrapeptide repeats similar to those in other histone-like proteins from prokaryotes (Perara, Ganem et al. 1992; Sharadamma, Harshavardhana et al. 2010). What is also notable with regard to the DNA-binding domain region is the variation in these repeats between orthologous proteins from different *Streptomyces* species. This variation is also evident in orthologs of both the H-NS-like protein from *M. tuberculosis* (Sharadamma, Harshavardhana et al. 2010) and the

H1 Hc2-like protein of *Chlamydia* (Klint, Thollesson et al. 2010). For the latter, although there is no data available to suggest the number of pentapeptide repeats required to facilitate binding to DNA, a mechanism has been put forward which suggests the repeats kink the helix structure so that it is compatible with the major groove of B-form DNA (Brickman, Barry et al. 1993).

8.3 Sco2075's expression profile

During the life cycle of *S. coelicolor*, expression of SCO2075 appeared to be minimal through vegetative growth but then increased during aerial hyphal erection and sporulation (Chapters 6/ 7). Expression of SCO2075 in aerial hyphae appeared to precede the expression of FtsZ prior to Z-ring formation, with nucleoid prespore compartments larger in DSCO2075 compared to M145 shown in Chapter 7, suggesting a role in nucleoid condensation. With the link to nucleoid condensation, the protein DpsA which has been shown to be intimately involved in nucleoid condensation during sporulation (Facey, Hitchings et al. 2009) and has a similar expression profile to SCO2075 was analysed in the DSCO2075 mutant strain. The basal level of DpsA was elevated in DSCO2075 (Figure 6.13) which could possibly suggest a compensatory mechanism for the absence of SCO2075 or that SCO2075 plays a role in repressing basal expression of DpsA. Regulation of the DksA protein does vary between species. Perron, Comte et al. (2005) showed the DksA protein from *P. aeruginosa* having a high expression in early exponential phase, reaching maximal expression in mid exponential phase then completely absent in early stationary phase with a slight increase in late stationary phase and postulated that this was the result of post transcriptional

modification. Also *P. aeruginosa*'s DksA2 protein is completely repressed by exogenous Zn^{2+} (Perron, Comte et al. 2005; Blaby-Haas, Furman et al. 2011). In *C. pneumonia* during the transition from reticulate to elementary body formation, DksA has a 3.2 fold increase in mRNA transcript, with only a 1.2 fold increase in protein abundance (Mukhopadhyay, Good et al. 2006). These discrepancies with the mRNA profiles compared to protein profiles are similar to data from *P. aeruginosa* (Perron, Comte et al. 2005).

Interestingly in *E. coli,* DksA protein concentration is relatively constant throughout the life cycle and under differing growth concentrations with 3000 to 10,000 copies per cell (Paul, Barker et al. 2004) and declines slightly (two-fold) only after many hours in stationary phase (Rutherford, Lemke et al. 2007). DksA only appears as a prominent band using western analysis when using a multicopy plasmid containing *dksA* under its native promoter (Brown, Gentry et al. 2002). The expression profile of SCO2075 in *S. coelicolor* has no similarities to the expression of DksA in *P. aeruginosa*, however, like *E. coli* DksA, SCO2075 has low expression levels in vegetative hyphae. This is where the similarities end, as expression increases during aerial hyphae, prior to Z-ring expression and sporulation (Chapter 6 & 7). The constant level of *E. coli* DksA is attributed to recent data that implicates DksA as a very stable protein with a half-life of between 35 and 53 minutes, with constant protein levels maintained by a negative feedback loop in which transcription from the *dksA* promoter is inhibited by DksA in conjunction with ppGpp (Chandrangsu, Lemke et al. 2011). This gives an insight into the possible mechanism of DksA regulation within *Streptomyces* during vegetative growth, as 50bp upstream of the gene *sco2075*, there is a possible -10 element

(GATTTA) very similar to that of *E. coli dksA* (TATTTA) that is involved in the negative feedback. This negative feedback loop could potentially be part of a mechanism to regulate *sco2075* during vegetative growth. During aerial growth/ sporulation SCO2075 could be either modified or bound permitting the observed increase in expression. Post-translational modification could be a possible mechanism of regulation with the apparent two species of SCO2075 visible on PAGE gels (Figure 6.11). Alternatively, expression could be from a single developmentally-regulated promoter.

Beyond preliminary phenotypic analysis, DSCO6164 and DSCO6165 mutant strains were not analysed further in this study. It is interesting how both mutants have very similar phenotypes, with DSCO6164 having a more pronounced defect in actinorhodin production on LB and 2xYT than DSCO6165 (Figure 4.6). No papers to date have been published regarding *sco6164* but interestingly *sco6165* has been shown to be translationally coupled with *sco6166*, an MreB-like protein, and is strongly expressed during vegetative growth but is absent during sporulation (Heichlinger, Ammelburg et al. 2011).

8.4 SCO2075 is a dimer

Native page analysis has shown that the predominant form of the SCO2075 protein is potentially a dimer (Figure 6.3), although due to protein aggregation it was difficult to use a higher concentration of protein to determine the presence of any other oligomeric states present. This data is consistent with the 2.0 Å resolution crystalline structure of DksA from *E. coli* which showed the presence of two types of dimers, where type I were connected by a non-proper two-fold symmetry with ~110° rotation, while

type II had more physiological structural characteristics with a proper two-fold symmetry and possesses quite an extensive symmetric interface involving their long coiled-coil domain (Perederina, Svetlov et al. 2004). Only eight out of ten monomers formed the type II dimers, which suggested that the intermolecular interactions are easily disrupted in solution (Perederina, Svetlov et al. 2004). The major functional state of the *E. coli* DksA was proposed to be a monomer, however due to the multifunctional regulatory role it was not ruled out that it could function in an oligomeric state. (Perederina, Svetlov et al. 2004).

From SDS-PAGE analysis of N- and C-terminally His-tagged recombinant SCO2075 protein, two species appeared evident, with molecular weights of ~23KDa and~35KDa. The dominant form migrating around ~35KDa and a lower band at ~ 23KDa, with SCO2075 having a theoretical expected size of ~27KDa. This phenomenon was reproduced with both N- and C- terminally His-tagged protein using Western blot analysis (Figure 6.11B), suggesting that the difference is not the result of degradation or an alternate start codon. Twenty three internal lysine residues are predicted to be acetylated, suggesting the variation in molecular weight could be the result of post-translational modification. Interestingly, two genes up stream there appears to be a partially conserved Acetyltransferase (*sco2072*) which could potentially be involved in SCO2075's acetylation. To investigate this anomaly, a trypsin digest of the two bands cut from a PAGE can be used to perform mass spectrometry.

8.5 *sigR* expression is repressed under thiol stress in DSCO2075

Maintaining thiol oxidation state within the cytoplasm is an important mechanism to maintain enzymatic activity, while preventing over-oxidation resulting in protein inactivation. DksA in *E.coli* has been shown to be involved in the response to stress conditions such as interaction in some way to TrxA, which encodes thioredoxin (Kumar, Tabor et al. 2004) and also to regulate the extracytoplasmic stress factor Sigma E (Costanzo, Nicoloff et al. 2008), and regulation of *rpoS* expression (Brown, Gentry et al. 2002) in conjunction with ppGpp. Unlike *E. coli* where *oxyR* regulates both thiol and peroxide stress responses (Christman, Storz et al. 1989), in *Streptomyces* the alternative sigma factor, Sigma R regulates thiol stress (Paget, Kang et al. 1998). As the DSCO2075 mutant strain showed sensitivity to diamide stress, qRT-PCR was used to look at transcription from *sigR,* which showed that the diamide sensitivity is more than likely the result of a reduction in levels of *sigR* transcription (Figure 4.4).

In *E. coli*, one function of DksA, in conjunction with ppGpp, is to liberate core RNAP, for example during starvation, which allows transcription from alternative sigma factors (Potrykus and Cashel 2008). The *sigR* gene in *S. coelicolor* has been shown to be positively regulated by σ^R, thereby increasing concentrations of σ^R. An explanation for the reduced expression of *sigR* transcript in the DSCO2075 mutant strain could be that SCO2075 may be required for the liberation of core RNAP and thereby reducing the availability of core RNAP, which results in increased competition of σ^R with other alternative sigma factors. Interestingly, *relA* has been shown to have a σ^R promoter region and is classed as a subclass B gene of σ^R (Paget, Molle et al. 2001), meaning that it retains a certain level of expression in a *sigR* mutant strain. As ppGpp has been shown

to be critical for antibiotic production in *Streptomyces*, with peak expression coinciding with onset of antibiotic production (Ochi 1986; Hesketh, Sun et al. 2001), it is interesting that the DSCO2075 mutant strain lacked any major alteration in antibiotic production except under osmotic stress (Chapter 4). This could be explained by the basal expression of ppGpp which appears to persist in the *sigR* mutant and as *sigR* transcription is not completely abolished within DSCO2075 during thiol stress, there is potentially an adequate amount of σ^R required to maintain cellular ppGpp levels during the life cycle, either with stress or without. Further investigation would be required to look at intracellular concentrations of ppGpp between DSCO2075 and parental strain M145 to determine whether there is an actual difference in cellular ppGpp concentration.

Phenotypic analysis also revealed a reduction in aerial hyphae and a possible increase in actinorhodin (although quantification in liquid culture is required to verify this) when grown on NMMP with 250mM KCl (Figure 4.1). This could be explained by topological alterations of DNA under osmotic stress and/ or reduced liberation of RNAP from *rrn* promoters, at a time in the life cycle that requires a number of genes to be transcribed. This could possibly alter expression of *osaB* which has a conditional phenotype on media with added osmolyte resulting in a bald phenotype producing an increased amount of pigmented antibiotics (Bishop, Fielding et al. 2004). Alternatively, SCO2075 could be pleiotropic and the phenotype a result of changes in transcription of other genes.

8.6 SCO2075 can bind DNA

Unlike the typical DksA protein, which has a pI of around 5 (as calculated from its primary amino acid sequence), SCO2075 has an extended 9.4KDa N-terminal domain consisting of 23 lysine and 33 alanines with a pI of 10.45, which gives the protein an average pI of 9.34, making the protein significantly more basic. Analysis of *in vitro* DNA binding with the full-length protein showed evidence of non-specific binding with both linear and supercoiled DNA using EMSA at sub μM concentrations (Figure 6.8/ 6.10). To further analyse whether this DNA binding is the direct result of the extended N-terminal domain, truncated proteins of both N- and C- terminal domains were constructed. Most DksA proteins do not bind DNA, however the DksA of *P. aeruginosa* has been shown to bind DNA containing *rrn* promoters *in vitro* with low affinity and without specificity via the C-terminal Zn-finger domain (Perron, Comte et al. 2005). Compared to SCO2075, a 20-fold greater concentration of the DksA from *P. aeruginosa* protein was required for *in vitro* binding (Perron, Comte et al. 2005). There was no evidence of DNA binding by the C-terminal DksA domain of SCO2075 with protein concentrations of 1μM and 1.8μM (i.e. at concentrations that allow binding of either the full-length protein or truncated N-terminal protein) (Figure 6.9). Further analysis is required to determine whether the zinc finger domain of SCO2075 binds DNA at higher concentrations and to examine if either SCO6164 or SCO6165 have the ability to bind DNA.

As certain nucleoid-associated proteins show preference to DNA sequence/ structure, preliminary characterisation of SCO2075's DNA specificity was conducted

using supercoiled and linearised DNA. Using pUC18 plasmid as a report in EMSAs showed no preference to linear or supercoiled DNA (Figure 6.10), although further analysis is required to determine whether there is a preference to certain sequences or DNA structure/ shape (e.g. high G+C or A+T content DNA, holliday junctions etc).

There are several examples of nucleoid-associated proteins that can alter the topological state of a reporter plasmid *in vivo*. For example, the DNA of a HU mutant strain of *E. coli* is in a more relaxed topological state (Hsieh, Rouviere-Yaniv et al. 1991; Mojica and Higgins 1997), whereas depletion of H-NS results in an increase in DNA supercoiling (Hsieh, Rouviere-Yaniv et al. 1991; Mojica and Higgins 1997). The plasmid DNA of a DSCO2075 mutant strain appeared to be in a more relaxed state with and without osmolyte, although the difference between the parental strain and mutant strain is more apparent after osmotic stress (Figure 5.5A). This is similar to a HU mutant strain of *E. coli,* although, Hsieh, Rouviere-Yaniv et al. (1991) reported that the HU mutant strain was still able to respond osmotic stress in terms of changes in DNA supercoiling. This is true to a degree with the DSCO2075 mutant strain, which responded with an increase in negative supercoiled topoisomers although not to the same extent as the wild type. The analysis of the *E. coli* HU mutant strain after osmotic stress was not compared with a parental strain, so it is difficult to determine whether there is full recovery of the superhelical state of the reporter plasmid under osmotic stress conditions in this mutant strain (Hsieh, Rouviere-Yaniv et al. 1991).

Hardy and Cozzarelli (2005) designed a genetic selection for mutations that resulted in reduced negative supercoiling in *E. coli* illustrating that Fis, H-NS and DksA mutant strains are sensitive to gyrase inhibitors and DNA damage and also that

expression of supercoiling-sensitive promoters is affected in a manner reflecting chromosomal relaxation. Interestingly when reporter plasmid analysis was carried out on the Fis, H-NS and DksA mutant strains, no difference in DNA topology was visible (Hardy and Cozzarelli 2005). This was shown to be the result of timing of plasmid extraction and when H-NS and Fis mutants were re-examined by another group, variations in DNA topology were shown for both mutants, however, the DksA mutant was not reanalysed (Blot, Mavathur et al. 2006). It has also been reported that the *E. coli* DksA mutant strain results in a 72% increase in *topA* activity (Hardy and Cozzarelli 2005). Whether SCO2075 affects DNA topology directly or indirectly remains to be elucidated.

While the chloroquine gel topoisomer data of the reporter plasmid gave insight into the DNA topology of the DSCO2075 mutant strain on a global scale (Figure 5.5A), it did not provide insight into alterations in supercoiling within chromosomal domains. In addition, it should be noted that when the DSCO2075 mutant strain was grown on agar plates, its phenotype did not significantly differ to that of the wild-type which could suggest that the observed alteration in DNA topology is specific to liquid cultures. As the analysis of DNA supercoiling represents changes in submerged cultures, when the sporulation cycle is absent, it is as yet unclear if SCO2075 has a significant impact on nucleoid structure and global transcription for surface-grown cultures that proceed through a typical streptomycete life-cycle. To investigate this further, a SCO2075 orthologous mutant strain of *Streptomyces venezuelae* would be required. *S. venezuelae* is able to sporulate in submerged cultures (Glazebrook, Doull et al. 1990). Once the mutant strain is constructed, analysis of plasmid topology could then be completed from

samples of vegetative and samples from early sporulation. An alternative approach, the *tipA* promoter has been shown to be induced with increased negative supercoiling (Ali, Herron et al. 2002). This could be used to construct a transcriptional fusion to a reporter gene such as *egfp* or *luxAB* cassette (luciferase).

8.7 Why does SCO2075 have both a DNA binding domain and a DksA domain?

It is intriguing why such a two domain protein should exist. Although the alanine and lysine enriched extended N-terminal domain DksA-like protein is predominantly found in *Streptomyces,* there is at least one other species in the actinomycetales, *Janibacter* sp. HTCC2649, which contains a similar protein with an alanine and lysine enriched N-terminal domain including the single highly conserved pentapeptide repeat (Chapter 3).

DksA is a transcription factor that binds specifically with RNAP; although *P. aeruginosa's* DksA protein has been shown to interact with DNA at high concentrations via its zinc finger domain (Perron, Comte et al. 2005), it is interesting what the DNA binding domain would be required for. The protein SCO2075 at least in part, has been shown to have similarities with the *E. coli* DksA. *E. coli* DksA has been shown to be a non-essential protein (Kang and Craig 1990), and partly rescues the *relA* phenotype in *E. coli* (Magnusson, Gummesson et al. 2007), which has also been shown in *Streptomyces* in this work (chapter 4). One could speculate that the DksA domain of SCO2075 is redundant in *Streptomyces*. For example, CarD from *M. tuberculosis* and other mycobacteria has been shown to functionally replace DksA in *E. coli* and mycobacteria lack any obvious *dksA* like genes in their genomes (Stallings, Stephanou et al. 2009). A

gene with similarities to *carD* in *M. tuberculosis* is present in the *S. coelicolor* genome (*sco4232*) and therefore has the potential of functionally substituting for the DksA domain of SCO2075. Alternatively, this function could be replaced by SCO6164 or SCO6165 even though these proteins lack the pair of highly conserved aspartic acid residues, which have been shown to be required for DksA function in other species.

The Hlp protein of *M. smegmatis* has an extended C-terminal domain enriched in alanine and lysine, which has been shown to bind DNA with high affinity and can promote end joining in the presence of T4 DNA ligase (Mukherjee, Bhattacharyya et al. 2008). It can also repress transcription by T7 RNA polymerase and is required for recognition of duplex DNA containing a nick or gap of 1-2 nucleotides and cruciform DNA (Mukherjee, Bhattacharyya et al. 2008; Kumar, Sardesai et al. 2010). Hlp, like SCO2075, has a low cellular abundance of protein during exponential growth and has been suggested to be involved in DNA repair or recombination processes (e.g. non-homologous end-joining) and regulation of gene expression due to stress (Mukherjee, Bhattacharyya et al. 2008).

This could be an alternate possibility of the function of the extended N-terminal domain of the SCO2075 protein, as it can bind DNA with high affinity and the mutant strain is sensitive to oxidative stress with H_2O_2. To determine whether this is true for SCO2075, further investigation would be required by following the protocol used by Mukherjee, Bhattacharyya et al. (2008), replacing hlp with recombinant SCO2075.

8.8 H_2O_2 sensitivity

Deletions and over-expression of *dksA* have pleiotropic effects in a number of bacterial species with effects in gene expression, chaperonin function, cell division, amino acid requirements, quorum sensing, phage sensitivity and virulence (Paul, Berkmen et al. 2005). DksA has also been implicated in acid and oxidative stress response in *Shigella flexneri*, partially through the regulation of *rpoS* induction (Mogull, Runyen-Janecky et al. 2001). H_2O_2 causes dissociation of σ^R -RsrA resulting in the release of σ^R to allow transcription of σ^R target genes such as *relA* implicating a possible role of ppGpp in thiol/ peroxide stress response (Kang, Paget et al. 1999; Paget, Molle et al. 2001). Up to 70% of total RNA transcripts are stable RNAs encoded in long operons (Costanzo, Nicoloff et al. 2008). DksA in conjunction with ppGpp has been shown to inhibit transcription of *rrn* genes and DksA decreases the lifetime of complexes formed dependent on the intrinsic kinetic properties of the promoter (Paul, Barker et al. 2004; Paul, Berkmen et al. 2005; Rutherford, Lemke et al. 2007). As *sigR* transcription is reduced (fold change of 0.62 at 15min) in the DSCO2075 mutant strain under oxidative stress, in theory, *relA* will have a reduced σ^R directed transcription. With the reduced ppGpp and the lack of SCO2075 in the DSCO2075 mutant strain, potentially, this could reduce the inhibition of *rrn* genes which in turn decreases the concentration of free RNAP (Zhou and Jin 1998; Barker, Gaal et al. 2001; Paul, Berkmen et al. 2005) for the transcription of *oxyR/ catA*.

Alternatively, in *E. coli*, DksA has been suggested to be intimately involved in maintaining the chromosome structure *in vivo* (Hardy and Cozzarelli 2005) showing characteristics of a domain barrier mutant by having interactions with *dnaK*, *mukB*, *ruv*,

recN, including gyrase inhibitor, hydroxyurea and Mitomycin-C sensitivity. DksA has been shown to be a multicopy suppressor of *dnaK* phenotype (Kang and Craig 1990) and of the temperature sensitivity of a *mukB* mutant (Yamanaka, Mitani et al. 1994). *dksA* has also been isolated in screens in *E.coli*, for hydroxyurea-sensitive mutants and screens for mutations in *ruv* mutant backgrounds for increased DNA damage sensitivity (Meddows, Savory et al. 2005). The *ruv* genes are required to resolve holliday junctions that accumulate after replication on damaged template DNA caused by, for example UV irradiation (Donaldson, Courcelle et al. 2006). DksA has also been shown to be involved with *recN* an SOS induced condensin like gene, where the double mutant strain has a severely impaired double-strand break repair defect (Meddows, Savory et al. 2005). RecN is related to the SMC family of proteins (Rostas, Morton et al. 1987) and is one of the most abundantly produced proteins induced as part of the SOS response to DNA damage (Finch, Chambers et al. 1985) where it is involved in recombinational repair of double stranded breaks (Picksley, Attfield et al. 1984; Reyes, Patidar et al. 2010). Microarray analysis in *E. coli* has also revealed that the *dksA* mutant strain was likely to have altered supercoiling sensitive promoter profiles consistent with widespread relaxation (Hardy and Cozzarelli 2005).

However, the contribution of *dksA* to maintaining the chromosome structure in *E. coli* is more than likely indirect via its interaction with RNAP. This remains unclear with respect to SCO2075, which has the additional histone-like domain, it is possibly involved directly with chromosomal structure, which has been shown at least during pre-spore nucleoid condensation (Chapter 7). H_2O_2 is a potent DNA damaging agent via the Fenton reaction, and the reduced survival of the DSCO2075 mutant strain potentially

could be a result of altered expression of SOS genes, or, if DSCO2075 has domain barrier defects, the single strand breaks could cause complete relaxation of the chromosome.

Further investigation is required to fully elucidate the true mechanism by which SCO2075 confers resistance to H_2O_2 stress. Initial investigation would require qRT-PCR analysis of *oxyR* and *catA* genes to determine if expression is altered in the DSCO2075 mutant strain.

8.9 SCO2075 can restore antibiotic production in *relA* mutant

High-copy number plasmids containing the native promoter upstream of a full length *dksA* have been able to restore the phenotype of a number of *E. coli* mutant strains such as, Δ*dnaK,* Δ*dnaJ,* Δ*grpE,* Δ*mukB* and the restoration of *rpoS* on entry into stationary phase in a ppGpp^0 (Δ*relA* Δ*spoT*) mutant in an *E. coli* background (Kang and Craig 1990; Yamanaka, Mitani et al. 1994; Brown, Gentry et al. 2002). The phenotype of a ppGpp^0 *E. coli* mutant can also be rescued by a high copy number *dksA* plasmid with respect to filamentation, motility, cell-cell aggregation, stationary phase morphology, transcription as well as amino acid auxotrophy (Magnusson, Gummesson et al. 2007).

In *S. coelicolor*, intracellular ppGpp accumulates in the transition phase between exponential growth and stationary phase and has been shown to be critical for the onset of secondary metabolism such as antibiotic production (Ochi 1986; Hesketh, Sun et al. 2001). The *relA* mutant strain, M570 grown on SMMS shows *redD* transcription is abolished and *act*II-ORF4 expression is reduced below threshold levels required for

transcription of the cognate biosynthetic genes and subsequent production (Chakraburtty and Bibb 1997).

To investigate whether over-expression of SCO2075 can restore the antibiotic production in the *relA* mutant strains in *S. coelicolor*, the integrative plasmid pDksA3/H containing *sco2075* under the control of a *tipA* promoter was inserted into two *S.coelicolor* backgrounds (M570, DSCO1513) by intergeneric conjugal transfer. With induction of the promoter via thiostrepton from 0-20μg/ml there was a dosage dependent recovery of antibiotic production on SMMS agar, suggesting at least that the C-terminal portion of SCO2075 is functionally similar to that of *E. coli,* even though the 2D gel analysis failed to show binding to RNAP (Figure 6.12). This could be explained by the transient nature in which DksA binds RNAP and further investigation is required to show its binding. The exact mechanism however of how antibiotic production is restored within the *relA* mutant strains remains to be explained.

Interaction of DSCO2075 and RNAP could be investigated further via two alternate methods. The first method is cross-linking of the proteins using formaldehyde, or secondly immobilising SCO2075 on a HisTrap column and passing native RNAP through the column. After a large wash volume, if RNAP is co-eluted this would prove interaction.

8.10 Conclusions

Computational analysis revealed three paralogs of *dksA* in *S. coelicolor* with SCO2075 being the most conserved of the three with an extended alanine lysine rich N-terminal domain. *sco2075,* is non-essential, however, it appears to be one of several

nucleoid-associated proteins involved in nucleoid compaction during aerial hyphal erection and sporulation. Absence of *sco2075,* however, does not affect the production of unigenomic spore chains.

The N-terminal domain has been shown to bind to DNA non-specifically with high affinity. The C-terminal domain has shown similarly to *E. coli*, with phenotypic recovery in *RelA* mutant strains and SCO2075 has been implicated in oxidative stress response with a reduced level of σ^R in the DSCO2075 mutant strain compared to wild type.

Over-expression of SCO2075 can recover antibiotic production in *relA* mutant strains of *S. coelicolor*. As pleiotropic regulators such as σ^B cannot account for the vast majority of osmotically stress induced genes in *S. coelicolor,* one could speculate, given the data in the results (Ch4-7) that SCO2075 is potentially a novel regulator involving both DNA-binding domain and DksA-like domain, integrating stress and physiological signals via modulation of compaction of the nucleoid/ DNA topology, in conjunction with its ability to interact with RNAP directly.

8.11 Future analysis

The work presented in this thesis provides an insight into a potentially new regulator, which has the ability to integrate stress responses and physiological cues with modulation of DNA topology, resulting in altered transcription of antibiotic production in Δ*relA* backgrounds of *S. coelicolor*.

This study can be a starting point for future research to not only understand SCO2075's role in DNA topology modulation, but also to further characterise its ability

to alter transcription. Below are a few suggestions/ hypotheses which would be interesting to look into:

- Over expression of DksA in *E. coli* has been shown to recover the temperature sensitivity of a *mukB* mutant strain. *smc* in *S. coelicolor* is a homology of *mukB*. It would be interesting to see if SCO2075 can recover the anucleate spore compartments and enlarged nuceloids of a *Streptomyces* Δ*smc* mutant strain.
- The protein Hlp in *M. smegmatis* has been shown to mediate end-joining of DNA. It would be of interest to examine whether SCO2075 increases efficiency of ligation of DNA in the presence of T4 DNA ligase.
- Further investigation into the discrepancy in the molecular weight of SCO2075 using in gel trypsin digest and mass spectrometry to determine if post translational modification is taking place.
- (Transposon) mutational analysis of *sco4232* (*carD)* to determine whether it is essential in *Streptomyces*, and the construction of a double mutant strain with *sco2075*$^{-}$ and a triple mutant consisting of *sco2075*$^{-}$, *sco6164*$^{-}$ and *sco6165*$^{-}$ to determine whether there is cross-talk/ compensatory mechanism for the loss of *sco2075.*
- QRT-PCR of genes involved with amino acid biosynthesis and rRNA genes in DSCO2075 compared to wild-type and the Δ*relA* mutant. This would provide further evidence to whether SCO2075 functions similarly to DksA in other species.

- Further investigation into the mechanism of antibiotic recovery with p*tipA* induced expression of SCO2075 in *ΔrelA* mutant strains, such as quantification of intracellular ppGpp within DSC2075 compared to M145.
- Further investigation into the mechanism of H_2O_2 sensitivity. Initially via comparison of *oxyR* and *catA* expression using qRT-PCR in M145 and DSCO2075 strains.

References

Ainsa, J. A., H. D. Parry, et al. (1999). "A response regulator-like protein that functions at an intermediate stage of sporulation in *Streptomyces coelicolor* A3(2)." Mol Microbiol **34**(3): 607-619.

Aki, T. and S. Adhya (1997). "Repressor induced site-specific binding of HU for transcriptional regulation." EMBO J **16**(12): 3666-3674.

Ali Azam, T., A. Iwata, et al. (1999). "Growth phase-dependent variation in protein composition of the *Escherichia coli* nucleoid." J Bacteriol **181**(20): 6361-6370.

Ali, N., P. R. Herron, et al. (2002). "Osmotic regulation of the *Streptomyces lividans* thiostrepton-inducible promoter, *ptipA*." Microbiology **148**(Pt 2): 381-390.

Alice, A. F. and C. Sanchez-Rivas (1997). "DNA supercoiling and osmoresistance in *Bacillus subtilis* 168." Curr Microbiol **35**(5): 309-315.

Almiron, M., A. J. Link, et al. (1992). "A novel DNA-binding protein with regulatory and protective roles in starved *Escherichia coli*." Genes Dev **6**(12B): 2646-2654.

Altschul, S. F., W. Gish, et al. (1990). "Basic local alignment search tool." J Mol Biol **215**(3): 403-410.

Anderson, A. S. and E. M. Wellington (2001). "The taxonomy of *Streptomyces* and related genera." Int J Syst Evol Microbiol **51**(Pt 3): 797-814.

Angell, S., C. G. Lewis, et al. (1994). "Glucose repression in *Streptomyces coelicolor* A3(2): a likely regulatory role for glucose kinase." Mol Gen Genet **244**(2): 135-143.

Arner, E. S. and A. Holmgren (2000). "Physiological functions of thioredoxin and thioredoxin reductase." Eur J Biochem **267**(20): 6102-6109.

Artsimovitch, I., V. Patlan, et al. (2004). "Structural basis for transcription regulation by alarmone ppGpp." Cell **117**(3): 299-310.

Aslund, F., M. Zheng, et al. (1999). "Regulation of the OxyR transcription factor by hydrogen peroxide and the cellular thiol-disulfide status." Proc Natl Acad Sci U S A **96**(11): 6161-6165.

Atlung, T. and H. Ingmer (1997). "H-NS: a modulator of environmentally regulated gene expression." Mol Microbiol **24**(1): 7-17.

Ausmees, N., H. Wahlstedt, et al. (2007). "SmeA, a small membrane protein with multiple functions in *Streptomyces* sporulation including targeting of a

SpoIIIE/FtsK-like protein to cell division septa." Mol Microbiol **65**(6): 1458-1473.

Baaklini, I., V. Usongo, et al. (2008). "Hypernegative supercoiling inhibits growth by causing RNA degradation." J Bacteriol **190**(22): 7346-7356.

Babcock, M. J., M. J. Buttner, et al. (1997). "Characterization of the rpoC gene of *Streptomyces coelicolor* A3(2) and its use to develop a simple and rapid method for the purification of RNA polymerase." Gene **196**(1-2): 31-42.

Bao, K. and S. N. Cohen (2001). "Terminal proteins essential for the replication of linear plasmids and chromosomes in *Streptomyces*." Genes Dev **15**(12): 1518-1527.

Barker, M. M., T. Gaal, et al. (2001). "Mechanism of regulation of transcription initiation by ppGpp. I. Effects of ppGpp on transcription initiation in vivo and in vitro." J Mol Biol **305**(4): 673-688.

Bates, A. D., A, Maxwell (1993). DNA Topology, Oxford University Press.

Becker, N. A., J. D. Kahn, et al. (2007). "Effects of nucleoid proteins on DNA repression loop formation in *Escherichia coli*." Nucleic Acids Res **35**(12): 3988-4000.

Bentley, S. D., K. F. Chater, et al. (2002). "Complete genome sequence of the model actinomycete *Streptomyces coelicolor* A3(2)." Nature **417**(6885): 141-147.

Berdy, J. (2005). "Bioactive microbial metabolites." J Antibiot (Tokyo) **58**(1): 1-26.

Berger, M., A. Farcas, et al. (2010). "Coordination of genomic structure and transcription by the main bacterial nucleoid-associated protein HU." EMBO Rep **11**(1): 59-64.

Bibb, M. J. (2005). "Regulation of secondary metabolism in *streptomycetes*." Curr Opin Microbiol **8**(2): 208-215.

Bierman, M., R. Logan, et al. (1992). "Plasmid cloning vectors for the conjugal transfer of DNA from *Escherichia coli* to *Streptomyces spp*." Gene **116**(1): 43-49.

Bishop, A., S. Fielding, et al. (2004). "Systematic insertional mutagenesis of a streptomycete genome: a link between osmoadaptation and antibiotic production." Genome Res **14**(5): 893-900.

Blaby-Haas, C. E., R. Furman, et al. (2011). "Role of a Zn-independent DksA in Zn homeostasis and stringent response." Mol Microbiol **79**(3): 700-715.

Bliska, J. B. and N. R. Cozzarelli (1987). "Use of site-specific recombination as a probe of DNA structure and metabolism in vivo." J Mol Biol **194**(2): 205-218.

Blot, N., R. Mavathur, et al. (2006). "Homeostatic regulation of supercoiling sensitivity coordinates transcription of the bacterial genome." EMBO Rep **7**(7): 710-715.

Brickman, T. J., C. E. Barry, 3rd, et al. (1993). "Molecular cloning and expression of hctB encoding a strain-variant chlamydial histone-like protein with DNA-binding activity." J Bacteriol **175**(14): 4274-4281.

Brown, K. L., S. Wood, et al. (1992). "Isolation and characterization of the major vegetative RNA polymerase of *Streptomyces coelicolor* A3(2); renaturation of a sigma subunit using GroEL." Mol Microbiol **6**(9): 1133-1139.

Brown, L., D. Gentry, et al. (2002). "DksA affects ppGpp induction of RpoS at a translational level." J Bacteriol **184**(16): 4455-4465.

Brun, Y. and L. J. Shimkets (2000). Prokaryotic development. Washington, DC, ASM Press.

Bryson, K., L. J. McGuffin, et al. (2005). "Protein structure prediction servers at University College London." Nucleic Acids Res **33**(Web Server issue): W36-38.

Buttner, M. J., K. F. Chater, et al. (1990). "Cloning, disruption, and transcriptional analysis of three RNA polymerase sigma factor genes of Streptomyces coelicolor A3(2)." J Bacteriol **172**(6): 3367-3378.

Buttner, M. J. and C. G. Lewis (1992). "Construction and characterization of Streptomyces coelicolor A3(2) mutants that are multiply deficient in the nonessential hrd-encoded RNA polymerase sigma factors." J Bacteriol **174**(15): 5165-5167.

Ceci, P., S. Cellai, et al. (2004). "DNA condensation and self-aggregation of *Escherichia coli* Dps are coupled phenomena related to the properties of the N-terminus." Nucleic Acids Res **32**(19): 5935-5944.

Ceci, P., A. Ilari, et al. (2003). "The Dps protein of *Agrobacterium tumefaciens* does not bind to DNA but protects it toward oxidative cleavage: x-ray crystal structure, iron binding, and hydroxyl-radical scavenging properties." J Biol Chem **278**(22): 20319-20326.

Ceci, P., A. Ilari, et al. (2005). "Reassessment of protein stability, DNA binding, and protection of *Mycobacterium smegmatis* Dps." J Biol Chem **280**(41): 34776-34785.

Chakraburtty, R. and M. Bibb (1997). "The ppGpp synthetase gene (relA) of *Streptomyces coelicolor* A3(2) plays a conditional role in antibiotic production and morphological differentiation." J Bacteriol **179**(18): 5854-5861.

Challis, G. L. and D. A. Hopwood (2003). "Synergy and contingency as driving forces for the evolution of multiple secondary metabolite production by *Streptomyces* species." Proc Natl Acad Sci U S A **100 Suppl 2**: 14555-14561.

Champness, W. C. (1988). "New loci required for *Streptomyces coelicolor* morphological and physiological differentiation." J Bacteriol **170**(3): 1168-1174.

Champoux, J. J. (2001). "DNA topoisomerases: structure, function, and mechanism." Annu Rev Biochem **70**: 369-413.

Chandrangsu, P., J. J. Lemke, et al. (2011). "The dksA promoter is negatively feedback regulated by DksA and ppGpp." Mol Microbiol **80**(5): 1337-1348.

Chater, K. F. (1998). " Taking a genetic scalpel to the *Streptomyces* colony." Microbiology

144: 1465-1478.

Chater, K. F. (2006). "*Streptomyces* inside-out: a new perspective on the bacteria that provide us with antibiotics." Philos Trans R Soc Lond B Biol Sci **361**(1469): 761-768.

Chavez, A., A. Forero, et al. (2011). "Interaction of SCO2127 with BldKB and its possible connection to carbon catabolite regulation of morphological differentiation in *Streptomyces coelicolor*." Appl Microbiol Biotechnol **89**(3): 799-806.

Chen, J. M., H. Ren, et al. (2008). "Lsr2 of *Mycobacterium tuberculosis* is a DNA-bridging protein." Nucleic Acids Res **36**(7): 2123-2135.

Chen, N., A. A. Zinchenko, et al. (2008). "ATP-induced shrinkage of DNA with MukB protein and the MukBEF complex of *Escherichia coli*." J Bacteriol **190**(10): 3731-3737.

Cheung, K. J., V. Badarinarayana, et al. (2003). "A microarray-based antibiotic screen identifies a regulatory role for supercoiling in the osmotic stress response of *Escherichia coli*." Genome Res **13**(2): 206-215.

Cho, Y. H., E. J. Lee, et al. (2001). "SigB, an RNA polymerase sigma factor required for osmoprotection and proper differentiation of *Streptomyces coelicolor*." Mol Microbiol **42**(1): 205-214.

Choy, H. E. (2000). "The study of guanosine 5'-diphosphate 3'-diphosphate-mediated transcription regulation in vitro using a coupled transcription-translation system." J Biol Chem **275**(10): 6783-6789.

Christman, M. F., G. Storz, et al. (1989). "OxyR, a positive regulator of hydrogen peroxide-inducible genes in *Escherichia coli* and *Salmonella typhimurium*, is

homologous to a family of bacterial regulatory proteins." Proc Natl Acad Sci U S A **86**(10): 3484-3488.

Claessen, D., W. de Jong, et al. (2006). "Regulation of *Streptomyces* development: reach for the sky!" Trends Microbiol **14**(7): 313-319.

Colangeli, R., A. Haq, et al. (2009). "The multifunctional histone-like protein Lsr2 protects mycobacteria against reactive oxygen intermediates." Proc Natl Acad Sci U S A **106**(11): 4414-4418.

Cole, C., J. D. Barber, et al. (2008). "The Jpred 3 secondary structure prediction server." Nucleic Acids Res **36**(Web Server issue): W197-201.

Colquhoun, J. A., S. C. Heald, et al. (1998). "Taxonomy and biotransformation activities of some deep-sea *actinomycetes*." Extremophiles **2**(3): 269-277.

Colquhoun, J. A., J. Zulu, et al. (2000). "Rapid characterisation of deep-sea actinomycetes for biotechnology screening programmes." Antonie Van Leeuwenhoek **77**(4): 359-367.

Costanzo, A., H. Nicoloff, et al. (2008). "ppGpp and DksA likely regulate the activity of the extracytoplasmic stress factor sigmaE in *Escherichia coli* by both direct and indirect mechanisms." Mol Microbiol **67**(3): 619-632.

Cui, Y., Z. M. Petrushenko, et al. (2008). "MukB acts as a macromolecular clamp in DNA condensation." Nat Struct Mol Biol **15**(4): 411-418.

Darvasi, A. and A. Pisante-Shalom (2002). "Complexities in the genetic dissection of quantitative trait loci." Trends Genet **18**(10): 489-491.

Datsenko, K. A. and B. L. Wanner (2000). "One-step inactivation of chromosomal genes in Escherichia coli K-12 using PCR products." Proc Natl Acad Sci U S A **97**(12): 6640-6645.

Dedrick, R. M., H. Wildschutte, et al. (2009). "Genetic interactions of smc, ftsK, and parB genes in *Streptomyces coelicolor* and their developmental genome segregation phenotypes." J Bacteriol **191**(1): 320-332.

Del Sol, R., I. Armstrong, et al. (2007). "Characterization of changes to the cell surface during the life cycle of *Streptomyces coelicolor*: atomic force microscopy of living cells." J Bacteriol **189**(6): 2219-2225.

Del Sol, R., J. G. Mullins, et al. (2006). "Influence of CrgA on assembly of the cell division protein FtsZ during development of *Streptomyces coelicolor*." J Bacteriol **188**(4): 1540-1550.

Demerec, M. a. H., P.E. (1959). "Complex Loci in Microorganisms." Annual Review of Microbiology **13**: 377-406.

Depew, D. E. and J. C. Wang (1975). "Conformational fluctuations of DNA helix." Proc Natl Acad Sci U S A **72**(11): 4275-4279.

Dickerson, R. E., H. R. Drew, et al. (1982). "The anatomy of A-, B-, and Z-DNA." Science **216**(4545): 475-485.

Dillon, S. C. and C. J. Dorman (2010). "Bacterial nucleoid-associated proteins, nucleoid structure and gene expression." Nat Rev Microbiol **8**(3): 185-195.

Donaldson, J. R., C. T. Courcelle, et al. (2006). "RuvABC is required to resolve holliday junctions that accumulate following replication on damaged templates in Escherichia coli." J Biol Chem **281**(39): 28811-28821.

Dorman, C. J. (2006). "DNA supercoiling and bacterial gene expression." Sci Prog **89**(Pt 3-4): 151-166.

Dorman, C. J. and C. P. Corcoran (2009). "Bacterial DNA topology and infectious disease." Nucleic Acids Res **37**(3): 672-678.

Drlica, K. (1992). "Control of bacterial DNA supercoiling." Mol Microbiol **6**(4): 425-433.

Drlica, K. and J. Rouviere-Yaniv (1987). "Histonelike proteins of bacteria." Microbiol Rev **51**(3): 301-319.

Drolet, M. (2006). "Growth inhibition mediated by excess negative supercoiling: the interplay between transcription elongation, R-loop formation and DNA topology." Mol Microbiol **59**(3): 723-730.

Facey, P. D., M. D. Hitchings, et al. (2009). "*Streptomyces coelicolor* Dps-like proteins: differential dual roles in response to stress during vegetative growth and in nucleoid condensation during reproductive cell division." Mol Microbiol **73**(6): 1186-1202.

Fahal, A. H. and M. A. Hassan (1992). "Mycetoma." Br J Surg **79**(11): 1138-1141.

Fennell-Fezzie, R., S. D. Gradia, et al. (2005). "The MukF subunit of *Escherichia coli* condensin: architecture and functional relationship to kleisins." EMBO J **24**(11): 1921-1930.

Fernandez-Martinez, L. T., R. Del Sol, et al. (2011). "A transposon insertion single-gene knockout library and new ordered cosmid library for the model organism *Streptomyces coelicolor* A3(2)." Antonie Van Leeuwenhoek **99**(3): 515-522.

Fernandez Martinez, L., A. Bishop, et al. (2009). "Osmoregulation in *Streptomyces coelicolor*: modulation of SigB activity by OsaC." Mol Microbiol **71**(5): 1250-1262.

Figueroa-Bossi, N., M. Guerin, et al. (1998). "The supercoiling sensitivity of a bacterial tRNA promoter parallels its responsiveness to stringent control." EMBO J **17**(8): 2359-2367.

Finch, P. W., P. Chambers, et al. (1985). "Identification of the *Escherichia coli* recN gene product as a major SOS protein." J Bacteriol **164**(2): 653-658.

Fisher, S. H. (1992). "Glutamine synthesis in Streptomyces--a review." Gene **115**(1-2): 13-17.

Flardh, K. and M. J. Buttner (2009). "*Streptomyces* morphogenetics: dissecting differentiation in a filamentous bacterium." Nat Rev Microbiol **7**(1): 36-49.

Flardh, K., K. C. Findlay, et al. (1999). "Association of early sporulation genes with suggested developmental decision points in *Streptomyces coelicolor* A3(2)." Microbiology **145 (Pt 9)**: 2229-2243.

Flett, F., V. Mersinias, et al. (1997). "High efficiency intergeneric conjugal transfer of plasmid DNA from Escherichia coli to methyl DNA-restricting *streptomycetes*." FEMS Microbiol Lett **155**(2): 223-229.

Frenkiel-Krispin, D., S. Levin-Zaidman, et al. (2001). "Regulated phase transitions of bacterial chromatin: a non-enzymatic pathway for generic DNA protection." EMBO J **20**(5): 1184-1191.

Fuller, F. B. (1971). "The writhing number of a space curve." Proc Natl Acad Sci U S A **68**(4): 815-819.

Gallant, J. A. (1979). "Stringent control in *E. coli*." Annu Rev Genet **13**: 393-415.

Garner, M. M. and A. Revzin (1981). "A gel electrophoresis method for quantifying the binding of proteins to specific DNA regions: application to components of the *Escherichia coli* lactose operon regulatory system." Nucleic Acids Res **9**(13): 3047-3060.

Gellert, M., M. H. O'Dea, et al. (1976). "Novobiocin and coumermycin inhibit DNA supercoiling catalyzed by DNA gyrase." Proc Natl Acad Sci U S A **73**(12): 4474-4478.

Georgopoulos, C. P. (1977). "A new bacterial gene (groPC) which affects lambda DNA replication." Mol Gen Genet **151**(1): 35-39.

Gerber, N. N. and H. A. Lechevalier (1965). "Geosmin, an earthly-smelling substance isolated from *actinomycetes*." Appl Microbiol **13**(6): 935-938.

Ghosh, A. and M. Bansal (2003). "A glossary of DNA structures from A to Z." Acta Crystallogr D Biol Crystallogr **59**(Pt 4): 620-626.

Giladi, H., S. Koby, et al. (1998). "Participation of IHF and a distant UP element in the stimulation of the phage lambda PL promoter." Mol Microbiol **30**(2): 443-451.

Glazebrook, M. A., J. L. Doull, et al. (1990). "Sporulation of Streptomyces venezuelae in submerged cultures." J Gen Microbiol **136**(3): 581-588.

Gordon, B. R., R. Imperial, et al. (2008). "Lsr2 of *Mycobacterium* represents a novel class of H-NS-like proteins." J Bacteriol **190**(21): 7052-7059.

Gray, D. I., G. W. Gooday, et al. (1990). "Apical hyphal extension in *Streptomyces coelicolor* A3(2)." J Gen Microbiol **136**(6): 1077-1084.

Gropp, M., Y. Strausz, et al. (2001). "Regulation of *Escherichia coli* RelA requires oligomerization of the C-terminal domain." J Bacteriol **183**(2): 570-579.

Grove, A. (2011). "Functional Evolution of Bacterial Histone-Like HU Proteins." Curr Issues Mol Biol **13**(1): 1-12.

Guo, F. and S. Adhya (2007). "Spiral structure of *Escherichia coli* HUalphabeta provides foundation for DNA supercoiling." Proc Natl Acad Sci U S A **104**(11): 4309-4314.

Gust, B., G. L. Challis, et al. (2003). "PCR-targeted *Streptomyces* gene replacement identifies a protein domain needed for biosynthesis of the sesquiterpene soil odor geosmin." Proc Natl Acad Sci U S A **100**(4): 1541-1546.

Guzman, S., A. Carmona, et al. (2005). "Pleiotropic effect of the SCO2127 gene on the glucose uptake, glucose kinase activity and carbon catabolite repression in *Streptomyces peucetius var. caesius*." Microbiology **151**(Pt 5): 1717-1723.

Guzman, S., I. Ramos, et al. (2005). "Sugar uptake and sensitivity to carbon catabolite regulation in *Streptomyces peucetius var. caesius*." Appl Microbiol Biotechnol **69**(2): 200-206.

Hahn, J. S., S. Y. Oh, et al. (2000). "H2O2-sensitive fur-like repressor CatR regulating the major catalase gene in *Streptomyces coelicolor*." J Biol Chem **275**(49): 38254-38260.

Hahn, J. S., S. Y. Oh, et al. (2002). "Role of OxyR as a peroxide-sensing positive regulator in *Streptomyces coelicolor* A3(2)." J Bacteriol **184**(19): 5214-5222.

Hardy, C. D. and N. R. Cozzarelli (2005). "A genetic selection for supercoiling mutants of *Escherichia coli* reveals proteins implicated in chromosome structure." Mol Microbiol **57**(6): 1636-1652.

Haseltine, W. A. and R. Block (1973). "Synthesis of guanosine tetra- and pentaphosphate requires the presence of a codon-specific, uncharged transfer

ribonucleic acid in the acceptor site of ribosomes." Proc Natl Acad Sci U S A **70**(5): 1564-1568.

Heichlinger, A., M. Ammelburg, et al. (2011). "The MreB-like protein Mbl of *Streptomyces coelicolor* A3(2) depends on MreB for proper localization and contributes to spore wall synthesis." J Bacteriol **193**(7): 1533-1542.

Hesketh, A., W. J. Chen, et al. (2007). "The global role of ppGpp synthesis in morphological differentiation and antibiotic production in *Streptomyces coelicolor* A3(2)." Genome Biol **8**(8): R161.

Hesketh, A., J. Sun, et al. (2001). "Induction of ppGpp synthesis in *Streptomyces coelicolor* A3(2) grown under conditions of nutritional sufficiency elicits actII-ORF4 transcription and actinorhodin biosynthesis." Mol Microbiol **39**(1): 136-144.

Hillyard, D. R., M. Edlund, et al. (1990). "Subunit-specific phenotypes of *Salmonella typhimurium* HU mutants." J Bacteriol **172**(9): 5402-5407.

Hirano, T. (1999). "SMC-mediated chromosome mechanics: a conserved scheme from bacteria to vertebrates?" Genes Dev **13**(1): 11-19.

Hodgson, D. A. (1982). "Glucose repression of carbon uptake and metabolism in *Streptomyces coelicolor* A3(2) and its perturbation in mutants resistant to 2 deoxyglucose. ." J Gen Microbiol **128**: 2417-2430.

Hodgson, D. A. (2000). "Primary metabolism and its control in *streptomycetes*: a most unusual group of bacteria." Adv Microb Physiol **42**: 47-238.

Hoffmann, H. J., S. K. Lyman, et al. (1992). "Activity of the Hsp70 chaperone complex--DnaK, DnaJ, and GrpE--in initiating phage lambda DNA replication by sequestering and releasing lambda P protein." Proc Natl Acad Sci U S A **89**(24): 12108-12111.

Hogg, T., U. Mechold, et al. (2004). "Conformational antagonism between opposing active sites in a bifunctional RelA/SpoT homolog modulates (p)ppGpp metabolism during the stringent response [corrected]." Cell **117**(1): 57-68.

Hommais, F., E. Krin, et al. (2001). "Large-scale monitoring of pleiotropic regulation of gene expression by the prokaryotic nucleoid-associated protein, H-NS." Mol Microbiol **40**(1): 20-36.

Hopwood, D. A. (1958). Genetic recombination in *Streptomyces coelicolor*. PhD, University of Cambridge.

Hopwood, D. A. (1999). "Forty years of genetics with Streptomyces: from in vivo through in vitro to in silico." Microbiology **145 (Pt 9)**: 2183-2202.

Hopwood, D. A. (2006). "Soil to genomics: the *Streptomyces* chromosome." Annu Rev Genet **40**: 1-23.

Hsieh, L. S., J. Rouviere-Yaniv, et al. (1991). "Bacterial DNA supercoiling and [ATP]/[ADP] ratio: changes associated with salt shock." J Bacteriol **173**(12): 3914-3917.

Hwang, D. S. and J. M. Kaguni (1991). "dnaK protein stimulates a mutant form of dnaA protein in *Escherichia coli* DNA replication." J Biol Chem **266**(12): 7537-7541.

Ikeda, H., E. T. Seno, et al. (1984). "Genetic mapping, cloning and physiological aspects of the glucose kinase gene of *Streptomyces coelicolor*." Mol Gen Genet **196**(3): 501-507.

Jiang, J., X. He, et al. (2007). "Biosynthesis of the earthy odorant geosmin by a bifunctional *Streptomyces coelicolor* enzyme." Nat Chem Biol **3**(11): 711-715.

Jishage, M., K. Kvint, et al. (2002). "Regulation of sigma factor competition by the alarmone ppGpp." Genes Dev **16**(10): 1260-1270.

Kang, J. G., M. S. Paget, et al. (1999). "RsrA, an anti-sigma factor regulated by redox change." EMBO J **18**(15): 4292-4298.

Kang, P. J. and E. A. Craig (1990). "Identification and characterization of a new *Escherichia coli* gene that is a dosage-dependent suppressor of a dnaK deletion mutation." J Bacteriol **172**(4): 2055-2064.

Kelemen, G. H., P. Brian, et al. (1998). "Developmental regulation of transcription of whiE, a locus specifying the polyketide spore pigment in *Streptomyces coelicolor* A3 (2)." J Bacteriol **180**(9): 2515-2521.

Keller, W. and I. Wendel (1975). "Stepwise relaxation of supercoiled SV40 DNA." Cold Spring Harb Symp Quant Biol **39 Pt 1**: 199-208.

Khodakaramian, G., S. Lissenden, et al. (2006). "Expression of Cre recombinase during transient phage infection permits efficient marker removal in *Streptomyces*." Nucleic Acids Res **34**(3): e20.

Kieser, H. M., T. Kieser, et al. (1992). "A combined genetic and physical map of the *Streptomyces coelicolor* A3(2) chromosome." J Bacteriol **174**(17): 5496-5507.

Kieser, T., Bibb, M. J., Buttner, M. J., Chater, K. F. & Hopwood,D. A. (2000). Practical Streptomyces Genetics. Norwich: John Innes Foundation.

Kikuchi, Y. and H. A. Nash (1978). "The bacteriophage lambda int gene product. A filter assay for genetic recombination, purification of int, and specific binding to DNA." J Biol Chem **253**(20): 7149-7157.

Kirby, R. and D. A. Hopwood (1977). "Genetic determination of methylenomycin synthesis by the SCP1 plasmid of *Streptomyces coelicolor* A3(2)." J Gen Microbiol **98**(1): 239-252.

Klint, M., M. Tholleson, et al. (2010). "Mosaic structure of intragenic repetitive elements in histone H1-like protein Hc2 varies within serovars of *Chlamydia trachomatis*." BMC Microbiol **10**: 81.

Klug, W. S., M. R. Cummings, et al. (1997). Concepts of genetics. Upper Saddle River, N.J., Prentice Hall.

Kois, A., M. Swiatek, et al. (2009). "SMC protein-dependent chromosome condensation during aerial hyphal development in *Streptomyces*." J Bacteriol **191**(1): 310-319.

Kolmsee, T., D. Delic, et al. (2011). "Differential stringent control of E. coli rRNA promoters: effects of ppGpp, DksA and the initiating nucleotides." Microbiology.

Kosower, N. S. and E. M. Kosower (1995). "Diamide: an oxidant probe for thiols." Methods Enzymol **251**: 123-133.

Kostrewa, D., J. Granzin, et al. (1992). "Crystal structure of the factor for inversion stimulation FIS at 2.0 A resolution." J Mol Biol **226**(1): 209-226.

Krasny, L. and R. L. Gourse (2004). "An alternative strategy for bacterial ribosome synthesis: *Bacillus subtilis* rRNA transcription regulation." EMBO J **23**(22): 4473-4483.

Kumar, J. K., S. Tabor, et al. (2004). "Proteomic analysis of thioredoxin-targeted proteins in *Escherichia coli*." Proc Natl Acad Sci U S A **101**(11): 3759-3764.

Kumar, S., A. A. Sardesai, et al. (2010). "DNA clasping by mycobacterial HU: the C-terminal region of HupB mediates increased specificity of DNA binding." PLoS One **5**(9).

Kwakman, J. H. and P. W. Postma (1994). "Glucose kinase has a regulatory role in carbon catabolite repression in *Streptomyces coelicolor*." J Bacteriol **176**(9): 2694-2698.

Lambert, D. H., and R. Loria. (1989). "*Streptomyces acidiscabies sp. nov.*" Int. J. Syst. Bacteriol. **39**: 393-396.

Larkin, M. A., G. Blackshields, et al. (2007). "Clustal W and Clustal X version 2.0." Bioinformatics **23**(21): 2947-2948.

Lawlor, E. J., H. A. Baylis, et al. (1987). "Pleiotropic morphological and antibiotic deficiencies result from mutations in a gene encoding a tRNA-like product in Streptomyces coelicolor A3(2)." Genes Dev **1**(10): 1305-1310.

Lee, E. J., Y. H. Cho, et al. (2004). "Regulation of sigmaB by an anti- and an anti-anti-sigma factor in *Streptomyces coelicolor* in response to osmotic stress." J Bacteriol **186**(24): 8490-8498.

Lee, E. J., N. Karoonuthaisiri, et al. (2005). "A master regulator sigmaB governs osmotic and oxidative response as well as differentiation via a network of sigma factors in *Streptomyces coelicolor*." Mol Microbiol **57**(5): 1252-1264.

Leslie, A. G., S. Arnott, et al. (1980). "Polymorphism of DNA double helices." J Mol Biol **143**(1): 49-72.

Lewis, D. E., M. Geanacopoulos, et al. (1999). "Role of HU and DNA supercoiling in transcription repression: specialized nucleoprotein repression complex at gal promoters in *Escherichia coli*." Mol Microbiol **31**(2): 451-461.

Lezhava, A., T. Mizukami, et al. (1995). "Physical map of the linear chromosome of *Streptomyces griseus*." J Bacteriol **177**(22): 6492-6498.

Lilley, D. (1986). "Bacterial chromatin. A new twist to an old story." Nature **320**(6057): 14-15.

Lin, Y. S., H. M. Kieser, et al. (1993). "The chromosomal DNA of *Streptomyces lividans* 66 is linear." Mol Microbiol **10**(5): 923-933.

MacNeil, D. J. (1988). "Characterization of a unique methyl-specific restriction system in Streptomyces avermitilis." J Bacteriol **170**(12): 5607-5612.

Magnusson, L. U., A. Farewell, et al. (2005). "ppGpp: a global regulator in *Escherichia coli*." Trends Microbiol **13**(5): 236-242.

Magnusson, L. U., B. Gummesson, et al. (2007). "Identical, independent, and opposing roles of ppGpp and DksA in *Escherichia coli*." J Bacteriol **189**(14): 5193-5202.

Mallik, P., B. J. Paul, et al. (2006). "DksA is required for growth phase-dependent regulation, growth rate-dependent control, and stringent control of fis expression in Escherichia coli." J Bacteriol **188**(16): 5775-5782.

Martinez-Costa, O. H., M. A. Fernandez-Moreno, et al. (1998). "The relA/spoT-homologous gene in Streptomyces coelicolor encodes both ribosome-dependent (p)ppGpp-synthesizing and -degrading activities." J Bacteriol **180**(16): 4123-4132.

McCormick, J. R., E. P. Su, et al. (1994). "Growth and viability of *Streptomyces coelicolor* mutant for the cell division gene ftsZ." Mol Microbiol **14**(2): 243-254.

McGhee, J. D. and G. Felsenfeld (1980). "Nucleosome structure." Annu Rev Biochem **49**: 1115-1156.

Meddows, T. R., A. P. Savory, et al. (2005). "RecN protein and transcription factor DksA combine to promote faithful recombinational repair of DNA double-strand breaks." Mol Microbiol **57**(1): 97-110.

Menzel, R. and M. Gellert (1983). "Regulation of the genes for *E. coli* DNA gyrase: homeostatic control of DNA supercoiling." Cell **34**(1): 105-113.

Menzel, R. and M. Gellert (1987). "Fusions of the *Escherichia coli* gyrA and gyrB control regions to the galactokinase gene are inducible by coumermycin treatment." J Bacteriol **169**(3): 1272-1278.

Merrick, M. J. (1976). "A morphological and genetic mapping study of bald colony mutants of *Streptomyces coelicolor*." J Gen Microbiol **96**(2): 299-315.

Meury, J. and M. Kohiyama (1991). "Role of heat shock protein DnaK in osmotic adaptation of *Escherichia coli*." J Bacteriol **173**(14): 4404-4410.

Miguelez, E. M., C. Hardisson, et al. (1999). "Hyphal death during colony development in Streptomyces antibioticus: morphological evidence for the existence of a process of cell deletion in a multicellular prokaryote." J Cell Biol **145**(3): 515-525.

Mistry, B. V., R. Del Sol, et al. (2008). "FtsW is a dispensable cell division protein required for Z-ring stabilization during sporulation septation in *Streptomyces coelicolor*." J Bacteriol **190**(16): 5555-5566.

Mogull, S. A., L. J. Runyen-Janecky, et al. (2001). "dksA is required for intercellular spread of *Shigella flexneri* via an RpoS-independent mechanism." Infect Immun **69**(9): 5742-5751.

Mojica, F. J. and C. F. Higgins (1997). "In vivo supercoiling of plasmid and chromosomal DNA in an *Escherichia coli* hns mutant." J Bacteriol **179**(11): 3528-3533.

Mukherjee, A., G. Bhattacharyya, et al. (2008). "The C-terminal domain of HU-related histone-like protein Hlp from *Mycobacterium smegmatis* mediates DNA end-joining." Biochemistry **47**(33): 8744-8753.

Mukhopadhyay, S., D. Good, et al. (2006). "Identification of *Chlamydia pneumoniae* proteins in the transition from reticulate to elementary body formation." Mol Cell Proteomics **5**(12): 2311-2318.

Nagai, A., S. T. Khan, et al. (2011). "*Streptomyces aomiensis sp. nov.*, isolated from a soil sample using the membrane-filter method." Int J Syst Evol Microbiol **61**(Pt 4): 947-950.

Nair, S. and S. E. Finkel (2004). "Dps protects cells against multiple stresses during stationary phase." J Bacteriol **186**(13): 4192-4198.

Niki, H., R. Imamura, et al. (1992). "*E.coli* MukB protein involved in chromosome partition forms a homodimer with a rod-and-hinge structure having DNA binding and ATP/GTP binding activities." EMBO J **11**(13): 5101-5109.

Niki, H., A. Jaffe, et al. (1991). "The new gene mukB codes for a 177 kd protein with coiled-coil domains involved in chromosome partitioning of *E. coli*." EMBO J **10**(1): 183-193.

Nothaft, H., S. Parche, et al. (2003). "In vivo analysis of HPr reveals a fructose-specific phosphotransferase system that confers high-affinity uptake in *Streptomyces coelicolor*." J Bacteriol **185**(3): 929-937.

Ochi, K. (1986). "Occurrence of the stringent response in *Streptomyces sp.* and its significance for the initiation of morphological and physiological differentiation." J Gen Microbiol **132**(9): 2621-2631.

Omer, C. A. and S. N. Cohen (1984). "Plasmid formation in *Streptomyces*: excision and integration of the SLP1 replicon at a specific chromosomal site." Mol Gen Genet **196**(3): 429-438.

Paget, M. S., J. G. Kang, et al. (1998). "sigmaR, an RNA polymerase sigma factor that modulates expression of the thioredoxin system in response to oxidative stress in *Streptomyces coelicolor* A3(2)." EMBO J **17**(19): 5776-5782.

Paget, M. S., V. Molle, et al. (2001). "Defining the disulphide stress response in Streptomyces coelicolor A3(2): identification of the sigmaR regulon." Mol Microbiol **42**(4): 1007-1020.

Paradkar, A., A. Trefzer, et al. (2003). "Streptomyces genetics: a genomic perspective." Crit Rev Biotechnol **23**(1): 1-27.

Park, J. W., Y. Jung, et al. (2002). "Alteration of stringent response of the *Escherichia coli* rnpB promoter by mutations in the -35 region." Biochem Biophys Res Commun **290**(4): 1183-1187.

Paul, B. J., M. M. Barker, et al. (2004). "DksA: a critical component of the transcription initiation machinery that potentiates the regulation of rRNA promoters by ppGpp and the initiating NTP." Cell **118**(3): 311-322.

Paul, B. J., M. B. Berkmen, et al. (2005). "DksA potentiates direct activation of amino acid promoters by ppGpp." Proc Natl Acad Sci U S A **102**(22): 7823-7828.

Perara, E., D. Ganem, et al. (1992). "A developmentally regulated chlamydial gene with apparent homology to eukaryotic histone H1." Proc Natl Acad Sci U S A **89**(6): 2125-2129.

Perederina, A., V. Svetlov, et al. (2004). "Regulation through the secondary channel--structural framework for ppGpp-DksA synergism during transcription." Cell **118**(3): 297-309.

Perron, K., R. Comte, et al. (2005). "DksA represses ribosomal gene transcription in Pseudomonas aeruginosa by interacting with RNA polymerase on ribosomal promoters." Mol Microbiol **56**(4): 1087-1102.

Peter, B. J., J. Arsuaga, et al. (2004). "Genomic transcriptional response to loss of chromosomal supercoiling in *Escherichia coli*." Genome Biol **5**(11): R87.

Petrushenko, Z. M., C. H. Lai, et al. (2006). "DNA reshaping by MukB. Right-handed knotting, left-handed supercoiling." J Biol Chem **281**(8): 4606-4615.

Petrushenko, Z. M., C. H. Lai, et al. (2006). "Antagonistic interactions of kleisins and DNA with bacterial Condensin MukB." J Biol Chem **281**(45): 34208-34217.

Picksley, S. M., P. V. Attfield, et al. (1984). "Repair of DNA double-strand breaks in *Escherichia coli* K12 requires a functional recN product." Mol Gen Genet **195**(1-2): 267-274.

Piuri, M., C. Sanchez-Rivas, et al. (2003). "Adaptation to high salt in Lactobacillus: role of peptides and proteolytic enzymes." J Appl Microbiol **95**(2): 372-379.

Pizarro-Cerda, J. and K. Tedin (2004). "The bacterial signal molecule, ppGpp, regulates *Salmonella* virulence gene expression." Mol Microbiol **52**(6): 1827-1844.

Potrykus, K. and M. Cashel (2008). "(p)ppGpp: still magical?" Annu Rev Microbiol **62**: 35-51.

Potrykus, K., G. Wegrzyn, et al. (2004). "Direct stimulation of the lambdapaQ promoter by the transcription effector guanosine-3',5'-(bis)pyrophosphate in a defined in vitro system." J Biol Chem **279**(19): 19860-19866.

Pruss, G. J., R. J. Franco, et al. (1986). "Effects of DNA gyrase inhibitors in *Escherichia coli* topoisomerase I mutants." J Bacteriol **168**(1): 276-282.

Quintana, E. T., K. Wierzbicka, et al. (2008). "Streptomyces sudanensis sp. nov., a new pathogen isolated from patients with actinomycetoma." Antonie Van Leeuwenhoek **93**(3): 305-313.

Redenbach, M., H. M. Kieser, et al. (1996). "A set of ordered cosmids and a detailed genetic and physical map for the 8 Mb *Streptomyces coelicolor* A3(2) chromosome." Mol Microbiol **21**(1): 77-96.

Reyes, E. D., P. L. Patidar, et al. (2010). "RecN is a cohesin-like protein that stimulates intermolecular DNA interactions in vitro." J Biol Chem **285**(22): 16521-16529.

Rice, P. A., S. Yang, et al. (1996). "Crystal structure of an IHF-DNA complex: a protein-induced DNA U-turn." Cell **87**(7): 1295-1306.

Roca, J. (1995). "The mechanisms of DNA topoisomerases." Trends Biochem Sci **20**(4): 156-160.

Rostas, K., S. J. Morton, et al. (1987). "Nucleotide sequence and LexA regulation of the *Escherichia coli* recN gene." Nucleic Acids Res **15**(13): 5041-5049.

Roth, V., B. Aigle, et al. (2004). "Differential and Cross-Transcriptional Control of Duplicated Genes Encoding Alternative Sigma Factors in *Streptomyces ambofaciens*." J. Bacteriol. **186**(16): 5355-5365.

Rudd, B. A. and D. A. Hopwood (1979). "Genetics of actinorhodin biosynthesis by *Streptomyces coelicolor* A3(2)." J Gen Microbiol **114**(1): 35-43.

Rutherford, S. T., J. J. Lemke, et al. (2007). "Effects of DksA, GreA, and GreB on transcription initiation: insights into the mechanisms of factors that bind in the secondary channel of RNA polymerase." J Mol Biol **366**(4): 1243-1257.

Saitou, N. and M. Nei (1987). "The neighbor-joining method: a new method for reconstructing phylogenetic trees." Mol Biol Evol **4**(4): 406-425.

Salerno, P., J. Larsson, et al. (2009). "One of the two genes encoding nucleoid-associated HU proteins in *Streptomyces coelicolor* is developmentally regulated and specifically involved in spore maturation." J Bacteriol **191**(21): 6489-6500.

Sanglier, J. J., H. Haag, et al. (1993). "Novel bioactive compounds from Actinomycetes: a short review (1988-1992)." Res Microbiol **144**(8): 633-642.

Sanglier, J. J., E. M. Wellington, et al. (1993). "Novel bioactive compounds from *actinomycetes*." Res Microbiol **144**(8): 661-663.

Schwedock, J., J. R. McCormick, et al. (1997). "Assembly of the cell division protein FtsZ into ladder-like structures in the aerial hyphae of *Streptomyces coelicolor*." Mol Microbiol **25**(5): 847-858.

Segall, A. M., S. D. Goodman, et al. (1994). "Architectural elements in nucleoprotein complexes: interchangeability of specific and non-specific DNA binding proteins." Embo J **13**(19): 4536-4548.

Sevcikova, B., O. Benada, et al. (2001). "Stress-response sigma factor sigma(H) is essential for morphological differentiation of *Streptomyces coelicolor* A3(2)." Arch Microbiol **177**(1): 98-106.

Sharadamma, N., Y. Harshavardhana, et al. (2010). "*Mycobacterium tuberculosis* nucleoid-associated DNA-binding protein H-NS binds with high-affinity to the

Holliday junction and inhibits strand exchange promoted by RecA protein." Nucleic Acids Res **38**(11): 3555-3569.

Shure, M., D. E. Pulleyblank, et al. (1977). "The problems of eukaryotic and prokaryotic DNA packaging and in vivo conformation posed by superhelix density heterogeneity." Nucleic Acids Res **4**(5): 1183-1205.

Simon, R., U. Priefer, and A. Puhler (1983). "A broad host range mobilization system for in vivo genetic engineering: transposon mutagenesis in gram-negative bacteria." Bio/Technology **1**: 784-790.

Sinden, R. R. (1994). DNA structure and function. San Diego, Academic Press.

Smulczyk-Krawczyszyn, A., D. Jakimowicz, et al. (2006). "Cluster of DnaA boxes involved in regulation of *Streptomyces* chromosome replication: from in silico to in vivo studies." J Bacteriol **188**(17): 6184-6194.

Stallings, C. L., N. C. Stephanou, et al. (2009). "CarD is an essential regulator of rRNA transcription required for *Mycobacterium tuberculosis* persistence." Cell **138**(1): 146-159.

Stephens, J. C., S. W. Artz, et al. (1975). "Guanosine 5'-diphosphate 3'-diphosphate (ppGpp): positive effector for histidine operon transcription and general signal for amino-acid deficiency." Proc Natl Acad Sci U S A **72**(11): 4389-4393.

Strauch, E., E. Takano, et al. (1991). "The stringent response in *Streptomyces coelicolor* A3(2)." Mol Microbiol **5**(2): 289-298.

Stuger, R., C. L. Woldringh, et al. (2002). "DNA supercoiling by gyrase is linked to nucleoid compaction." Mol Biol Rep **29**(1-2): 79-82.

Sun, J., A. Hesketh, et al. (2001). "Functional analysis of relA and rshA, two relA/spoT homologues of *Streptomyces coelicolor* A3(2)." J Bacteriol **183**(11): 3488-3498.

Sun, J., G. H. Kelemen, et al. (1999). "Green fluorescent protein as a reporter for spatial and temporal gene expression in *Streptomyces coelicolor* A3(2)." Microbiology **145 (Pt 9)**: 2221-2227.

Szalewska-Palasz, A., G. Wegrzyn, et al. (2007). "Mechanisms of physiological regulation of RNA synthesis in bacteria: new discoveries breaking old schemes." J Appl Genet **48**(3): 281-294.

Tamura, K., J. Dudley, et al. (2007). "MEGA4: Molecular Evolutionary Genetics Analysis (MEGA) software version 4.0." Mol Biol Evol **24**(8): 1596-1599.

Tamura, K., D. Peterson, et al. (2011). "MEGA5: molecular evolutionary genetics analysis using maximum likelihood, evolutionary distance, and maximum parsimony methods." Mol Biol Evol **28**(10): 2731-2739.

Tanaka, K., T. Shiina, et al. (1988). "Multiple principal sigma factor homologs in eubacteria: identification of the "rpoD box"." Science **242**(4881): 1040-1042.

Towbin, H., T. Staehelin, et al. (1979). "Electrophoretic transfer of proteins from polyacrylamide gels to nitrocellulose sheets: procedure and some applications." Proc Natl Acad Sci U S A **76**(9): 4350-4354.

Travers, A. and G. Muskhelishvili (2005). "Bacterial chromatin." Curr Opin Genet Dev **15**(5): 507-514.

Travers, A. and G. Muskhelishvili (2005). "DNA supercoiling - a global transcriptional regulator for enterobacterial growth?" Nat Rev Microbiol **3**(2): 157-169.

Travers, A. A. (1980). "Promoter sequence for stringent control of bacterial ribonucleic acid synthesis." J Bacteriol **141**(2): 973-976.

Tse-Dinh, Y. C. and J. C. Wang (1986). "Complete nucleotide sequence of the topA gene encoding *Escherichia coli* DNA topoisomerase I." J Mol Biol **191**(3): 321-331.

Ventura, M., C. Canchaya, et al. (2007). "Genomics of Actinobacteria: tracing the evolutionary history of an ancient phylum." Microbiol Mol Biol Rev **71**(3): 495-548.

Verbeek, H., L. Nilsson, et al. (1992). "The mechanism of trans-activation of the Escherichia coli operon thrU(tufB) by the protein FIS. A model." Nucleic Acids Res **20**(15): 4077-4081.

Viollier, P. H., G. H. Kelemen, et al. (2003). "Specialized osmotic stress response systems involve multiple SigB-like sigma factors in *Streptomyces coelicolor*." Mol Microbiol **47**(3): 699-714.

Volff, J. N. and J. Altenbuchner (2000). "A new beginning with new ends: linearisation of circular chromosomes during bacterial evolution." FEMS Microbiol Lett **186**(2): 143-150.

Waksman, S. A. and A. T. Henrici (1943). "The Nomenclature and Classification of the Actinomycetes." J Bacteriol **46**(4): 337-341.

Wang, F., X. Xiao, et al. (2002). "Streptomyces olivaceoviridis possesses a phosphotransferase system that mediates specific, phosphoenolpyruvate-dependent uptake of N-acetylglucosamine." Mol Genet Genomics **268**(3): 344-351.

Wang, J. C. (1971). "Interaction between DNA and an *Escherichia coli* protein omega." J Mol Biol **55**(3): 523-533.

Wang, J. C. (1996). "DNA topoisomerases." Annu Rev Biochem **65**: 635-692.

Wang, J. C. (1998). "Moving one DNA double helix through another by a type II DNA topoisomerase: the story of a simple molecular machine." Q Rev Biophys **31**(2): 107-144.

Watson, J. D. and F. H. Crick (1953). "Molecular structure of nucleic acids; a structure for deoxyribose nucleic acid." Nature **171**(4356): 737-738.

Watve, M. G., R. Tickoo, et al. (2001). "How many antibiotics are produced by the genus Streptomyces?" Arch Microbiol **176**(5): 386-390.

Wehmeier, U. F. (1995). "New multifunctional *Escherichia coli-Streptomyces* shuttle vectors allowing blue-white screening on XGal plates." Gene **165**(1): 149-150.

Wendrich, T. M., G. Blaha, et al. (2002). "Dissection of the mechanism for the stringent factor RelA." Mol Cell **10**(4): 779-788.

Werlang, I. C., C. Z. Schneider, et al. (2009). "Identification of Rv3852 as a nucleoid-associated protein in *Mycobacterium tuberculosis*." Microbiology **155**(Pt 8): 2652-2663.

Witz, G. and A. Stasiak (2010). "DNA supercoiling and its role in DNA decatenation and unknotting." Nucleic Acids Res **38**(7): 2119-2133.

Wood, J. M., E. Bremer, et al. (2001). "Osmosensing and osmoregulatory compatible solute accumulation by bacteria." Comp Biochem Physiol A Mol Integr Physiol **130**(3): 437-460.

Worcel, A. and E. Burgi (1972). "On the structure of the folded chromosome of *Escherichia coli*." J Mol Biol **71**(2): 127-147.

Wu, H. Y., S. H. Shyy, et al. (1988). "Transcription generates positively and negatively supercoiled domains in the template." Cell **53**(3): 433-440.

Yamanaka, K., T. Mitani, et al. (1994). "Cloning, sequencing, and characterization of multicopy suppressors of a mukB mutation in Escherichia coli." Mol Microbiol **13**(2): 301-312.

Yamanaka, K., T. Ogura, et al. (1996). "Identification of two new genes, mukE and mukF, involved in chromosome partitioning in *Escherichia coli*." Mol Gen Genet **250**(3): 241-251.

Yamasaki, M. and H. Kinashi (2004). "Two chimeric chromosomes of *Streptomyces coelicolor* A3(2) generated by single crossover of the wild-type chromosome and linear plasmid scp1." J Bacteriol **186**(19): 6553-6559.

Yamazoe, M., T. Onogi, et al. (1999). "Complex formation of MukB, MukE and MukF proteins involved in chromosome partitioning in *Escherichia coli*." EMBO J **18**(21): 5873-5884.

Yang, C. C., C. H. Huang, et al. (2002). "The terminal proteins of linear *Streptomyces chromosomes* and plasmids: a novel class of replication priming proteins." Mol Microbiol **43**(2): 297-305.

Yang, X. and E. E. Ishiguro (2001). "Dimerization of the RelA protein of *Escherichia coli*." Biochem Cell Biol **79**(6): 729-736.

Yang, X. and E. E. Ishiguro (2001). "Involvement of the N terminus of ribosomal protein L11 in regulation of the RelA protein of Escherichia coli." J Bacteriol **183**(22): 6532-6537.

Yanisch-Perron, C., J. Vieira, et al. (1985). "Improved M13 phage cloning vectors and host strains: nucleotide sequences of the M13mp18 and pUC19 vectors." Gene **33**(1): 103-119.

Yokoyama, E., K. Doi, et al. (1997). "Cloning and sequencing of the hup gene encoding the histone-like protein HSl of *Streptomyces lividans*." Biochim Biophys Acta **1353**(2): 103-106.

Yuan, H. S., S. E. Finkel, et al. (1991). "The molecular structure of wild-type and a mutant Fis protein: relationship between mutational changes and recombinational enhancer function or DNA binding." Proc Natl Acad Sci U S A **88**(21): 9558-9562.

Zhang, X., C. A. Clark, et al. (2003). "Interstrain inhibition in the sweet potato pathogen Streptomyces ipomoeae: purification and characterization of a highly specific bacteriocin and cloning of its structural gene." Appl Environ Microbiol **69**(4): 2201-2208.

Zhou, Y. N. and D. J. Jin (1998). "The rpoB mutants destabilizing initiation complexes at stringently controlled promoters behave like "stringent" RNA polymerases in *Escherichia coli*." Proc Natl Acad Sci U S A **95**(6): 2908-2913.